High Resolution NMR Studies Concerning the Solvation/Hydration and Coordination Chemistry of Pt(II/IV) Compounds

Arjan Nicolaas Westra

Dissertation presented for the Degree of Doctor of Philosophy

at the University of Stellenbosch

Promoter: Professor Klaus R. Koch

December 2005

Stellenbosch University http://scholar.sun.ac.za

I, the undersigned, hereby declare that the work contained in this dissertation is my own original work and that I have not previously in its entirety or in part submitted it at any university for a degree.

SIGNATURE:

DATE:

Stellenbosch University http://scholar.sun.ac.za

Summary

Pt(IV) complexes with S,O-donating aroylthioureas have been synthesized by oxidative addition of elemental halogens to the Pt(II) precursors, leading to the first-reported crystal structures of Pt(IV) with this class of ligand.

The treatment of Pt(II) complexes of *N,N*-diethyl-*N'*-benzoylthiourea with I_2, Br_2 and Cl_2 leads to facile oxidative addition of the halogens to the platinum center, yielding several geometric isomers, as determined by ^{195}Pt NMR; the products *cis*-bis(*N,N*-diethyl-*N'*-benzoylthioureato)diiodoplatinum(IV), **26**, and *cis*-bis(*N,N*-diethyl-*N'*-benzoylthioureato)dibromo-platinum(IV), **27**, have been isolated and structurally characterized. Reaction of *cis-/trans*-bis(*N*-benzoyl-*N'*-propylthiourea-κS)dibromoplatinum(II) with Br_2, similarly results in oxidative addition of the dihalogen, yielding the product *trans*-bis(*N*-benzoyl-*N'*-propylthiourea-κS)tetrabromoplatinum(IV), **29**. I_2, however, does not undergo oxidative addition to *cis-/trans*-bis(*N*-benzoyl-*N'*-propylthiourea-κS)diiodoplatinum(II), instead the iodine inclusion compound *trans*-bis(*N*-benzoyl-*N'*-propylthiourea-κS)diiodoplatinum(II) diiodine, **28**, was isolated. Short intermolecular I···I interactions in crystals of compounds **26** and **28** lead to infinite chains of weakly linked molecules in the respective solids.

^{195}Pt NMR reveals that the 3 : 3 Pt(II) metallamacrocycle of 3,3,3',3'-tetra(*n*-butyl)-1,1'-terephthaloylbis(thiourea) undergoes stepwise oxidative addition of I_2 or Br_2 to each of the Pt(II) centers, upon treatment with the dihalogens. Treatment of the 2 : 2 Pt(II) complex of 3,3,3',3'-tetraethyl-1,1'-isophthaloylbis(thiourea) with I_2 also results in the oxidative addition of the halogen, yielding a 2 : 2 *trans*-Pt(IV)-iodo metallamacrocycle, **35**. The corresponding *trans*-Pt(IV)-X (X = Br, Cl) complexes were synthesized by oxidative addition in an electrolytic cell containing the 2 : 2 Pt(II) precursor and an appropriate halide salt in dichloromethane. The 2 : 2 *trans*-Pt(IV)-X (X = I, Br, Cl) metallamacrocycles, **36** an **37**, were isolated and structurally characterized. Intermolecular I···I interactions between molecules of **35**, in crystals of the compound, result in chains of weakly connected molecules in the lattice.

^{195}Pt NMR is used as a sensitive probe for studying the hydration/solvation spheres of the PtX_6^{2-} (X = Cl, Br) anions, and to investigate the occurrence of $\{Na^+[PtCl_6^{2-}]\}^-$ contact ion-pairing in non-aqueous solutions.

The ^{195}Pt NMR chemical shifts of the PtX_6^{2-} (X = Cl, Br) anions in D_2O and in various organic solvents have been determined, and are discussed with regard to solvent polarities and donor and acceptor properties. The non-linear variations of $\delta_{Pt\text{-}195}$ for the anions with changing bulk composition in aqueous binary mixtures with the organic solvents, suggest that the anions are preferentially solvated by the organic solvents relative to water. The anion solvation sphere compositions with changing bulk composition, as well as preferential solvation equilibrium constants, $K^{1/n}$, are determined from the NMR data.

Significant non-linear variations of the ^{195}Pt NMR chemical shift for methanol and acetonitrile solutions of PtX_6^{2-} (X = Cl, Br) with increasing $NaClO_4$ concentrations indicate the occurrence of $\{Na^+[PtX_6^{2-}]\}^-$

Stellenbosch University http://scholar.sun.ac.za

contact ion-pair formation in these solutions. By contrast, the variation of $\delta_{Pt\text{-}195}$ for aqueous solutions of the halogenoplatinate anions with increasing sodium perchlorate concentration is slight, revealing that $Na^{+}\cdots PtX_6^{2-}$ ion association is not favoured in the aqueous medium. The ^{195}Pt chemical shift variations are used to estimate conditional ion-pair formation equilibrium quotients, Q (M^{-1}), for $\{Na^{+}[PtX_6^{2-}]\}^{-}$ contact ion-pair formation in water, methanol and acetonitrile. The estimated Q values illustrate that the extent of $\{Na^{+}[PtX_6^{2-}]\}^{-}$ ion-pairing increases in these solvents in the order water < methanol < acetonitrile, which is in accordance with the solvent donor and acceptor properties.

Opsomming

Pt(IV) komplekse met S,O-donerende aroïeltioüreum ligande is deur middel van die oksidatiewe addisie van halogene aan Pt(II) uitgangskomplekse gesintetiseer; die kristalstrukture van die Pt(IV) komplekse met hierdie tipe ligande word vir die eerste keer gerapporteer.

Die behandeling van die Pt(II) komplekse van *N,N*-diëtiel-*N*'-bensoïeltioüreum met I_2, Br_2 en Cl_2 gee geredelik aanleiding tot die oksidatiewe addisie van die halogene aan die platinum sentrum, en lei, volgens bepaling met ^{195}Pt KMR, tot die vorming van verskeie geometriese isomere; die produkte *cis*-bis(*N,N*-diëtiel-*N*'-bensoïeltioüreato)di-jodoplatinum(IV), **26**, en *cis*-bis(*N,N*-diëtiel-*N*'-bensoïeltioüreato)dibromo-platinum(IV), **27**, is geïsoleer en kristallografies gekarakteriseer. Reaksie van *cis-/trans*-bis(*N*-bensoïel-*N*'-propieltioüreum-κS)dibromoplatinum(II) met Br_2, lei ooreenkomstiglik tot oksidatiewe addisie van die halogeen, met *trans*-bis(*N*-bensoïel-*N*'-propieltioüreum-κS)tetrabromoplatinum(IV) as produk, **29**. I_2 ondergaan egter nie oksidatiewe addisie aan *cis-/trans*-bis(*N*-bensoïel-*N*'-propieltioüreum-κS)di-jodoplatinum(II) nie; 'n verbinding waarin I_2 ingesluit word in 'n kristalstruktuur met *trans*-bis(*N*-bensoïel-*N*'-propieltioüreum-κS)di-jodoplatinum(II), word geïsoleer, **28**. Kort intermolekulêre I···I interaksies in die kristalstrukture van verbindings **26** en **28** lei tot die ontstaan van swak-gebonde molekuul-kettings in die kristalle.

^{195}Pt KMR dui aan dat met behandeling van die 3 : 3 Pt(II) metallomakrosikliese kompleks van die 3,3,3',3'-tetra(*n*-butiel)-1,1'-tereftaloïelbis(tioüreum) ligand met I_2 of Br_2, daar stapsgewyse oksidatiewe addisie van die halogene aan die Pt(II) ione in die kompleks plaasvind. Behandeling van die 2 : 2 Pt(II) kompleks van 3,3,3',3'-tetraëtiel-1,1'-isoftaloïelbis(tioüreum) met I_2 gee ook aanleiding tot oksidatiewe addisie, met 'n 2 : 2 *trans*-Pt(IV)-jodo metallomakrosikliese kompleks as produk, **35**. Die ooreenkomstige *trans*-Pt(IV)-X (X = Br, Cl) komplekse is gesintetiseer deur middel van oksidatiewe addisie in 'n elektrolitiese sel wat die 2 : 2 Pt(II) uitgangskompleks bevat tesame met 'n toepaslike haliedsout in dichlorometaan. Die 2 : 2 *trans*-Pt(IV)-X (X = I, Br, Cl) komplekse, **36** en **37**, is geïsoleer en kristallografies gekarakteriseer. Intermolekulêre I···I interaksies tussen molekule in kristalle van verbinding **35**, gee aanleiding tot kettings van swak-gebonde molekule in die struktuur.

Stellenbosch University http://scholar.sun.ac.za

^{195}Pt KMR word gebruik om die hidraterings-/solvaterings-sfere van die PtX_6^{2-} (X = Cl, Br) anione te ondersoek, asook om die voorkoms van $\{Na^+[PtClX_6^{2-}]\}^-$ kontak-ioonparing in nie-waterige oplosmiddels te bestudeer.

Die ^{195}Pt KMR chemise verskuiwing van die PtX_6^{2-} (X = Cl, Br) anione in D_2O en in verskeie organiese oplosmiddels is bepaal, en word bespreek met verwysing na die polariteite asook die donor- en akseptoreienskappe van die oplosmiddels. Die nie-lineêre variasies van $\delta_{Pt\text{-}195}$ vir die anione met veranderende oplosmiddelsamestelling in waterige binêre mengsels met die organiese oplosmiddels, dui aan dat die anione by voorkeur deur die organiese oplosmiddels gesolvateer word. Die solvaterings-samestelling van die anione met veranderende oplosmiddelsamestelling, asook ewewigskonstantes vir die voorkeur-solvatering deur die organiese oplosmiddels, $K^{1/n}$, word met behulp van die KMR data bepaal.

Beduidende nie-lineêre variasies van $\delta_{Pt\text{-}195}$ in metanol en asetonitriel oplossings van PtX_6^{2-} (X = Cl, Br) met toenemende $NaClO_4$ konsentrasies, dui op die voorkoms van $\{Na^+[PtClX_6^{2-}]\}^-$ kontak-ioonparing in die oplossings. Die variasies van $\delta_{Pt\text{-}195}$ in waterige oplosings van die anione met toenemende $NaClO_4$ konsentrasies is egter minder beduidend, waaruit afgelei kan word dat ioonparing nie in die waterige medium bevoordeel word nie. Die ^{195}Pt chemiese verskuiwings word gebruik om kondisionele ioonpaarvormings-ewewigskwosiënte, Q (M^{-1}), vir die vorming van $\{Na^+[PtClX_6^{2-}]\}^-$ in water, metanol en asetonitriel af te lei. Die Q-waardes dui in ooreenstemming met die donor- en akseptoreienskappe van die onderskeie oplosmiddels aan dat die voorkoms van kontak-ioonparing toeneem vir die oplosmiddels in die volgorde water < metanol < asetonitriel.

Stellenbosch University http://scholar.sun.ac.za

mam

arno centa christel elisabeth jos jurjen keith luke matthew petra richard terry wesley

Stellenbosch University http://scholar.sun.ac.za

ek wil graag in besonder my dank betuig aan Professor Koch wat met onuitputbare entoesiasme, energie en inspirasie, hierdie werk gerig en ondersteun het

dankie ook aan

lede van die Platinum Metals Chemistry Research Group (US), vir vriendskap en ondersteuning

studente en personeel van die Departement Chemie en Polimeerwetenskap (US)

Susan Bourne

Dave Robinson

my familie en vriende

die Universiteit van Stellenbosch, die National Research Foundation, en Angloplatinum

Stellenbosch University http://scholar.sun.ac.za

CONTENTS

Stellenbosch University http://scholar.sun.ac.za

Stellenbosch University http://scholar.sun.ac.za

Stellenbosch University http://scholar.sun.ac.za

Stellenbosch University http://scholar.sun.ac.za

Chapter 1

General Introduction

In this thesis, studies of two aspects of the chemistry of Pt(IV) complexes are described. In the first, the coordination chemistry of Pt(IV) complexes of *S,O*-donating aroylthioureas is investigated, based on complex synthesis and characterization (Chapters 2 and 3), and in the second, the nature of the hydration and solvation spheres of Pt(IV) chloro- and bromo-anions in various media, by means of high resolution ^{195}Pt NMR spectroscopy, is undertaken (Chapters 4 and 5). Although neither of the two investigations involves specifically a study of the selective separation of platinum *per se*, both have been initiated with a view to elucidating, at a fundamental level, the nature of the separation of this precious metal, and the other platinum group metals, by modern analytical techniques (such as solvent extraction and ion exchange). The investigation of Pt(IV) complexes of the aroylthioureas also includes ligands which incorporate two *S,O*-donating moieties, so-called bipodal ligands (Chapter 3), since these molecules have shown considerable potential as building blocks for synthesizing new 3-dimensional metal-organic frameworks.

Stellenbosch University http://scholar.sun.ac.za

Pt(IV) complexes of S,O-donating aroylthioureas.

Ligands based on the *N,N*-alkyl-*N'*-aroyl(acyl)thiourea motif, shown below, have shown remarkable potential in medicinal, as well as technical and analytical applications. These compounds have been investigated due to their potential anticancer,[1,2] antifungal,[3,4] and antimalarial[5] properties, and have been successfully utilized in the separation and trace determination of particularly the platinum group metals (PGMs).[6-12]

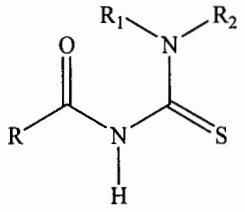

R = aryl or alkyl, R_1 and R_2 = alkyl; ***N,N*-dialkyl-*N'*-aroyl(acyl)thiourea** **HL^1**
R = aryl or alkyl, R_1 = H, R_2 = alkyl; ***N*-alkyl-*N'*-aroyl(acyl)thiourea** **H_2L^2**

Extensive studies of the coordination chemistry of this class of ligand to various transition metal ions such as Co(III), Ni(II), Cu(II), Pd(II), Ag(I), Hg(II), and Pb(II),[13] as well as their potential in practical applications,[7] were initiated by the work of Beyer and Hoyer in 1981. These authors reported the potential of the *N'*-aroylthioureas in liquid-liquid extraction of such ions as Cu(II), Hg(II), Au(III) and Pd(II),[7] and König, Schuster and co-workers found that the *N,N*-dialkyl-*N'*-benzoylthioureas show a pronounced selectivity toward the *platinum group metals*, resulting in very effective extractions of these precious elements.[6,14] König *et al.*[6] found that by controlling the pH of the aqueous phase in liquid-liquid extraction experiments with *N,N*-dialkyl-*N'*-benzoylthioureas, the platinum group metals can be separated from interfering elements such as iron, cobalt, nickel, copper and zinc; the selectivity for the PGMs was found to increase at higher acid concentrations. Moreover, the platinum group metals can, to some degree, be separated from each other by controlling solution pH and temperature in extraction processes. In a subsequent investigation by Vest *et al.*,[14] the *N,N*-dialkyl-*N'*-benzoylthioureas were shown to be more efficient extractants than the *N*-alkyl-*N'*-benzoylthioureas.

Several studies have highlighted the separation and trace determination of PGMs by high-performance thin layer chromatography (HPTLC) after complexation of the metal ions with *N,N*-disubstituted *N'*-aroyl(acyl)thioureas,[15-18] and recently Koch *et al.*[11] have applied reversed-phase high performance liquid chromatography (RP-HPLC) for the trace determination of Pd(II), Pt(II) and Rh(II), after metal coordination with suitable *N,N*-dialkyl-*N'*-acylthioureas. Schuster and co-workers have also investigated the potential of using *fluorescent N*-aroylthioureas for the determination of traces of PGMs by means of HPTLC,[19,20] and have recently described an on-line separation and preconcentration system for the trace determination of Pd(II) by graphite furnace atomic absorption spectrometry, after complexation of the palladium with *N,N*-diethyl-*N'*-benzoylthiourea.[8]

Stellenbosch University http://scholar.sun.ac.za

A number of recent investigations have elucidated the coordination of several platinum group metal ions with a variety of *N,N*-dialkyl-*N'*-aroyl(acyl)thioureas (**HL**^{1}), with structural characterization reported for *tris*-(*N,N*-diethyl-*N'*-benzoylthioureato)ruthenium(III),[21] *tris*-(*N,N*-diethyl-*N'*-benzoylthioureato)-rhodium(III),[22] *fac*-tris[*N*-pyrrolidyl-*N'*-(2,2-dimethylpropyl)thioureato]rhodium(III),[11] *cis*-bis(*N,N*-diethyl-*N'*-benzoylthioureato)palladium(II),[10,23] *cis*-bis(*N,N*-diethyl-*N'*-benzoylthioureato)platinum(II),[24] *cis*-bis(*N,N*-di(*n*-butyl)-*N'*-benzoylthioureato)platinum(II),[25] and *cis*-bis[*N*-piperidyl-*N'*-(2,2-dimethylpropyl)thioureato]platinum(II).[11] The **HL**^{1} ligands have been found to coordinate to the platinum group metal ions *via* both the *S*- and *O*-atoms with loss of the thioamidic proton, forming, in the case of Pd(II) and Pt(II), predominantly *cis* complexes; *cis*-[M(**L**^{1}-***S,O***)$_2$] (M = Pd(II), Pt(II)) . The structural characterization of only one *trans* complex of an **HL**^{1} ligand with Pt(II) has been reported to date, *viz.* *trans*-bis(*N,N*-di(*n*-butyl)-*N'*-naphthoylthioureato)platinum(II).[26] Koch *et al.*[27] have recently reported that *cis* Pt(II) and Pd(II) complexes of the *N,N*-dialkyl-*N'*-aroylthioureas undergo reversible photoinduced isomerization to the corresponding *trans* isomer, and are currently investigating the mechanism of the photoisomerization.

Only a small number of published studies concerning the coordination of the *N*-alkyl-*N'*-aroyl(acyl)thioureas (**H$_2$L**^{2}) to the platinum group metals are available; crystallographic characterization for chloro(η^2,η^2-1,5-cyclo-octadiene)-(*N*-benzoyl-*N'*-propylthiourea-κS)rhodium(I),[28] *trans*-bis(*N*-benzoyl-*N'*-propylthiourea-κS)dibromopalladium(II),[29] and *cis*-bis(*N*-benzoyl-*N'*-propylthiourea-κS)dichloroplatinum(II)[30] are reported. The mode of coordination of the **H$_2$L**^{2} ligands to the platinum group metals differs from that of the **HL**^{1} ligands; an intramolecular hydrogen-bond between the thiourea –C(S)NHR moiety and the carbonyl *O*-atom in the former, leads to monodentate coordination *via* the *S*-atom only.

The synthesis of complexes of the platinum group metals with **HL**^{1} ligands are typically carried out in *basic* medium, to ensure deprotonation of the thioamidic proton and allow bidentate coordination via the *S*- and *O*-donors. The application of the *N,N*-dialkyl-*N'*-aroyl(acyl)thioureas as extractants in the separation of the platinum group metals by liquid-liquid extraction, however, requires an *acidic* extractive medium.[6,14] Very little is known with regard to the nature of the PGM complexes which exist in these acidic media. We have recently shown in a ^{1}H and ^{195}Pt NMR speciation study that acidification (HCl) of a chloroform solution of *cis*-bis(*N*-morpholino-*N'*-propanoylthioureato)platinum(II) (*cis*-[Pt^{II}(**L**^{11}-***S,O***)$_2$]) leads to the formation of three major species in the organic phase, *viz.* [Pt^{II}(**L**^{11}-***S,O***)(**HL**^{11}-***S***)Cl], *cis*-[Pt^{II}(**HL**^{11}-***S***)$_2$Cl$_2$] and *trans*-[Pt^{II}(**HL**^{11}-***S***)$_2$Cl$_2$], i.e. protonated analogues of *cis*-[Pt^{II}(**L**^{11}-***S,O***)$_2$][31]* (general structures for these protonated species are shown below). These results suggest that in acidic solvent extraction processes of **Pt(II)** with **HL**^{1}-type ligands, the three Pt(II) complexes shown below are likely to predominate in the

* Reference [31] is included as Addendum C.

Stellenbosch University http://scholar.sun.ac.za

R = aryl or alkyl, R_1 and R_2 = alkyl

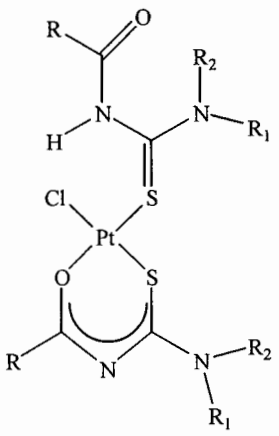

$[Pt^{II}(L^1\text{-}S,O)(HL^1\text{-}S)Cl]$

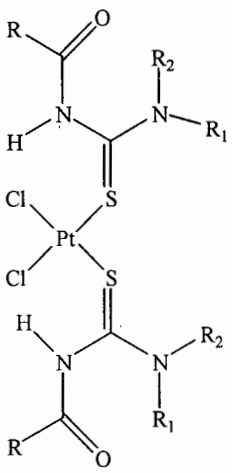

cis-$[Pt^{II}(HL^1\text{-}S)_2Cl_2]$

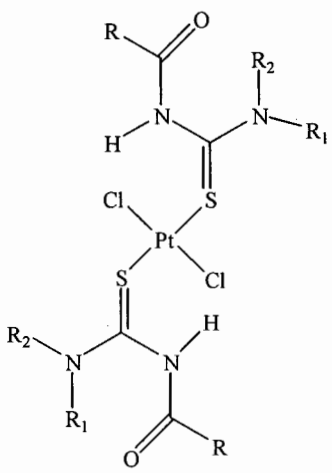

trans-$[Pt^{II}(HL^1\text{-}S)_2Cl_2]$

organic phase. Extraction of **Pt(IV)** into chloroform containing excess HL^1 from an acidic aqueous (HCl) source phase containing only $PtCl_6^{2-}$ ($PtCl_6^{2-}$ being the predominant species present in strongly acidic refining-process solutions[32]) resulted in a significantly more complicated distribution of both Pt(II) and Pt(IV) complex species in the organic phase, arising *inter alia* from redox reactions between Pt(IV) and the ligand.[31] No conclusions could be drawn regarding the nature of the extracted Pt(IV) species present in the extraction mixtures, since very little is known about the coordination of Pt(IV) with HL^1, or H_2L^2. Initial attempts to synthesize Pt(IV) complexes of *N*,*N*-diethyl-*N*'-benzoylthiourea by reacting $PtCl_6^{2-}$ with the ligand under various experimental conditions, led to the isolation of predominantly the Pt(II) complex of this ligand, evidently due to redox reactions between Pt(IV) and the ligand. The complete absence of any published studies concerning the coordination chemistry of ligands of the type HL^1 and H_2L^2 with Pt(IV), motivated the investigation to synthesize and characterize Pt(IV) complexes of this class of ligand.

The symmetrical bipodal analogues of the *N*'-aroylthioureas, the 3,3,3',3'-tetraalkyl-1,1'-phenylenedicarbonylbis(thioureas), illustrated below, have been shown to be 'pre-programmed' to self-assemble into discrete metallamacrocycles with metal ions such as Ni(II),[33,34] Pt(II),[34,35] and Pd(II).[35] Metal-to-ligand stoichiometries of 2 : 2 are achieved with *meta* substitution of the carbonylthiourea moieties to the phenylene spacer, while *para* substitution leads to 3 : 3 metallamacrocycles. Recently Bourne and Koch *et al.* have shown that *octahedral* adducts of 2 : 2 and 3 : 3 Ni(II) metallamacrocycles of the bipodal aroylthioureas can be obtained by addition of pyridines.[35-37] Moreover, by using a bipodal isophthaloylbis(thiourea) ligand with hydroxyethyl side branches, i.e. using a spacer with *meta* substitution and with R = 2-hydroxyethyl, an octahedral metallamacrocyclic adduct which assembles into a complex 3-

Stellenbosch University http://scholar.sun.ac.za

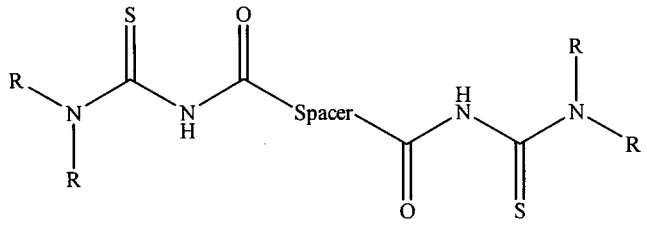

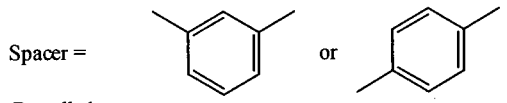

R = alkyl

dimensional supramolecular framework, is isolated.[36] These results suggest that the 2 : 2 metallamacrocyclic complexes of bipodal aroylthioureas may potentially be used for the self-assembly of infinite metal-organic frameworks. With a view to exploring the potential of exploiting axial ligating sites on Pt(IV) centres in analogous 2 : 2 and 3 : 3 Pt(IV) complexes as sites for further assembly of Pt(IV) metallamacrocycles, an investigation was initiated to synthesize and characterize Pt(IV) complexes of bipodal 3,3,3',3'-tetraalkyl-1,1'-phenylenedicarbonylbis(thioureas).

Hydration and solvation spheres of Pt(IV)-chloro and -bromo anions.

Industrial processes for the separation and refinement of the platinum group metals rely on solvent extraction or ion-exchange techniques in which the PGM chloro-anions are transferred from an aqueous to a non-aqueous phase,[32] and favourable phase transfer of the anions depends to a large degree on the hydration and solvation energies of the ions in the solvents used.[38] Although the hydration/solvation of cations is well understood,[39,40] that of anions, which are generally regarded to be relatively poorly solvated,[39] remains scarcely studied. In order to elucidate the fundamental aspects of the nature and degree of hydration/solvation of the PGM chloro-anions, Naidoo and Koch *et al.* have recently used density functional theory (DFT) calculations and molecular dynamics simulations to develop detailed models of the solvation-sphere structures of several of the PGM chloro-anions.[41-43] Not only have the structural arrangements of water and methanol molecules around such ions as $PtCl_6^{2-}$, $PtCl_4^{2-}$, $RhCl_6^{3-}$ and $PdCl_4^{2-}$ been determined by computation,[42,43] but the authors have also shown that the formation of solvent-shared and contact ion-pairs of Na^+ and $PtCl_6^{2-}$ is favoured in methanol.[43] With the aim of providing experimental verification and support for the computational observations, we have explored the potential of utilizing ^{195}Pt NMR spectroscopy as a probe for studying the environment directly around such anions as $PtCl_6^{2-}$ and $PtBr_6^{2-}$. The ^{195}Pt NMR chemical shift is known to be sensitive to the nature of the ligands coordinated to the platinum centre, as well as to factors such as solvent, temperature and concentration,[44-47] and it was of interest to determine whether this sensitivity could be exploited to study not only the hydration/solvation

Stellenbosch University http://scholar.sun.ac.za

spheres of the PtX_6^{2-} (X = Cl, Br) anions, but also the occurrence of ion-pairing of these anions with Na^+ in non-aqueous solvents.

The research described in this thesis has as aim the synthesis and characterization of Pt(IV) complexes of *N*-alkyl- and *N,N*-dialkyl-*N'*-acyl(aroyl)thioureas, as well as the bipodal analogues 3,3,3',3'-tetraalkyl-1,1'-phenylenedicarbonylbis(thioureas), and the utilization of ^{195}Pt NMR spectroscopy as a probe for studying the solvation spheres of the $PtCl_6^{2-}$ and $PtBr_6^{2-}$ anions.

Chapter 2 describes the synthesis of the first Pt(IV) complexes of $\mathbf{HL^1}$ and $\mathbf{H_2L^2}$ ligands, by means of oxidative addition of elemental halogens (I_2, Br_2 and Cl_2) to the Pt(II) complexes of these ligands. Various Pt(IV) products, as well as an interesting iodine inclusion compound, were isolated, and have been structurally characterized.

The facile synthesis of the Pt(IV) complexes of $\mathbf{HL^1}$ and $\mathbf{H_2L^2}$ by halogen oxidative addition motivated a similar approach for metallamacrocyclic Pt(IV) compounds; this is described in **Chapter 3**. ^{195}Pt NMR is used to monitor the oxidative addition of I_2 and Br_2 to the 3 : 3 Pt(II) metallamacrocyclic complex of 3,3,3',3'-tetraethyl-1,1'-terephthaloylbis(thiourea). The synthesis of 2 : 2 Pt(IV) metallamacrocyclic complexes of 3,3,3',3'-tetraethyl-1,1'-isophthaloylbis(thiourea) by oxidative addition of halogens, added directly or produced *in situ* in an electrolytic cell, is described; the isolated compounds have been characterized by single crystal X-ray diffraction.

The solvent dependence of the ^{195}Pt chemical shift of $PtCl_6^{2-}$ and $PtBr_6^{2-}$ in D_2O and in various organic solvents, as well as in aqueous binary mixtures with the organic solvents, is described in **Chapter 4**. The $\delta_{Pt\text{-}195}$ data in pure solvents are interpreted with reference to the properties of the solvents, and results for the binary solvent mixtures are discussed in terms of the preferential solvation of the anion.

The utilization of ^{195}Pt NMR as a probe for studying the occurrence of $Na^+\cdots[PtX_6^{2-}]$ (X = Cl, Br) contact ion-pair formation, is presented in **Chapter 5**. Conditional ion-pair formation equilibrium quotients for $Na^+\cdots[PtX_6^{2-}]$ contact ion-pairing in water, methanol and acetonitrile are calculated from the observed NMR data, and are related to the properties of the respective solvents.

Stellenbosch University http://scholar.sun.ac.za

References

1 U. Bierbach and N. Farrel, *Journal of Inorganic Biochemistry*, 1995, **59**, 233.
2 C. Sacht and M. S. Datt, *Polyhedron*, 2000, **19**, 1347.
3 E. Rodriguez-Fernandez, E. Garcia, M. R. Hermosa, A. Jimenez-Sanchez, M. M. Sanchez, E. Monte and J. J. Criado, *Journal of Inorganic Biochemistry*, 1999, **75**, 181.
4 R. del Campo, J. J. Criado, E. Garcia, M. R. Hermosa, A. Jimenez-Sanchez, J. L. Manzano, E. Monte, E. Rodriguez-Fernandez and F. Sanz, *Journal of Inorganic Biochemistry*, 2002, **89**, 74.
5 T. Egan, K. R. Koch, P. L. Swan, C. Clarkson, D. A. van Schalkwyk and P. J. Smith, *Journal of Medicinal Chemistry*, 2004, **47**, 2926.
6 K.-H. König, M. Schuster, B. Steinbrech, G. Schneeweis and R. Schlodder, *Fresenius Zeitschrift für Analitische Chemie*, 1985, **321**, 457.
7 P. Mühl, K. Głoe, F. Dietze, E. Hoyer and L. Beyer, *Zeitschrift für Chemie*, 1986, **26**, 81.
8 M. Schuster and M. Schwarzer, *Analytica Chimica Acta*, 1996, **328**, 1.
9 M. Merdivan, A. Gungor, S. Savasci and R. S. Aygun, *Talanta*, 2000, **53**, 141.
10 M. Dominguez, E. Antico, L. Beyer, A. Aguirre, S. Garcia-Granda and V. Salvado, *Polyhedron*, 2002, **21**, 1429.
11 A. N. Mautjana, J. D. S. Miller, A. Gie, S. A. Bourne and K. R. Koch, *Dalton Transactions*, 2003, 1952.
12 K. R. Koch, *Coordination Chemistry Reviews*, 2001, **216-217**, 473.
13 L. Beyer, E. Hoyer, H. Hartman and J. Liebscher, *Z. Chem*, 1981, **21**, 81.
14 P. Vest, M. Schuster and K. H. Koenig, *Fresenius Zeitschrift für Analitische Chemie*, 1989, **335**, 759.
15 K.-H. König, M. Schuster, G. Schneeweis and B. Steinbrech, *Fresenius Zeitschrift für Analitische Chemie*, 1984, **319**, 66.
16 K.-H. König, M. Schuster, G. Schneeweis and B. Steinbrech, *Fresenius Zeitschrift für Analitische Chemie*, 1985, **325**, 321.
17 M. Schuster, B. Kugler and K. H. Koenig, *Fresenius Journal of Analytical Chemistry*, 1990, **338**, 717.
18 M. Schuster, *Fresenius Zeitschrift für Analitische Chemie*, 1992, **342**, 791.
19 M. Schuster and E. Unterreitmaier, *Fresenius Journal of Analytical Chemistry*, 1993, **346**, 630.
20 M. Schuster and M. Sandor, *Fresenius Journal of Analytical Chemistry*, 1996, **356**, 326.
21 J. Sieler, R. Richter, E. Hoyer, L. Beyer, O. Lindqvist and L. Andersen, *Zeitschrift fur Anorganische und Allgemeine Chemie*, 1990, **580**, 167.
22 W. Bensch and M. Schuster, *Zeitschrift fur Anorganische und Allgemeine Chemie*, 1992, **615**, 93.
23 G. Fitzl, L. Beyer, J. Sieler, R. Richter, J. Kaiser and E. Hoyer, *Zeitschrift für Anorganische und Allgemeine Chemie*, 1977, **433**, 237.
24 C. Sacht, M. Datt, S. Otto and A. Roodt, *Journal of the Chemical Society, Dalton Transactions*, 2000, 727.
25 A. Irving, K. R. Koch and M. Matoetoe, *Inorganica Chimica Acta*, 1993, **206**, 193.
26 K. R. Koch, J. du Toit, M. R. Caira and C. Sacht, *Journal of the Chemical Society, Dalton Transactions*, 1994, 785.
27 D. Hanekom, J. M. McKenzie, N. M. Derix and K. R. Koch, *Chemical Communications*, 2005, 767.
28 D. Cauzzi, M. Lanfranchi, G. Marzolini, G. Predieri, A. Tiripicchio, M. Costa and R. Zanoni, *Journal of Organometallic Chemistry*, 1995, **488**, 115.
29 K. R. Koch, Y. Wang and A. Coetzee, *Journal of the Chemical Society, Dalton Transactions*, 1999, 1013.
30 S. Bourne and K. R. Koch, *Journal of the Chemical Society, Dalton Transactions*, 1993, 2071.
31 K. R. Koch, J. D. C. Miller and A. N. Westra, in *International Solvent Extraction Conference, ISEC 2002*, ed. P. M. C. K. C. Sole, J. S. Preston and D. J. Robinson, South African Institute of Mining and Metallurgy, Johannesburg, 2002, 327.
32 R. I. Edwards, A. J. Bird and G. J. Berfeld, in *Gmelin Handbook of Inorganic Chemistry, Platinum Supplement*, Springer-Verlag, Berlin, 8th edn., 1986.
33 R. Richter, J. Sieler, R. Kohler, E. Hoyer, L. Beyer and L. K. Hansen, *Zeitschrift für Anorganische und Allgemeine Chemie*, 1989, **578**, 191.
34 K. R. Koch, S. A. Bourne, A. Coetzee and J. Miller, *Journal of the Chemical Society, Dalton Transactions*, 1999, 3157.

Stellenbosch University http://scholar.sun.ac.za

35 K. R. Koch, O. Hallale, S. A. Bourne, J. Miller and J. Bacsa, *Journal of Molecular Structure*, 2001, **561**, 185.
36 S. A. Bourne, O. Hallale and K. R. Koch, *Crystal Growth & Design*, 2005, **5**, 307.
37 O. Hallale, S. A. Bourne and K. R. Koch, *Crystal Engineering Communication*, 2005, **7**, 161.
38 B. A. Moyer and P. V. Bonnesen, in *Supramolecular Chemistry of Anions*, Wiley-VCH, New York, 1997.
39 Y. Marcus, in *Ion Solvation*, Wiley-Interscience, Chichester, 1985.
40 Y. Marcus, in *Ion Properties*, Marcel Dekker, Inc., New York, 1997.
41 A. Lienke, G. Klatt, D. J. Robinson, K. R. Koch and K. J. Naidoo, *Inorganic Chemistry*, 2001, **40**, 2352.
42 K. J. Naidoo, G. Klatt, K. R. Koch and D. J. Robinson, *Inorganic Chemistry*, 2002, **41**, 1845.
43 K. J. Naidoo, A. S. Lopis, A. N. Westra, D. J. Robinson and K. R. Koch, *Journal of the American Chemical Society.*, 2003, **125**, 13330.
44 R. K. Harris and B. E. Mann, in *NMR and the Periodic Table*, Academic Press INC., London, 1978.
45 S. M. Cohen and T. H. Brown, *Journal of Chemical Physics*, 1974, **61**, 2985.
46 J. J. Pesek and W. R. Mason, *Journal of Magnetic Resonance*, 1977, **25**, 519.
47 P. S. Pregosin, *Coordination Chemistry Reviews*, 1982, **44**, 247.

Stellenbosch University http://scholar.sun.ac.za

Chapter 2

Reactions of Halogens with Pt(II) Complexes of *N*-alkyl- and *N,N*-dialkyl-*N'*-benzoylthioureas: Oxidative Addition and Formation of an I_2 Inclusion Compound.*

Platinum(II) complexes of *N,N*-diethyl-*N'*-benzoylthiourea and *N,N*-di(*n*-butyl)-*N'*-benzoylthiourea have been treated with I_2, Br_2 or Cl_2 in chloroform, leading to facile oxidative addition of the dihalogens to the platinum center. The oxidative addition reaction can be monitored by ^{195}Pt NMR, which reveals the formation of one major and at least four minor Pt(IV) products in solution. The compounds *cis*-bis(*N,N*-diethyl-*N'*-benzoylthioureato)diiodoplatinum(IV), **26**, and *cis*-bis(*N,N*-diethyl-*N'*-benzoylthioureato)dibromoplatinum(IV), **27**, which are the predominant Pt(IV) products in the respective synthesis solutions, have been isolated and structurally characterized; the chloride analogue could not be isolated. Reaction of *cis-/trans*-bis(*N*-benzoyl-*N'*-propylthiourea-κS)dibromoplatinum(II) with Br_2, similarly results in oxidative addition of the dihalogen; the product *trans*-bis(*N*-benzoyl-*N'*-propylthiourea-κS)tetrabromoplatinum(IV), **29**, was isolated and characterized. Diiodine, however, does not undergo oxidative addition to *cis-/trans*-bis(*N*-benzoyl-*N'*-propylthiourea-κS)diiodoplatinum(II), instead the iodine inclusion compound *trans*-bis(*N*-benzoyl-*N'*-propylthiourea-κS)diiodoplatinum(II) diiodine, **28**, precipitates from solution. Compounds **26**, **27**, and **29** are the first-reported complexes of Pt(IV) with this class of ligand.

* This chapter is based on the papers:
A. N. Westra, C. Esterhuysen, K. R. Koch, *Acta Cryst. C*, 2004, m395-m398.
A. N. Westra, S. A. Bourne, C. Esterhuysen, K. R. Koch, *DaltonTrans.*, 2005, 2162-2172.

UNIVERSITEIT STELLENBOSCH
BIBLIOTEEK

Stellenbosch University http://scholar.sun.ac.za

2.1 Introduction

Ligands of type *N,N*-dialkyl-*N'*-aroyl(acyl)thiourea (**HL^1**; $R^1_2NC(S)NHC(O)R^2$, R^1 = alkyl, R^2 = alkyl or aryl) are known to form stable, neutral coordination compounds with a variety of transition metal ions,[1,2] a number of which have been structurally characterized; for example, Co(III),[3] Ni(II),[4,5] Cu(II),[6] Zn(II),[7] Ru(III),[8] Rh(III),[9,10] Pd(II),[11] Ag(I),[12] Cd(II),[7] Re(I),[13] Pt(II),[10,14] and Hg(II).[15] These ligands show a pronounced affinity for coordination to the platinum group metals (PGMs),[16,17] which allows for their potential application in the solvent extraction, preconcentration, separation and trace determination of the PGMs.[16-22] Koch and co-workers have studied the complexation of **HL^1**, as well as the analogous *N*-alkyl-*N'*-aroyl(acyl)thioureas (**H_2L^2**; $R^1NHC(S)NHC(O)R^2$, R^1 = alkyl, R^2 = alkyl or aryl), to Pd(II), Rh(III) and particularly Pt(II) with the aim of fully understanding the coordination chemistry of these complexes, and with a view to developing practically useful analytical and process chemical applications for these ligands.[10,23]

The molecules **HL^1** and **H_2L^2** are easily synthesised in high yields in a two-step, 'one-pot' procedure,[24] and readily coordinate to Pt(II).[10,25] An intramolecular hydrogen bond between the thiourea RNHC(S)-moiety and the carbonyl *O*-atom in **H_2L^2** generally leads to coordination of such ligands with PtX_4^{2-} (X = I, Br, Cl) *via* the *S*-atom only, resulting in mixtures of *cis*- and *trans*-[Pt^{II}(**H_2L^2-*S***)$_2X_2$] (X = I, Br, Cl).[26] On the other hand, **HL^1** ligands generally coordinate to Pt(II) via both the *S*- and *O*-atoms with loss of a thioamidic proton, forming predominantly *cis*-[Pt^{II}(**L^1-*S,O***)$_2$] complexes, several of which have been structurally characterized,[10,14,27] with only a single authenticated *trans* complex of Pt^{II} having been reported to date.[28] Recently Koch *et al.* discovered that the *cis*-[M(**L^1-*S,O***)$_2$] (M = Pt(II), Pd(II)) complexes undergo photochemically induced *cis-trans* isomerization.[29]

To date, very little is known about the coordination of **HL^1** or **H_2L^2** to Pt(IV); initial attempts to synthesise Pt(IV) complexes of *N,N*-diethyl-*N'*-benzoylthiourea (**HL^{1a}**) directly, by reacting $PtCl_6^{2-}$ with this ligand under various conditions and in various media, resulted in the isolation of predominantly the Pt(II) complex *cis*-bis(*N,N*-diethyl-*N'*-benzoylthioureato)platinum(II) *cis*-[Pt^{II}(**L^{1a}-*S,O***)$_2$], evidently due to redox reactions between Pt(IV) and the ligand. The reduction of Pt(IV) by **HL^{1a}** is not unexpected since several investigations into anti-cancer drugs have revealed that many sulphur-containing biomolecules act as reducing agents, reducing antitumour-active Pt(IV) drugs to their Pt(II) analogues.[30] We have thus explored an alternative strategy to the synthesis of Pt(IV) complexes with these ligands, by means of oxidative addition of molecular halogens to the corresponding Pt(II) complexes. Many square-planar Pt(II) complexes can be oxidised to the octahedral Pt(IV) compounds by addition of I_2, Br_2 or Cl_2.[31,32]

We here report the facile synthesis of the first Pt(IV) complexes of *N,N*-diethyl-*N'*-benzoylthiourea (**HL^{1a}**), *N,N*-di(n-butyl)-*N'*-benzoylthiourea (**HL^{1b}**) and *N*-propyl-*N'*-benzoylthiourea (**H_2L^{2a}**) by direct oxidation of *cis*-[Pt^{II}(**L^{1a}-*S,O***)$_2$] **21** and *cis*-[Pt^{II}(**L^{1b}-*S,O***)$_2$] **22** with I_2 and Br_2, and of *cis*- and *trans*-[Pt^{II}(**H_2L^{2a}-**

Stellenbosch University http://scholar.sun.ac.za

S)$_2$Br$_2$] **24** with Br_2 in organic solvents. Whereas treatment of **21** and **22** with I_2 or Br_2, and **24** with Br_2, leads to simple oxidative addition of the halogens, treatment of *cis*- and *trans*-[Pt^{II}($\mathbf{H_2L^{2a}}$-*S*)$_2$$I_2$] **23** with I_2 does *not* result in oxidative addition, but in the formation of an interesting iodine inclusion compound, *trans*-[Pt^{II}($\mathbf{H_2L^{2a}}$-*S*)$_2$$I_2$]·$I_2$.

2.2 Experimental

2.2.1 Methods and instruments

The ligands *N,N*-diethyl-*N'*-benzoylthiourea ($\mathbf{HL^{1a}}$), *N,N*-di(n-butyl)-*N'*-benzoylthiourea ($\mathbf{HL^{1b}}$), and *N*-propyl-*N'*-benzoylthiourea ($\mathbf{H_2L^{2a}}$) were synthesized and recrystallized according to a method described by Douglass *et al.*[24] The Pt^{II} complexes of $\mathbf{HL^{1a}}$, *cis*-[Pt^{II}($\mathbf{L^{1a}}$-*S,O*)$_2$] **21**, and $\mathbf{HL^{1b}}$, *cis*-[Pt^{II}($\mathbf{L^{1b}}$-*S,O*)$_2$] **22**, and the Pt^{II} complexes of $\mathbf{H_2L^{2a}}$, *cis*-/*trans*-[Pt^{II}($\mathbf{H_2L^{2a}}$-*S*)$_2$$X_2$] (X= I, Br or Cl; **23**, **24**, **25**, respectively), were synthesized, purified and characterized as previously reported.[10,25] All reagents and solvents were commercially available, and all were used without further purification except for the acetone used in ligand synthesis, which was distilled before use.

^{1}H and ^{13}C NMR spectra (25°C) were recorded in chloroform-d using either a Varian INOVA 600 MHz spectrometer operating at 600 or 151 MHz respectively, or a Varian VXR 300 MHz spectrometer operating at 300 or 76 MHz respectively. ^{195}Pt NMR spectra (30°C) were recorded in chloroform-d using the Varian INOVA 600 MHz spectrometer operating at 128 MHz. ^{1}H chemical shifts are quoted relative to the residual $CDCl_3$ solvent resonance at 7.26 ppm, and ^{13}C chemical shifts relative to the $CDCl_3$ triplet. All ^{195}Pt chemical shifts are quoted relative to external H_2PtCl_6 (500 mg ml^{-1} in 30% v/v D_2O/1 M HCl), and are estimated to be accurate to ±2 ppm. Chromatographic analyses were carried out using a Waters 2690 'Alliance' fully automatic HPLC system equipped with automatic sample injection system and a Waters 996 photodiode array detector, using a 4.6 × 150 mm, 5 μm, Zorbax Eclipse XDB-C18 column. All eluents were filtered through a 0.45 μm (Microsep) nitrocellulose membrane and degassed by bubbling helium gas through eluent reservoirs for at least 1 hr prior to use. The column was conditioned with an acetonitrile-aqueous buffer mixture [90:10 (% v/v)], usually at 1 cm^3 min^{-1} for 15-30 min before commencing with sample (20 μl) injections. Acetate buffer of pH ~ 6 was prepared by mixing exactly 25 cm^3 of 0.1 mol dm^{-3} acetic acid with 475 cm^3 of 0.1 mol dm^{-3} sodium acetate solution. UV-vis spectrophotometric experiments were carried out on an Agilent 8453E UV-visible spectrophotometer (Agilent Technologies). Melting points were determined using an Electrothermal IA9000 Digital Melting Point Apparatus. Elemental analyses were performed using a Carlo Erba EA 1108 elemental analyser in the microanalytical laboratory of the University of Cape Town. Thin layer chromatography was performed on Alugram® Sil G/UV_{254} aluminium sheets (Marchery-Nagel).

Stellenbosch University http://scholar.sun.ac.za

2.2.2 Preparative methods and compound characterization

2.2.2.1 trans-Bis(N-benzoyl-N'-propylthiourea-κS)diiodoplatinum(II), trans-[Pt^{II}(H$_2$L^{2a}-S)$_2$I$_2$] 23^{trans}, and trans-bis(N-benzoyl-N'-propylthiourea-κS)dibromoplatinum(II), trans-[Pt^{II}(H$_2$L^{2a}-S)$_2$Br$_2$] 24^{trans} *

^{195}Pt NMR spectra of the product mixtures obtained in the synthesis of **23** (*cis*-/*trans*-[Pt^{II}(**H$_2$L^{2a}-*S***)$_2$I$_2$]) and **24** (*cis*-/*trans*-[Pt^{II}(**H$_2$L^{2a}-*S***)$_2$Br$_2$]), revealed resonances at δ_{Pt} -4846 ppm and -4670 ppm for *trans*- and *cis*-[Pt^{II}(**H$_2$L^{2a}-*S***)$_2$I$_2$], respectively, and at δ_{Pt} -3662 ppm and -3681 ppm for *trans*- and *cis*-[Pt^{II}(**H$_2$L^{2a}-*S***)$_2$Br$_2$], respectively, confirming the presence of both isomers as previously assigned.[25] However, good quality crystals of only the dominant *trans* isomers (**23**^{trans} and **24**^{trans}) could be isolated by recrystallization from chloroform-ethanol; suitable crystals of the *cis* complexes (**23**^{cis} and **24**^{cis}) could not be obtained.

2.2.2.2 cis-Bis(N,N-diethyl-N'-benzoylthioureato)diiodoplatinum(IV), cis-[Pt^{IV}(L^{1a}-S,O)$_2$I$_2$] 26

0.394 mmol (262 mg) of *cis*-[Pt^{II}(**L^{1a}-*S*,*O***)$_2$] **21** was dissolved in 3 cm^3 of chloroform and treated with a stoichiometric 100 mg of solid I_2. Crystals of *cis*-bis(*N,N*-diethyl-*N'*-benzoylthioureato)diiodoplatinum(IV) **26** were obtained by diffusion crystallization with pentane, and analysed. M.p.: 154-157°C. Found: C, 31.4; H, 3.0; N, 6.3; S, 6.8. $C_{24}H_{30}N_4S_2O_2PtI_2$ requires: C, 31.3; H, 3.3; N, 6.1; S, 7.0%. δ_H(600 MHz; solvent $CDCl_3$): 8.25 (4H, d, C_6H_5), 7.52 (2H, t, C_6H_5), 7.44 (4H, t, C_6H_5), 3.93 (4H, q, $2CH_2$), 3.89 (4H, q, $2CH_2$), 1.42 (6H, t, $2CH_3$), 1.38 (6H, t, $2CH_3$). δ_C(151 MHz; solvent $CDCl_3$): 171.23 (C(O)), 167.43 (C(S)), 136.27-128.06 (C_6H_5), 47.54 ($2CH_2$), 46.95 ($2CH_2$), 13.46 ($2CH_3$), 13.26 ($2CH_3$). δ_{Pt}(128 MHz; solvent $CDCl_3$): -2422 (s). TLC (silica gel, $CHCl_3$): R_f = 0.95.

2.2.2.3 cis-Bis(N,N-diethyl-N'-benzoylthioureato)dibromoplatinum(IV), cis-[Pt^{IV}(L^{1a}-S,O)$_2$Br$_2$] 27

0.394 mmol (262 mg) of *cis*-[Pt^{II}(**L^{1a}-*S*,*O***)$_2$] **21** was dissolved in 3 cm^3 of chloroform and treated stoichiometrically with 20.3 µl of Br_2 (3.1 g.ml^{-1}) using a gastight syringe. Crystals of *cis*-bis(*N,N*-diethyl-*N'*-benzoylthioureato)dibromoplatinum(IV) **27** were obtained by diffusion crystallization with pentane, and analysed. M.p.: 177-180°C. Found: C, 35.1; H, 3.4; N, 6.9; S, 7.8. $C_{24}H_{30}N_4S_2O_2PtBr_2$ requires: C, 34.9; H, 3.7; N, 6.8; S, 7.8%. δ_H(600 MHz; solvent $CDCl_3$): 8.27 (4H, d, C_6H_5), 7.53 (2H, t, C_6H_5), 7.43 (4H, t, C_6H_5), 3.92 (4H, q, $2CH_2$), 3.89 (4H, q, $2CH_2$), 1.42 (6H, t, $2CH_3$), 1.36 (6H, t, $2CH_3$). δ_C(151 MHz; solvent $CDCl_3$): 171.17 (C(O)), 166.82 (C(S)), 136.39-128.06 (C_6H_5), 47.80 ($2CH_2$), 46.99 ($2CH_2$), 13.43 ($2CH_3$), 13.17 ($2CH_3$). δ_{Pt}(128 MHz; solvent $CDCl_3$): -1322 (s). TLC (silica gel, $CHCl_3$): R_f = 0.92.

* The crystal structure of *cis*-[Pt^{II}(**H$_2$L^{2a}-*S***)$_2$Cl$_2$] has been previously reported,[19] but our efforts to isolate good quality crystals of *trans*-[Pt^{II}(**H$_2$L^{2a}-*S***)$_2$Cl$_2$] for characterization by X-ray diffraction were unsuccessful. The difficulty in isolating the *trans* isomer most likely arises from the fact that the *cis* complex is predominant in solution (*cis* : *trans* isomer ratio 75 : 25[18]).

Stellenbosch University http://scholar.sun.ac.za

2.2.2.4 trans-Bis(N-benzoyl-N'-propylthiourea-κS)diiodoplatinum(II) diiodine, trans-[$Pt^{II}(H_2L^{2a}$-S)$_2I_2$]·I_2 28

The addition of 28.3 mg of solid I_2 to 0.111 mmol (99.5 mg) of a mixture of *cis*- and *trans*-bis(*N*-benzoyl-*N'*-propylthiourea-κ*S*)diiodoplatinum(II) **23**$^{cis/trans}$ (*cis* : *trans* isomer ratio of 5 : 95[25]) dissolved in 0.7 cm^3 of chloroform, led to the formation of a dark purple precipitate. Careful dissolution of the precipitate in dichloromethane, and diffusion crystallization with pentane, allowed the isolation of crystals of *trans*-bis(*N*-benzoyl-*N'*-propylthiourea-κ*S*)diiodoplatinum(II) diiodine **28**. M.p.: 153-155°C. Found: C, 23.2; H, 2.1; N, 4.9; S, 5.5. $C_{22}H_{28}N_4S_2O_2PtI_4$ requires: C, 23.1; H, 2.5; N, 4.9; S, 5.6%.

2.2.2.5 trans-Bis(N-benzoyl-N'-propylthiourea-κS)tetrabromoplatinum(IV), trans-[$Pt^{IV}(H_2L^{2a}$-S)$_2Br_4$] 29

0.196 mmol (156 mg) of a mixture of *cis*- and *trans*-bis(*N*-benzoyl-*N'*-propylthiourea-κ*S*)dibromoplatinum(II) **24**$^{cis/trans}$ (*cis* : *trans* isomer ratio of 42 : 58[25]) was dissolved in 3 cm^3 of dichloromethane and stoichiometrically treated with 10.1 µl of Br_2 (3.1 $g.ml^{-1}$) using a gastight syringe. Good quality crystals of *trans*-bis(*N*-benzoyl-*N'*-propylthiourea-κ*S*)tetrabromoplatinum(IV) **29** were obtained by slow evaporation from a toluene/dichloromethane solvent mixture. Crystals of *cis*-[Pt^{IV}(**H_2L^{2a}**-*S*)$_2Br_4$] suitable for structure determination could not be obtained. The recrystallized product, a mixture of *cis*- and *trans*- isomers, shows two melting points; m.p.: 183-187 and 196-198°C. Found: C, 27.9; H, 2.6; N, 5.9; S, 7.3. $C_{22}H_{28}N_4S_2O_2PtBr_4$ requires C, 27.6; H, 3.0; N, 5.9; S, 6.7%. δ_H(600 MHz; solvent $CDCl_3$; based on relative peak intensities): 11.65 (1H, s, H(6)), 11.16 (1H, s, H(7)), 8.26 (4H, d, C_6H_5), 7.63 (2H, t, C_6H_5), 7.51 (4H, t, C_6H_5), 3.82 (4H, $2CH_2$), 1.88 (4H, $2CH_2$), 1.10 (6H, $2CH_3$). δ_C(151 MHz; solvent $CDCl_3$; based on relative peak intensities): 174.92 (C(S)), 169.62 (C(O)), 134.63-129.21 (C_6H_5), 48.27 ($2CH_2$), 22.10 ($2CH_2$), 11.56 ($2CH_3$). δ_{Pt}(128 MHz; solvent $CDCl_3$; based on relative peak intensities): -2440 (s).

2.2.3 Crystallography and structure refinement

Suitable crystals were mounted on a thin glass fiber and data were collected either on a Nonius Kappa CCD or Bruker-Nonius SMART Apex diffractometer using graphite monochromated Mo-Kα radiation (λ = 0.7107 Å). The structures were solved using SHELXS-97 and refined using SHELXL-97[33] with the aid of the interface program X-SEED.[34] Peaks of electron density in the Fourier map for compound **27** indicated that one of the ethyl chains in structure B is disordered over two positions. The disorder alternatives are labelled C(11B)-C(12B) and C(11C)-C(12C), and C-C distances have been constrained to reasonable values using the SADI command in SHELXL. In each structure all non-hydrogen atoms were modelled anisotropically, with the exception of C(11C) in compound **27**. Hydrogen atoms involved in hydrogen bonding in structures **23**^{trans} and **24**^{trans}, *i.e.* those attached to nitrogen atoms, were located in a difference electron-density map and refined isotropically. All other hydrogen atoms, in all the structures, were placed in geometrically calculated positions, with C-H = 0.99 (for $-CH_2-$), 0.98 (for $-CH_3$), or 0.95 Å (for phenyl),

Stellenbosch University http://scholar.sun.ac.za

and N-H = 0.88 Å. These were refined using a riding model, with U_{iso}(H) = 1.2U_{eq}(parent) (for $-CH_2-$, phenyl, and N-H) or 1.5U_{eq}(parent) (for $-CH_3$). Crystal structure interpretation was performed with the aid of the programs PLATON[35] and MERCURY.[36] Selected bond lengths and angles for the structures are presented in Tables 2.1 - 2.5, and relevant crystallographic data is shown in Table 2.6.

2.3 Results and Discussion

2.3.1 Oxidative addition of I_2, Br_2 and Cl_2 to cis-[Pt^{II}(L^{1a}-S,O)$_2$] 21 and cis-[Pt^{II}(L^{1b}-S,O)$_2$] 22 by direct treatment with the halogens

^{195}Pt NMR spectroscopic as well as UV-visible spectrophotometric experiments revealed that the oxidative addition reaction is rapid in chloroform, and can readily be monitored by 'titrating' chloroform solutions of *cis*-[Pt^{II}(L^{1a}-*S,O*)$_2$] **21** or *cis*-[Pt^{II}(L^{1b}-*S,O*)$_2$] **22** with appropriate quantities of halogen.

Fig. 2.1 shows the reaction of I_2 with compound **21** as monitored by UV-vis spectrophotometry; the spectra display two isosbestic points, indicating the occurrence of at least two predominant species in solution.

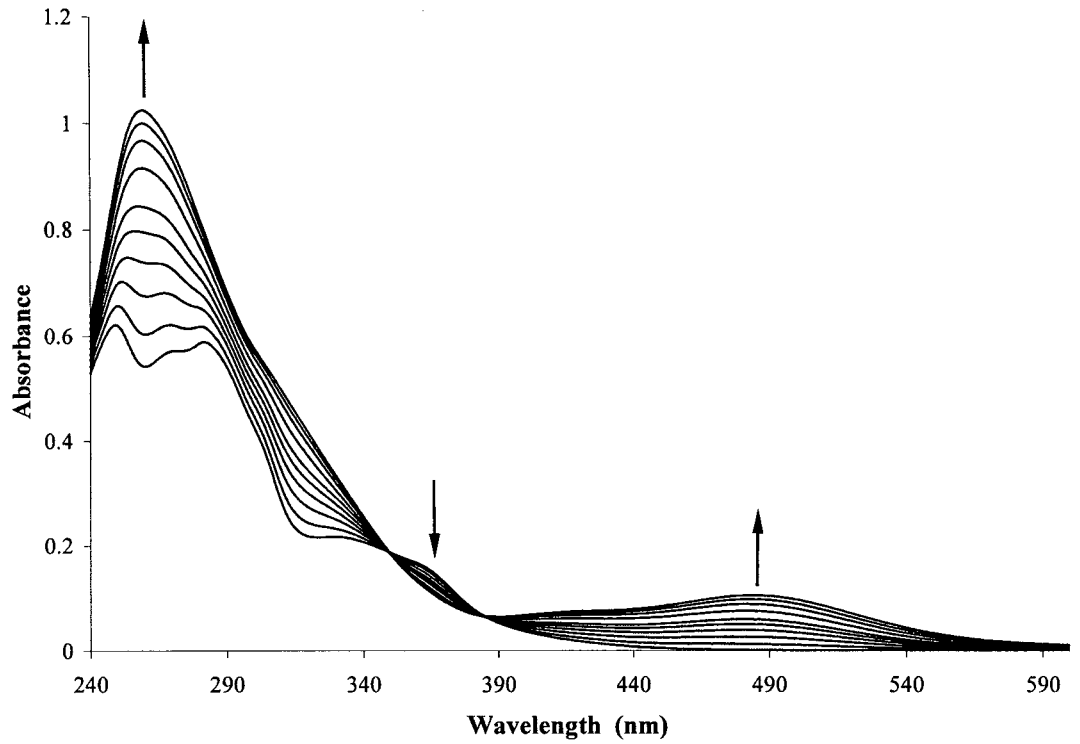

Fig. 2.1 Distribution of UV-visible spectra obtained by 'titration' of *cis*-[Pt^{II}(L^{1a}-*S,O*)$_2$] **21** (9.17×10^{-6} mol in 100 cm^3 $CHCl_3$) with small volumes of 0.15 M I_2 in chloroform, to equimolarity (the arrows indicate changes in absorbance with increase of I_2 added).

Stellenbosch University http://scholar.sun.ac.za

Fig. 2.2 shows the corresponding ^{195}Pt NMR spectra obtained by treatment of *cis*-[Pt^{II}(**L**^{1a}-***S,O***)$_2$] **21** in $CDCl_3$ with small quantities of I_2 (s), up to a mole ratio I_2 : Pt of 1 : 1, directly in an NMR tube at room temperature. Addition of I_2 results in the diminution of the ^{195}Pt NMR peak of complex **21** ($\delta_{Pt\ 21}$ = -2719 ppm), and the appearance of a major and several minor peaks of varying intensities to lower field: δ_{Pt} = -2422 ppm (70 % by relative peak intensity at mole ratio Pt : I_2 of 1 : 1), -2325 ppm (9 %), -2160 ppm (18 %), -2114 ppm (2 %), -2076 ppm (1 %). Similar treatment of compound **22** with a sub-stoichiometric quantity of Br_2 (l), results in the appearance of a comparable distribution of ^{195}Pt resonances (δ_{Pt} = -1320 ppm (82 % by relative product peak intensities), -1230 ppm (6 %), -1087 ppm (9 %), -1037 ppm (2 %), -1005 ppm (1 %)), and diminution of the peak corresponding to complex **22** ($\delta_{Pt\ 22}$ = -2713 ppm). Since generally it is found that ^{195}Pt NMR shifts of Pt(IV) complexes appear significantly more downfield relative to Pt(II) complexes,[37,38] the downfield shift in ^{195}Pt peaks suggests oxidative addition of I_2 or Br_2, resulting in one predominant Pt(IV) species in addition to several minor species in solution.

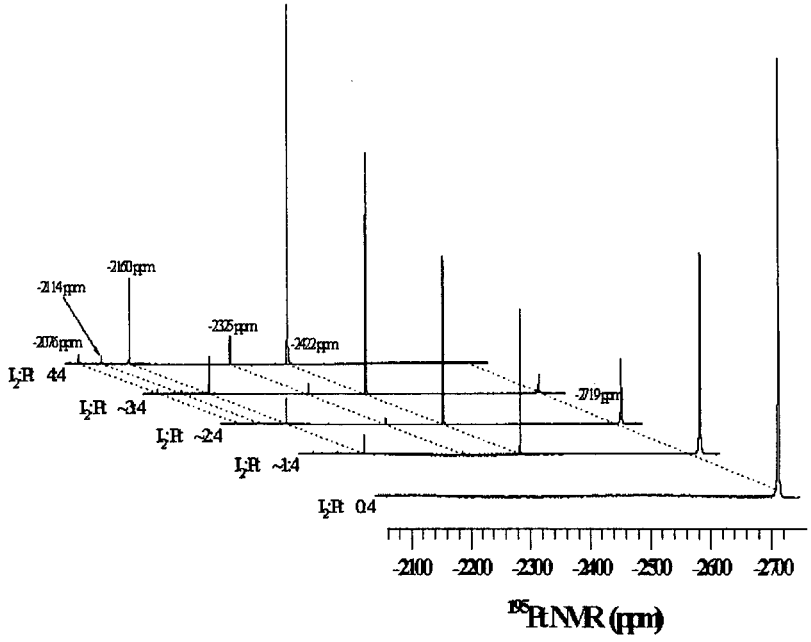

Fig. 2.2 ^{195}Pt NMR spectra obtained by 'titration' of *cis*-[Pt^{II}(**L**^{1a}-***S,O***)$_2$] **21** (9.96×10^{-5} mol in 0.7 cm^3 $CDCl_3$) with small quantities of I_2 to a mole ratio of 1 : 1.

Treatment of **21** in chloroform with stoichiometric quantities of I_2 (s) or Br_2 (l), led to the isolation and characterization by single crystal X-ray diffraction of *cis*-bis(*N,N*-diethyl-*N'*-benzoylthioureato)diiodoplatinum(IV), **26** (Fig. 2.3), and *cis*-bis(*N,N*-diethyl-*N'*-benzoylthioureato)dibromoplatinum(IV), **27** (Fig. 2.4), respectively, confirming the expected oxidative addition of the halogens to Pt(II) in **21**. Complexes **26** and **27** are to our knowledge, the first authenticated Pt(IV) complexes with *N,N*-dialkyl-*N'*-aroyl(acyl)thiourea ligands.

Stellenbosch University http://scholar.sun.ac.za

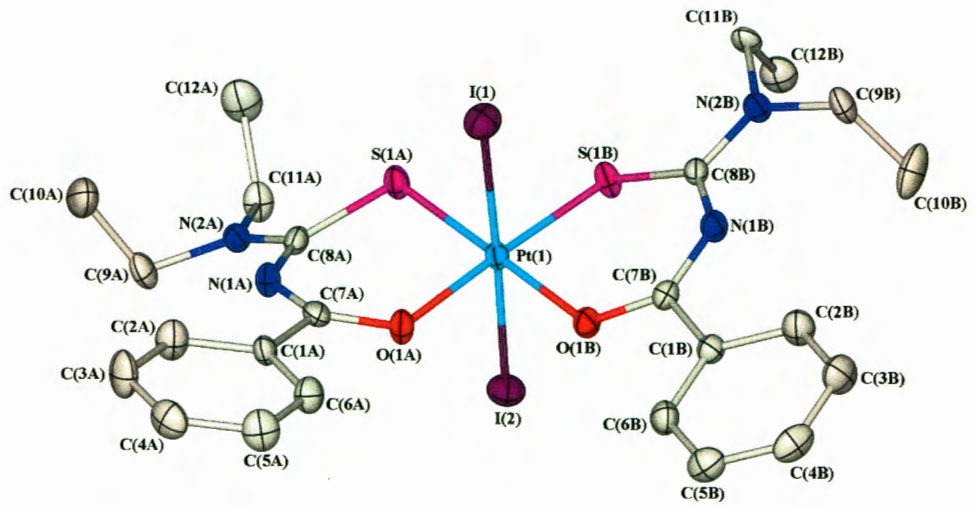

Fig. 2.3 The molecular structure of *cis*-bis(*N,N*-diethyl-*N'*-benzoylthioureato)diiodoplatinum(IV) **26** with atom numbering scheme. Displacement ellipsoids are drawn at the 50 % probability level and H atoms have been omitted for clarity. Selected bond lengths and angles are given in Table 2.1.

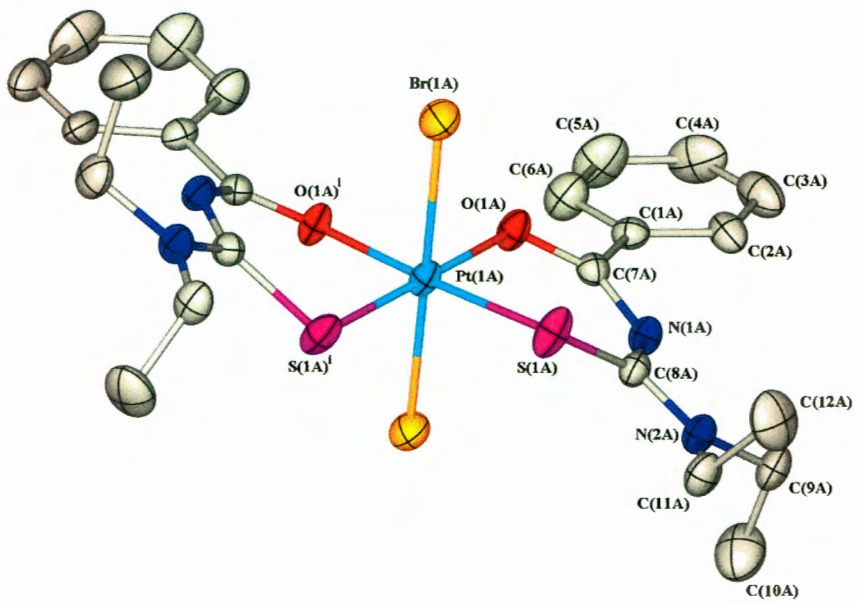

Fig. 2.4 Compound **27**, *cis*-bis(*N,N*-diethyl-*N'*-benzoylthioureato)dibromoplatinum(IV), crystallizes with two independent half molecules (denoted A and B) in the asymmetric unit; component A is shown with atom numbering scheme. Displacement ellipsoids are drawn at the 50 % probability level and H atoms have been omitted for clarity. Symmetry code: (i) 1-x, y, 3/2-z. Selected bond lengths and angles are given in Table 2.1.

Stellenbosch University http://scholar.sun.ac.za

Preliminary investigations of acetonitrile solutions of **21** treated with sub-stoichiometric quantities of I_2 and analysed by reversed-phase high performance liquid chromatography (RP-HPLC), showed that the product species formed elute in fairly rapid succession well before **21**, but appear chromatographically separable under the conditions of the experiment. A peak in the chromatograms with a retention time of 14.4 min is assignable to the Pt(II) starting compound **21**.[29,39] A peak at 3.1 min is assigned to the dominant oxidative addition product **26**, based on relative peak intensities, and at least three further minor peaks with retention times of 1.3 min, 2.6 min and 7.0 min are also evident. The minor products are most probably isomers of the isolated *cis*-bis(*N,N*-diethyl-*N'*-benzoylthioureato)diiodoplatinum(IV) **26**.

Attempts to isolate well defined single oxidative addition products by direct treatment of **21** (*cis*-[Pt^{II}(**L^{1a}-*S,O*)$_2$]) or **22** (*cis*-[Pt^{II}(**L^{1b}-*S,O*)$_2$]) with Cl_2 were unsuccessful, partly due to the difficulty in controlling the reaction with gaseous chlorine. Experiments in which Cl_2 (g) was bubbled through solutions of **21** in chloroform for several minutes resulted in mixtures from which droplets containing $PtCl_6^{2-}$ separated, indicating destructive oxidation of **21** which is not surprising in view of the higher oxidative strength of Cl_2. Efforts at more controlled addition of Cl_2 (g) to chloroform solutions of **22**, yielded solutions of which the ^{195}Pt NMR show a five-peak distribution (as was observed for the addition of I_2 and Br_2 to these complexes) in the range -500 to -1000 ppm: δ_{Pt} = -923 ppm (4.8 % by relative product peak intensities), -704 ppm (77.0 %), -617 ppm (6.5 %), -557 ppm (7.4 %), -513 ppm (4.3 %); a peak corresponding to **22** was still evident in the spectra, but controlling the Cl_2 addition to a stoichiometric **22** : Cl_2 ratio of 1 : 1 was found to be very difficult. The ^{195}Pt NMR results nevertheless suggest the formation of several Pt(IV)-chloro complexes. Cl_2 oxidative addition to **22** was also monitored by spectrophotometric experiments in which UV-vis spectra were recorded after repeatedly running a controlled number of Cl_2 (g) bubbles through a solution of *cis*-[Pt^{II}(**L^{1b}-*S,O*)$_2$] **22** in chloroform. A distribution of spectra very similar to that shown in Fig. 2.1 was obtained, indicating reaction of the halogen with the Pt(II) center. Unfortunately, good quality crystals of Pt(IV)-chloro oxidative addition products could not be isolated from any of the reaction mixtures.

2.3.2 Crystal and molecular structure of cis-bis(N,N-diethyl-N'-benzoylthioureato)diiodoplatinum(IV) 26

The crystal structure of **26** (Fig. 2.3) shows that in the dominant product (confirmed by ^{195}Pt NMR) of oxidative addition of I_2 to **21**, the thiourea ligands (**L^{1a}**) remain coordinated in a *cis-S,O* fashion to the Pt(IV) centre, with the iodide ligands *trans* in the octahedral complex. The Pt-I bond lengths (2.674(1)/2.676(1) Å) and the I-Pt-I bond angle (178.2(1)°), presented in Table 2.1, compare well with values reported for the Pt(IV) complex *trans*-Pt(acac)$_2$I$_2$ (acac = acetylacetonate) in which the iodide ligands are similarly coordinated axially to the planar Pt(acac)$_2$ moiety (Pt-I, 2.667(1) Å; I-Pt-I, 180.0°).[40]

Stellenbosch University http://scholar.sun.ac.za

A particularly interesting feature of complex **26**, is the short intermolecular I···I contact between adjacent molecules as a result of their alignment in the crystal lattice (shown in Fig. 2.5). The molecules pack such that their I-Pt-I axes are essentially parallel, but slightly off-centre relative to each other (Pt(1)-I(2)···I(1^{ii}), 163.75(1)°; symmetry code: (ii) x-1, y, z), with intermolecular distances between nearest-neighbour iodide ligands of 3.553(1) Å. These intermolecular I···I distances are considerably shorter than the sum of the van der Waals radii for two iodine atoms (4.20 Å[41]), and are only slightly longer than the range of distances (3.3 to 3.5 Å) found for covalent bond formation in poly-iodide anions.[42,43] These intermolecular interactions seem to be only slightly 'weaker' than those in crystalline I_2, for which intermolecular I···I distances are 3.496(6) Å.[44] Octahedral *trans*-Pt(IV)-iodo compounds with intermolecular I···I distances shorter than twice the van der Waals radius of iodine have been reported; for example in *trans*-Pt(acetylacetonate)$_2$I$_2$,[40] [*cis*-Pt(ethylamine)I$_4$],[45] and [Pt(*o*-diaminobenzene)I$_3$].[46] In these compounds, the intermolecular I···I distances lie in the range 3.48-3.56 Å.

In compound **26**, the Pt-S bond lengths (2.283(1)/2.281(1) Å) and the Pt-O bond lengths (2.058(2)/2.055(3) Å) are longer than in the platinum(II) complex **21** (Pt-S: 2.231(2)/2.233(2) Å; Pt-O: 2.018(5)/2.023(6) Å).[14] The Pt(IV) complexes might be expected to have shorter Pt-S and Pt-O bond lengths, but the observed elongation of these bonds can probably be ascribed to the presence of the bulky

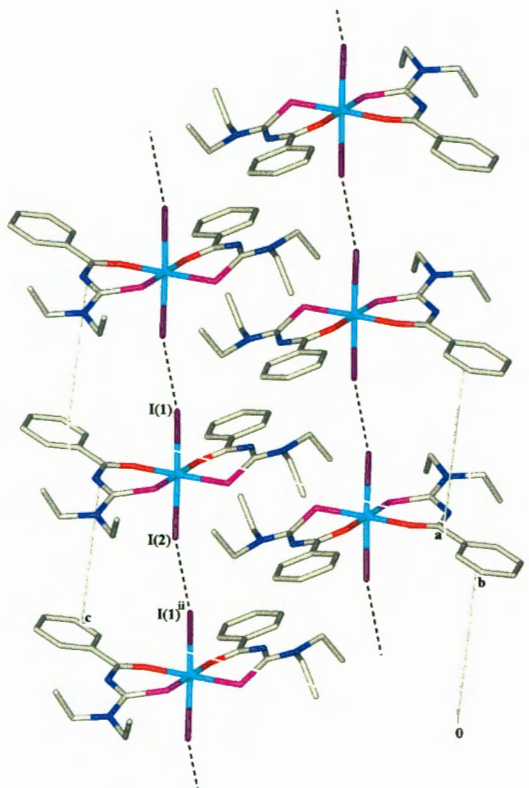

Fig. 2.5 Molecules in the crystal structure of **26** pack with unusually short nearest neighbour iodide distances (I(2)···I(I^{ii}), 3.553(1) Å; symmetry code: (ii) x-1, y, z) suggesting intermolecular I···I interactions in the solid. Molecules are shown in wireframe style for clarity; H atoms have been omitted. The unit cell is also shown.

Stellenbosch University http://scholar.sun.ac.za

iodide ligands in the octahedral coordination sphere. Complex **26** crystallizes in a $P\bar{1}$ space group. The atoms Pt(1)/S(1A)/O(1A)/S(1B)/O(1B) lie in a plane (a maximum deviation of 0.003(1) Å from a least-squares plane through these atoms is calculated for O(1B)), but the two ligands coordinated to the metal centre do not lie in this coordination plane. Ligand B is twisted significantly out of the $Pt^{IV}S_2O_2$ plane, while ligand A is twisted through the coordination plane with the ethyl end-groups below and the phenyl group above the plane. The chains of weakly connected molecules, which result from the intermolecular I···I interactions, pack such that adjacent chains appear to slot into one another with molecules inverted, the phenyl groups of one chain overlaying amine *N*-atoms of an adjacent chain, and *vice versa* (this can be seen in Fig. 2.5).

2.3.3 Crystal and molecular structure of cis-bis(N,N-diethyl-N'-benzoylthioureato)dibromoplatinum(IV) 27

The major product of the oxidative addition of Br_2 to **21** crystallizes in the *C2/c* space group with two independent half molecules, denoted A and B, in the asymmetric unit. In both structures A and B the thiourea ligands (L^{1a}) remain *cis-S,O* coordinated to the metal centre, with the bromide ligands *trans* in the resulting complex (component A is shown in Fig. 2.4). A two-fold axis of symmetry lies in the coordination plane, through the metal centre and between the thiourea ligands in A and B. The Pt-Br bond lengths (2.460(1)/2.462(1) Å) and Br-Pt-Br bond angles (177.4(1)/178.1(1)°), presented in Table 2.1, compare well with corresponding values for *trans*-$Pt(acac)_2Br_2$ (acac = acetylacetonate; Pt-Br, 2.451(2) Å; Br-Pt-Br, 180.0°).[47]

Table 2.1 Selected bond lengths (Å) and angles (°) for compounds **26** and **27**.

	26		**27**	
	Ligand A	**Ligand B**	**Structure A**	**Structure B**
Pt(1)-S(1)	2.283(1)	2.281(1)	2.280(1)	2.280(1)
S(1)-C(8)	1.737(4)	1.742(4)	1.744(4)	1.745(4)
C(8)-N(1)	1.345(4)	1.340(4)	1.347(4)	1.346(4)
N(1)-C(7)	1.307(5)	1.325(4)	1.316(4)	1.313(4)
C(7)-O(1)	1.277(4)	1.276(5)	1.283(4)	1.269(4)
O(1)-Pt(1)	2.058(2)	2.055(3)	2.044(2)	2.043(3)
C(8)-N(2)	1.334(5)	1.324(4)	1.329(4)	1.339(4)
Pt(1)-S(1)-C(8)	104.1(1)	104.6(1)	103.3(1)	104.8(1)
S(1)-C(8)-N(1)	127.0(3)	128.1(3)	128.5(3)	130.1(3)
C(8)-N(1)-C(7)	128.1(3)	128.8(4)	126.6(3)	128.0(3)
N(1)-C(7)-O(1)	129.9(4)	130.3(4)	131.0(3)	130.8(3)
C(7)-O(1)-Pt(1)	125.4(2)	126.2(2)	125.1(2)	127.4(2)
N(1)-C(8)-N(2)	115.8(3)	115.1(4)	115.7(3)	115.2(3)
O(1)-Pt(1)-S(1)	95.56(8)	93.24(8)	91.89(7)	94.73(8)

26				
Pt(1)-I(1)	**Pt(1)-I(2)**	**I(1)-Pt(1)-I(2)**	**S(1A)-Pt(1)-O(1B)**	**O(1A)-Pt(1)-I(1)**
2.676(1)	2.674(1)	178.2(1)	179.5(1)	87.83(8)
O(1B)-Pt(1)-I(1)	**S(1A)-Pt(1)-I(1)**	**S(1B)-Pt(1)-I(1)**		
89.80(8)	90.31(4)	92.06(4)		
27				
Pt(1A)-Br(1A)	**Pt(1B)-Br(1B)**	**Br(1A)-Pt(1A)-Br(1A^{ii})**	**Br(1B)-Pt(1B)-Br(1B^{ii})**	**S(1A)-Pt(1A)-O(1A^{ii})**
2.460(1)	2.462(1)	177.4(1)	178.1(1)	177.3(1)
S(1B)-Pt(1B)-O(1B^{ii})	**O(1A)-Pt(1A)-Br(1A)**	**O(1B)-Pt(1B)-Br(1B)**	**S(1A)-Pt(1A)-Br(1A)**	**S(1B)-Pt(1B)-Br(1B)**
177.3(1)	89.11(8)	88.55(9)	92.65(3)	90.56(4)

Symmetry codes: (ii) 1-x, y, 3/2-z.

Stellenbosch University http://scholar.sun.ac.za

The coordinating atoms Pt(1)/S(1)/O(1)/S(1^{i})/O(1^{i}) (symmetry code: (i) 1-x, y, 3/2-z) in both structures A and B are planar, with maximum deviations from these plane of 0.033(2) Å for O(1) in A and 0.012(2) Å for O(1) in B. The ethyl end-groups extend from, and the phenyl groups are bent or twisted out of planes defined by the atoms S(1)/C(8)/N(2)/N(1)/C(7)/O(1). The chelating ligands are, however, twisted significantly out of the Pt(1)/S(1)/O(1)/S(1^{i})/O(1^{i}) coordination planes, giving the structures distinctly puckered shapes when viewed side-on along the two-fold axes, as illustrated in Fig. 2.4. This puckering is more pronounced for one of the molecules in the asymmetric unit than for the other. The angle between least squares planes through the coordinating *S*- and *O*-atoms (coordination plane), and the atoms S(1)/C(8)/N(2)/N(1)/C(7)/O(1) (ligand plane) is 33.78(14)° for structure A (Fig. 2.4) and 18.80(10)° for structure B. The two molecules are orientated at 65.68(7)° with respect to each other and appear to slot into one another along the two-fold axes.

The Pt-S bond lengths in **26** and **27** are very similar (2.283(1)/2.281(1) Å and 2.280(1)/2.280(1) Å, respectively), but longer than in **21** (2.231(2)/2.233(2) Å[14]), while the Pt-O bond lengths for **21**, **26**, and **27** are respectively 2.018(5)/2.023(6) Å, 2.058(2)/2.055(3) Å, and 2.044(2)/2.043(3) Å.[14] One of the ethyl chains in structure B is disordered over two positions; the alternative chains are labelled C(11B)-C(12B) (sof refined to 74 %) and C(11C)-C(12C) (sof refined to 26 %). There are no other significant intermolecular contacts in this structure.

2.3.4 Treatment of cis-/trans-[Pt^{II}(H_2L^{2a}-S)$_2I_2$] 23 with I_2, cis-/trans-[Pt^{II}(H_2L^{2a}-S)$_2Br_2$] 24 with Br_2 and cis-/trans-[Pt^{II}(H_2L^{2a}-S)$_2Cl_2$] 25 with Cl_2

The invariable UV-visible spectra obtained by 'titration' with I_2 of **23** (*cis*-/*trans*-bis(*N*-benzoyl-*N'*-propylthiourea-κ*S*)diiodoplatinum(II) mixture, *cis* : *trans* isomer ratio 5 : 95[25]) in chloroform at room temperature, suggested that **23** is apparently *not* oxidized by I_2 to any significant extent under these conditions. 'Titration' experiments with higher reagent concentrations, examined by ^{195}Pt NMR spectroscopy (δ_{Pt}(*cis*-[Pt^{II}(**H_2L^{2a}-*S***)$_2I_2$]) = -4693 ppm, δ_{Pt}(*trans*-[Pt^{II}(**H_2L^{2a}-*S***)$_2I_2$]) = -4870 ppm[25]), resulted in a dark precipitate forming during the 'titration' prior to its completion, although careful examination of the ^{195}Pt spectrum did indicate the emergence of two very low intensity peaks at -4934 ppm and -5082 ppm with the addition of increasing quantities of I_2. Oxidative addition of I_2 to **23** might be expected to result in only *cis*-[Pt^{IV}(**H_2L^{2a}-*S***)$_2I_4$] and *trans*-[Pt^{IV}(**H_2L^{2a}-*S***)$_2I_4$] in solution, so that it is tempting to assign the two small ^{195}Pt peaks to these complexes. The ^{195}Pt chemical shift of Pt(IV) species might however be expected somewhat downfield of the corresponding Pt(II) complexes,[38] so that unambiguous assignment of the low intensity peaks at -4934 ppm and -5082 ppm has not yet been possible. Interestingly, careful recrystallization of the precipitate formed during the I_2 'titration' allowed the isolation and characterization of compound **28** which is actually an I_2 inclusion compound of *trans*-[Pt^{II}(**H_2L^{2a}-*S***)$_2I_2$], as determined by X-ray diffraction (Fig. 2.6).

Stellenbosch University http://scholar.sun.ac.za

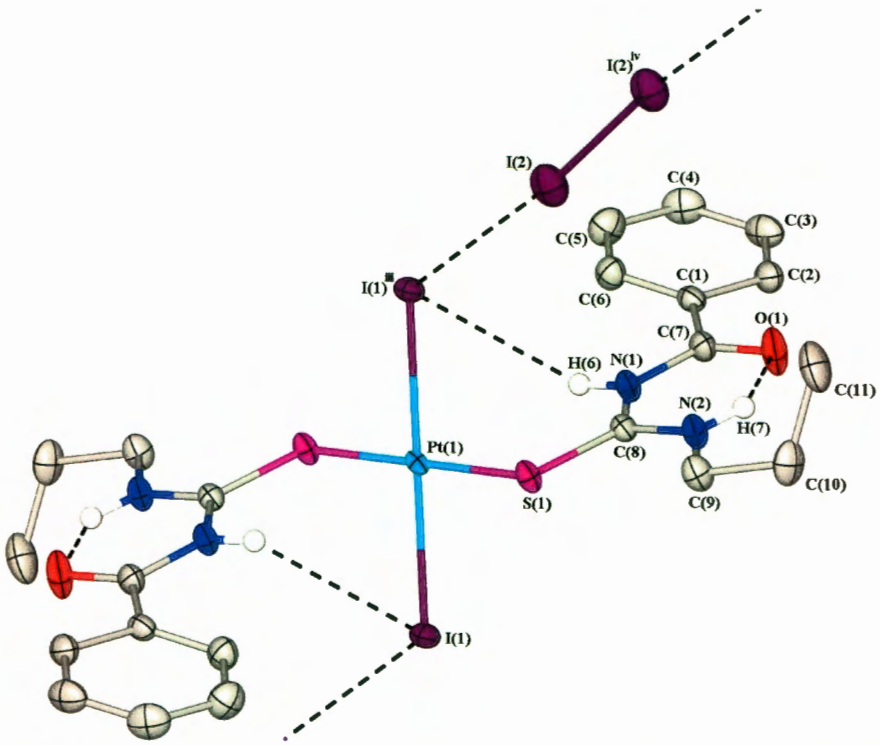

Fig. 2.6 Molecular structure of *trans*-bis(*N*-benzoyl-*N'*-propylthiourea-κ*S*)diiodoplatinum(II) diiodine **28**, with atom numbering scheme. Displacement ellipsoids are drawn at the 50 % probability level; H(6) and H(7) are shown as small spheres of arbitrary radius, and the H atoms not involved in hydrogen bonding have been omitted for clarity. Molecular iodine is included in the structure at short nearest-neighbour I(1^{iii})···I(2) distances (3.453(1) Å; symmetry code: (iii) 1-x, 1-y, -z; (iv) 2-x, 2-y, -z), indicative of intermolecular I···I interaction. Selected bond lengths and angles are given in Tables 2.4 and 2.5.

A survey of the literature shows that treatment of Pt(II) compounds with I_2 need not necessarily always lead to oxidative addition. Reactions of platinum(II) complexes of, for example, Group 15 donor ligands with iodine can give Pt(IV)-iodides (e.g. [Pt(4,7-Ph_2phenanthroline)I_4],[48] and [*cis*-Pt(ethylamine)I_4] [45]), but may also leave the metal centre un-oxidised (leading reportedly to Pt(II) poly-iodides as in the case of [Pt(1,2-dimethylimidazole)$_4$](I_3)$_2$ [49]).

Treatment of **24** (*cis*-/*trans*-bis(*N*-benzoyl-*N'*-propylthiourea-κ*S*)dibromoplatinum(II) mixture, *cis* : *trans* isomer ratio 42 : 58[25]) in chloroform with a stoichiometric quantity of Br_2 (l), results, in contrast to the formation of **28** above, in oxidative addition of the halogen and formation of compound **29**, *trans*-bis(*N*-benzoyl-*N'*-propylthiourea-κ*S*)tetrabromoplatinum(IV), as shown in Fig. 2.7. A ^{195}Pt NMR spectrum of the pre-recrystallization mixture shows two peaks, one major signal at -2440 ppm, assigned to **29** based on relative resonance intensities, and one at -2426 ppm, most likely due to *cis*-bis(*N*-benzoyl-*N'*-propylthiourea-κ*S*)tetrabromoplatinum(IV). If this assignment is correct, the ^{195}Pt chemical shift of *trans*-[Pt^{IV}(H_2L^2-*S*)$_2$$Br_4$] occurs upfield to that of the *cis* isomer. This is in contrast to the relative shift positions of the Pt(II) precursors (δ_{Pt}(*cis*-[Pt^{II}(H_2L^{2a}-*S*)$_2$$Br_2$]) = -3693 ppm, δ_{Pt}(*trans*-[Pt^{II}(H_2L^{2a}-*S*)$_2$$Br_2$]) = -3678

Stellenbosch University http://scholar.sun.ac.za

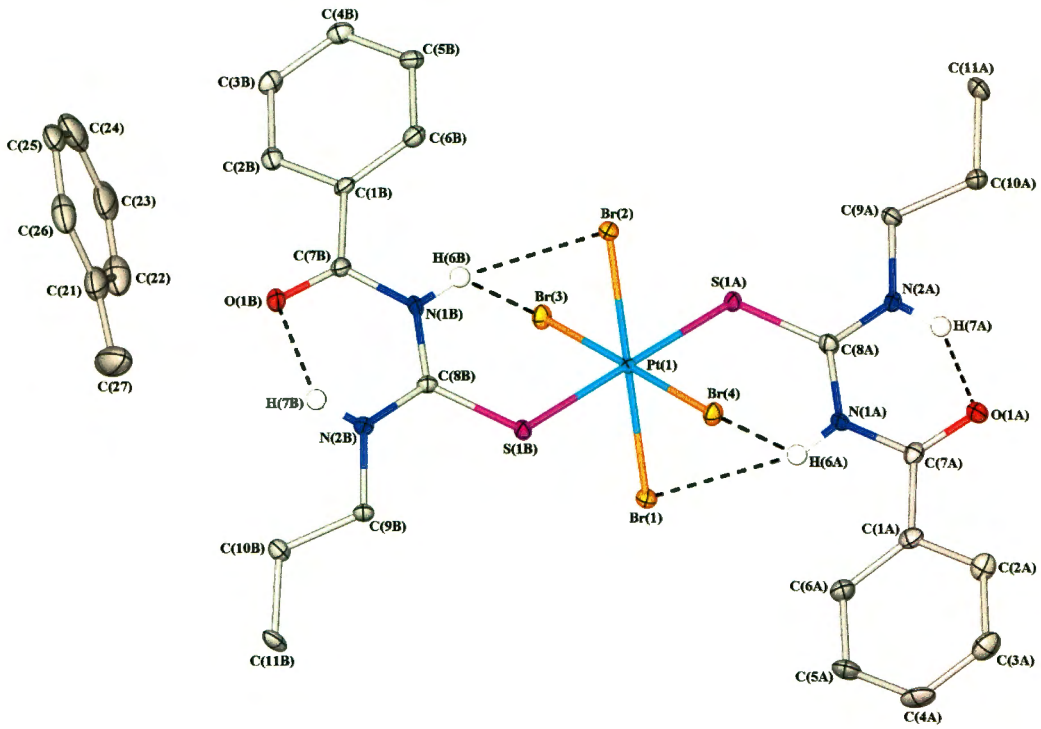

Fig. 2.7 Molecular structure of *trans*-bis(*N*-benzoyl-*N'*-propylthiourea-κ*S*)tetrabromoplatinum(IV) **29**, with atom numbering scheme. Displacement ellipsoids are drawn at the 50 % probability level; H(6A), H(7A), H(6B) and H(7B) are shown as small spheres of arbitrary radius, and the H atoms not involved in hydrogen bonding have been omitted for clarity. One toluene solvent guest molecule per *trans*-[Pt^{IV}(**H_2L^{2a}-*S***)$_2Br_4$] molecule was located in the model refinement. Selected bond lengths and angles are given in Table 2.4. N-H···O and N-H···Br intramolecular hydrogen bonding is illustrated, with details given in Table 2.5.

ppm[25]), but is consistent with the results obtained for [Pt^{IV}(**L^{1a}-*S,O***)$_2X_2$] (X = I, Br) in the present study in which the shifts for the *trans*-halide isomers appear farthest upfield in the distribution of Pt(IV) product peaks. Crystals of *cis*-[Pt^{IV}(**H_2L^{2a}-*S***)$_2Br_4$] suitable for structure determination, could not be obtained.

Efforts to isolate single products from the oxidative addition of Cl_2 to **25** (*cis-/trans*-bis(*N*-benzoyl-*N'*-propylthiourea-κ*S*)dichloroplatinum(II) mixture, *cis* : *trans* isomer ratio 75 : 25[25]) were unsuccessful, as had been found in the attempts with *cis*-[Pt^{II}(**L^{1a}-*S,O***)$_2$] **21** and *cis*-[Pt^{II}(**L^{1b}-S,O**)$_2$] **22** (Section 2.3.1), despite repeated experiments.

The Pt^{II} complexes of **H_2L^{2a}**, *cis-/trans*-[Pt^{II}(**H_2L^{2a}-*S***)$_2X_2$] (X= I, Br or Cl; **23**, **24**, **25**, respectively) have been previously synthesized and characterised,[25] but the crystal structure of only *cis*-bis(*N*-benzoyl-*N'*-propylthiourea-κ*S*)dichloroplatinum(II) has been reported.[26] To allow detailed crystallographic description of the compounds *trans*-bis(*N*-benzoyl-*N'*-propylthiourea-κ*S*)diiodoplatinum(II) diiodine **28** and *trans*-bis(*N*-benzoyl-*N'*-propylthiourea-κ*S*)tetrabromoplatinum(IV) **29**, the platinum precursor complexes from which **28** and **29** were prepared, *viz.* *trans*-bis(*N*-benzoyl-*N'*-propylthiourea-κ*S*)diiodoplatinum(II) **23**^{trans}

Stellenbosch University http://scholar.sun.ac.za

(Fig. 2.8) and *trans*-bis(*N*-benzoyl-*N'*-propylthiourea-κ*S*)dibromoplatinum(II) **24**^{trans} (Fig. 2.9), respectively, were first isolated and structurally characterized. The crystal and molecular structures of **23**^{trans} and **24**^{trans} are described below, followed by the crystallographic characterization of compounds **28** and **29**.

2.3.5 Crystal and molecular structures of trans-bis(N-benzoyl-N'-propylthiourea-κS)diiodoplatinum(II) 23^{trans}, and trans-bis(N-benzoyl-N'-propylthiourea-κS)dibromoplatinum(II) 24^{trans}

Both compounds **23**^{trans} and **24**^{trans} crystallize in space group $P\bar{1}$ with the Pt(II) ion located on an inversion center, but they are not isomorphous. Because of the inversion symmetry, both PtS_2X_2 (X = I, Br) moieties are strictly planar.

The molecular structures of **23**^{trans} (Fig. 2.8) and **24**^{trans} (Fig. 2.9) reveal that, despite the potentially bidentate nature of the ligand (*N*-propyl-*N'*-benzoylthiourea, $\mathbf{H_2L^{2a}}$), only the sulphur atom coordinates to the metal, while the carbonyl oxygen atom is locked into an O-C-N-C-N-H ring by means of an intramolecular N(2)-H(7)···O(1) hydrogen bond (Table 2.3), similar to that in the previously reported compounds *cis*-dichlorobis(*N*-propyl-*N'*-benzoylthiourea)platinum(II)[26] and *trans*-dibromobis(*N*-propyl-*N'*-benzoylthiourea)palladium(II).[25] The six-membered O(1)-C(7)-N(1)-C(8)-N(2)-H(7) rings in both structures are virtually planar, with a maximum deviation from planarity of 0.013(4) Å for atom N(1) in **23**^{trans} and of 0.05(2) Å for atom H(7) in **24**^{trans}.

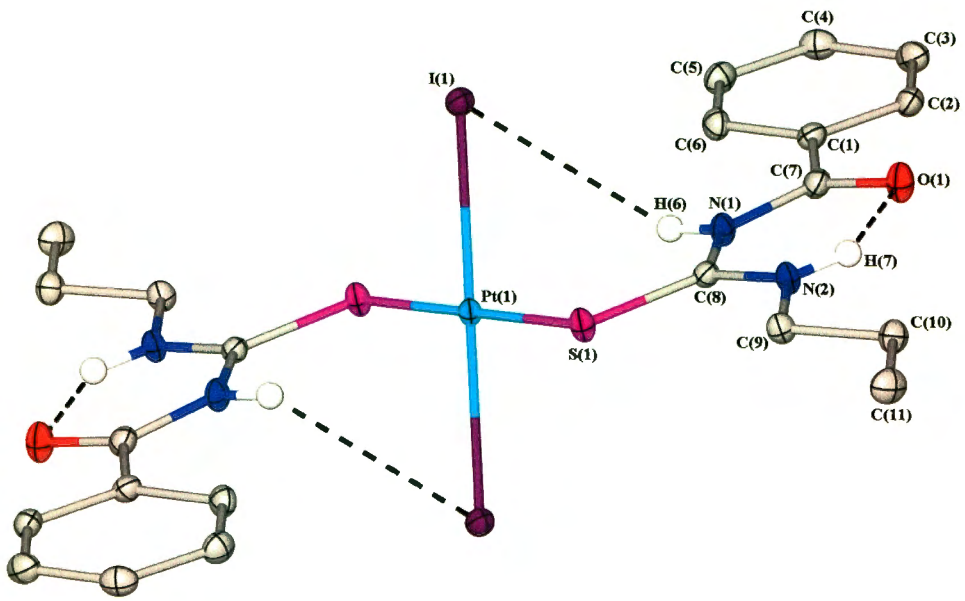

Fig. 2.8 The molecular structure of *trans*-bis(*N*-benzoyl-*N'*-propylthiourea-κ*S*)diiodoplatinum(II) **23**^{trans}, with atom numbering scheme. Displacement ellipsoids are drawn at the 50 % probability level; H(6) and H(7) are shown as small spheres of arbitrary radius, and the H atoms not involved in hydrogen bonding have been omitted for clarity. Selected bond lengths and angles are presented in Tables 2.2 and 2.3.

Stellenbosch University http://scholar.sun.ac.za

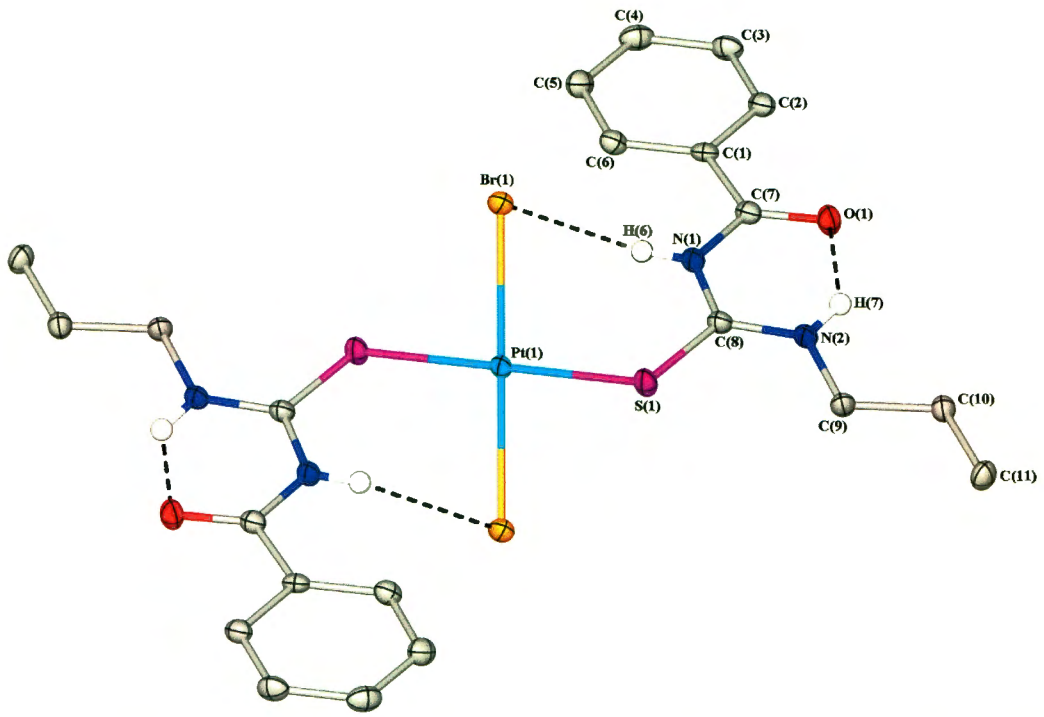

Fig. 2.9 The molecular structure of *trans*-bis(*N*-benzoyl-*N'*-propylthiourea-κ*S*)dibromoplatinum(II) **24**^{trans}, with atom numbering scheme. Displacement ellipsoids are drawn at the 50 % probability level; H(6) and H(7) are shown as small spheres of arbitrary radius, and the H atoms not involved in hydrogen bonding have been omitted for clarity. Selected bond lengths and angles are presented in Tables 2.2 and 2.3.

The Pt-I and Pt-S bond lengths for **23**^{trans} (2.617(1) Å and 2.315(1) Å), respectively) compare well with the corresponding distances in the previously reported *trans*-Pt(II) complexes of *S*-donor ligands and iodide, $[Pt\{C_2H_5NHC(S)OC_2H_5\}_2I_2]$ (Pt-I, 2.610(2) Å; Pt-S, 2.314(4) Å),[50] $[Pt\{(CH_3)_2S\}_2I_2]$ (Pt-I, 2.604(1) Å; Pt-S, 2.310(2) Å)[51] and $[Pt\{(C_4H_9)_2NC(S)NHC(O)Ph\}_2I_2]$ (Pt-I, 2.608(2) Å; Pt-S, 2.294(3) Å).[52] The Pt-Br and Pt-S bond distances in **24**^{trans} (2.441(1) Å and 2.305(1) Å, respectively) are somewhat longer than the corresponding distances in *trans*-dibromobis(1,4-oxathian)platinum(II) (Pt-Br, 2.420(1) Å; Pt-S, 2.281(3) Å).[53] The latter is the only *trans*-Pt(II) complex of *S*-donor ligands and Br^- reported in the CSD.

The torsion angles in Table 2.2 illustrate that there is no distortion of the thiourea ligands in compounds **23**^{trans} and **24**^{trans}. The atoms of the central carbonyl-thiourea moieties, O(1)/C(7)/N(1)/C(8)/S(1)/N(2), are nearly planar, with deviations of less than 0.04 Å for **23**^{trans} and **24**^{trans}. The carbonyl-thiourea moiety (O(1)/C(7)/N(1)/C(8)/S(1)/N(2)) in **23**^{trans} is tilted at an angle of 68.96(3)° to the coordination plane, while the corresponding angle in **24**^{trans} is 54.17(7)°. These angles allow for the relatively short interatomic distances of 3.600(2) Å between atoms N(1) and I(1) in **23**^{trans}, and 3.290(3) Å between atoms N(1) and

Stellenbosch University http://scholar.sun.ac.za

Br(1) in **24**^{trans}. The sums of the van der Waals radii for the N···I and N···Br contacts are *ca.* 3.65 and 3.45 Å, respectively,[41] so the corresponding distances in **23**^{trans} and **24**^{trans} indicate intramolecular N(1)-H(6)···I(1) and N(1)-H(6)···Br(1) hydrogen bonds (Table 2.3). Such interactions also account for the distortions of the coordination spheres of the Pt^{II} centers from ideal square-planar geometry, leading to angles slightly larger than 90° for the S(1)-Pt(1)-I(1) (92.03(2)°) and S(1)-Pt(1)-Br(1) (94.43(3)°).

The intramolecular N-H···O hydrogen bond in **23**^{trans} and **24**^{trans} is also observed in the free ligand *N*-propyl-*N'*-benzoylthiourea, $\mathbf{H_2L^{2a}}$.[54] Analogous intramolecular N-H···O interactions are a common phenomenon in related molecules which, as in $\mathbf{H_2L^{2a}}$, feature a central carbonyl-thiourea moiety –NHC(S)NHC(O)–; examples include molecules such as *N*-(*n*-butyl)-*N'*-benzoylthiourea,[55] *N*-(2-pyridyl)-*N'*-benzoylthiourea,[56] *N*-benzoylthiourea,[57] *N*-(*p*-bromophenyl)-*N'*-benzoylthiourea,[58] 3-(3-benzoylthioureido)propionic acid,[59] *N*-benzoyl-*N'*-(2-hydroxyethyl)thiourea,[60] and *N*-ethoxycarbonyl-*N'*-phenylthiourea.[61]

Thus, for the $\mathbf{H_2L^{2a}}$ ligand, the relatively stable six-membered O-C-N-C-N-H hydrogen-bonded ring persists upon coordination to 'softer' transition metal ions, without the loss of an H-atom. This is confirmed by the observations on **23**^{trans} and **24**^{trans} in the present study, and can be seen in several related structures, *e.g.* $[\{Cu[PhNHC(S)NHC(O)C_3H_5]_2Cl\}_2]$,[62] $[Rh\{C_3H_7NHC(S)NHC(O)Ph\}(C_8H_{12})Cl]$,[63] *trans*-$[Pd\{C_3H_7NHC(S)NHC(O)Ph\}_2Br_2]$,[25] $[\{Cu[C_5NH_4NHC(S)NHC(O)Ph]Cl_2\}_2]$,[64] and $[Cu\{CH_3PhNHC(S)NHC(O)OC_2H_5\}_2Cl]$.[65]

Table 2.2 Selected bond lengths (Å) and angles (°) for compounds **23**^{trans} and **24**^{trans}.

	23^{trans}	**24**^{trans}
Pt(1)-S(1)	2.315(1)	2.305(1)
S(1)-C(8)	1.701(2)	1.702(4)
C(8)-N(1)	1.380(3)	1.372(4)
N(1)-C(7)	1.377(3)	1.389(5)
C(7)-O(1)	1.226(3)	1.220(4)
C(8)-N(2)	1.314(3)	1.313(4)
Pt(1)-I(1)	2.617(1)	
Pt(1)-Br(1)		2.441(1)
Pt(1)-S(1)-C(8)	108.10(8)	113.44(13)
S(1)-C(8)-N(2)	120.49(18)	119.2(3)
C(8)-N(1)-C(7)	127.3(2)	125.9(3)
N(1)-C(7)-O(1)	121.4(2)	121.5(5)
N(1)-C(8)-N(2)	118.8(2)	119.0(3)
S(1)-Pt(1)-I(1)	92.03(2)	
I(1)-Pt(1)-I(1^{v})	180.0	
S(1)-Pt(1)-Br(1)		94.43(3)
Br(1)-Pt(1)-Br(1^{vi})		180.0
C(2)-C(1)-C(7)-N(1)	172.2(2)	179.6(3)
C(7)-N(1)-C(8)-N(2)	2.1(4)	4.3(5)
C(7)-N(1)-C(8)-S(1)	-178.4(2)	-175.3(3)
C(8)-N(2)-C(9)-C(10)	-170.2(2)	174.5(3)

Symmetry codes: (v) 1-x, -y, -z; (vi) 1-x, 1-y, 1-z.

Stellenbosch University http://scholar.sun.ac.za

Table 2.3 Hydrogen-bonding geometry (Å, °) for compounds **23**^{trans} and **24**^{trans}.

	Donor-H···Acceptor	Donor-H	H···Acceptor	Donor···Acceptor	Donor-H···Acceptor
23^{trans}	N(2)-H(7)···O(1)	0.84(3)	1.98(3)	2.639(3)	134(2)
	N(1)-H(6)···I(1)	0.80(3)	3.06(3)	3.600(2)	127(2)
24^{trans}	N(2)-H(7)···O(1)	0.83(5)	1.95(5)	2.603(4)	135(4)
	N(1)-H(6)···Br(1)	0.78(5)	2.62(5)	3.290(3)	145(4)

2.3.6 Crystal and molecular structure of the inclusion compound trans-bis(N-benzoyl-N'-propylthiourea-κS)diiodoplatinum(II) diiodine 28

The crystal structure of *trans*-bis(*N*-benzoyl-*N'*-propylthiourea-κ*S*)diiodoplatinum(II) diiodine (*trans*-[Pt^{II}(**H$_2$L^{2a}**-*S*)$_2$I$_2$]·I$_2$) reveals that the *trans*-[Pt^{II}(**H$_2$L^{2a}**-*S*)$_2$I$_2$] molecules alternate with I$_2$ molecules diagonally to the *a*-,*b*-axes, in the *ab*-plane (Fig. 2.10). Nearest-neighbour I(1^{iii})···I(2) distances at 3.453(1) Å are considerably shorter than the sum of the van der Waals radii for two iodine atoms (4.20 Å[41]), and connote the occurrence of intermolecular I···I interactions in the structure, resulting in infinite zigzag chains of weakly linked *trans*-[Pt^{II}(**H$_2$L^{2a}**-*S*)$_2$I$_2$]···I$_2$ groups. Moreover, interatomic distances of 3.771(1) Å are found between iodide ligands of *trans*-[Pt^{II}(**H$_2$L^{2a}**-*S*)$_2$I$_2$] molecules in adjacent chains (I(1)···I(1^{vii});

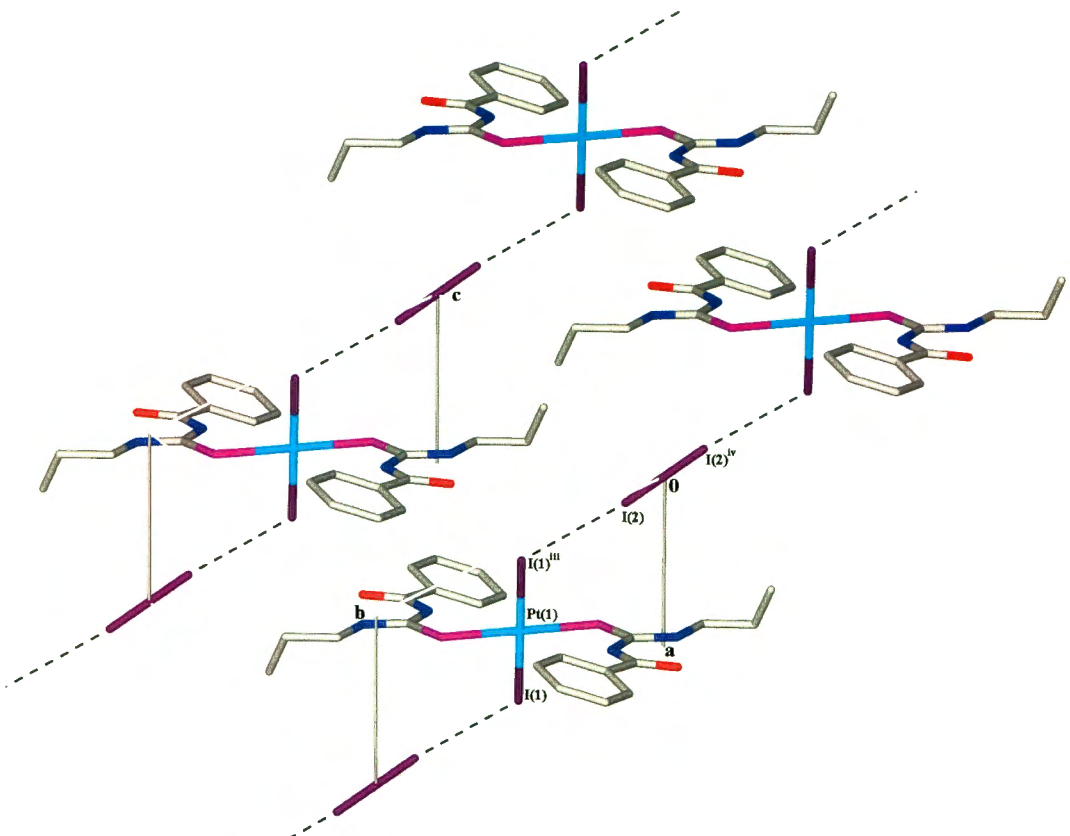

Fig. 2.10 In compound **28** molecules of *trans*-[Pt^{II}(**H$_2$L^{2a}**-*S*)$_2$I$_2$] alternate with I$_2$ diagonally to the *a*- and *b*-axes in the *ab*-plane (the unit cell is shown), leading to infinite zigzag chains of weakly linked *trans*-[Pt^{II}(**H$_2$L^{2a}**-*S*)$_2$I$_2$]···I$_2$ groups. Molecules are shown in wireframe style for clarity; H atoms have been omitted.

Stellenbosch University http://scholar.sun.ac.za

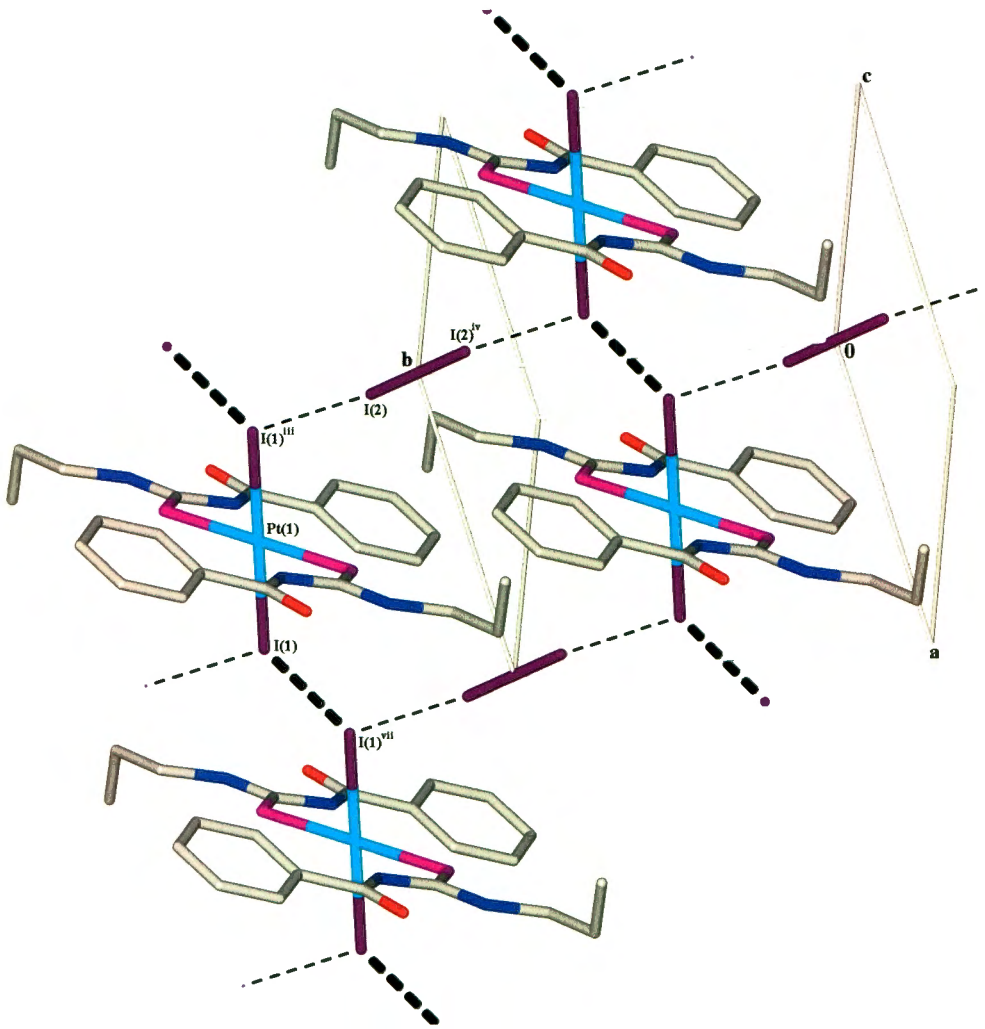

Fig. 2.11 Distances between iodide ligands of *trans*-[Pt^{II}(**H$_2$L^{2a}-*S***)$_2$I$_2$] molecules in adjacent chains (bold fragmented bonds, I(1)···I(1^{vii}), 3.771(1) Å; symmetry code: (vii) 2-x, 1-y, -z) indicate the occurrence of intermolecular I···I interactions which connect the *trans*-[Pt^{II}(**H$_2$L^{2a}-*S***)$_2$I$_2$]···I$_2$ chains into sheets of weakly linked molecules. Molecules are shown in wireframe style for clarity; H atoms have been omitted. The unit cell is shown.

symmetry code: (vii) 2-x, 2-y, -z; Fig. 2.11); these distances indicate the possible occurrence of further intermolecular I···I interactions in the structure, connecting the chains to form sheets, or layers, of weakly linked molecules.

The product crystallizes in a $P\bar{1}$ space group with the Pt(II) ion located at an inversion centre, which ensures that the coordinated PtS_2I_2 moiety is strictly planar. The potentially bidentate thiourea ligands in **28** remain bound to Pt(II) *via* the sulphur atom only, with the carbonyl *O*-atom locked into a six-membered O-C-N-C-N-H ring by means of an intramolecular N(2)-H(7)···O(1) hydrogen bond (Fig. 2.6, Table 2.5), similar to that observed for *trans*-bis(*N*-benzoyl-*N'*-propylthiourea-*κS*)diiodoplatinum(II) **23**^{trans}. The maximum deviation from a least-squares plane through the carbonyl-thiourea atoms

Stellenbosch University http://scholar.sun.ac.za

N(2)/C(8)/S(1)/N(1)/C(7)/O(1) in **28** is 0.057(2) Å for O(1), while the maximum deviation from a plane through the -NC(S)NC(O)-moiety in pure *trans*-[Pt^{II}(**H_2L^{2a}-*S***)$_2I_2$] is 0.013(2) Å for the carbonyl carbon. The torsion angles of -16.4(4)° for N(1)-C(7)-C(1)-C(6) and -63.1(4)° for N(2)-C(9)-C(10)-C(11) in the *trans*-[Pt^{II}(**H_2L^{2a}-*S***)$_2I_2$] molecule of **28** illustrate that the thiourea ligands are more distorted in **28** than those in **23**^{trans}, for which the corresponding torsion angles are -8.4(4)° and -178.4(4)° respectively. The central carbonyl-thiourea moiety (N(2)/C(8)/S(1)/N(1)/C(7)/O(1)) in compound **28** is tilted at an angle of 68.03(6)° to the PtS_2I_2 coordination plane. This angle allows for the interatomic distance between N(1) and I(1^{iii}) of 3.652(3) Å (symmetry code: (iii) 1-x, 1-y, -z), a distance which is practically identical to the sum of the van der Waals radii for N···I contact (*ca.* 3.65 Å[41]) suggesting possible weak intramolecular N(1)-H(6)···I(1^{iii}) hydrogen bonding (Table 2.5). The increased steric hindrance which results from the tilted thiourea ligand, leads to the enlargement of the S(1)-Pt(1)-I(1^{iii}) angle to 92.68(3)°, leaving the Pt(II) centre with a slightly distorted square-planar coordination geometry. Similar N-H···I interactions were also observed in **23**^{trans}. The Pt-I bond distance (2.597(1) Å) and the Pt-S bond distance (2.308(1) Å) in **28** (Table 2.4) are only slightly shorter than the corresponding distances in *trans*-bis(*N*-benzoyl-*N'*-propylthiourea-κS)diiodoplatinum(II) (2.617(1) Å and 2.315(1) Å, respectively; Table 2.2), and are also comparable to those determined for *trans*-bis(*N,N*-di(*n*-butyl)-*N'*-benzoylthiourea)diiodoplatinum(II) (2.608(2) Å and 2.294(3) Å respectively).[52]

Iodine inclusion compounds with Pt-iodide complexes, which lead to arrays of four iodine atoms in the structure (Pt-**I···I-I···I**-Pt) similar to **28**, have been reported (e.g., [Pt^{IV}(1,10-phenanthroline)I_4·I_2], [(Pt^{IV}(1,10-phenanthroline)I_4)$_2$·I_2],[66] and [Pt^{III}_2(Me_2CHCS)$_4I_2$·I_2][67]). In fact the I_4 array is a common feature in several metal iodide-iodine structures,[43] but *trans*-[Pt^{II}(**H_2L^{2a}-*S***)$_2I_2$]·I_2 is, to our knowledge, the first of such structures reported for Pt(II).[68] In the previously reported Pt structures,[66,67] the I_4-arrays are linear or slightly bent, with the distance between 'inner' iodine atoms (**I-I**, 2.739-2.759 Å) somewhat longer than that found in crystalline iodine (2.715(6) Å[44]) and the 'outer' distances (**I···I**, 3.288-3.518 Å) in a range which suggest weaker I···I interactions. The elongation of the central I-I bond occurs as a result of donation of electron density from the iodide ligands into the I_2 LUMO, an antibonding σ^* orbital, leading to net bond order decrease.[69] The 'inner' distance in the symmetrical, slightly bent I_4-array of **28** (I(2)-I(2^{iv}), 2.768(1) Å; I(1^{iii})···I(2)-I(2^{iv}), 174.49(2)°; symmetry code: (iii) 1-x, 1-y, -z, (iv) 2-x, 2-y, -z) is just longer than that found in the reported structures, while the 'outer' distances (I(1^{iii})···I(2), 3.453(1) Å) lie within the range of previously reported values.[66,67]

The I_4-array in metal iodide-iodine structures has sometimes alternatively been considered to be a poly-iodide (I_4^{2-}); for example in [Pt(1,10-phenanthroline)I_4·I_2],[66] [Cu($C_9H_{13}N_5$)I_2·I_2],[70] [Pd(*cis*-$Ph_2PCHCHPPh_2$)I_4],[71] and [$(NH_4)_2$[(AuI_4)(AuI_2(μ_2-I_4))]].[72] Svensson *et al.*[43] however caution that in these cases, the characterization of the array as an I_4^{2-} ion is questionable and that the notation is only a formal one, since the terminal iodides of the I_4-arrays in metal iodide-iodine structures are more weakly

Stellenbosch University http://scholar.sun.ac.za

bound than in 'pure' tetraiodides (e.g. in $[Ni\{(CH_3)_2SO\}_6][I_4]$[73] and $[V(MeCN)_6][I_4]$[74]), and should thus more appropriately be seen as a part of the metal ion complex. Deplano *et al.*[69] have proposed an empirical criterion to determine whether or not iodine atom arrays in structures may be considered as discrete polyiodide entities; the 'building blocks' of the iodine arrays are accepted to be I^- ions and/or I_3^- ions with I_2 molecules. The criterion is based on the value of the bond order (n) of an I_2 'building block' in the array. The bond order, n, is calculated as a function of the I_2 bond lengthening, which results from the donor-acceptor interactions between the I^- (and/or I_3^-) and I_2 'building blocks', using the equation: $d = d_o - c \log n$ (where d and d_o are the I-I bond distances in coordinated, or interacting, and free I_2 respectively, and c is an empirical constant, 0.85 Å). For values of $n > 0.6$, the arrays are considered non-discrete, weakly interacting adducts of I^- (and/or I_3^-) and I_2, but if $n \sim 0.5$ the iodine atoms in the array may be described as being covalently bonded to give discrete poly-iodide entities. The bond order for the 'inner' bond in the I_4-array of **28** (I(2)-I(2^{iv})) is 0.75 (d = 2.768 Å; bond distance of I_2 in the gas phase, *i.e.* d_o, is 2.662 Å[75]), and hence the array cannot be described as a discrete I_4^{2-} polyanion. Instead, the 4-atom iodine array should be seen as arising from van der Waals interactions between iodide ligands of *trans*-$[Pt^{II}(\mathbf{H_2L^{2a}}\text{-}S)_2I_2]$ and I_2 molecules, leading to the zigzag $^1{}_\infty[\cdots I\text{-}I\cdots I\text{-}Pt\text{-}I\cdots I\text{-}I\cdots]$ chains[43] in the solid form of compound **28**.

Table 2.4 Selected bond lengths (Å) and angles (°) for compounds **28** and **29**.

	28	**29**	
		Ligand A	**Ligand B**
Pt(1)-S(1)	2.308(1)	2.378(1)	2.372(1)
S(1)-C(8)	1.700(3)	1.722(4)	1.721(4)
C(8)-N(1)	1.381(3)	1.366(4)	1.373(5)
N(1)-C(7)	1.387(3)	1.395(5)	1.390(5)
C(7)-O(1)	1.222(3)	1.221(5)	1.229(4)
C(8)-N(2)	1.315(3)	1.313(5)	1.310(5)
Pt(1)-S(1)-C(8)	111.1(1)	114.4(1)	115.2(1)
S(1)-C(8)-N(1)	121.9(2)	122.5(3)	122.9(3)
C(8)-N(1)-C(7)	126.2(2)	126.0(3)	127.0(3)
N(1)-C(7)-O(1)	121.1(3)	120.9(3)	120.8(3)
N(1)-C(8)-N(2)	118.8(2)	119.0(3)	118.6(3)
28			
Pt(1)-I(1)	**I(1)-Pt(1)-I(1^{iii})**	**I(1^{iii})···I(2)**	**I(2)-I(2^{iv})**
2.597(1)	180	3.453(1)	2.768(1)
29			
Pt(1)-Br(1)	**Pt(1)-Br(2)**	**Pt(1)-Br(3)**	**Pt(1)-Br(4)**
2.468(1)	2.472(1)	2.467(1)	2.477(1)
Br(3)-Pt(1)-Br(4)	**S(1A)-Pt(1)-S(1B)**	**Br(1)-Pt(1)-S(1A)**	**Br(4)-Pt(1)-S(1A)**
179.6(1)	179.5(3)	91.59(3)	98.29(3)
Br(3)-Pt(1)-S(1B)	**Br(2)-Pt(1)-Br(3)**	**Br(1)-Pt(1)-Br(4)**	
97.86(3)	90.84(2)	91.09(2)	
Br(1)-Pt(1)-Br(2)	**Br(2)-Pt(1)-S(1B)**		
179.7(1)	92.24(3)		

Symmetry codes: (iii) 1-x, 1-y, -z; (iv) 2-x, 2-y, -z.

Stellenbosch University http://scholar.sun.ac.za

Table 2.5 Hydrogen-bonding geometry (Å, °) for compounds **28** and **29**.

	Donor-H···Acceptor	Donor-H	H···Acceptor	Donor···Acceptor	Donor-H···Acceptor
28	**N(2)-H(7)···O(1)**	0.88	1.92	2.608(3)	133.5
	N(1)-H(6)···I(1^{iii})	0.88	3.11	3.652(3)	122.3
29	**N(2A)-H(7A)···O(1A)**	0.88	2.003	2.635(4)	127.6
	N(2B)-H(7B)···O(1B)	0.88	1.934	2.622(4)	133.9
	N(1A)-H(6A)···Br(1)	0.88	2.638	3.500(3)	153.8
	N(1A)-H(6A)···Br(4)	0.88	2.854	3.199(3)	105.2
	N(1B)-H(6B)···Br(2)	0.88	2.635	3.418(3)	148.1
	N(1B)-H(6B)···Br(3)	0.88	2.763	3.258(3)	117.0
	N(2A)-H(7A)···O(1B^{ix})	0.88	2.522	3.272(4)	143.6

Symmetry codes: (iii) 1-x, 1-y, -z; (ix) x-1/2, 1/2-y, 1/2+z.

2.3.7 Crystal and molecular structure of trans-bis(N-benzoyl-N'-propylthiourea-κS)tetrabromoplatinum(IV) 29

The octahedral six-coordinate environment of the Pt centre in compound **29** (Fig. 2.7, see Table 2.4) confirms oxidative addition of bromine to *trans*-[Pt^{II}(**H$_2$L^{2a}-*S***)$_2$Br$_2$] **24^{trans}**. Recrystallization from a toluene/dichloromethane mixture, led to inclusion of one toluene solvent guest molecule per *trans*-[Pt^{IV}(**H$_2$L^{2a}-*S***)$_2$Br$_4$] molecule. This product crystallizes in a $P2_1/n$ space group, with an inversion centre at the origin of the chosen unit cell.

The four bromide ligands and the Pt(IV) centre lie in a plane (a maximum deviation of only 0.007(1) Å is calculated for Br(3) and Br(4)), with Pt-Br bond distances varying only slightly in the range 2.467-2.477 Å. These distances are only slightly longer than the Pt-Br bond lengths in *cis*-[Pt^{IV}(**L^{1a}-*S,O***)$_2$Br$_2$] **27** (see Table 2.1), but are longer than the Pt-Br distances in *trans*-bis(*N*-benzoyl-*N'*-propylthiourea-κ*S*)dibromoplatinum(II) (*trans*-[Pt^{II}(**H$_2$L^{2a}-*S***)$_2$Br$_2$] **24^{trans}**; Pt-Br, 2.441(1) Å; Table 2.2) despite the higher oxidation state of the platinum ion in **29**, possibly as a result of the steric requirements in the octahedral coordination sphere. The Pt-S bond distances in **29** (Pt(1)-S(1A), 2.378(1) Å; Pt(1)-S(1B), 2.372(1) Å) are also considerably longer than those in *trans*-[Pt^{II}(**H$_2$L^{2a}-*S***)$_2$Br$_2$] **24^{trans}** (Pt-S, 2.305(1) Å). In both compounds **29** and **24^{trans}** the thiourea ligands are monodentately *S*-bound to the metal, resulting in longer Pt-S bond lengths than in *cis*-[Pt^{IV}(**L^{1a}-*S,O***)$_2$Br$_2$] **27**, which has the thiourea ligands chelated *via S*- and *O*-atoms. The intramolecular N-H···O hydrogen bonds (propylamine side) observed in *trans*-bis(*N*-benzoyl-*N'*-propylthiourea-κ*S*)dibromoplatinum(II), are also evident in the thiourea ligands of *trans*-[Pt^{IV}(**H$_2$L^{2a}-*S***)$_2$Br$_4$] (N(2A)-H(7A)···O(1A) and N(2B)-H(7B)···O(1B); Table 2.5); these interactions lock the carbonyl oxygen atoms into six-membered O-C-N-C-N-H rings, thereby resulting in the monodentate *S*-coordination of the ligands. The two *S*-donor ligands however assume different conformations (denoted A and B in Fig. 2.7) in the Pt(IV) compound **29**, and are more distorted than in the Pt(II) complex in which

Stellenbosch University http://scholar.sun.ac.za

the two thiourea ligands are related by an inversion centre located at the Pt(II) ion. The N(2A)/C(8A)/S(1A)/N(1A)/C(7A)/O(1A) moiety of ligand A in **29** is tilted at an angle of 63.96(6)° to the Pt(1)/S(1A)/Br(1)/S(1B)/Br(2) coordination plane (maximum deviation from the coordination plane is 0.003(1) Å for Br(1)), which results in interatomic N(1A)···Br(1) and N(1A)···Br(4) distances of 3.500(3) Å and 3.199(3) Å respectively (Table 2.5). The central carbonyl-thiourea moiety of ligand B is tilted at 55.63(6)° to the coordination plane, leading to N(1B)···Br(2) and N(1B)···Br(3) distances of 3.418(3) Å and 3.258(3) Å respectively (Table 2.5). All these N···Br distances are shorter than, or practically identical to, the sum of the van der Waals radii for N···Br contact (3.45 Å[41]). This suggests that the N(1A)-H(6A) group in ligand A acts as a donor for intramolecular hydrogen bonds to Br(1) and Br(4), and that the N(1B)-H(6B) group in ligand B similarly acts as hydrogen bond donor to Br(2) and Br(3) (Table 2.5). Such interactions account for the distortions from ideal octahedral geometry, leading to the larger than 90° bond angles for the coordination sphere of the Pt(IV) centre (see Table 2.4).

In crystals of compound **29**, molecules of *trans*-bis(*N*-benzoyl-*N'*-propylthiourea-κS)tetrabromoplatinum(IV) may be paired, with molecules of a pair oriented with their Br(1) atoms pointing toward each other (the orientations are related by an inversion centre). Furthermore, the pairs of molecules can have two different orientations with the orientations related by a two-fold screw axis or an n-glide plane normal to the *b*-axis. The Br(1)-Pt(1)-Br(2) axes of a pair of molecules (Br(1)-Pt(1)-Br(2) 179.7(1)°) are essentially parallel but slightly off-centre (Pt(1)-Br(1)···Br(1^{viii}) 170.6(1)°; symmetry code: (viii) –x, 1-y, 1-z), with nearest-neighbour Br(1)···Br(1^{viii}) distances of 3.396(1) Å. This intermolecular Br(1)···Br(1^{viii}) distance is considerably shorter than twice the van der Waals radius of bromine (3.90 Å[41]), and suggests the possible occurrence of Br···Br intermolecular interactions between molecules of a pair. Moreover, intermolecular N(2A)-H(7A)···O($1B^{ix}$) hydrogen bonds (symmetry code: (ix) x-½, ½-y, ½+z; Table 2.5) exist between adjacent molecules which have orientations related by the n-glide plane normal to the *b*-axis, resulting in a complicated network of intermolecular Br(1)···Br(1^{viii}) and N(2A)-H(7A)···O($1B^{ix}$) interactions in the solid. A search in the Cambridge Structural Database[68] revealed that only a limited number of Pt(IV)-bromo complexes with intermolecular Br···Br distances shorter than twice the van der Waals radius of bromine have been synthesized and structurally characterized; examples are [Pt(2-pyridyldiphenylphosphineoxide)Br_4],[76] [*trans*-Pt(acetylacetonate)$_2Br_2$],[47] [Pt(ethylenediamine)Br_4].[77] In these complexes the intermolecular Br···Br distances lie in the range of 3.46-3.54 Å.

2.4 Concluding Remarks

The treatment of *cis*-[Pt^{II}($\mathbf{L^{1a/b}}$-***S,O***)$_2$] complexes of *N,N*-diethyl- ($\mathbf{HL^{1a}}$) and *N,N*-di(n-butyl)-*N'*-benzoylthiourea ($\mathbf{HL^{1b}}$) with I_2 or Br_2 in chloroform, leads to rapid oxidative addition to yield several geometric isomers of [Pt^{IV}(**L-*S,O***)$_2X_2$] (X=I, Br); the reactions can be monitored by ^{195}Pt NMR and UV-

Stellenbosch University http://scholar.sun.ac.za

visible spectrophotometry. Mechanistically the oxidative addition is possibly initiated by an end-on interaction of X_2 (X=Cl, Br, I) with the metal centre;[32] a useful model for this initial stage of oxidative addition of molecular halogens to transition metal centres is given by the isolated η^1-I_2 Pt(II) adduct formed by the reaction of I_2 with [PtI(C_6H_3{CH_2NMe_2}$_2$-2,6)].[78] The X-X bond is presumably cleaved in an S_N2-type process, forming a cationic five-coordinate Pt(IV) intermediate and X^-, followed by attack of the anion to produce a neutral Pt(IV)(X_2) product, and subsequent isomerization.

The products *cis*-[Pt^{IV}(**L^{1a}-*S,O***)$_2I_2$] **26** and *cis*-[Pt^{IV}(**L^{1a}-*S,O***)$_2Br_2$] **27**, which have been isolated and structurally characterized, are the first-reported crystal structures of complexes of Pt(IV) with this class of ligand. Molecules of **26** pack such that I-Pt-I axes are essentially aligned, with unusually close nearest-neighbour iodide contacts (3.553(1) Å). These short I···I intermolecular interactions lead to infinite chains of weakly connected molecules in crystals of the compound. No such interactions are evident in the corresponding crystals of **27**. Reaction of the Pt(II) complex of *N*-propyl-*N'*-benzoylthiourea (**H_2L^{2a}**) *cis*-/*trans*-[Pt^{II}(**H_2L^{2a}-*S***)$_2Br_2$] with Br_2 also results in oxidative addition, to yield *trans*-Pt^{IV}(**H_2L^2-*S***)$_2Br_4$ **29**. By contrast, treatment of *cis*-/*trans*-[Pt^{II}(**H_2L^{2a}-*S***)$_2I_2$] with I_2 does not lead to an oxidative addition product, yielding instead an interesting iodine inclusion compound of Pt^{II}, *trans*-[Pt^{II}(**H_2L^{2a}-*S***)$_2I_2$]·I_2 **28**. In **28**, short intermolecular I···I distances of 3.453(1) Å between I_2 and coordinated iodide ions in *trans*-[Pt^{II}(**H_2L^{2a}-*S***)$_2I_2$] molecules, result in infinite chains of weakly linked *trans*-[Pt^{II}(**H_2L^{2a}-*S***)$_2I_2$]···I_2 groups in the lattice. However, the empirically estimated bond order of 0.75 for the included I_2 molecules does not support the possible existence of discrete tetraiodide ions (I_4^{2-}) in the lattice of compound **28**.

It is unfortunate that no Pt(IV)-*chloro* complexes of **HL^1** ligands ([Pt^{IV}(**L^1-*S,O***)$_2Cl_2$]) could be isolated and characterized. An understanding of the coordination chemistry of the [Pt^{IV}(**L^1-*S,O***)$_2Cl_2$]-type complexes will certainly contribute to elucidating the speciation in extraction processes of Pt(IV) from an acidic aqueous phase containing $PtCl_6^{2-}$ into an organic phase containing **HL^1**. This study has shown, however, that the oxidative addition of halogens to *cis*-[Pt^{II}(**L^1-*S,O***)$_2$] complexes is an effective means of synthesizing the Pt(IV) analogues; it remains to determine the appropriate experimental conditions which will allow isolation of [Pt^{IV}(**L^1-*S,O***)$_2Cl_2$] compounds. In this regard, we may refer to a comment made by one of the referees for the paper on this work who suggested that *controlled* oxidative addition of Cl_2 to *cis*-[Pt^{II}(**L^1-*S,O***)$_2$] complexes might also be achieved by making a standard solution of chlorine in CCl_4, and adding a calculated quantity of this standard reagent to a frozen solution of the Pt(II) complex. Alternatively, the application of an electrolytic cell containing a Pt(II) precursor and a chloride salt in an appropriate solvent, as discussed in the following chapter, may be attempted.

Table 2.6 Crystal and structure refinement data for compounds **26**, **27**, **23**^{trans}, **24**^{trans}, **28** and **29**.

	***cis*-[Pt^{IV}(L^1-*S*,*O*)$_2$I$_2$]** **26**	***cis*-[Pt^{IV}(L^1-*S*,*O*)$_2$Br$_2$]** **27**	***trans*-[Pt^{II}(H$_2$L^{2a}-*S*)$_2$I$_2$]** **23^{trans}**	***trans*-[Pt^{II}(H$_2$L^{2a}-*S*)$_2$Br$_2$]** **24^{trans}**	***trans*-[Pt(H$_2$L^2-*S*)$_2$I$_2$]·I$_2$** **28**	**{*trans*-[Pt(H$_2$L^2-*S*)$_2$Br$_4$]}(C$_7$H$_8$)** **29**
Molecular formula	$C_{24}H_{30}I_2N_4O_2PtS_2$	$C_{24}H_{30}Br_2N_4O_2PtS_2$	$C_{22}H_{28}I_2N_4O_2PtS_2$	$C_{22}H_{28}Br_2N_4O_2PtS_2$	$C_{22}H_{28}I_4N_4O_2PtS_2$	$C_{29}H_{36}Br_4N_4O_2PtS_2$
Formula weight	919.53	825.55	893.49	799.51	1147.29	1051.47
Crystal system	Triclinic	Monoclinic	Triclinic	Triclinic	Triclinic	Monoclinic
Space group	$P\bar{1}$	C 2/c	$P\bar{1}$	$P\bar{1}$	$P\bar{1}$	$P2_1/n$
Unit cell dimensions	a = 8.810(2) Å	a = 26.321(5) Å	a = 7.349(1) Å	a = 8.664(1) Å	a = 8.513(2) Å	a = 13.568(4) Å
	b = 10.920(2) Å	b = 15.743(3) Å	b = 10.246(1) Å	b = 8.818(1) Å	b = 9.400(2) Å	b = 13.739(4) Å
	c = 16.228(2) Å	c = 18.693(4) Å	c = 10574(1) Å	c = 9.747(1) Å	c = 10.064(2) Å	c = 18.962(6) Å
	α =74.23(3)°	α =90°	α = 67.73(1)°	α = 104.61(1)°	α =77.00(3)°	α =90°
	β =78.50(3)°	β =130.64(3)°	β = 74.74(1)°	β = 112.26(1)°	β =80.70(3)°	β =103.34(1)°
	γ =75.76(3)°	γ =90°	γ = 70.47(1)°	γ = 98.66(1)°	γ =86.19(3)°	γ =90°
Volume (Å^3)	1441.7(6)	5878(3)	685.76(7)	641.18(14)	773.9(3)	3439(2)
μ (mm^{-1})	7.181	7.663	7.55	8.78	8.683	8.881
Z	2	8	1	1	1	4
Temperature (K)	193(2)	193(2)	100(2)	100(2)	193(2)	100(2)
Reflections collected/unique	14013/7598 [R(int)=0.0363]	14663/7786 [R(int)=0.0394]	7162/2682 [R(int)=0.019]	6491/2490 [R(int)=0.022]	21068/3020 [R(int)=0.0254]	34743/6745 [R(int)=0.0442]
Goodness-of-fit	0.959	1.012	1.057	1.062	1.048	1.040
Final R [$I > 2\sigma(I)$] (all data)	0.0564	0.0592	0.0151	0.0248	0.0158	0.0326
$wR2$ [$I \geq 2\sigma(I)$] (all data)	0.0608	0.0681	0.0373	0.0603	0.0314	0.0639
Largest remaining feature in electron density map, max/min (e. Å^3)	1.32 (1.66 Å from H(14A)) -0.95 (0.83 Å from Pt(1))	1.35 (1.19 Å from Pt(1A)) -0.98 (0.84 Å from Pt(1A))	0.85 (0.98 Å from Pt(1)) -0.59 (1.29 Å from Pt(1))	2.68 (0.91 Å from Pt(1)) -1.20 (0.99 Å from Pt(1))	0.93 (0.78 Å from I(2)) -0.93 (0.75 Å from I(2))	1.80 (1.43 Å from H(21)) -0.50 (1.09 Å from Pt(1))

Stellenbosch University http://scholar.sun.ac.za

Stellenbosch University http://scholar.sun.ac.za

References

1 L. Beyer, E. Hoyer, H. Hartman and J. Liebscher, *Zeitschrift fur Chemie*, 1981, **21**, 81.
2 P. Mühl, K. Gloe, F. Dietze, E. Hoyer and L. Beyer, *Zeitschrift fur Chemie*, 1986, **26**, 8.
3 L. Beyer, R. Richter and O. Seidelmann, *Journal fur Praktische Chemie, Chemische Zeitung*, 1999, **341**, 704.
4 G. Binzet, U. Florke, N. Kulcu and H. Arslan, *Acta Crystallographica Section E*, 2003, **59**, m705.
5 R. del Campo, J. J. Criado, E. Garcia, M. R. Hermosa, A. Jimenez-Sanchez, J. L. Manzano, E. Monte, E. Rodriguez-Fernandez and F. Sanz, *Journal of Inorganic Biochemistry*, 2002, **89**, 74.
6 R. Flores-Centurion, R. Richter, J. Angulo-Comejo and L. Beyer, *Boletin de la Sociedad Quimica del Peru*, 1999, **65**, 211.
7 M. Reinel, R. Richter and R. Kirmse, *Zeitschrift fur Anorganische und Allgemeine Chemie*, 2002, **628**, 41.
8 J. Sieler, R. Richter, E. Hoyer, L. Beyer, O. Lindqvist and L. Andersen, *Zeitschrift fur Anorganische und Allgemeine Chemie*, 1990, **580**, 167.
9 W. Bensch and M. Schuster, *Zeitschrift fur Anorganische und Allgemeine Chemie*, 1992, **615**, 93.
10 A. N. Mautjana, J. D. S. Miller, A. Gie, S. A. Bourne and K. R. Koch, *Journal of the Chemical Society, Dalton Transactions*, 2003, 1952.
11 M. Dominguez, E. Antico, L. Beyer, A. Aguirre, S. Garcia-Granda and V. Salvado, *Polyhedron*, 2002, **21**, 1429.
12 R. Richter, F. Dietze, S. Schmidt, E. Hoyer, W. Poll and D. Mootz, *Zeitschrift fur Anorganische und Allgemeine Chemie*, 1997, **623**, 135.
13 U. Abram, S. Abram, R. Alberto and R. Schibli, *Inorganica Chimica Acta*, 1996, **248**, 193.
14 C. Sacht, M. Datt, S. Otto and A. Roodt, *Journal of the Chemical Society, Dalton Transactions*, 2000, 727.
15 R. Richter, J. Sieler, L. Beyer, O. Lindqvist and L. Andersen, *Zeitschrift fur Anorganische und Allgemeine Chemie*, 1985, **522**, 171.
16 K.-H. König, M. Schuster, B. Steinbrech, G. Schneeweis and R. Schlodder, *Fresenius Zeitschrift für Analitische Chemie*, 1985, **321**, 457.
17 P. Vest, M. Schuster and K. H. Koenig, *Fresenius Zeitschrift für Analitische Chemie*, 1989, **335**, 759.
18 K.-H. König, M. Schuster, G. Schneeweis and B. Steinbrech, *Fresenius Zeitschrift für Analitische Chemie*, 1984, **319**, 66.
19 M. Merdivan, A. Gungor, S. Savasci and R. S. Aygun, *Talanta*, 2000, **53**, 141.
20 M. Schuster, B. Kugler and K. H. König, *Fresenius Journal of Analytical Chemistry*, 1990, **338**, 717.
21 M. Schuster and M. Sandor, *Fresenius' Journal of Analytical Chemistry*, 1996, **356**, 326.
22 M. Schuster and M. Schwarzer, *Analytica Chimica Acta*, 1996, **328**, 1.
23 K. R. Koch, *Coordination Chemistry Reviews*, 2001, **216-217**, 473.
24 I. B. Douglass and F. B. Dains, *Journal of the American Chemical Society*, 1934, **56**, 719.
25 K. R. Koch, Y. Wang and A. Coetzee, *Journal of the Chemical Society, Dalton Transactions*, 1999, 1013.
26 S. Bourne and K. R. Koch, *Journal of the Chemical Society, Dalton Transactions*, 1993, 2071.
27 A. Irving, K. R. Koch and M. Matoetoe, *Inorganica Chimica Acta*, 1993, **206**, 193.
28 K. R. Koch, J. du Toit, M. R. Caira and C. Sacht, *Journal of the Chemical Society, Dalton Transactions*, 1994, 785.
29 D. Hanekom, J. M. McKenzie, N. M. Derix and K. R. Koch, *Chemical Communications*, 2005, 767.
30 T. Shi, J. Berglund and L. I. Elding, *Journal of the Chemical Society, Dalton Transactions*, 1997, 2073.
31 J. J. Zuckerman and J. D. Atwood, in *Inorganic Reactions and Methods, Formation of bonds to transition and inner-transition metals*, Wiley-VCH, New York, 1998.
32 L. M. Rendina and R. J. Puddephatt, *Chemical Reviews*, 1997, **97**, 1735.
33 G. M. Sheldrick, SHELXS-97 and SHELXL-97, Programs for the Solution and Refinement of Crystal Structures, University of Göttingen, Germany, 1997.
34 L. J. Barbour, *Journal of Supramolecular Chemistry*, 2003, **1**, 189.
35 A. L. Spek, PLATON, A Multipurpose Crystallographic Tool, University of Utrecht, Netherlands, 1999.
36 I. J. Bruno, J. C. Cole, P. R. Edgington, M. Kessler, C. F. Macrae, P. McCabe, J. Pearson and R. Taylor, *Acta Crystallographica Section B*, 2002, **58**, 389.

Stellenbosch University http://scholar.sun.ac.za

37 J. J. Pesek and W. R. Mason, *Journal of Magnetic Resonance*, 1977, **25**, 519.
38 P. S. Pregosin, *Coordination Chemistry Reviews*, 1982, **44**, 247.
39 D. Hanekom, *Thesis presented for M.Sc.*, University of Stellenbosch, 2005.
40 P. M. Cook, L. F. Dahl, D. Hopgood and R. A. Jenkins, *Journal of the Chemical Society; Dalton Transactions*, 1973, 294.
41 J. E. Huheey, E. A. Keiter and R. L. Keiter, in *Inorganic Chemistry: Principles of Structure and Reactivity*, Harper-Collins, New York, 4th edn., 1993.
42 F. A. Cotton and G. Wilkinson, in *Advanced Inorganic Chemistry*, Wiley-Interscience, New York, 5th edn., 1988.
43 P. H. Svensson and L. Kloo, *Chemical Reviews*, 2003, **103**, 1649.
44 F. van Bolhuis, P. B. Koster and T. Migchelsen, *Acta Crystallographica*, 1967, **23**, 90.
45 G. Thiele, D. O. F., H. W. Rotter and M. Goanta, *Journal of Molecular Structure*, 1999, **482-483**, 93.
46 O. F. Danzeisen, M. Goanta, H. W. Rotter and G. Thiele, *Inorganica Chimica Acta*, 1999, **287**, 218.
47 D. Rickert and W. Preetz, *Zeitschrift fur Naturforschung*, 1996, **51**, 1400.
48 F. P. Fanizzi, G. Natile, M. Lanfranchi, A. Tiripicchio, F. Laschi and P. Zanello, *Inorganic Chemistry*, 1996, **35**, 3173.
49 H.-J. Korte, B. Krebs, C. G. van Kralingen, A. T. M. Marcelis and J. Reedijk, *Inorganica Chimica Acta*, 1981, **52**, 61.
50 R. Bardi, A. M. Piazzesi, A. Del Pra and L. Trincia, *Acta Crystallographica Section C*, 1987, **43**, 1281.
51 K. C. Lövqvist, O. F. Wendt and J. G. Leipoldt, *Acta Chemica Scandinavica*, 1996, **50**, 1069.
52 K. R. Koch and S. Bourne, *Journal of Molecular Structure*, 1998, **441**, 11.
53 J. C. Barnes, G. Hunter and M. W. Lown, *Journal of the Chemical Society, Dalton Transactions*, 1977, 458.
54 A. Dago, Y. Shepelev, F. Fajardo, F. Alvarez and R. Pomés, *Acta Crystallographica*, 1989, **C45**, 1192.
55 K. R. Koch, C. Sacht, T. Grimmbacher and S. Bourne, *South African Journal of Chemistry*, 1995, **48**, 71.
56 W. Kaminsky, K. I. Goldberg and D. X. West, *Journal of Molecular Structure*, 2002, **605**, 9.
57 P. Wagner, S. Niemczyk-Baltro and M. Kubicki, *Acta Crystallographica Section C*, 2003, **C59**, o83.
58 B. M. Yamin and M. S. M. Yusof, *Acta Crystallographica Section E*, 2003, o340.
59 M. S. M. Yusof and B. M. Yamin, *Acta Crystallographica Section E*, 2003, **E59**, o828.
60 Y.-M. Zhang, L. Xian, T.-B. Wei and L.-X. Cai, *Acta Crystallographica Section E*, 2003, **E59**, o817.
61 Y.-M. Zhang, T.-B. Wei, L. Xian, Q. Lin and K.-B. Yu, *Acta Crystallographica Section E*, 2003, **59**, o905.
62 J. Cernak, J. Chomic, P. Kutschy, D. Svrcinova and M. Dzurilla, *Inorganica Chimica Acta*, 1991, **181**, 85.
63 D. Cauzzi, M. Lanfranchi, G. Marzolini, G. Predieri, A. Tiripicchio, M. Costa and R. Zanoni, *Journal of Organometallic Chemistry*, 1995, **488**, 115.
64 G. Li, D.-J. Che, Z.-F. Li, Y. Zhu and D.-P. Zou, *New Journal of Chemistry*, 2002, **26**, 1629.
65 Y.-M. Zhang, L. Xian and T.-B. Wei, *Acta Crystallographica Section C*, 2003, **59**, m473.
66 K. D. Buse, H. J. Keller and H. Pritzkow, *Inorganic Chemistry*, 1977, **16**, 1072.
67 C. Bellitto, M. Bonamico, G. Dessy, V. Fares and A. Flamini, *Journal of the Chemical Society, Dalton Transactions*, 1986, 595.
68 F. H. Allen, *Acta Crystallographica Section B*, 2002, **58**, 380.
69 P. Deplano, J. R. Ferraro, M. L. Mercuri and E. F. Trogu, *Coordination Chemistry Reviews*, 1999, **188**, 71.
70 M. F. Belicchi, G. G. Fava and C. Pelizzi, *Acta Crystallographica*, 1981, **B37**, 924.
71 L. R. Gray, D. J. Gulliver, W. Levason and M. Webster, *Inorganic Chemistry*, 1983, **22**, 2362.
72 E. Schulz Lang and J. Strahle, *Zeitschrift fur Anorganische und Allgemeine Chemie*, 1996, **622**, 981.
73 D.-L. Long, H.-M. Hu, J.-T. Chen and J.-S. Huang, *Acta Crystallographica Section C*, 1999, **C55**, 339.
74 P. B. Hitchcock, D. L. Hughes, G. J. Leigh, J. R. Saers, J. Desouza, C. J. Mcgarry and L. F. Larkworthy, *Journal of the Chemical Society, Dalton Transactions*, 1994, **24**, 3683.
75 I. L. Karle, *Journal of Chemical Physics*, 1955, **23**, 1739.
76 F. E. Wood, M. M. Olmstead, J. P. Farr and A. L. Balch, *Inorganica Chimica Acta*, 1985, **97**, 77.
77 K. Hindmarsh, D. A. House and M. M. Turnbull, *Inorganica Chimica Acta*, 1997, **257**, 11.
78 R. A. Gossage, A. D. Ryabov, A. L. Spek, D. J. Stufkens, J. A. M. van Beek, R. van Eldik and G. van Koten, *Journal of the American Chemical Society*, 1999, **121**, 2488.

Stellenbosch University http://scholar.sun.ac.za

Chapter 3

First Metallamacrocyclic Complexes of Pt(IV) with 3,3,3',3'-tetraalkyl-1,1'-phenylenedicarbonylbis(thioureas): Synthesis by Direct or Electrolytic Oxidative Addition of I_2, Br_2 and Cl_2.*

The 3 : 3 Pt(II) metallamacrocycle of 3,3,3',3'-tetra(*n*-butyl)-1,1'-terephthaloylbis(thiourea) was reacted with I_2 and Br_2 resulting in the stepwise oxidative addition of the dihalogens to each of the Pt(II) centers, yielding initially mixed valence Pt(II)/Pt(IV) species and finally the fully oxidized Pt(IV) complex, depending on the mole ratio of halogen to Pt(II) precursor. Treatment of the 2 : 2 Pt(II) complex of 3,3,3',3'-tetraethyl-1,1'-isophthaloylbis(thiourea) with I_2 also results in the oxidative addition of the halogen, yielding a 2 : 2 *trans*-Pt(IV)-iodo metallamacrocycle. The corresponding *trans*-Pt(IV)-X (X = Br, Cl) complexes were synthesized by oxidative addition in an electrolytic cell containing the 2 : 2 Pt(II) precursor and an appropriate halide salt in dichloromethane. Each of the first-reported 2 : 2 *trans*-Pt(IV)-X (X = I, Br, Cl) metallamacrocycles were isolated and structurally characterized.

* This chapter is based on the paper:
A. N. Westra, S. A. Bourne and K. R. Koch, *Dalton Trans.*, 2005, 2916-2924.

Stellenbosch University http://scholar.sun.ac.za

3.1 Introduction

The design and synthesis of novel metallamacrocycles has been stimulated not only by the fascinating structures of many of these metallo-organic architectures, but also by their potential applications, *viz.* in molecular recognition, host-guest chemistry, nanotechnology and catalysis.[1-4] The synthetic strategy for the preparation of these structures is based on molecular self-assembly, a phenomenon in which compounds are spontaneously formed by mixing component ligands and metals in solution.[5-9] As part of our studies of the coordination chemistry of molecules with the acyl-thiourea motif, we have become interested in the symmetrical bipodal 3,3,3',3'-tetraalkyl-1,1'-phenylenedicarbonylbis(thioureas); these molecules appear to be 'pre-programmed' to form, through self-assembly, discrete metallamacrocyclic complexes with d^8 metal ions (Ni(II), Pd(II) and Pt(II)), in high yields. This organised self-assembly occurs as a result of the tendency of the *S,O*-donating acylthioureas to coordinate to these metals in a predominantly *cis* fashion.[10-15] Metallamacrocyclic complexes with well-defined metal-to-ligand ratios are exclusively formed depending on the relative substitution positions of the carbonyl-thiourea moieties on the phenylene spacer: *meta* substitution ($\mathbf{H_2L^m}$; Scheme 3.1) leads to 2 : 2 complexes (*cis*-[$M_2(\mathbf{L^m}$-***S,O***$)_2$] with M = Ni, Pd, Pt; Scheme 3.1), and *para* substitution ($\mathbf{H_2L^p}$; Scheme 3.1) to 3 : 3 metallamacrocycles (*cis*-[$M_3(\mathbf{L^p}$-***S,O***$)_3$] with M = Ni, Pd, Pt; Scheme 3.1).[12-15]

The structural characterisation of 2 : 2 metallamacrocycles of Ni(II) and Pt(II) with 3,3,3',3'-tetraethyl-1,1'-isophthaloylbis(thiourea)[12,15] and of Pd(II) with 3,3,3',3'-tetra(*n*-butyl)-1,1'-isophthaloylbis(thiourea),[13] has been reported, and crystallographic data is also available for the 3 : 3 complexes of Pt(II) with 3,3,3',3'-tetra(*n*-butyl)-1,1'-terephthaloylbis(thiourea)[12] and Ni(II) with 3,3,3',3'-tetraethyl-1,1'-terephthaloylbis(thiourea).[11] König *et al.* reported preparation of Ni(II) and Pd(II) complexes with related 3,3,3',3'-tetraethyl-1,1'-adipoylbis(thiourea) in 1987, but these complexes were not structurally characterised.[16]

It has recently been shown that 2 : 2 and 3 : 3 Ni(II) metallamacrocycles of the bipodal aroylthioureas readily form adducts with pyridines to yield octahedrally coordinated Ni(II) complexes of the general structure *cis*-[$Ni_2(\mathbf{L^m}$-***S,O***$)_2(py)_4$] (py = pyridine or 4-dimethylaminopyridine)[13,14] and *cis*-[$Ni_3(\mathbf{L^p}$-***S,O***$)_3(py)_6$] (py = pyridine),[15] which also display interesting host -guest chemistry. This illustrates the potential of such essentially planar metallamacrocyclic Ni(II) complexes to function as secondary building blocks for further assembly into 3-dimensional higher ordered structures, using suitable linker molecules.

With a view to exploiting the kinetic inertness of analogous Pt(II) complexes, as well as the ease of oxidation of Pt(II) to Pt(IV) resulting in axial coordination sites at the Pt(IV) centres, we have investigated the synthesis of Pt(IV) complexes with the bipodal $\mathbf{H_2L^m}$ and $\mathbf{H_2L^p}$ ligands. We have found that Pt(IV) complexes of **HL** can be readily prepared by simple oxidative addition of I_2 and Br_2 to the Pt(II) complexes of these ligands, *cis*-[Pt^{II}(**L-*S,O***$)_2$] in Scheme 3.1; this work is described in Chapter 2. We here report the

Stellenbosch University http://scholar.sun.ac.za

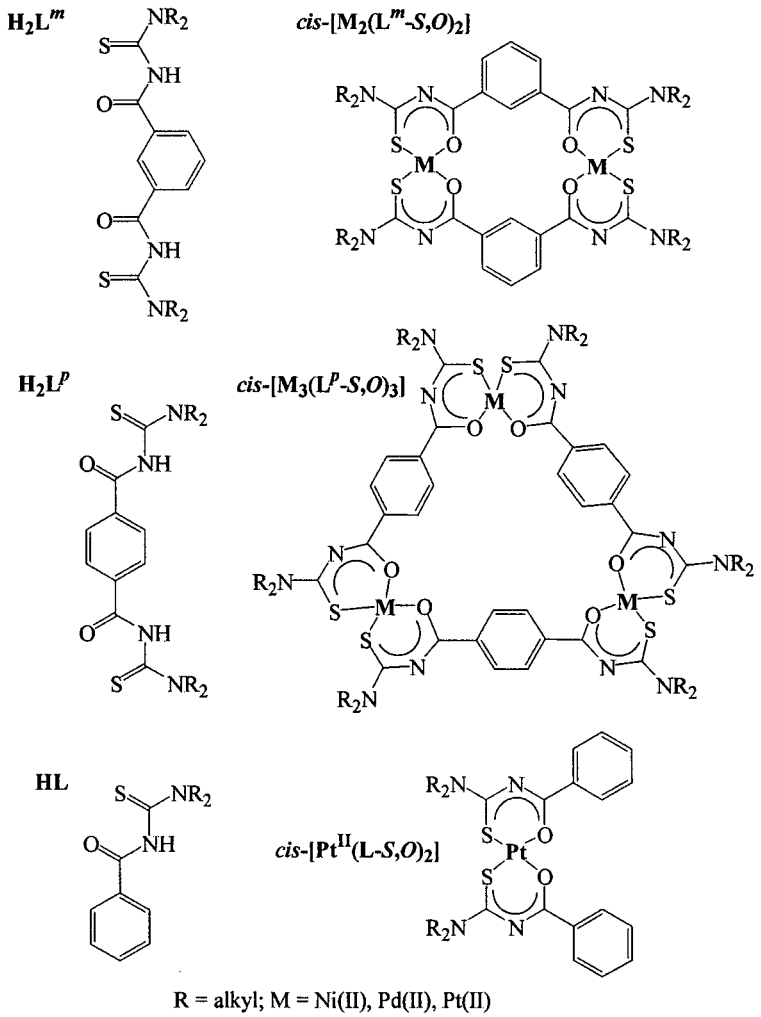

Scheme 3.1 Carbonylthiourea moieties bound *meta* to the phenylene linker ($\mathbf{H_2L^m}$) lead to 2 : 2 metallamacrocycles (*cis*-[$M_2(\mathbf{L^m}$-*S,O*)$_2$]), while the *para* substituted bipodal thioureas ($\mathbf{H_2L^p}$) give rise to 3 : 3 complexes (*cis*-[$M_3(\mathbf{L^p}$-*S,O*)$_3$]). *N,N*-dialkyl-*N'*-benzoylthioureas (**HL**) coordinate to these metals in a predominantly *cis* fashion.

facile preparation and characterisation of a series of *trans*-Pt(IV)-X (X = I, Br, Cl) 2 : 2 and 3 : 3 metallamacrocyclic complexes of the 3,3,3',3'-tetraalkyl-1,1'-phenylenedicarbonylbis(thioureas) by oxidative addition of diatomic halogens to the Pt(II) centers of *cis*-[$Pt^{II}_2(\mathbf{L^m}$-*S,O*)$_2$] and *cis*-[$Pt^{II}_3(\mathbf{L^p}$-*S,O*)$_3$]. In solution the oxidative addition can readily be achieved by reaction directly with I_2, although by utilising a simple electrolytic cell in which presumably Br_2 or Cl_2 are produced *in situ* at the anode, the bromo- and chloro- complexes can also be prepared in high purity.

Stellenbosch University http://scholar.sun.ac.za

3.2 Experimental

3.2.1 Methods and instruments

3,3,3',3'-tetra(*n*-butyl)-1,1'-terephthaloylbis(thiourea), $\mathbf{H_2L^{p1}}$ **31**, and 3,3,3',3'-tetraethyl-1,1'-isophthaloylbis(thiourea), $\mathbf{H_2L^{m1}}$ **32**, as well as the complexes *cis*-[$Pt^{II}_3(\mathbf{L^{p1}}$-***S,O***$)_3$] **33** and *cis*-[$Pt^{II}_2(\mathbf{L^{m1}}$-***S,O***$)_2$] **34**, were synthesised and characterized as previously reported.[12] All reagents and solvents were commercially available, and all were used without further purification except for the acetone used in ligand synthesis, which was distilled before use. ^{195}Pt NMR spectra (30°C) were recorded in chloroform-d using a Varian INOVA 600 MHz spectrometer operating at 128 MHz. All ^{195}Pt chemical shifts are quoted relative to external H_2PtCl_6 (500 mg ml^{-1} in 30% v/v D_2O/1 M HCl), and are estimated to be accurate to ± 2 ppm. UV-visible spectrophotometric experiments were carried out on an Agilent 8453E UV-visible spectrophotometer (Agilent Technologies). Melting points were determined using an Electrothermal IA9000 Digital Melting Point Apparatus. Elemental analyses were performed using a Carlo Erba EA 1108 elemental analyzer in the microanalytical laboratory of the University of Cape Town.

3.2.2 Preparative methods and compound characterization

3.2.2.1 cis-[$Pt^{IV}_2(L^{m1}$-S,O$)_2I_4$] 35. Synthesis by direct oxidative addition

0.0351 mmol (41.3 mg) of the sparingly soluble *cis*-[$Pt^{II}_2(\mathbf{L^{m1}}$-***S,O***$)_2$] **34** was dissolved in 25 cm^3 of dichloromethane and treated with a solution of 0.0780 mmol (19.8 mg) I_2 in 5 cm^3 of CH_2Cl_2; *i.e.* a slight excess of I_2 with regard to total Pt(II). From the dark red/brown mixture, crystals of *cis*-[$Pt^{IV}_2(\mathbf{L^{m1}}$-***S,O***$)_2I_4$] **35**, were obtained by diffusion crystallization with pentane; the product was washed with chloroform, dried and analysed. Mp > 190 °C (decomp.). Found: C, 25.9; H, 2.5; N, 6.6; S, 7.5. $C_{36}H_{48}I_4N_8O_4Pt_2S_4$ requires C, 25.7; H, 2.9; N, 6.7; S, 7.6 %.

3.2.2.2 cis-[$Pt^{IV}_2(L^{m1}$-S,O$)_2Br_4$] 36. Oxidative addition in an electrolytic cell

An electrolytic process with the set-up shown in Fig. 3.1, was used to prepare compound **36**. The custom-made cell consisted simply of two connected glass tubes (90 mm in height and 30 mm in diameter), separated in the connecting-bridge by a sintered-glass frit (porosity 3). A platinum electrode was used as the cathode (rotary-foil), and as the anode (rotary-gauze). 30 cm^3 of an electrolyte solution comprising 0.143 mol dm^{-3} tetrabutylammoniumbromide in dichloromethane was measured into each compartment, and 0.0655 mmol (77.0 mg) of *cis*-[$Pt^{II}_2(\mathbf{L^{m1}}$-***S,O***$)_2$] **34** was also added to the electrolyte solution in the anodic compartment; the compartments were covered with glass caps. A large portion of the sparingly soluble *cis*-[$Pt^{II}_2(\mathbf{L^{m1}}$-***S,O***$)_2$] remained undissolved and settled at the bottom of the compartment. A potential difference of 2.2 V applied across the electrodes resulted in an initial current of 0.30 mA through the cell. After 24 hrs the solution in the anodic compartment had become dark yellow/orange and no

Stellenbosch University http://scholar.sun.ac.za

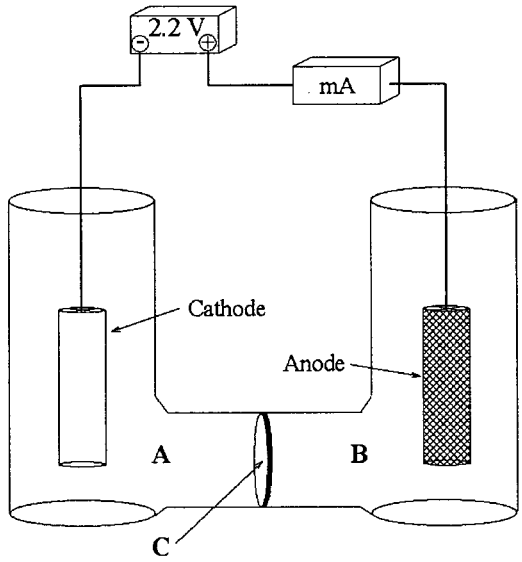

Fig. 3.1 Diagram of the electrolytic cell used for the synthesis of compounds **36** and **37**. In compartment A, a platinum rotary-foil electrode (cathode) was immersed in 30 cm^3 of electrolyte solution, *ca.* 0.143 mol dm^{-3} tetrabutylammoniumbromide, or tetrabutylammoniumchloride, in dichloromethane. A platinum rotary-gauze electrode was used as anode in compartment B, immersed in 30 cm^3 of electrolyte solution and a known quantity of an appropriate Pt(II) complex. A sintered-glass frit C (porosity 3) separated the two compartments. Under the conditions of the experiments, a potential difference of 2.2 V applied across the electrodes, resulted in an initial current of *ca.* 0.3 mA through the cell, and resulted in the formation of crystals of **36** or **37** in the anodic compartment B.

undissolved remnants of compound **34** could be seen, and after 48 hrs dark orange crystals were visible on the anode. The cell was allowed to function undisturbed for 140 hrs; a suitable quantity of good quality crystals precipitated on the anode. The crystals were washed with chloroform, dried and analysed. Mp > 195 °C (decomp.). Found: C, 29.4; H, 2.9; N, 7.5; S, 8.7. $C_{36}H_{48}Br_4N_8O_4Pt_2S_4$ requires C, 28.9; H, 3.2; N, 7.5; S, 8.6 %.

3.2.2.3 cis-[$Pt^{IV}_2(L^{m1}$-S,O)$_2Cl_4$] 37. Oxidative addition in an electrolytic cell

Compound **37** was also prepared in a set-up as shown in Fig. 3.1. In each compartment was measured 30 cm^3 of an electrolyte solution comprising 0.143 mol dm^{-3} tetrabutylammoniumchloride in dichloromethane, and 0.0630 mmol (74.0 mg) of compound **34** was added to the electrolyte solution in the anodic compartment. A large portion of the sparingly soluble *cis*-[$Pt^{II}_2(\mathbf{L^{m1}}$-***S,O***$)_2$] settled at the bottom of the compartment, remaining undissolved. A potential difference of 2.2 V applied across the electrodes resulted in an initial current of 0.34 mA through the cell. After 24 hrs the solution in the anodic compartment had become dark yellow and compound **34** appeared to have dissolved completely; after 48 hrs dark yellow crystals were growing on the anode. The cell was left to function undisturbed for 141 hrs, allowing a suitable quantity of good quality crystals to form on the anode. The crystals were washed with chloroform,

Stellenbosch University http://scholar.sun.ac.za

dried and analysed. Mp > 210 °C (decomp.). Found: C, 32.5; H, 3.4; N, 8.2; S, 9.3. $C_{36}H_{48}Cl_4N_8O_4Pt_2S_4$ requires C, 32.8; H, 3.7; N, 8.5; S, 9.7 %.

3.2.2.4 cis-[$Pt^{IV}_3(L^{p1}$-S,O)$_3Br_6$]. Synthesis by direct oxidative addition

0.0257 mmol (54.0 mg) of *cis*-[$Pt^{II}_3(\mathbf{L}^{p1}$-***S,O***$)_3$] **33** was dissolved in 1 cm^3 of chloroform, and treated with 4 µl of Br_2 (3.1 g ml^{-1}) using a gastight syringe. Crystals isolated by diffusion crystallization with pentane, were washed with chloroform and dried. Characterization by single crystal diffractometry confirmed oxidative addition of Br_2 to all three platinum centres, but considerable disorder in the structure did not allow complete refinement.

No yields were determined for the isolated compounds; NMR spectroscopic monitoring of the oxidative addition indicated that the reactions are practically quantitative. Furthermore, the presence of background electrolyte in the solutions used for electrolytic syntheses hindered the determination of product yields in these solutions, and cells were kept operational only until sufficient crystals for analyses had formed on the anode.

3.2.3 Crystallography and structure refinement

Suitable crystals were mounted on a thin glass fiber and data were collected either on a Nonius Kappa CCD or Bruker-Nonius SMART Apex diffractometer using graphite monochromated Mo-Kα radiation (λ = 0.7107 Å). The structures were solved using SHELXS-97 and refined using SHELXL-97[17] with the aid of the interface program X-SEED.[18] All non-hydrogen atoms were modeled anisotropically. Hydrogen atoms were placed in geometrically calculated positions, with C-H = 0.99 (for $-CH_2-$), 0.98 (for $-CH_3$), or 0.95 Å (for phenyl). These were refined using a riding model, with U_{iso}(H) = 1.2U_{eq}(parent) (for $-CH_2-$, and phenyl) or 1.5U_{eq}(parent) (for $-CH_3$). Crystal structure interpretation was performed with the aid of the programs PLATON[19] and MERCURY.[20] Selected bond lengths and angles are presented in Tables 3.1 and 3.2, and relevant crystallographic data is shown in Table 3.3.

3.3 Results and Discussion

Complexation of equimolar quantities of 3,3,3',3'-tetra(*n*-butyl)-1,1'-terephthaloylbis(thiourea), $\mathbf{H_2L}^{p1}$ **31**, and 3,3,3',3'-tetraethyl-1,1'-isophthaloylbis(thiourea), $\mathbf{H_2L}^{m1}$ **32**, with $PtCl_4^{2-}$ led to high yields of the corresponding 3 : 3 and 2 : 2 metallamacrocyclic complexes *cis*-[$Pt^{II}_3(\mathbf{L}^{p1}$-***S,O***$)_3$] **33** and *cis*-[$Pt^{II}_2(\mathbf{L}^{m1}$-***S,O***$)_2$] **34**, respectively, which were re-crystallized and characterized as before.[12]

Stellenbosch University http://scholar.sun.ac.za

3.3.1 Oxidative addition of I_2 and Br_2 to 3 : 3 cis-[$Pt^{II}_3(L^{p1}$-S,O)$_3$] 33

The treatment of a $CDCl_3$ solution of *cis*-[$Pt^{II}_3(\mathbf{L}^{p1}$-*S,O*)$_3$] **33** with a stoichiometric quantity of I_2 (s), i.e. Pt : I_2 at 1 : 1, leads to the disappearance of the ^{195}Pt NMR peak due to **33** ($\delta_{Pt\ 33}$ = -2710 ppm), and the emergence of a single peak at δ_{Pt} = -2430 ppm, suggesting facile oxidative addition of iodine to all three metal centres of metallamacrocycle **33**. We have shown previously that I_2 readily reacts with *cis*-bis(*N,N*-diethyl-*N'*-benzoylthioureato)platinum(II) (*cis*-[$Pt^{II}(\mathbf{L}^{1a}$-*S,O*)$_2$], δ_{Pt} = -2719 ppm), the mononuclear analogue of **33**, to yield *cis*-[$Pt^{IV}(\mathbf{L}^{1a}$-*S,O*)$_2I_2$] (δ_{Pt} = -2422 ppm), in which the iodo ions bind *trans* axially to Pt(IV) (Chapter 2). Interestingly, oxidative addition of I_2 to the various Pt(II) centres of **33** takes place in a stepwise manner. The course of this stepwise addition can conveniently be monitored by means of ^{195}Pt NMR, by 'titrating' a $CDCl_3$ solution of **33** with sub-stoichiometric quantities of I_2 directly in an NMR tube; ^{195}Pt NMR spectra for such a titration are shown in Fig. 3.2(a). As increasing quantities of I_2 are added, three distinct resonances emerge *ca.* 280 ppm downfield of the ^{195}Pt NMR peak of **33**, corresponding to three Pt(IV)-containing product species with relative concentrations dependent on the quantity of I_2 added. Peaks at -2432 ppm and -2430 ppm emerge and diminish on addition of more I_2, while

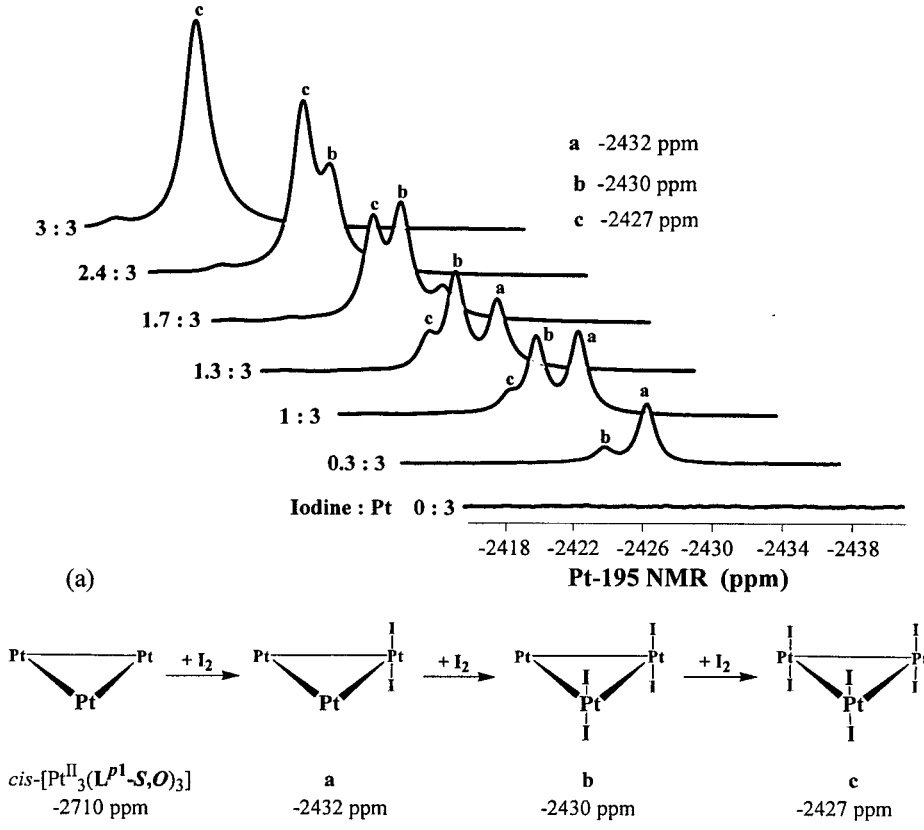

Fig. 3.2 (a) Partial ^{195}Pt NMR spectra obtained by 'titration' of *cis*-[$Pt^{II}_3(\mathbf{L}^{p1}$-*S,O*)$_3$] **33** ($1.20\times10^{-4}$ mol of **33**, i.e. 3.60×10^{-4} mol Pt(II), in 0.7 cm^3 $CDCl_3$) with small quantities of I_2 to equimolarity (I_2 : Pt at 1 : 1), at room temperature. The appearance of signals in the observed chemical shift range, suggests facile oxidative addition of iodine to each of the three metal centres in *cis*-[$Pt^{II}_3(\mathbf{L}^{p1}$-*S,O*)$_3$], leading to the formation and subsequent diminution of the mixed valence species shown schematically as **a** and **b** in (b) (corresponding to peaks **a** and **b** in (a), respectively), and the eventual predominance of compound **c** (peak **c**) in solution.

Stellenbosch University http://scholar.sun.ac.za

a third peak at -2427 ppm grows to be the only resonance after addition of a stoichiometric quantity of iodine. (The slight discrepancy between the resonance positions of peak **c** in Fig. 3.2(a), -2427 ppm, and that obtained after direct stoichiometric addition of I_2, -2430 ppm, is accounted for if one considers that the ^{195}Pt chemical shifts are estimated to be accurate to ± 2 ppm). Inspection of Fig. 3.2(a) shows that in chloroform, for an I_2 : Pt(II) ratio of 1 : 3, oxidative addition to all three Pt(II) centres occurs readily, and apparently indiscriminately, yielding the mixed valence species *cis*-$[Pt^{II}_2Pt^{IV}I_2(\mathbf{L}^{p1}\text{-}\boldsymbol{S,O})_3]$ and *cis*-$[Pt^{II}Pt^{IV}_2I_4(\mathbf{L}^{p1}\text{-}\boldsymbol{S,O})_3]$ as well as the 3:3 Pt(IV) metallamacrocycle *cis*-$[Pt^{IV}_3I_6(\mathbf{L}^{p1}\text{-}\boldsymbol{S,O})_3]$ (Fig. 3.2(b)), for which the ^{195}Pt NMR chemical shifts of the Pt(IV) environments differ by a few ppm respectively. The expected similar distribution of peaks corresponding to the Pt(II) environments in these species (at *ca.* -2710 ppm) is unfortunately not seen, presumably due to the significant broadening of the Pt(II) resonance observed in both **33** ($\nu_{½}$ ~ 772 Hz) and its oxidative addition products. This is in contrast to the somewhat narrower Pt(IV) resonances ($\nu_{½}$ ~ 257 Hz), allowing their resolution. The broadness of the ^{195}Pt resonance of **33** is understandable in terms of an expected field dependent contribution to the T_2 relaxation of the Pt(II) nuclei in the essentially planar metallamacrocycle **33**.[21,22] On addition of I_2 to the chloroform solution of *cis*-$[Pt^{II}_3(\mathbf{L}^{p1}\text{-}\boldsymbol{S,O})_3]$, the observed diminution of the -2710 ppm resonance intensity with a concomitant slight downfield shift is not resolved into three separate peaks as seen for the Pt(IV) environment.

The most widely accepted mechanism for oxidative halogen addition reactions to square-planar Pt(II) complexes,[23,24] adapted to **33**, is shown in Scheme 3.2. The initial step is believed to be an end-on η^1-complexation of the dihalogen molecule to a Pt(II) center (**A** in Scheme 3.2); a model for this first step is the isolated η^1-I_2 Pt(II) adduct formed by the reaction of I_2 with $[PtI(C_6H_3\{CH_2NMe_2\}_2\text{-}2,6)]$.[25] This is followed by a two-electron intramolecular transfer from the d_z^2 orbital on the Pt(II) to the empty σ_u^* orbital of X_2, yielding a cationic intermediate in which one of the metal centres is five-coordinate (**B** in Scheme 3.2), and an X^- ion. The final step involves migration of the anion to the vacant coordination site of the Pt(IV) centre, leading to a *trans*-Pt(IV)-halogenide arrangement (**C** in Scheme 3.2). Repetition of this process for the second and third metal centers, yields the fully oxidized 3 : 3 hexa-iodo-Pt(IV) macrocycle.

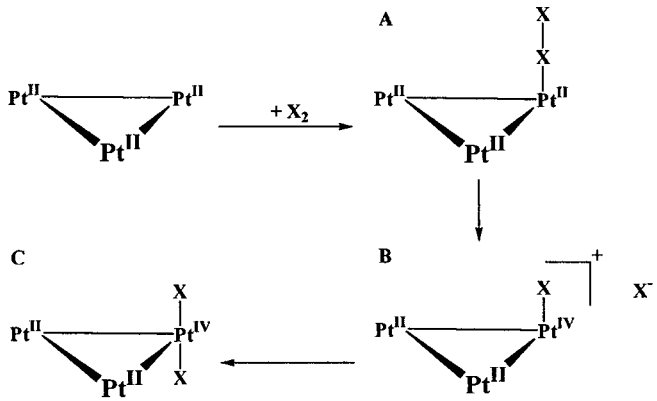

Scheme 3.2 Proposed mechanism for the oxidative addition of a dihalogen to a metal centre of a Pt(II) 3 : 3 metallamacrocycle such as *cis*-$[Pt^{II}_3(\mathbf{L}^{p1}\text{-}\boldsymbol{S,O})_3]$.

Stellenbosch University http://scholar.sun.ac.za

Although preliminary results of our studies of oxidative halogen addition to the *mononuclear* analogue *cis*-[$Pt^{II}(\mathbf{L^{1a}}$-***S,O***$)_2$] (Chapter 2) indicated possible isomerization of the resulting Pt(IV) complexes, the bipodal nature of $\mathbf{H_2}L^{p1}$ in metallamacrocyclic complexes presumably precludes re-arrangement of the ligands, ruling out the possibility of isomers in this case.

A similar 'titration' of a $CDCl_3$ solution of **33** with small quantities of Br_2 (l) directly in an NMR tube also results in the emergence of three ^{195}Pt NMR peaks *ca.* 1380 ppm downfield of the peak of **33**. The resonances at -1334 ppm and -1332 ppm emerge and again disappear with increasing quantities of Br_2 added. Finally, a third peak at -1330 ppm appears and grows to be the only resonance after stoichiometric addition of Br_2; the peak at -2710 ppm corresponding to complex **3** disappears completely. The resonance position of the remaining peak (-1330 ppm) compares well with the chemical shift reported for *cis*-bis(*N,N*-diethyl-*N'*-benzoylthioureato)dibromoplatinum(IV) (*cis*-[$Pt^{IV}(\mathbf{L^{1a}}$-***S,O***$)_2Br_2$], δ_{Pt} = -1322 ppm), which was isolated after treatment of *cis*-[$Pt^{II}(\mathbf{L^{1a}}$-***S,O***$)_2$] with Br_2 (Chapter 2), confirming the oxidative addition of Br_2 to all three platinum centres in **33**. The observed product peaks are assigned to the Pt(IV) *trans* axially coordinated bromo analogues of the species shown in Fig. 1(b). X-ray diffraction analysis of crystals isolated from a mixture in which **33** had been treated with a stoichiometric quantity of Br_2 (l) (see Experimental Section), confirmed the oxidative addition of dibromine to all three metal centers of the macrocycle, but considerable disorder in the structure precluded satisfactory refinement.

3.3.2 Oxidative addition of I_2 to 2 : 2 cis-[$Pt^{II}_2(L^{m1}$-S,O$)_2$] 34, and the crystal structure of cis-[$Pt^{IV}_2(L^{m1}$-S,O$)_2I_4$] 35

Treatment of dilute chloroform, or dichloromethane, solutions of the sparingly soluble *cis*-[$Pt^{II}_2(\mathbf{L^{m1}}$-***S,O***$)_2$] **34** with stoichiometric quantities of I_2 (equivalent to Pt(II)), resulted in good quality crystals being obtained by diffusion crystallization. These were determined by elemental analysis and single crystal diffractometry to be *cis*-[$Pt^{IV}_2(\mathbf{L^{m1}}$-***S,O***$)_2I_4$] **35** (Fig. 3.3), confirming oxidative addition of the dihalogen to *both* metal centres. The poor solubility of **34** unfortunately prevented similar ^{195}Pt NMR studies as with **33**; dilute solutions suitable for UV-visible spectrophotometry could however be prepared, and allowed the course of the oxidative addition to be monitored by this technique. A chloroform solution of *cis*-[$Pt^{II}_2(\mathbf{L^{m1}}$-***S,O***$)_2$] **34** was 'titrated' with appropriate quantities of I_2, to equimolarity, and the UV-vis spectrum of the solution recorded after each addition; spectra are shown in Fig. 3.4. The spectrum for *cis*-[$Pt^{II}_2(\mathbf{L^{m1}}$-***S,O***$)_2$] **34** is similar to that for *cis*-bis(*N,N*-diethyl-*N'*-benzoylthioureato)platinum(II) *cis*-[$Pt^{II}(\mathbf{L^{1a}}$-***S,O***$)_2$] (the spectrum is shown in Fig. 2.1), and the distributions of the spectra in Figures 2.1 and 3.4 are comparable; this is not surprising considering the structural similarities of compound **34** with *cis*-[$Pt^{II}(\mathbf{L^{1a}}$-***S,O***$)_2$], and of **35** with *cis*-[$Pt^{IV}(\mathbf{L^{1a}}$-***S,O***$)_2I_2$]. Based on the observations in Section 3.3.1, it is likely that during the course of the 'titration' the three species *cis*-[$Pt^{II}_2(\mathbf{L^{m1}}$-***S,O***$)_2$], *cis*-[$Pt^{II}Pt^{IV}I_2(\mathbf{L^{m1}}$-***S,O***$)$] and *cis*-[$Pt^{IV}_2(\mathbf{L^{m1}}$-***S,O***$)_2I_4$] exist in solution., which is in accordance with the occurrence of two isosbestic points in the distribution.

Stellenbosch University http://scholar.sun.ac.za

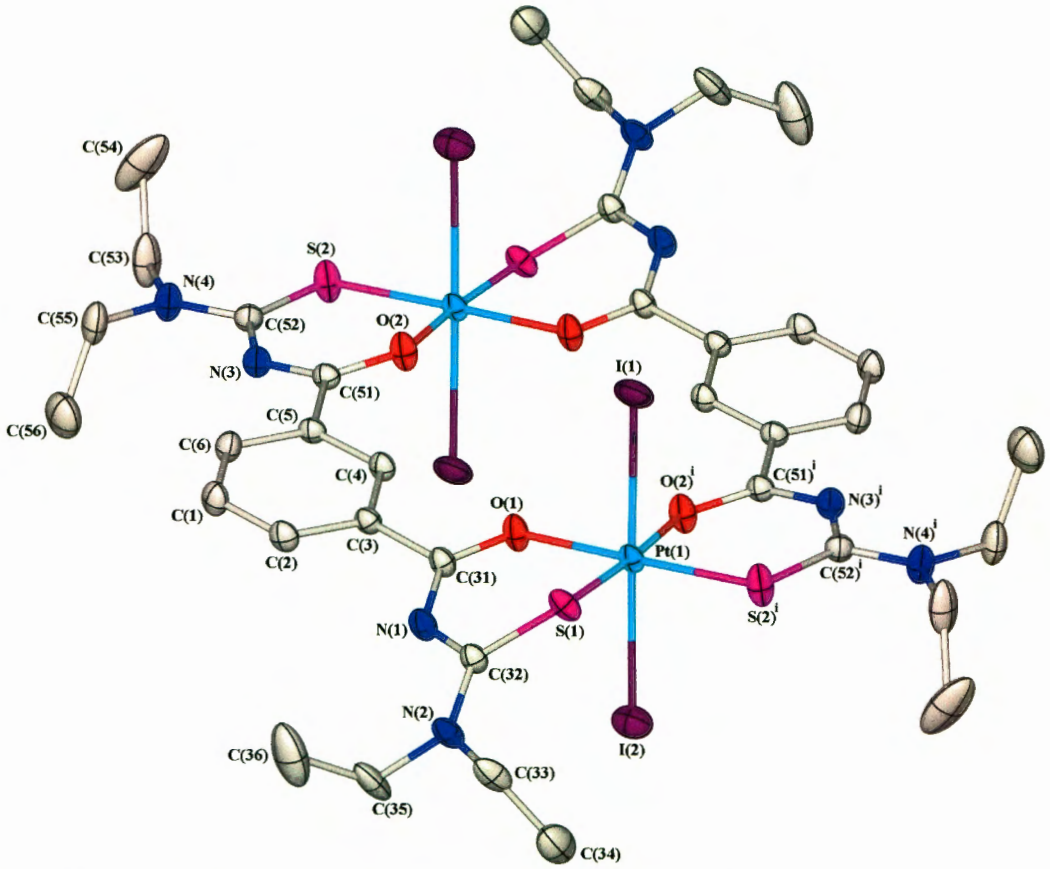

Fig. 3.3 The molecular structure of *cis*-[Pt^{IV}_2(L^{m1}-*S*,*O*)$_2I_4$] **35** with atom numbering scheme. Displacement ellipsoids are drawn at the 50% probability level, and H atoms have been omitted for clarity. Although the $Pt^{IV}S_2O_2$ planes are parallel, they are displaced by 1.313(6) Å relative to each other; this displacement leads to considerable deformation of the bipodal ligands. Selected bond lengths and angles are given in Table 3.1. Symmetry code: (i) 1-x, 1-y, 1-z.

Several recent reports attest to the continued interest in the well-known oxidative addition of iodine to Pt(II) in various complexes,[26-30] and the structural data of a number of *trans*-Pt(IV)-iodo complexes are documented in the Cambridge Structural Database.[31] In these structures, Pt(IV) is coordinated to the remaining ligands via C, N, O, P, or As atoms (in either mono- or bidentate mode), and we have reported the structure of a *trans*-Pt(IV)-iodo complex incorporating S-donor atoms, *viz*. the mononuclear analogue of **35**, *cis*-bis(*N*,*N*-diethyl-*N*'-benzoylthioureato)diiodoplatinum(IV) *cis*-[Pt^{IV}(L^{1a}-*S*,*O*)$_2I_2$] (Chapter 2). In compound **35**, the bipodal ligands (L^{m1}) remain *cis* *S*,*O*-coordinated to the Pt(IV) centres, with the halides in *trans* axial positions. To our knowledge, *cis*-[Pt^{IV}_2(L^{m1}-*S*,*O*)$_2I_4$] **35** is the first fully characterized *metallamacrocyclic* complex with a *trans*-Pt(IV)-iodo arrangement.

Compound **35** crystallizes in the space group $P\bar{1}$, with half a molecule in the asymmetric unit; the full molecule is generated from the asymmetric half by an inversion centre at (1/2 1/2 1/2). The Pt-I bond lengths and I-Pt-I bond angle in **35** (2.667(1)/2.672(1) Å and 178.86(1)°, respectively; see Table 3.1) compare well with the values for corresponding parameters in *cis*-bis(*N*,*N*-diethyl-*N*'-

Stellenbosch University http://scholar.sun.ac.za

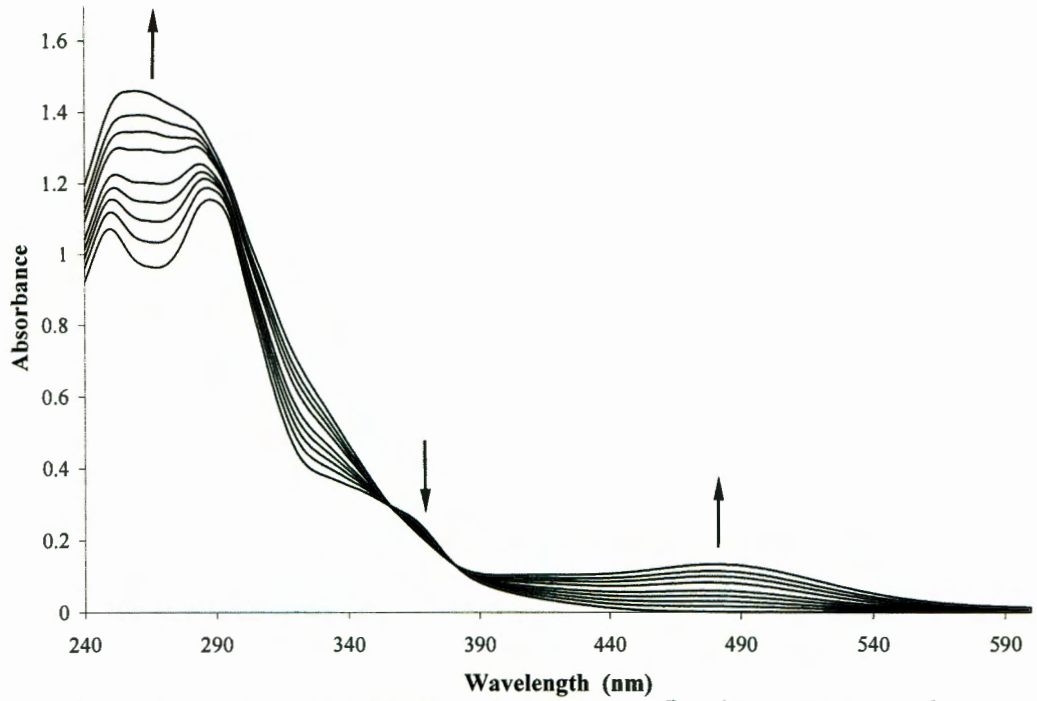

Fig. 3.4 Distribution of UV-vis spectra obtained by 'titration' of *cis*-$[Pt^{II}_2(\mathbf{L}^{m1}\text{-}\boldsymbol{S,O})_2]$ **34** (8.00×10^{-6} mol of **34**, i.e. 1.60×10^{-5} mol Pt(II), in 100 cm^3 of $CHCl_3$) with small volumes of 0.15 M I_2 in chloroform, to equimolarity (the arrows indicate changes in absorbance with increase of I_2 added).

benzoylthioureato)diiodoplatinum(IV) *cis*-$[Pt^{IV}(\mathbf{L}^{1a}\text{-}\boldsymbol{S,O})_2I_2]$ (2.676(1)/2.674(1) Å and 178.2(1)°, respectively; see Table 2.1). The Pt-S bond lengths for the two compounds *cis*-$[Pt^{IV}_2(\mathbf{L}^{m1}\text{-}\boldsymbol{S,O})_2I_4]$ and *cis*-$[Pt^{IV}(\mathbf{L}^{1a}\text{-}\boldsymbol{S,O})_2I_2]$ are on average very similar (2.271(11)/2.301(11) Å and 2.283(1)/2.281(1) Å, respectively), as are the Pt-O bond lengths (2.049(2)/2.057(2) Å for **35**, and 2.058(2)/2.055(3) for *cis*-$[Pt^{IV}(\mathbf{L}^{1a}\text{-}\boldsymbol{S,O})_2I_2]$). A comparison of the average of the Pt-S bond lengths ($Pt\text{-}S_{avg}$) and the average of the Pt-O bond lengths ($Pt\text{-}O_{avg}$) for the Pt(IV) product **35** and the Pt(II) starting compound **34**, reveals that while $Pt\text{-}O_{avg}$ for **35** (2.053 Å) is only slightly longer than $Pt\text{-}O_{avg}$ for **34** ($Pt\text{-}O_{avg}$, 2.038 Å[12]), the $Pt\text{-}S_{avg}$ value for the Pt(IV) compound (2.286 Å) is considerably longer than that for *cis*-$[Pt^{II}_2(\mathbf{L}^{m1}\text{-}\boldsymbol{S,O})_2]$ ($Pt\text{-}S_{avg}$, 2.230 Å[12]). Similar bond elongation is observed in *cis*-$[Pt^{IV}(\mathbf{L}^{1a}\text{-}\boldsymbol{S,O})_2I_2]$ compared to the Pt(II) precursor (Chapter 2). The increase in the formal oxidation state of the metal centres in the oxidative addition product might be expected to lead to shorter Pt-S and Pt-O bond distances, but the observed elongation is likely to be due to the steric requirements of the bulky iodo ligands in the platinum coordination sphere.

The maximum deviation from a least squares plane through the atoms Pt(1)/S(1)/O(1)/S(2^i)/O(2^i) (symmetry code: (i) 1-x, 1-y, 1-z) is calculated to be 0.011(1) Å for Pt(1), indicating a planarity of these atoms similar to that observed for *cis*-$[Pt^{IV}(\mathbf{L}^{1a}\text{-}\boldsymbol{S,O})_2I_2]$. In the molecular structure of compound **35**, one of the *S,O*-donating moieties coordinated to a Pt(IV) centre is twisted considerably out of the $Pt^{IV}S_2O_2$ plane; the angle between a plane through S(1)/C(32)/N(2)/N(1)/C(31) (maximum deviation from this plane is 0.120(2) Å for N(1)) and the Pt(1)/S(1)/O(1)/S(2^i)/O(2^i) coordination plane is 44.63(10)°. The angle

Stellenbosch University http://scholar.sun.ac.za

between a plane through S(2)/C(52)/N(4)/N(3)/C(51) (maximum deviation from this plane is 0.074(2) Å for N(3)) and the $Pt^{IV}S_2O_2$ plane is only 6.54(13)°. These angles illustrate considerable ligand buckling in the crystal structure of compound **35**. Moreover, the ligands are also bent along the length of the molecule, due to a 1.313(6) Å relative displacement of the coordination planes (as seen in Fig. 3.5). Two intramolecular weak hydrogen bonds (C(33)-H(33B)···S(1) and C(53)-H(53B)···S(2)) are evident in the crystal structure of *cis*-$[Pt^{IV}_2(L^{m1}$-*S*,*O*$)_2I_4]$; details are presented in Table 3.2.

A particularly noteworthy feature in compound **35**, is that the molecules of *cis*-$[Pt^{IV}_2(L^{m1}$-*S*,*O*$)_2I_4]$ pack with I(1)-Pt(1)-I(2) axes essentially parallel, but offset (Pt(1)-I(1)···I(1^{ii}), 149.4(1)°; symmetry code: (ii) 1-x, 1-y, 2-z), with nearest-neighbour I(1)···I(1^{ii}) distances of 3.775(1) Å (Fig. 3.5). These distances are significantly shorter than the sum of the van der Waals radii for two iodine atoms (4.2 Å[32]), and suggest the occurrence of intermolecular I(1)···I(1^{ii}) interactions in the solid. These interactions occur only between iodine I(1) atoms, thus leading to *chains* of weakly linked *cis*-$[Pt^{IV}_2(L^{m1}$-*S*,*O*$)_2I_4]$ metallamacrocycles in the solid. Similar intermolecular I···I interactions were also seen to occur in crystals of *cis*-bis(*N*,*N*-diethyl-*N'*-benzoylthioureato)diiodoplatinum(IV) *cis*-$[Pt^{IV}(L^{1a}$-*S*,*O*$)_2I_2]$, for which nearest-neighbour iodide distances

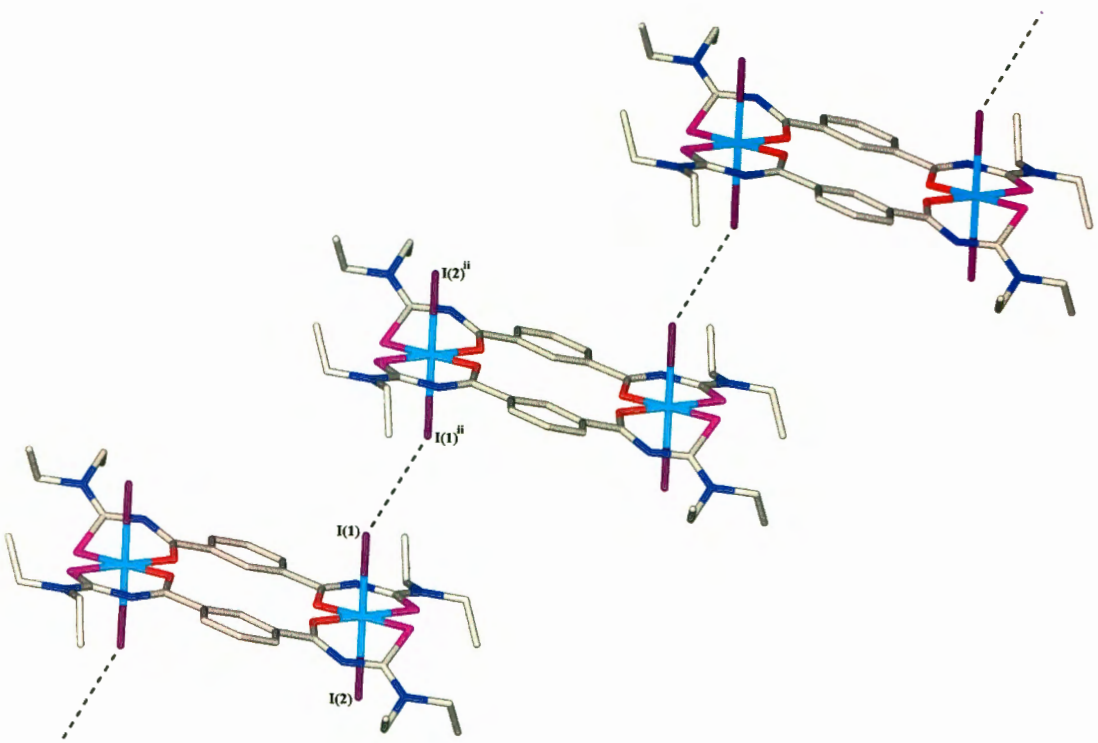

Fig. 3.5 In crystals of compound **35**, molecules of *cis*-$[Pt^{IV}_2(L^{m1}$-*S*,*O*$)_2I_4]$ pack with nearest-neighbour I(1)···I(1^{ii}) distances of 3.775(1) Å. These distances suggest intermolecular I···I interactions, leading to *chains* of weakly connected *cis*-$[Pt^{IV}_2(L^{m1}$-*S*,*O*$)_2I_4]$ molecules in the solid. Molecules are shown in wireframe style for clarity; H atoms have been omitted. Symmetry code: (ii) 1-x, 1-y, 2-z.

Table 3.1 Selected bond lengths (Å) and angles (°) for structures **35**, **36**, and **37**, with esds in parentheses.

	35	36	37	Disorder Alternative		35	36	37	Disorder Alternative
Pt(1)-S(1)	2.301(11)	2.282(1)	2.265(15)	2.27(2)	**Pt(1)-S(1)-C(32)**	100.21(11)	103.45(19)	105.8(6)	106.6(11)
Pt(1')-S(2)	2.271(11)	2.282(1)	2.312(3)	2.270(4)	**Pt(1')-S(2)-C(52)**	106.11(11)	104.04(19)	103.8(2)	105.0(3)
S(1)-C(32)	1.760(3)	1.743(6)	1.729(15)	1.70(2)	**S(1)-C(32)-N(1)**	118.1(2)	128.7(4)	128.1(6)	129.2(8)
S(2)-C(52)	1.734(3)	1.743(6)	1.707(6)	1.724(6)	**S(2)-C(52)-N(3)**	129.6(2)	128.1(4)	124.5(4)	129.0(4)
C(32)-N(1)	1.341(4)	1.352(7)	1.344(6)		**C(32)-N(1)-C(31)**	127.4(3)	128.1(5)	130.4(4)	
C(52)-N(3)	1.344(4)	1.353(7)	1.347(6)		**C(52)-N(3)-C(51)**	128.9(3)	128.5(5)	130.9(4)	
N(1)-C(31)	1.317(4)	1.329(7)	1.304(6)		**N(1)-C(31)-O(1)**	130.0(3)	130.4(5)	130.5(4)	
N(3)-C(51)	1.312(4)	1.312(7)	1.301(6)		**N(3)-C(51)-O(2)**	130.9(3)	131.7(5)	130.2(4)	
C(31)-O(1)	1.273(4)	1.277(7)	1.267(5)		**C(31)-O(1)-Pt(1)**	125.7(2)	126.1(4)	126.9(3)	
C(51)-O(2)	1.275(4)	1.286(7)	1.253(5)		**C(51)-O(2)-Pt(1')**	125.6(2)	124.2(3)	126.8(3)	
O(1)-Pt(1)	2.057(2)	2.040(4)	2.040(3)		**N(1)-C(32)-N(2)**	116.9(3)	114.9(5)	116.5(4)	
O(2)-Pt(1')	2.049(2)	2.064(4)	2.055(3)		**N(3)-C(52)-N(4)**	115.1(3)	115.7(5)	116.8(4)	
C(32)-N(2)	1.321(4)	1.317(7)	1.319(6)		**O(1)-Pt(1)-S(1)**	92.56(7)	95.03(12)	96.0(4)	96.0(4)
C(52)-N(4)	1.330(4)	1.328(7)	1.307(6)		**O(2)-Pt(1')-S(2)**	95.98(7)	94.10(11)	92.94(14)	96.54(14)
35									
Pt(1)-I(1)	2.667(1)	**I(1)-Pt(1)-I(2)**	178.86(1)	**S(1)-Pt(1)-I(1)**	89.84(3)	**S(2')-Pt(1)-I(1)**	89.75(4)	**O(2')-Pt(1)-S(1)**	175.99(7)
Pt(1)-I(2)	2.672(1)	**O(1)-Pt(1)-I(1)**	89.62(8)	**O(2')-Pt(1)-I(1)**	89.28(8)	**S(2')-Pt(1)-O(1)**	179.21(7)		
36									
Pt(1)-Br(1)	2.425(1)	**Br(1)-Pt(1)-Br(2)**	177.80(3)	**S(1)-Pt(1)-Br(1)**	89.59(4)	**S(2')-Pt(1)-Br(1)**	92.62(4)	**O(2')-Pt(1)-S(1)**	178.53(12)
Pt(1)-Br(2)	2.437(1)	**O(1)-Pt(1)-Br(1)**	87.83(12)	**O(2')-Pt(1)-Br(1)**	89.17(12)	**S(2')-Pt(1)-O(1)**	178.18(12)		
37									
Pt(1)-Cl(1A)	2.246(2)	**Cl(1A)-Pt(1)-Cl(2A)**	178.23(11)	**S(1A)-Pt(1)-Cl(1A)**	92.1(3)	**S(2A')-Pt(1)-Cl(1A)**	92.96(12)	**O(2')-Pt(1)-S(1A)**	176.9(3)
Pt(1)-Cl(2A)	2.420(4)	**O(1)-Pt(1)-Cl(1B)**	94.82(16)	**O(2')-Pt(1)-Cl(1A)**	84.78(18)	**S(2A')-Pt(1)-O(1)**	171.38(19)		
Pt(1)-Cl(1B)	2.456(5)	**Cl(1B)-Pt(1)-Cl(2B)**	174.93(16)	**S(1B)-Pt(1)-Cl(1B)**	88.7(5)	**S(2B')-Pt(1)-Cl(1B)**	87.2(2)	**O(2')-Pt(1)-S(1B)**	173.3(5)
Pt(1)-Cl(2B)	2.189(6)	**O(1)-Pt(1)-Cl(1B)**	79.6(2)	**O(2')-Pt(1)-Cl(1B)**	97.9(2)	**S(2B')-Pt(1)-O(1)**	166.7(3)		

Symmetry code: (s) 1-x, 1-y, 1-z.

Stellenbosch University http://scholar.sun.ac.za

Stellenbosch University http://scholar.sun.ac.za

were observed to be 3.553(1) Å. Several neutral *trans*-Pt(IV)-iodo compounds with intermolecular iodine distances less than twice the van der Waals radius of iodine have been documented.[31] Some examples (with nearest-neighbour iodide distances in parentheses) include diiodomethyl(bis(pyrazol-1-yl)(thien-2-yl)methane-*N*,*N*')platinum(IV) (3.787 Å),[33] diiodo(heptafluoro-*n*-propyl)-methyl-(*N*,*N*,*N*',*N*'-tetramethyl-ethylenediamine)platinum(IV) (3.834 Å),[28] diiododimethyl-bis(4-(2-((4-heptoxy)phenyl)ethenyl)-pyridyl)platinum(IV) (3.844 Å),[34] *trans*-Pt(acetylacetonato)$_2$I$_2$ (3.558 Å),[35] [*cis*-Pt(ethylamine)I$_4$] (3.480 Å),[36] and [Pt(*o*-diaminobenzene)I$_3$] (3.487 Å),[37] but only the latter three reports refer to the occurrence of *trans*-Pt(IV)-iodo chains in the solids.

3.3.3 Synthesis by electrolysis: oxidative addition of Br_2 and Cl_2 to 2 : 2 cis-[$Pt^{II}_2(L^{m1}$-S,O)$_2$] 34

An alternative approach to the synthesis of Pt(IV) compounds, which has been used successfully for the preparation of for example *trans*-[Pt^{IV}(acac)$_2$X$_2$] (acac = acetylacetonate; X = Br, Cl) from Pt^{II}(acac)$_2$, is by means of electrolysis in a cell containing a suitable Pt(II) compound and a chosen halide.[38] This method was explored due to difficulty experienced in isolating product crystals from solutions of **34** treated with dibromine. Moreover, our previous studies of oxidative halogen addition to the mononuclear analogue *cis*-bis(*N*,*N*-diethyl-*N*'-benzoylthioureato)platinum(II) *cis*-[Pt^{II}(L^{1a}-*S*,*O*)$_2$], had indicated the *destructive* oxidation of these types of compounds on treatment with gaseous dichlorine (Chapter 2). A simple and easy to use electrolytic cell was custom-made; a description of the cell and set-up is given in the Experimental Section and shown in Fig. 3.1. The electrolyte solution of tetrabutylammoniumbromide in dichloromethane was placed in each compartment of the cell, with a known quantity of compound **34** added to the solution in the anodic compartment; a potential difference of 2.2V was applied across the immersed platinum electrodes. After several days good quality crystals had formed directly on the anode of the cell, and characterization of the isolated, washed and dried crystals by single crystal X-ray diffraction and elemental analysis, confirmed the product to be *cis*-[Pt^{IV}_2(L^{m1}-*S*,*O*)$_2$Br$_4$] **36** (Fig. 3.6).

Similarly, the application of the electrolysis cell with tetrabutylammonium*chloride* in dichloromethane as electrolyte, and **34** as starting compound, led to the formation of crystals identified by elemental analysis and single crystal diffractometry to be the product *cis*-[Pt^{IV}_2(L^{m1}-*S*,*O*)$_2$Cl$_4$] **37** (Fig. 3.7).

Considering the large excess of bromide and chloride relative to the starting compound **34** in the cells (more than 32 times in excess), and the large potential difference applied to the cells, it is likely that the observed Pt(IV) products are formed *predominantly* by oxidative addition of Br_2 or Cl_2 that is produced *in situ* at the anode. Application of the electrolysis cell presumably leads to a slower and more 'controlled' release of the oxidants, which benefits the crystallization of the sparingly soluble Pt(IV) products.

Stellenbosch University http://scholar.sun.ac.za

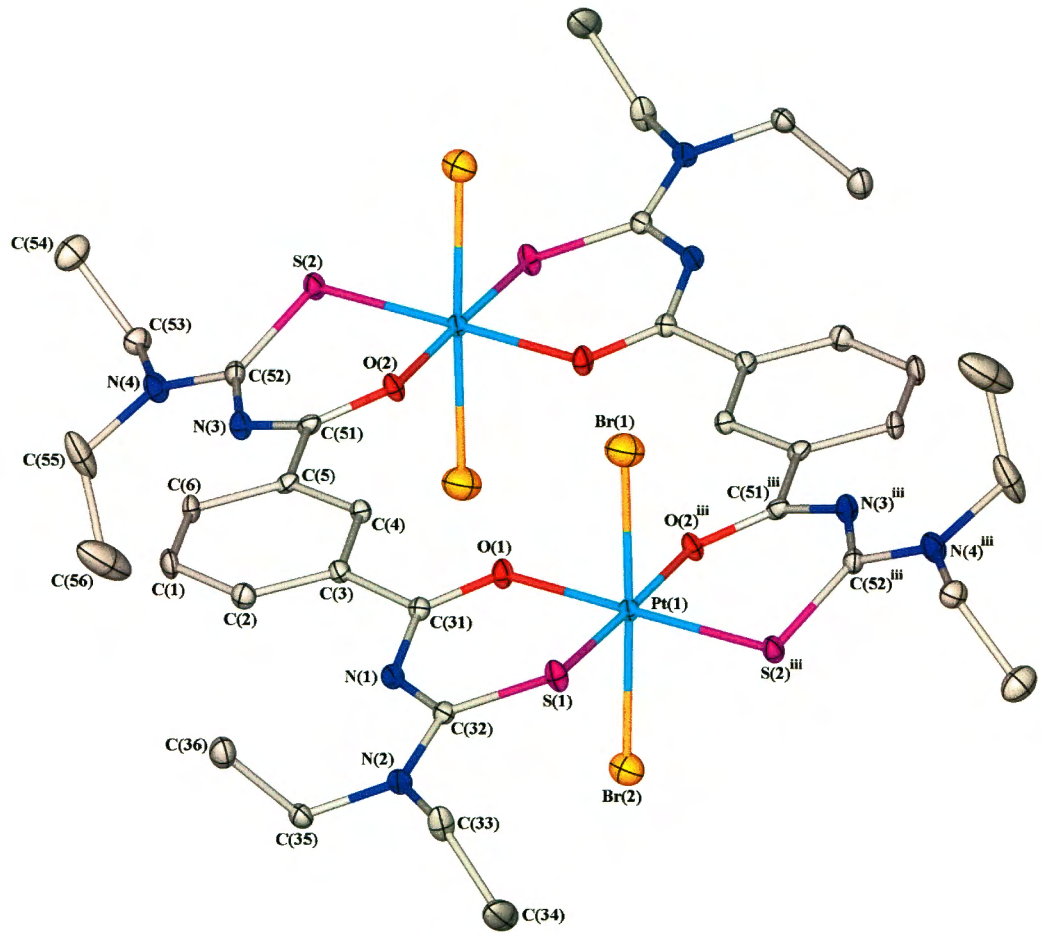

Fig. 3.6 The molecular structure of *cis*-[$Pt^{IV}_2(L^{m1}$-*S,O*$)_2Br_4$] **36** with atom numbering scheme. Displacement ellipsoids are drawn at the 50% probability level, and H atoms have been omitted for clarity. The bipodal ligands are twisted considerably out of the coordination planes, leading to significant puckering of the Pt-S-C-N-C-O chelating rings. Selected bond lengths and angles are given in Table 3.1. Symmetry code: (iii) 1-x, 1-y, 1-z.

3.3.4 Crystal and molecular structure of cis-[$Pt^{IV}_2(L^{m1}$-S,O$)_2Br_4$] 36

This compound crystallizes *P*21/*c*, with only one half of the molecule comprising the asymmetric unit; an inversion centre at (1/2 1/2 1/2) generates the full molecule from the asymmetric half. The bipodal ligands remain coordinated in a *cis S,O*-fashion, and bromide ions occupy the remaining sites in the octahedral Pt(IV) coordination sphere (Fig. 3.6). The atoms Pt(1)/S(1)/O(1)/S(2^{iii})/O(2^{iii}) (symmetry code: (iii) 1-x, 1-y, 1-z) are planar, with a maximum deviation of 0.018(2) Å calculated for O(2^{iii}). The two bipodal ligands do not lie in the coordination planes but are twisted considerably out of these planes, in opposite directions. The angle between the planar atoms S(1)/C(32)/N(2)/N(1)/C(31) (maximum deviation of 0.023(4) Å for N(1)) and the $Pt^{IV}S_2O_2$ coordination plane is 29.20(17)°. The angle between a least squares plane through S(2^{iii})/C(52^{iii})/N(4^{iii})/N(3^{iii})/C(51^{iii}) (a maximum deviation from this plane of 0.023(5) Å is calculated for C(52^{iii})) and the Pt(1)/S(1)/O(1)/S(2^{iii})/O(2^{iii}) plane is 30.56(15)°. These angles illustrate that the metallamacrocycle, when viewed side-on with the platinum centres eclipsed, has a puckered shape, very

Stellenbosch University http://scholar.sun.ac.za

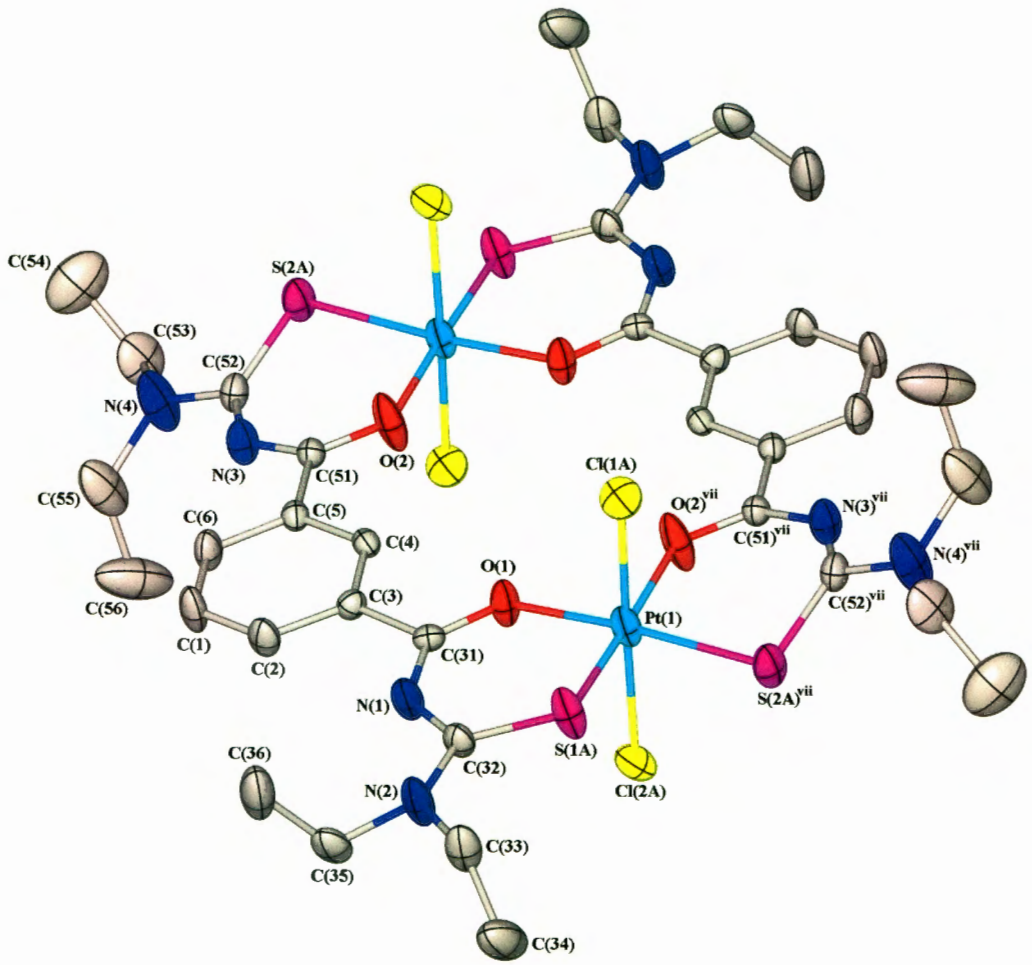

Fig. 3.7 The molecular structure of *cis*-[Pt^{IV}_2(L^{m1}-*S*,*O*)$_2Cl_4$] **37** with atom numbering scheme. Displacement ellipsoids are drawn at the 50% probability level, and H atoms have been omitted for clarity. The molecules in this compound are notably more planar than those in structures **35** and **36**. Selected bond lengths and angles are given in Table 3.1. Symmetry code: (vii) 1-x, 1-y, 1-z.

similar to that which has been reported for the corresponding mononuclear analogue *cis*-bis(*N*,*N*-diethyl-*N*'-benzoylthioureato)dibromoplatinum(IV) *cis*-[Pt^{IV}(L^{1a}-*S*,*O*)$_2Br_2$] (Chapter 2). As in compound **35**, the coordination planes of the metal centres are parallel, but not aligned, with one plane displaced by 0.528(9) Å relative to the other.

The Pt-Br bond lengths in **36** (2.437(1)/2.425(1) Å; see Table 3.1) are shorter than the Pt-Br distances in the mononuclear *cis*-[Pt^{IV}(L^{1a}-*S*,*O*)$_2Br_2$] (2.460(1)/2.462(1) Å; see Table 2.1). The Pt-O lengths in **36** (2.064(4)/2.040(4) Å) are on average slightly longer than the corresponding distances in *cis*-[Pt^{IV}(L^{1a}-*S*,*O*)$_2Br_2$] (2.044(2)/2.043(3) Å), while the Pt-S distances for **36** and *cis*-[Pt^{IV}(L^{1a}-*S*,*O*)$_2Br_2$] are comparable (2.282(1)/2.282(1) Å and 2.280(1)/2.280(1) Å, respectively). The slightly longer Pt-S and Pt-O distances

Stellenbosch University http://scholar.sun.ac.za

for **36**, by comparison to *cis*-[Pt^{IV}(**L^{1a}-*S*,*O***)$_2Br_2$], probably allow for the closer approach of the bromide ions to the metal centre in **36**.

The molecules in the crystal structure of compound **36** have two distinct orientations, the alternative orientation related to the asymmetric half molecule by a two-fold screw axis and a c-glide plane normal to the *b*-axis. A packing diagram viewed along the *a*-axis overlays molecules of similar orientation, and reveals *layers* of similarly oriented molecules parallel to the *a*,*c*-plane, with orientations alternating along the *b*-axis (Fig. 3.8). Four intermolecular weak hydrogen bonds were found to occur in the structure (see Table 3.2). The intermolecular C(56)-H(56A)···Br(1^{iv}) and C(53)-H(53A)···Br(1^{iv}) hydrogen bonds (symmetry code: (iv) x-1, y, z-1) connect molecules, which lie in a layer, diagonally across the *a*,*c*-plane, while the C(33)-H(33B)···Br(2^{v}) (symmetry code: (v) x, 1/2-y, 1/2+z) and C(34)-H(34A)···Br(1^{vi}) (symmetry code: (vi) 1-x, y-1/2, 3/2-z) hydrogen bonds link alternatively oriented molecules in adjacent layers. Two intramolecular weak hydrogen bonds (C(33)-H(33B)···S(1) and C(53)-H(53B)···S(2)) also occur in the structure (see Table 3.2). No intermolecular Br···Br interactions are apparent in this compound.

Although the structural data of several *trans*-Pt(IV)-bromo complexes are reported in the Cambridge Structural Database,[31] compound **36** appears to be the first of such structures which is classified as metallamacrocyclic.

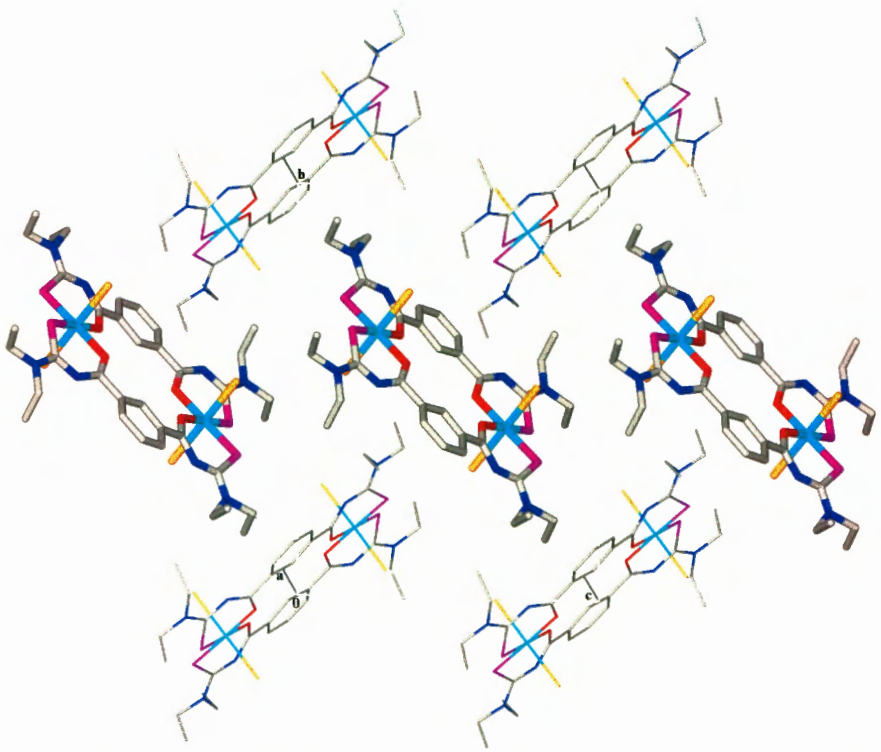

Fig. 3.8 A packing diagram for structure **36**, *cis*-[Pt^{IV}_2(**L^{m1}-*S*,*O***)$_2Br_4$], shows that the molecules have two different orientations in the crystal. A view along the *a*-axis overlays molecules of a similar orientation (the unit cell is shown; for clarity molecules have not been overlayed in this figure), and reveals layers of similarly oriented molecules parallel to the *a*,*c*-plane, with orientations alternating along the *b*-axis.

Stellenbosch University http://scholar.sun.ac.za

Table 3.2 Hydrogen-bonding geometry (Å, °) for structures **35**, **36**, and **37**.

Donor-H···Acceptor	Donor-H	H···Acceptor	Donor···Acceptor	Donor-H···Acceptor
35				
C(33)-H(33B)···S(1)	0.99	2.51	2.983(4)	109
C(53)-H(53B)···S(2)	0.99	2.47	2.892(4)	105
36				
C(33)-H(33B)···S(1)	0.99	2.44	2.898(6)	108
C(53)-H(53B)···S(2)	0.99	2.48	2.947(6)	108
C(56)-H(56A)···(Br1^{iv})	0.98	2.89	3.788(9)	154
C(53)-H(53A)···(Br1^{iv})	0.99	2.78	3.763(6)	174
C(33)-H(33B)···(Br2^{v})	0.99	2.87	3.739(6)	147
C(34)-H(34A)···(Br1^{vi})	0.98	2.88	3.847(8)	169
37				
C(33)-H(33B)···S(1A)	0.99	2.37	2.872(17)	110
C(53)-H(53A)···S(2A)	0.99	2.53	2.957(7)	106
C(53)-H(53B)···Cl(1A^{viii})	0.99	2.56	3.526(7)	164
C(33)-H(33B)···Cl(2A^{ix})	0.99	2.80	3.561(7)	134
C(38)-H(38C)···Cl(1A^{x})	0.98	2.56	3.490(15)	158
C(56)-H(56B)···Cl(2A^{xi})	0.98	2.62	3.494(16)	148
C(33)-H(33B)···S(1B)	0.99	2.42	2.841(24)	105
C(53)-H(53A)···S(2B)	0.99	2.25	2.818(7)	115
C(57)-H(57B)···Cl(1B^{xii})	0.99	2.11	2.779(15)	123
C(58)-H(58B)···Cl(1B^{xii})	0.98	2.98	3.394(21)	107
C(1)-H(1)···Cl(2B^{xiii})	0.95	2.93	3.551(8)	124

Symmetry codes: (iv) x-1, y, z-1; (v) x, 1/2-y, 1/2+z; (vi) 1-x, y-1/2, 3/2-z; (viii) x-1, y, z-1; (ix) x, 1/2-y, 1/2+z; (x) 1-x, y-1/2, 3/2-z; (xi) x-1, 1/2-y, z-1/2; (xii) –x, 1-y, 1-z; (xiii) x-1, y, z.

3.3.5 Crystal and molecular structure of cis-[$Pt^{IV}_2(L^{m1}$-S,O)$_2Cl_4$] 37

The molecular structure of **37** reveals that both platinum metal centres have been oxidized, the chloride ions occupying *trans* axial sites in the metal coordination sphere with the bipodal ligands *cis S,O*-coordinated (Fig. 3.7). The product crystallizes $P2_1/c$, with only half of the molecule in the asymmetric unit; the complete molecule is generated by an inversion centre at (1/2 1/2 1/2). Structure refinement indicates that two of the four ethyl chains in the asymmetric unit are disordered; alternative chains are labelled C(35)-C(36) (sof refined to 51%), C(37)-C(38) (sof refined to 49%), and C(55)-C(56) (sof refined to 51%), C(57)-C(58) (sof refined to 49%). The chloride ligands, and the sulphur donors of the thioureas, were also found to be disordered; the disorder alternatives being labelled Cl(1A)/Cl(1B), Cl(2A)/Cl(2B), S(1A)/S(1B) and S(2A)/S(2B). Comparison of the angles Cl(1A)-Pt(1)-S(1A) (92.12(31)°), Cl(1A)-Pt(1)-S(2A^{vii}) (92.96(12)°), and Cl(1A)-Pt(1)-S(1B) (101.91(47)°), Cl(1A)-Pt(1)-S(2B^{vii}) (72.09(25)°) (symmetry code: (vii) 1-x, 1-y, 1-z) with the X-Pt-S (X=I, Br) angles in structures **35** and **36** (these are all close to 90°, see Table 3.1), suggests that two arrangements of the chloride and sulphur coordinating atoms probably occur in the disorderd lattice, *viz.* Pt(1)/S(1A)/S(2A^{vii})/Cl(1A)/Cl(2A) (sof refined to 59%) and Pt(1)/S(1B)/S(2B^{vii})/Cl(1B)/Cl(2B) (sof refined to 41%), as shown in Fig. 3.9. Both disorder alternatives result in Cl-Pt-O angles notably different from 90° (see Table 3.1), but no disorder of the oxygen donors was apparent. Atoms with the highest site occupancy factors are shown in Fig. 3.7.

Stellenbosch University http://scholar.sun.ac.za

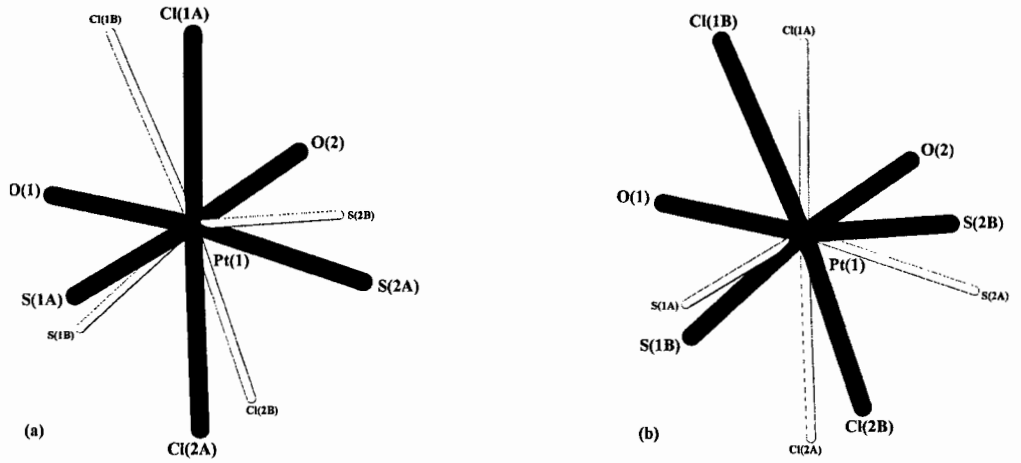

Fig. 3.9 Disordered chloride and sulphur donor positions in structure **37**; disorder alternatives have been labelled Cl(1A)/Cl(1B), Cl(2A)/Cl(2B), S(1A)/S(1B), S(2A)/S(2B). Two arrangements of the chloride and sulphur coordinating atoms most likely occur in the lattice, based on relative bond angles. In one arrangement the metal centre is coordinated to S(1A)/S(2A)/O(1)/O(2)/Cl(1A)/Cl(2A) ((a) above), and in another the atoms S(1B)/S(2B)/O(1)/O(2)/Cl(1B)/Cl(2B) are bonded to the metal ((b) above).

The Pt-Cl bond lengths in compound **37** are 2.246(2)/2.420(4) Å for Pt(1)-Cl(1A)/Pt(1)-Cl(2A) and 2.456(5)/2.189(6) Å for Pt(1)-Cl(1B)/Pt(1)-Cl(2B), with the angles Cl(1A)-Pt(1)-Cl(2A) and Cl(1B)-Pt(1)-Cl(2B) at 178.2(1)° and 174.9(2)°, respectively (see Table 3.1). No examples of neutral *trans*-Pt(IV)-chloro complexes with *S,O*-donating ligands that form six-membered chelating rings with the metal centre are described in the Cambridge Structural Database (CSD).[31] Several uncharged *trans*-Pt(IV)-chloro complexes with *N,N*-, *N,O*-, or *O,O*-donor ligands, are however structurally described; examples include *trans*-dichloro(6,8,15,17-tetramethyl-5,6,9,14,15,18-hexahydrodibenzo(*b,i*)-(1,4,8,11)-tetraazacyclotetradecine)platinum(IV) (Pt-Cl, 2.336(2)/2.337(2) Å),[39] *trans*-dichlorobis(3,5-dichlorosalicylaldoximato-*N,O*)platinum(IV) (Pt-Cl, 2.316(2) Å),[40] *tr ans*-dicloro(ethylenediamine-*N,N'*-di-3-propionato)platinum(IV) monohydrate (Pt-Cl, 2.296(2)/2.307(2) Å),[41] and *trans*-dichlorobis(acetylacetonato)platinum(IV) (Pt-Cl, 2.318(2) Å).[42] A wider search in the CSD of *all trans*-Pt(IV)-chloro compounds reveals that molecules have been characterized for which Pt-Cl bond lengths range from a short 2.228 Å to a long 2.397 Å (in e.g. 2,2'-bipyridyldichloropropane-1,3-di-ylplatinum(IV) with Pt-Cl 2.228(20) Å,[43] and *trans*-bis(1-(propoxy)propylideneamino)tetrachloroplatinum(IV) with Pt-Cl 2.228(15)/2.397(15) Å[44]). The Pt-Cl distances for structure **37** lie outside this range of bond lengths. Interestingly, the reported Pt-Cl range of bond lengths are observed in the same compound, *trans*-bis(1-(propoxy)propylideneamino)tetrachloroplatinum(IV) (Pt-Cl, 2.228(15)/2.397(15) Å[44]). Bokach *et al.*[44] report that the chloride with the longer Pt-Cl bond distance is involved in an intermolecular hydrogen bond with an imine H atom from a neighbouring molecule, while the chloride with the shorter Pt-Cl length is in a *trans* position relative to the former. Analysis of the crystal structure of compound **37** reveals that *both* chloride ligands in this complex, including the disorder alternatives, are involved in intermolecular

Stellenbosch University http://scholar.sun.ac.za

hydrogen bonding, leading to an intricate network of weakly bonded molecules similar to that observed in structure **36** (see Table 3.2). The intramolecular C-H···S hydrogen bonds observed in both compounds **35** and **36**, are also evident in *cis*-$[Pt^{IV}_2(\mathbf{L}^{m1}\text{-}\boldsymbol{S,O})_2Cl_4]$. No intermolecular Cl···Cl interactions were observed.

The $Pt\text{-}O_{avg}$ and $Pt\text{-}S_{avg}$ values for compounds **35** (2.053 Å and 2.286 Å, respectively), **36** (2.052 Å and 2.282 Å, respectively) and **37** (2.048 Å and 2.279 Å, respectively) are virtually indistinguishable. The disordered S-donors prohibit planarity of the $Pt^{IV}S_2O_2$ moiety, in contrast to that observed in compounds **35** and **36**, leading to rms deviations of 0.095 Å and 0.169 Å for the planes Pt(1)/S(1A)/O(1)/S(2A^{vii})/O(2^{vii}) and Pt(1)/S(1B)/O(1)/S(2B^{vii})/O(2^{vii}), respectively. The molecules as a whole in **37**, however, are significantly more planar than in either **35** or **36**, with the rms deviation for a plane through the phenylene spacer and $Pt^{IV}O$ moieties calculated at 0.030 Å in **37**. The molecular packing in crystals of compound **37** is similar to that described for structure **36** (shown in Fig. 3.8).

3.4 Concluding Remarks

Pt(IV) *metallamacrocyclic* complexes of the bipodal 3,3,3',3'-tetraalkyl-1,1'-phenylenedicarbonylbis(thioureas) may be readily synthesised by oxidative addition of dihalogens to the Pt(II) compounds of these ligands. Elemental I_2 and Br_2 cleanly react with the 3 : 3 Pt(II) metallamacrocycle of 3,3,3',3'-tetra(*n*-butyl)-1,1'-terephthaloylbis(thiourea) (*cis*-$[Pt^{II}_3(\mathbf{L}^{p1}\text{-}\boldsymbol{S,O})_3]$ **33**), in chloroform at room temperature, to yield oxidative addition products; ^{195}Pt NMR studies reveal that a stepwise oxidative addition readily occurs to each of the Pt(II) centres in the metallamacrocycle to yield the mixed valence species *cis*-$[Pt^{II}_2Pt^{IV}I_2(\mathbf{L}^{p1}\text{-}\boldsymbol{S,O})_3]$ and *cis*-$[Pt^{II}Pt^{IV}_2I_4(\mathbf{L}^{p1}\text{-}\boldsymbol{S,O})_3]$, and the fully oxidised *cis*-$[Pt^{IV}_3I_6(\mathbf{L}^{p1}\text{-}\boldsymbol{S,O})_3]$ in solution, depending on the mole ratio I_2 : **33**. Similar results are obtained on treatment of solutions of **33** with elemental Br_2. Treatment of the corresponding 2 : 2 Pt(II) complex of 3,3,3',3'-tetraethyl-1,1'-isophthaloylbis(thiourea) (*cis*-$[Pt^{II}_2(\mathbf{L}^{m1}\text{-}\boldsymbol{S,O})_2]$ **34**) with iodine, results in facile oxidative addition to yield *cis*-$[Pt^{IV}_2(\mathbf{L}^{m1}\text{-}\boldsymbol{S,O})_2I_4]$ **35**, with a *trans*-Pt(IV)-iodo arrangement. Molecules in the crystal structure of **35** have their *trans*-Pt(IV)-iodo axes essentially aligned, with very close intermolecular iodide contacts (3.775(1) Å), resulting in chains of weakly bound metallamacrocycles in the solid. An alternative electrolytic synthesis method using a simple two-compartment glass cell containing **34** and a chosen halide salt in dichloromethane, in which the Br_2 and Cl_2 oxidants are released *in situ* at the anode, led to the formation of *cis*-$[Pt^{IV}_2(\mathbf{L}^{m1}\text{-}\boldsymbol{S,O})_2Br_4]$ **36** and *cis*-$[Pt^{IV}_2(\mathbf{L}^{m1}\text{-}\boldsymbol{S,O})_2Cl_4]$ **37**, completing characterization of a series of first-reported *trans*-Pt(IV)-X (X = I, Br, Cl) metallamacrocyclic complexes.

Of particular interest for future work with regard to the 2 : 2 and 3 : 3 *trans*-Pt(IV)-X (X = Cl, Br, I) metallamacrocycles, is the possibility for the formation of ···Pt(II)···X-Pt(IV)-X··· mixed-valence complexes, leading to assembly of the metallamacrocycles into higher ordered structures. Aoyagi *et al.*[45] report that the reaction of the square Pt(II) or Pd(II) compounds $[(en)M(4,4'\text{-}bpy)]_4(NO_3)_8$ (M = Pt(II),

Stellenbosch University http://scholar.sun.ac.za

Pd(II); en = ethylene diamine; 4,4'-bpy = 4,4'-bipyridine) with $[Pt^{IV}Br_2(en)_2]^{2+}$ or PtX_6^{2-} (X = Cl, Br) lead to higher ordered infinite compounds due to the formation of ···Pt(II)···X-Pt(IV)-X··· mixed-valence complexes. Reaction of the isolated 2 : 2 *trans*-Pt(IV)-X (X = Cl, Br, I) metallamacrocycles with $PtCl_4^{2-}$, or the reaction of the 2 : 2 Pt(II) metallamacrocycle with such compounds as *cis*-$[Pt^{IV}(\mathbf{L^{1a}}\text{-}\boldsymbol{S,O})_2I_2]$ or *cis*-$[Pt^{IV}(\mathbf{L^{1a}}\text{-}\boldsymbol{S,O})_2Br_2]$ (described in Chapter 2), may similarly lead to the formation of mixed-valence complexes and new higher ordered structures. Alternatively, attempts may be made to remove the *trans* halide ligands of the 2 : 2 *trans*-Pt(IV)-X (X = Cl, Br, I) metallamacrocycles, by treatment with silver perchlorate in a suitable solvent, followed by the addition of linker molecules such as 4,4'-bipyridine to allow self-assembly into infinite metal-organic frameworks.

Table 3.3 Crystal and structure refinement data for compounds **35**, **36**, and **37**.

	cis-$[Pt^{IV}_2(\mathbf{L^{m1}}\text{-}\boldsymbol{S,O})_2I_4]$ **35**	*cis*-$[Pt^{IV}_2(\mathbf{L^{m1}}\text{-}\boldsymbol{S,O})_2Br_4]$ **36**	*cis*-$[Pt^{IV}_2(\mathbf{L^{m1}}\text{-}\boldsymbol{S,O})_2Cl_4]$ **37**
Molecular formula	$C_{36}H_{48}I_4N_8O_4Pt_2S_4$	$C_{36}H_{48}Br_4N_8O_4Pt_2S_4$	$C_{36}H_{48}Cl_4N_8O_4Pt_2S_4$
Formula weight	1682.84	1494.88	1317.04
Crystal system	Triclinic	Monoclinic	Monoclinic
Space group	$P\bar{1}$	$P2_1/c$	$P2_1/c$
a/ Å	10.087(2)	9.288(1)	9.260(2)
b/ Å	10.498(2)	18.736(2)	17.863(4)
c/ Å	11.975(2)	13.804(2)	14.504(3)
α / °	84.50(3)	90	90
β / °	87.24(3)	103.14(1)	107.08(3)
γ / °	80.80(3)	90	90
V / Å^3	1245.3(4)	2339.1(5)	2293.3(8)
μ / mm^{-1}	8.301	9.615	6.556
Z	1	2	2
T / K	173(2)	173(2)	173(2)
Reflections collected/unique	37186/5971 [R(int)=0.0308]	13755/5027 [R(int)=0.0313]	41212/4480 [R(int)=0.0804]
Goodness-of-fit	1.039	1.047	1.048
Final R [$I > 2\sigma(I)$] (all data)	0.0277	0.0386	0.0461
$wR2$ [$I \geq 2\sigma(I)$] (all data)	0.0479	0.0974	0.0653
Largest remaining feature in electron density map, max/min / e. Å^3	1.35 (0.75 Å from I2) -1.54 (0.70 Å from I1)	1.71 (0.19 Å from Pt1) -2.22 (0.43 Å from Br2)	1.35 (0.83 Å from Pt1) -1.29 (0.95 Å from Pt1)

References

1 S. Leininger, B. Olenyuk and P. J. Stang, *Chemical Reviews*, 2000, **100**, 853.
2 J. J. Bodwin, A. D. Cutland, R. G. Malkani and V. L. Pecoraro, *Coordination Chemistry Reviews*, 2001, **216-217**, 489.
3 F. Wurthner, C.-C. You and C. R. Saha-Moller, *Chemical Society Reviews*, 2004, **33**, 133.
4 P. Thanasekaran, R.-T. Liao, Y.-H. Liu, T. Rajendran, S. Rajagopal and K.-L. Lu, *Coordination Chemistry Reviews*, 2005, **249**, 1085.
5 M. Fujita, *Chemical Society Reviews*, 1998, **27**, 417.
6 B. Olenyuk, A. Fechtenkotter and P. J. Stang, *Journal of the Chemical Society, Dalton Transactions*, 1998, 1707.
7 G. F. Swiegers and T. J. Malefetse, *Chemical Reviews*, 2000, **100**, 3483.
8 M. Fujita, M. Tominaga, A. Hori and B. Therrien, *Accounts of Chemical Research*, 2005, **38**, 371.
9 P. J. Steel, *Accounts of Chemical Research*, 2005, **38**, 243.
10 K. R. Koch, *Coordination Chemistry Reviews*, 2001, **216-217**, 473.
11 R. Richter, J. Sieler, R. Kohler, E. Hoyer, L. Beyer and L. K. Hansen, *Zeitschrift für Anorganische und Allgemeine Chemie*, 1989, **578**, 191.

Stellenbosch University http://scholar.sun.ac.za

12 K. R. Koch, S. A. Bourne, A. Coetzee and J. Miller, *Journal of the Chemical Society, Dalton Transactions*, 1999, 3157.
13 K. R. Koch, O. Hallale, S. A. Bourne, J. Miller and J. Bacsa, *Journal of Molecular Structure*, 2001, **561**, 185.
14 S. A. Bourne, O. Hallale and K. R. Koch, *Crystal Growth & Design*, 2005, **5**, 307.
15 O. Hallale, S. A. Bourne and K. R. Koch, *Crystal Engineering Communication*, 2005, **7**, 161.
16 K.-H. König, M. Kuge, L. Kaul and H.-J. Pletsch, *Chemische Berichte*, 1987, **120**, 1251.
17 G. M. Sheldrick, SHELXS-97 and SHELXL-97, Programs for the Solution and Refinement of Crystal Structures, University of Goettingen, Germany, 1997.
18 L. J. Barbour, *Journal of Supramolecular Chemistry*, 2003, **1**, 189.
19 A. L. Spek, PLATON, A Multipurpose Crystallographic Tool, University of Utrecht, Netherlands, 1999.
20 I. J. Bruno, J. C. Cole, P. R. Edgington, M. Kessler, C. F. Macrae, P. McCabe, J. Pearson and R. Taylor, *Acta Crystallographica Section B*, 2002, **58**, 389.
21 P. S. Pregosin, *Coordination Chemistry Reviews*, 1982, **44**, 247.
22 J. Y. Lallemand, J. Soulie and J. C. Chottard, *Journal of the Chemical Society, Chemical Communications*, 1980, **10**, 436.
23 G. van Koten, J. Terheijden, J. A. M. van Beek and I. C. M. Wehman-Ooyevaar, *Organometallics*, 1990, **9**, 903.
24 L. M. Rendina and R. J. Puddephatt, *Chemical Reviews*, 1997, **97**, 1735.
25 R. A. Gossage, A. D. Ryabov, A. L. Spek, D. J. Stufkens, J. A. M. van Beek, R. van Eldik and G. van Koten, *Journal of the American Chemical Society*, 1999, **121**, 2488.
26 M. Ghedini, D. Pucci, A. Crispini and G. Barberio, *Organometallics*, 1999, **18**, 2116.
27 M. Panda, S. Das, G. Mostafa, A. Castineiras and S. Goswami, *Dalton Transactions*, 2005, 1249.
28 R. P. Hughes, J. T. Sweetser, M. D. Tawa, A. Williamson, C. D. Incarvito, B. Rhatigan, A. L. Rheingold and G. Rossi, *Organometallics*, 2001, **20**, 3800.
29 J. Ruiz, J. F. J. Lopez, V. Rodriguez, J. Perez, M. C. R. de Arellano and G. Lopez, *Journal of the Chemical Society, Dalton Transactions*, 2001, 2683.
30 M. A. Bennet, S. K. Bhargava, M. Ke and A. C. Willis, *Journal of the Chemical Society, Dalton Transactions*, 2000, 3537.
31 F. H. Allen, *Acta Crystallographica Section B*, 2002, **58**, 380.
32 J. E. Huheey, E. A. Keiter and R. L. Keiter, in *Inorganic Chemistry: Principles of Structure and Reactivity*, Harper-Collins, New York, 4th Ed., 1993.
33 A. J. Canty, R. T. Honeyman, B. W. Skelton and A. H. White, *Journal of Organometallic Chemistry*, 1990, **396**, 105.
34 P. Beagley, E. J. Starr, J. Bacsa, J. R. Moss and A. T. Hutton, *Journal of Organometallic Chemistry*, 2002, **645**, 206.
35 P. M. Cook, L. F. Dahl, D. Hopgood and R. A. Jenkins, *Journal of the Chemical Society; Dalton Transactions*, 1973, 294.
36 G. Thiele, O. F. Danzeisen, H. W. Rotter and M. Goanta, *Journal of Molecular Structure*, 1999, **482-483**, 93.
37 O. F. Danzeisen, M. Goanta, H. W. Rotter and G. Thiele, *Inorganica Chimica Acta*, 1999, **287**, 218.
38 A. Grabowski and W. Preetz, *Zeitschrift fur Anorganische und Allgemeine Chemie*, 1987, **544**, 95.
39 R. L. Paul, S. F. Gheller, G. A. Heath, D. C. R. Hochless, L. M. Rendina and M. Sterns, *Journal of the Chemical Society, Dalton Transactions*, 1997, 4143.
40 S. F. Kaplan, V. Y. Kukushkin, S. Shova, K. Suwinska, G. Wagner and A. J. L. Pombeiro, *European Journal of Inorganic Chemistry*, 2001, 1031.
41 G. N. Kaluderovic, G. A. Bogdanovic and T. J. Sabo, *Journal of Coordination Chemistry*, 2002, **55**, 817.
42 D. Rickert and W. Preetz, *Zeitschrift fur Naturforschung*, 1996, **51**, 1400.
43 R. J. Klingler, J. C. Huffman and J. K. Kochi, *Journal of the American Chemical Society*, 1982, **104**, 2147.
44 N. A. Bokach, V. Y. Kukushkin, M. L. Kuznetsov, D. A. Garnovskii, G. Natile and J. L. Pombeiro, *Inorganic Chemistry*, 2002, **41**, 2041.
45 M. Aoyagi, K. Biradha and M. Fujita, *Bulletin of the Chemical Society of Japan*, 1999, **72**, 2603.

Stellenbosch University http://scholar.sun.ac.za

Chapter 4

Hydration/Solvation Spheres of PtX_6^{2-} (X = Cl, Br) Anions Probed by ^{195}Pt NMR Spectroscopy: Preferential Solvation in Aqueous Binary Solvent Mixtures.*

The ^{195}Pt NMR chemical shifts of $PtCl_6^{2-}$ (as $H_2PtCl_6 \cdot H_2O$) in D_2O, and the organic solvents methanol, acetonitrile, acetone, hexamethylphosphorictriamide, ethylene glycol, 2-methoxyethanol, and 1,2-dimethoxyethane have been determined, and are discussed with regard to the polarities (as measured by μ, ε, and the $E_T(30)$ and Kamlet-Taft π^* parameters) and the donor and acceptor properties (measured by DN^N, AN and the Kamlet-Taft α parameter) of these solvents. The ^{195}Pt NMR chemical shifts of $PtCl_6^{2-}$ have also been measured in binary solvent mixtures of D_2O with the organic solvents. The non-linear variations of $\delta_{Pt\text{-}195}$ with changing bulk composition of the mixtures suggest that the anion is preferentially solvated by the organic solvents relative to water. Analysis of the $\delta_{Pt\text{-}195}$ variations allows estimation of the anion solvation sphere composition with changing bulk composition, as well as the quantitative characterization of the preferential solvation phenomenon in terms of preferential solvation equilibrium constants, $K^{1/n}$. The ^{195}Pt NMR chemical shift studies, and related analyses, were also carried out for $PtBr_6^{2-}$ (as H_2PtBr_6) in several of the above-mentioned solvent systems.

---

* Paper based in part on this chapter:
A. N. Westra, D. J. Robinson, A. S. Lopis, K. J. Naidoo, K. R. Koch, in *International Solvent Extraction Conference, ISEC 2005*, Conference Proceedings,Beijing China, 2005, *in press*.

Paper in progress, based on this chapter:
A. N. Westra, A. S. Lopis, K. J. Naidoo, D. J. Robinson, K. R. Koch, *Inorganic Chemistry*, 2005, *to be submitted*.

Stellenbosch University http://scholar.sun.ac.za

4.1 Introduction

Most chemical reactions which are carried out in laboratories or in industry (or which occur in natural processes), are conducted in liquid solutions and often involve ionic species. The behaviour of these ionic species depends to a large degree on the nature of the solvent present, and on the nature of the ion-solvent, ion-ion and solvent-solvent interactions which occur;[1] a growing awareness of the fundamental importance of these interactions in chemical processes, has resulted in detailed investigations over several decades.[1-9] The most common solvent, water, has received the most attention in studies of solvation, due to the practical as well as theoretical interest in ionic hydration.[1,9,10] Studies of ion solvation in non-aqueous and mixed aqueous-organic systems, which are more prevalent in 'real world' situations than single solvents, have however become more numerous in recent years as improved techniques for studying such systems, and new possibilities for applying them, have been developed.[1,9] Several methods have been introduced to study such aspects of ion solvation as ion-solvent distances, solvation numbers and ion-solvent interactions, the most useful of which are diffraction methods (X-ray, neutron, and electron diffraction, as well as EXAFS), spectroscopic methods (NMR, UV-visible and infrared-Raman), and computational methods (Monte Carlo and molecular dynamics simulations).[1,7-9]

The usefulness of molecular dynamics simulations for studying ion solvation was recently highlighted by Naidoo and Koch *et al.*, who have developed detailed models of the hydration sphere structures of a variety of anionic platinum group metal chloro complexes ($PtCl_6^{2-}$, $RhCl_6^{3-}$, $PtCl_4^{2-}$, and $PdCl_4^{2-}$), by means of DFT calculations and molecular dynamics simulations.[11,12] The detailed nature of the solvation shells of the PGM chloroanions is largely unknown, yet the degree of solvation of these anions is believed to be important in their selective separation by techniques such as ion-exchange and solvent extraction.[13] As part of our interest in understanding the fundamental aspects of the nature of the hydration and solvation of the PGM chloroanions, we have explored the potential of ^{195}Pt NMR spectroscopy as a method for studying the solvation/hydration spheres of the PtX_6^{2-} (X = Cl, Br) chloroanions.

The solvent dependence of solute-nucleus NMR chemical shifts has been used over several decades, particularly in the case of the alkali metal cations, to investigate ionic solutions of a large variety of solvents.[1,7,14] The dependence of alkali cation chemical shifts on the nature of the solvent, as well as the nature of the anion and the concentration of the salt, is exemplified by the extensive studies on sodium salts by Bloor *et al*[15] and Popov *et al.*[3,16-21] Bloor and co-workers, for example, found a fair correlation of ^{23}Na chemical shifts with solvent basicity,[15] while Popov's group were able to show a relationship between δ_{Na-23} and Gutmann donor numbers;[16-19,22] chemical shift dependence on anion nature and on concentration has been ascribed to the formation of contact ion-pairs in solution.[3,19-21] The sensitivity of alkali ion chemical shifts to species in direct contact with the cations, has allowed extensive investigations of preferential solvation phenomena of these ions in mixed solvent systems;[7,14] Popov and co-workers have studied ^{23}Na chemical shifts in a large number of binary solvent mixtures, and have found that in most cases the ability

Stellenbosch University http://scholar.sun.ac.za

of a solvent to preferentially solvate the Na^+ ion correlates well with the solvent's Gutmann donor number.[23,24] Far fewer investigations of the solvation of anions, which are generally believed to be less strongly solvated than cations,[1] by means of solute-nucleus NMR chemical shifts, are reported. The most detailed studies have been performed for F^-,[25,26] Cl^-,[25,27,28] Br^-,[28] and I^-,[28] and most have been carried out for binary solvent systems. Of particular interest are the investigations of the alkali fluorides[25] and chlorides[25] performed by Covington and co-workers in H_2O/H_2O_2 binary mixtures, since these authors developed a model for the calculation of preferential solvation equilibrium constants based on the observed solute-nucleus NMR chemical shifts.

The sensitivity of the ^{195}Pt NMR chemical shift of Pt(0), Pt(II) or Pt(IV) complexes to the nature of ligand donor atoms and their arrangement in the coordination sphere, as well as to factors such as solvent, temperature and concentration, has long been known,[14,29-36] and attempts to elucidate this sensitivity from a theoretical perspective have recently been presented.[37,38] In this work we describe the use of ^{195}Pt NMR as a sensitive probe for studying the solution environment directly around the PtX_6^{2-} (X = Cl, Br) anions. It is shown that the ^{195}Pt chemical shift for these anions at constant temperature is extremely sensitive not only to a complete change in the environment of the anion, for example with changing solvent, but that it is also sensitive to more subtle anion-environment changes, which may be brought about in binary solvent mixtures of varying composition. The data is analysed on the basis of methods developed for preferential solvation phenomena, to obtain solvation sphere structures and preferential solvation equilibrium constants.

4.2 Experimental

4.2.1 Reagents

The platinum salts $H_2PtCl_6 \cdot H_2O$ (Aldrich) and H_2PtBr_6 (Johnson Matthey PLC, Precious Metal Division) were of reagent grade quality; these were used without further purification and stored in a dessicator. The solvents used were: D_2O (Aldrich), methanol (Riedel de Haën, Chromasolv® for HPLC), acetonitrile (Aldrich, HPLC grade), acetone (Aldrich, HPLC grade), hexamethylphosphorictriamide (HMPA, Aldrich), 1,2-ethanediol (ethylene glycol, Aldrich), 2-methoxyethanol (2-MeOEt, Aldrich), and 1,2-dimethoxyethane (1,2-DME, Aldrich). All the solvents, except the ethylene glycol, were used without further purification, and all, except D_2O, were stored over freshly activated 4 Å molecular sieves (Aldrich).[39] Ethylene glycol was dried with NaOH, and distilled under vacuum; this solvent was stored under N_2.*

* *N,N*-dimethylformamide (DMF, Aldrich) was also used. Unfortunately this solvent was stored over solid potassium hydroxide, which may result in decomposition.[39] Data obtained with this solvent are shown in Table 4.8A-Adm, Table 4.8B-Adm and Fig. 4.8-Adm for $PtCl_6^{2-}$, and in Table 4.12A-Adm, Table 4.12B-Adm and Fig. 4.12-Adm for $PtBr_6^{2-}$, but are not included in the Results and Discussion.

Stellenbosch University http://scholar.sun.ac.za

4.2.2 Preparation of solutions in single solvents

For each non-aqueous solvent, and for D_2O, a stock solution of $PtCl_6^{2-}$ (as $H_2PtCl_6 \cdot H_2O$) in that solvent was prepared by weighing an appropriate mass of the platinum salt into a polytop container, pipetting 5 cm^3 of the solvent onto the salt, and weighing the resulting solution. This resulted in solutions with $[Pt^{IV}] \sim 0.1$ M; details are presented in Tables 4.1A-Adm - 4.7A-Adm, Addendum A. Similarly, stock solutions of $PtBr_6^{2-}$ (as H_2PtBr_6) were prepared in D_2O, methanol, acetonitrile, and acetone; details are presented in Tables 4.9A-Adm - 4.11A-Adm, Addendum A. ^{195}Pt NMR spectra were recorded of each of the solutions.

Solutions of $H_2PtCl_6 \cdot H_2O$ in D_2O ($[PtCl_6^{2-}] = 0.00846$ M), methanol ($[PtCl_6^{2-}] = 0.00874$ M), acetonitrile ($[PtCl_6^{2-}] = 0.00715$ M), acetone ($[PtCl_6^{2-}] = 0.00715$ M), and hexamethylphosphorictriamide ($[PtCl_6^{2-}] = 0.00879$ M) were also prepared, by weighing off appropriate quantities of the platinum salt, and dissolving in each solvent to a final volume of 5 cm^3. UV-visible spectra of the solutions were recorded.

4.2.3 Preparation of binary solvent mixtures

The stock solutions containing $PtCl_6^{2-}$ (see Section 4.2.2) were used to prepare the following binary solvent systems: D_2O/methanol (Table 4.1A-Adm), D_2O/ethylene glycol (Table 4.2A-Adm), D_2O/acetonitrile (Table 4.3A-Adm), D_2O/acetone (Table 4.4A-Adm), D_2O/2-methoxyethanol (Table 4.5A-Adm), D_2O/hexamethylphosphorictriamide (Table 4.6A-Adm), and D_2O/1,2-dimethoxyethane (Table 4.7A-Adm). For every binary solvent series, each mixed solvent solution was prepared by taring a polytop container, adding an appropriate quantity of **Solution A** ($PtCl_6^{2-}$ in D_2O, **Sol(A)** in Tables 4.1A-Adm - 4.7A-Adm), weighing, adding the desired quantity of **Solution B** ($PtCl_6^{2-}$ in non-aqueous solvent, **Sol(B)** in Tables 4.1A-Adm - 4.7A-Adm), and weighing again. Thus, each system comprised a series of solutions in which the platinum concentration did not vary significantly, and with increasing mole fraction non-aqueous solvent through the series. The mole fraction of the non-aqueous solvent in each mixed solvent solution (equation (4.1)) was calculated from the known masses of stock solutions used, the appropriate concentration term ("grams $H_2PtCl_6 \cdot H_2O$ per gram solution"), and the solvent molar masses.

$$\text{Mole fraction non - aqueous solvent} = \frac{\text{moles non - aqueous solvent}}{\text{total moles of solvent}} \qquad (4.1)$$

A concentration term, "grams $H_2PtCl_6 \cdot H_2O$ per gram solution", can be calculated from the masses of $H_2PtCl_6 \cdot H_2O$ and the stock solutions. Multiplying this term with the mass of the stock solution used for a particular mixed solvent sample, allows calculation of the contribution of $H_2PtCl_6 \cdot H_2O$ to the mass of the sample and thus the contribution of the solvent to the mass. The mass and molar mass of the solvent are used to calculate the moles of solvent, and subsequently the mole fraction non-aqueous solvent in each sample.

Stellenbosch University http://scholar.sun.ac.za

The following binary solvent systems with $PtBr_6^{2-}$ (as H_2PtBr_6) were also prepared as described above: D_2O/methanol (Table 4.9A-Adm), D_2O/acetonitrile (Table 4.10A-Adm), and D_2O/acetone (Table 4.11A-Adm).

4.2.4 Measurements

Appropriate volumes of all sample solutions were transferred to 5 mm OD NMR tubes and ^{195}Pt NMR spectra were recorded. All ^{195}Pt chemical shifts are quoted relative to an 'external' Pt(IV) reference solution contained in a 2mm OD coaxial insert tube which was inserted into each sample NMR tube prior to measurement. Different reference solutions were used for mixtures with $PtCl_6^{2-}$ (500 mg cm^{-3} $H_2PtCl_6{\cdot}H_2O$ in 30 % v/v D_2O / 1 M HCl), and for mixtures with $PtBr_6^{2-}$ (250 mg cm^{-3} H_2PtBr_6 in 67 % v/v D_2O / 3 M HBr). Positive chemical shifts indicate resonance positions downfield, and negative chemical shifts positions upfield, of the reference resonance peak. ^{195}Pt NMR spectra were recorded at 30°C using a Varian INOVA 600 MHz spectrometer operating at 128 MHz, and chemical shifts are estimated to be accurate to ± 2 ppm. The ^{195}Pt chemical shifts measured for the prepared solutions are given in Tables 4.1A-Adm - 4.12A-Adm in Addendum A. ^{195}Pt chemical shifts were not corrected for the difference in magnetic susceptibility between sample and reference (see Section 5.2.4, Chapter 5), since the corrections were found to be smaller than the estimated chemical shift errors.

UV-visible spectrophotometric experiments were carried out with an Agilent 8453E UV-visible spectrophotometer (Agilent Technologies). Spectra were recorded in 2 mm quartz cuvettes relative to the appropriate solvent.

4.3 Results and discussion

4.3.1 ^{195}Pt chemical shifts in single solvents

The non-aqueous solvents which could be used for the preparation of solutions in this investigation, were those that met the following criteria:

- solvents in which the platinum salts ($H_2PtCl_6{\cdot}H_2O$ and H_2PtBr_6) are soluble, to the extent that solutions with $[Pt^{IV}] \sim 0.1$ M can be prepared,
- solvents that do not react with the platinum salts, and
- solvents that are miscible with water (D_2O).

Solvents which met these requirements were methanol, 1,2-ethanediol (ethylene glycol), acetonitrile, acetone, 2-methoxyethanol (2-MeOEt), hexamethylphosphoric triamide (HMPA), and 1,2-dimethoxyethane (1,2-DME); abbreviations given in parentheses are sometimes used for simplicity. Formamide was tested as a potential solvent, but, although the $H_2PtCl_6{\cdot}H_2O$ was found to be soluble in this solvent, a black precipitate, presumably reduced platinum, was found to form in these solutions ca. 5 hrs after preparation,

Stellenbosch University http://scholar.sun.ac.za

precluding its use. A similar black precipitate also formed in solutions with methanol and $H_2PtCl_6 \cdot H_2O$ as salt, but this occurred only several days after solution preparation, allowing sufficient time for all the required measurements to be performed. Dioxane, although miscible with water, could not be used due to the low solubility of $H_2PtCl_6 \cdot H_2O$ in this solvent.

A ^{195}Pt NMR spectrum of each of the solutions with $PtCl_6^{2-}$, or $PtBr_6^{2-}$, *in a single solvent*, was measured in an NMR tube containing a coaxial insert filled with an appropriate platinum NMR reference solution. Each sample spectrum thus comprises two peaks: one resonance due to the reference solution, and the other arising from the anion ($PtCl_6^{2-}$ or $PtBr_6^{2-}$) in the sample solution. A typical ^{195}Pt spectrum obtained for the ethylene glycol-$PtCl_6^{2-}$ solution is shown in Fig. 4.1; the insert is an enlargement of the sample peak. In the spectrum, the peak at right is the reference peak and the peak at left the sample peak (127 ppm, relative to the reference resonance). The enlarged sample peak reveals fine structure, with the resonance resolved into five peaks. The multiplet splitting of the $PtCl_6^{2-}$ resonance in high fields, which was first reported by Ismail, Kerrison and Sadler in 1980,[40] is due to the occurrence of two chlorine isotopes ^{35}Cl and ^{37}Cl, which, due to a ^{35}Cl : ^{37}Cl natural abundance of 3 : 1, leads to the isotopomer distribution presented in Fig. 4.1; the relative isotopomer distribution shown, compares well with that reported by Ismail *et al.*[40] The fine structure of the $PtCl_6^{2-}$ resonance thus provides a convenient means of ensuring that the platinum species

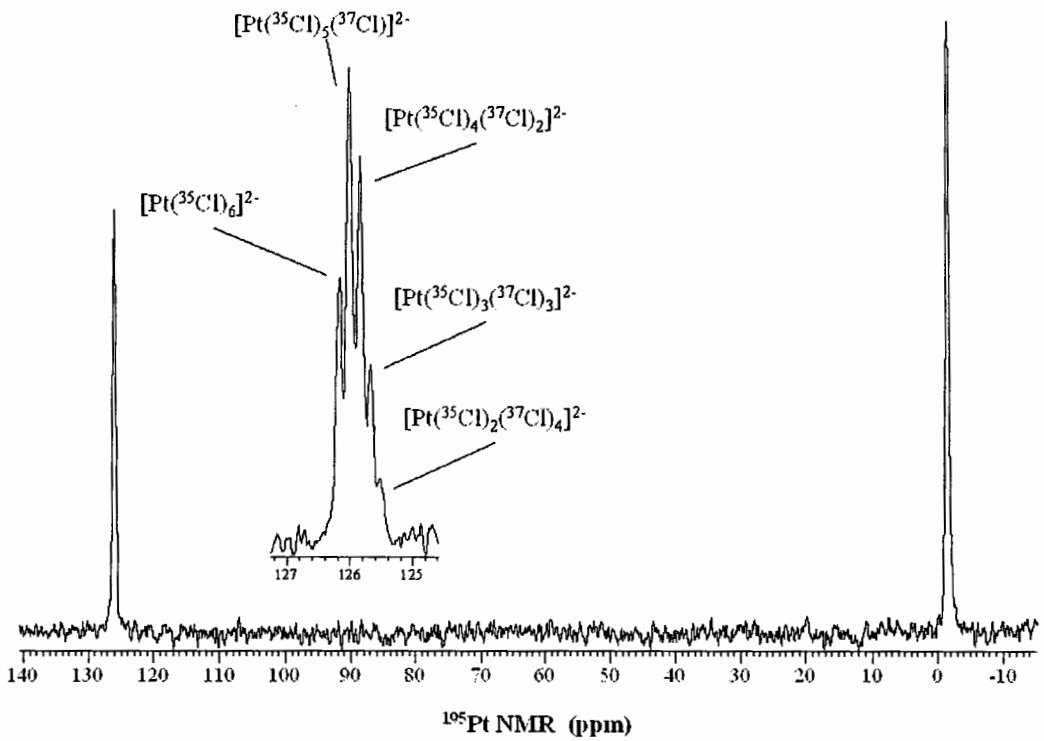

Fig. 4.1 A ^{195}Pt NMR spectrum for the ethylene glycol sample containing $PtCl_6^{2-}$ (as $H_2PtCl_6 \cdot H_2O$); the peak at right is the reference peak (500 mg cm^{-3} $H_2PtCl_6 \cdot H_2O$ in 30 % v/v D_2O / 1 M HCl) and the peak at left the sample peak (127 ppm relative to reference). The insert is an enlargement of the sample peak, illustrating the resolution of the ^{35}Cl, ^{37}Cl isotopomers.

Stellenbosch University http://scholar.sun.ac.za

being studied is in fact the hexachloroplatinate anion, and not a solvolysis product. Pesek and Mason reported ^{195}Pt chemical shifts for $[(n\text{-}C_4H_9)_4N]_2[PtCl_6]$ in a variety of solvents (H_2O, D_2O, CH_3OH, CH_2Cl_2, CH_3CN, acetone, and DMSO),[35] and these authors found no evidence of solvolysis reactions during the time required for their measurements. Nevertheless, preliminary investigations by Koch *et al.* have suggested that solvolysis of $PtCl_6^{2-}$ *may* occur with time in some solvents.[41] The present investigation, however, is focused solely on the solvation of the PtX_6^{2-} (X = Cl, Br) anions; ^{195}Pt NMR spectra for all the solvent systems in the present investigation were recorded immediately after sample preparation to minimize possible solvolysis reactions, and the isotopomer resolution of the $PtCl_6^{2-}$ sample peak was monitored to ensure that the $PtCl_6^{2-}$ species was being probed. Ismail *et al.* present evidence that the $PtBr_6^{2-}$ ^{195}Pt NMR peak splits into a seven line resonance at very high fields, due to bromine isotope effects (the ^{79}Br : ^{81}Br natural abundance ratio is 1 : 1),[40] but inspection of the $PtBr_6^{2-}$ sample peaks in the present study did not reveal fine structure. The isotope shift for $PtBr_6^{2-}$ is much smaller (0.028 ppm) than that for $PtCl_6^{2-}$ (0.167 ppm),[40] most probably disallowing resolution of the isotopomers for the former anion in the present study. The similarity of ^{195}Pt chemical shifts for the $PtBr_6^{2-}$-containing solutions with those for the $PtCl_6^{2-}$-containing solutions, in corresponding solvents, relative to the appropriate reference resonances, however confirmed that the $PtBr_6^{2-}$ anion was being probed in the former solutions.

The ^{195}Pt chemical shifts at constant temperature (30°C) for both anions in single solvents, are summarized in Table 4.1; the data are ordered according to increasing $\delta_{Pt\text{-}195}$. The range of chemical shifts in the pure solvents, from 5 ppm in D_2O to 411 ppm in hexamethylphosphorictriamide for $PtCl_6^{2-}$, and from -2 ppm in D_2O to 281 ppm in acetone for $PtBr_6^{2-}$, is considerable, and illustrates the remarkable sensitivity of the platinum nucleus in both anions to a change of solvent. The overall shift range is much larger than the

Table 4.1 ^{195}Pt chemical shifts for $PtCl_6^{2-}$ (as $H_2PtCl_6{\cdot}H_2O$) and $PtBr_6^{2-}$ as (H_2PtBr_6) in various solvents (30°C).

Solvent	$PtCl_6^{2-}$ $\delta_{Pt\text{-}195}$ (ppm)	$PtBr_6^{2-}$ $\delta_{Pt\text{-}195}$ (ppm)
D_2O	5	-2
Methanol	97	116
Ethylene glycol	127	-
2-Methoxyethanol	198	-
1,2-Dimethoxyethane	209	-
Acetonitrile	217	259
Acetone	240	281

Reference solution for $PtCl_6^{2-}$-containing solutions: 500 mg cm^{-3} $H_2PtCl_6{\cdot}H_2O$ in 30 % v/v D_2O / 1 M HCl; reference solution for $PtBr_6^{2-}$-containing solutions: 250 mg cm^{-3} H_2PtBr_6 in 67 % v/v D_2O / 3 M HBr.
Positive chemical shifts indicate resonances downfield, and negative shifts positions upfield, of the relevant reference resonance.
Total Pt^{IV} concentration ~ 0.1 M.

Stellenbosch University http://scholar.sun.ac.za

concentration dependent chemical shift variations which have been observed for the PtX_6^{2-} (X = Cl, Br) anions. In acetonitrile, we have found $\delta_{Pt\text{-}195}$ variations for $PtCl_6^{2-}$ and $PtBr_6^{2-}$ of 28 ppm and 39 ppm, respectively, over anion concentration ranges of 0 – 0.12 M, while in water and methanol $\delta_{Pt\text{-}195}$ for these anions, over similar concentration ranges, is concentration independent (see Section 5.3.1, Chapter 5). *Temperature dependent* ^{195}Pt chemical shift variations, reported for several platinum complexes (for example: *trans*-$PtCl_2((n\text{-}C_4H_9)_3P)_2$, 0.32 ppm $°K^{-1}$; *trans*-$PtEtBr((n\text{-}C_4H_9)_3P)_2$, 0.52 ppm $°K^{-1}$; upfield with decreasing temperature[31]), are also much smaller than the overall solvent dependent shift changes observed in the present study. Although $\delta_{Pt\text{-}195}$ for $PtBr_6^{2-}$ is consistently downfield to that for $PtCl_6^{2-}$ in corresponding solvents, except for D_2O, the resonance positions for the two anions do not differ markedly; this is not surprising considering that they are both simple halogeno complexes of the Pt(IV) ion. Interestingly, the data in Table 4.1 reveals a distinction between the protic and aprotic solvents used: protic solvents (D_2O, methanol, ethylene glycol, 2-methoxyethanol) result in relatively more upfield positions of $\delta_{Pt\text{-}195}$ (5 ppm to 198 ppm for $PtCl_6^{2-}$) than the aprotic solvents (1,2-dimethoxyethane, acetonitrile, acetone, hexamethylphosphorictriamide; 209 ppm to 411 ppm).

Pesek and Mason reported ^{195}Pt chemical shifts for $[(n\text{-}C_4H_9)_4N]_2[PtCl_6]$ at 26°C in D_2O (-11 ppm), CH_3OH (-222 ppm), CH_3CN (-327 ppm) and acetone (-370 ppm).[35] These values differ from those reported in Table 4.1 for corresponding solvents, but it should be noted that Pesek and Mason used a different platinum salt ($[(n\text{-}C_4H_9)_4N]_2[PtCl_6]$) at *considerably higher concentrations* (0.6 – 0.8 M; nearly saturated solutions[35]). Furthermore, the authors state only that their reference solution was H_2PtCl_6 in H_2O; $\delta_{Pt\text{-}195}$ for this solution would not be the same as that for the reference solution used in the present investigation, which was prepared in 1 M HCl. The fact that ^{195}Pt chemical shifts are somewhat concentration dependent,[36] and that ion-ion interactions may well occur at the near-saturation concentrations used in the previous study,[35] almost certainly contribute to the discrepancies in the reported shift values.

4.3.2 ^{195}Pt chemical shifts in aqueous binary solvent mixtures

Binary solvent mixtures (non-aqueous solvent + D_2O with $PtCl_6^{2-}$, or $PtBr_6^{2-}$) were prepared, and a ^{195}Pt NMR spectrum of each solution mixture was measured relative to the appropriate reference solution (see Experimental Section). Spectra for all the solvent systems were recorded immediately after sample preparation to minimize possible solvolysis reactions, and the isotopomer resolution of the $PtCl_6^{2-}$ sample peak was monitored to ensure that the correct platinum species was being probed. The similarity of $\delta_{Pt\text{-}195}$ ranges and trends for the mixtures containing $PtBr_6^{2-}$, compared with those for the $PtCl_6^{2-}$-containing solutions, confirmed that the $PtBr_6^{2-}$ anion was being probed in the former mixtures.

Stellenbosch University http://scholar.sun.ac.za

Selected ^{195}Pt NMR spectra obtained for the D_2O/methanol binary solvent solutions containing the $PtCl_6^{2-}$ anion are shown in Fig. 4.2. This distribution shows significant downfield shift of the sample resonance, relative to the reference peak, as the mole fraction of methanol in the bulk solvent increases. (The composition of a binary solvent mixture may be expressed in terms of mole fractions, mass fractions or volume fractions, but a definition in terms of the first, is preferred by most authors[1,7]). The complete data for the D_2O/methanol-$PtCl_6^{2-}$ binary solvent system are shown in Fig. 4.3. Similar graphical representations for all the binary solvent systems studied are shown in Figures 4.1-Adm - 4.7-Adm for $PtCl_6^{2-}$, and in Figures 4.9-Adm - 4.11-Adm for $PtBr_6^{2-}$ in Addendum A. Data for all the systems are shown together in Fig. 4.4 for $PtCl_6^{2-}$, and in Fig. 4.5 for $PtBr_6^{2-}$.

Figures 4.4 and 4.5 show that as one proceeds from one pure solvent to the other, there is a smooth, distinct *non-linear* transition of the ^{195}Pt resonance as a function of bulk solvent composition, for each binary solvent system. The trends observed for mixtures containing $PtBr_6^{2-}$ are comparable to those observed for the $PtCl_6^{2-}$-containing solutions in corresponding systems, although at slightly more downfield positions, illustrating that the behaviour of the two halogenoplatinate anions is very similar under these conditions. This suggests that the overall downfield shift observed is not dependent significantly on the halide ligand coordinated to the Pt(IV) centre, and supports the hypothesis that the variations in chemical shift are most likely the result of changes in the first solvation shell of the anions. The Pt nucleus in $PtCl_6^{2-}$ and $PtBr_6^{2-}$ is sensitive to not only an overall change in the environment of the anion, for example on going from one

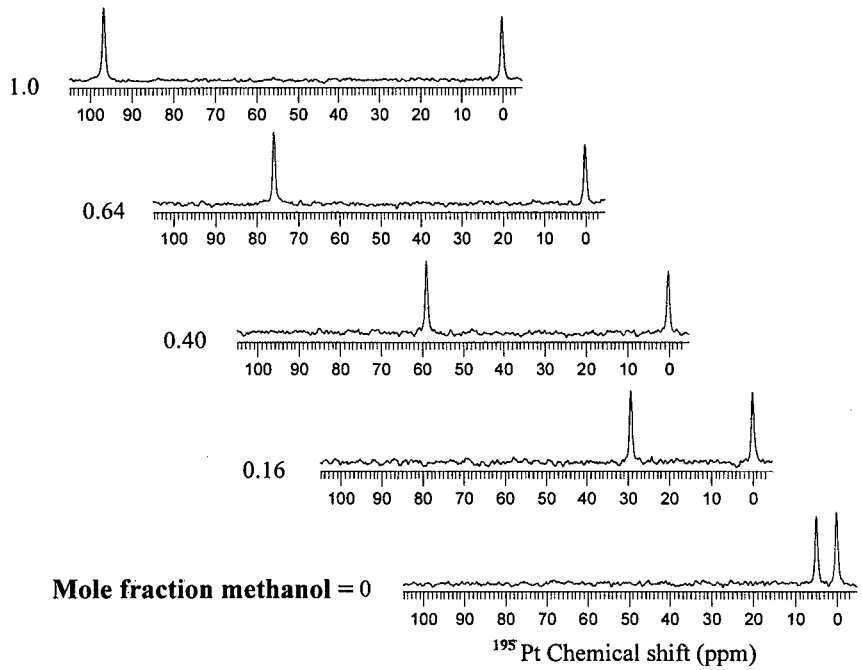

Fig. 4.2 Selected ^{195}Pt NMR spectra obtained for the D_2O/methanol binary solvent system containing $PtCl_6^{2-}$; the mole fraction methanol is indicated. With increasing mole fraction methanol in the series, the sample resonance (peak at left) shifts downfield relative to the reference resonance (peak at right).

Stellenbosch University http://scholar.sun.ac.za

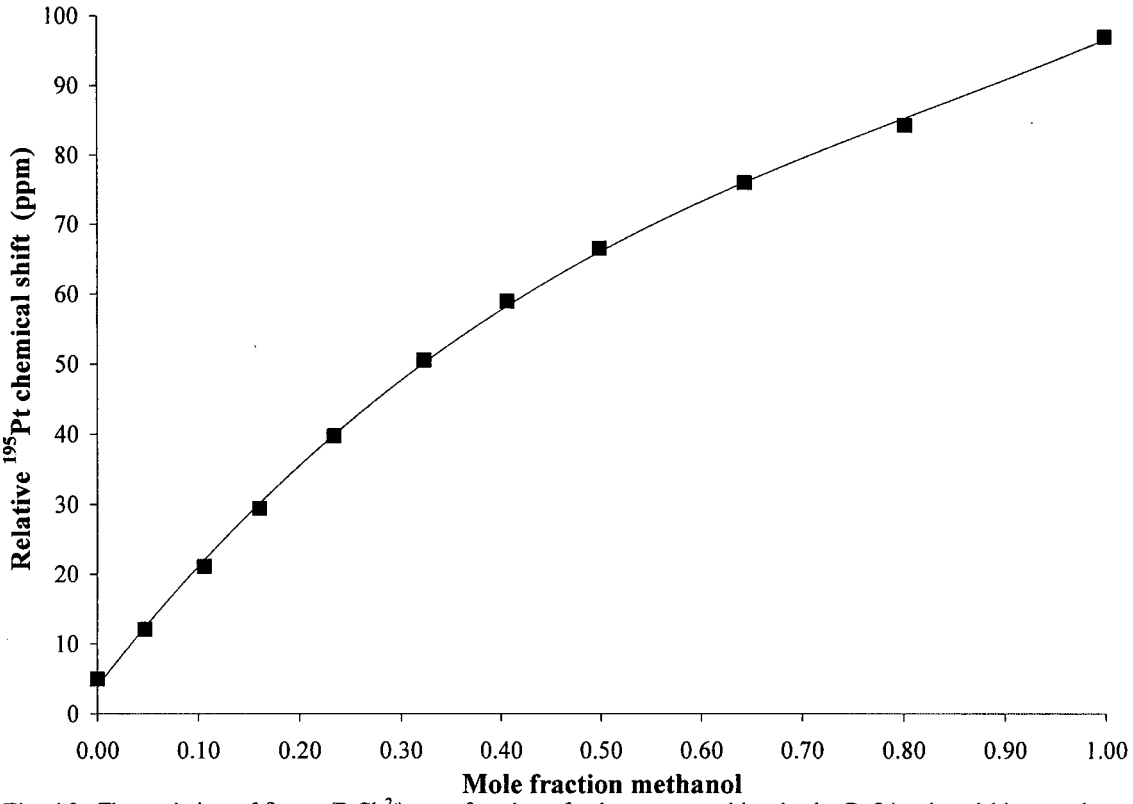

Fig. 4.3 The variation of $\delta_{Pt\text{-}195}$ ($PtCl_6^{2-}$) as a function of solvent composition in the D_2O/methanol binary solvent system; a best-fit polynomial trendline has been inserted.

solvent to another (as shown by the results in Section 4.3.1), but also to more subtle anion-environment changes, which have been brought about in the solutions of binary solvent mixtures, and reflects these changes in its resonance position.

4.3.3 ^{195}Pt chemical shifts in single solvents viewed with regard to solvent properties

Investigations of the effect of solvent on the NMR chemical shift of metal ions usually involve an attempt to correlate the observed shift with some solvent property, or some measure of solvent polarity. This is sometimes successful, but is not always achieved. Maciel *et al.*, for example, reported a linear relationship between ^{7}Li chemical shifts in various aprotic solvents and Kosower's solvent polarity parameter (Z)[42] for these solvents.[43] ^{23}Na chemical shifts have been correlated with solvent pK_a by Bloor *et al.*,[15] and with Gutmann's donor numbers[22] by Popov *et al.*.[17,18] Dechter *et al.*, however, found no simple correlation of the solvent dependence of the ^{205}Tl chemical shift with any measures of solvent polarity for a variety of solvents.[44]

Stellenbosch University http://scholar.sun.ac.za

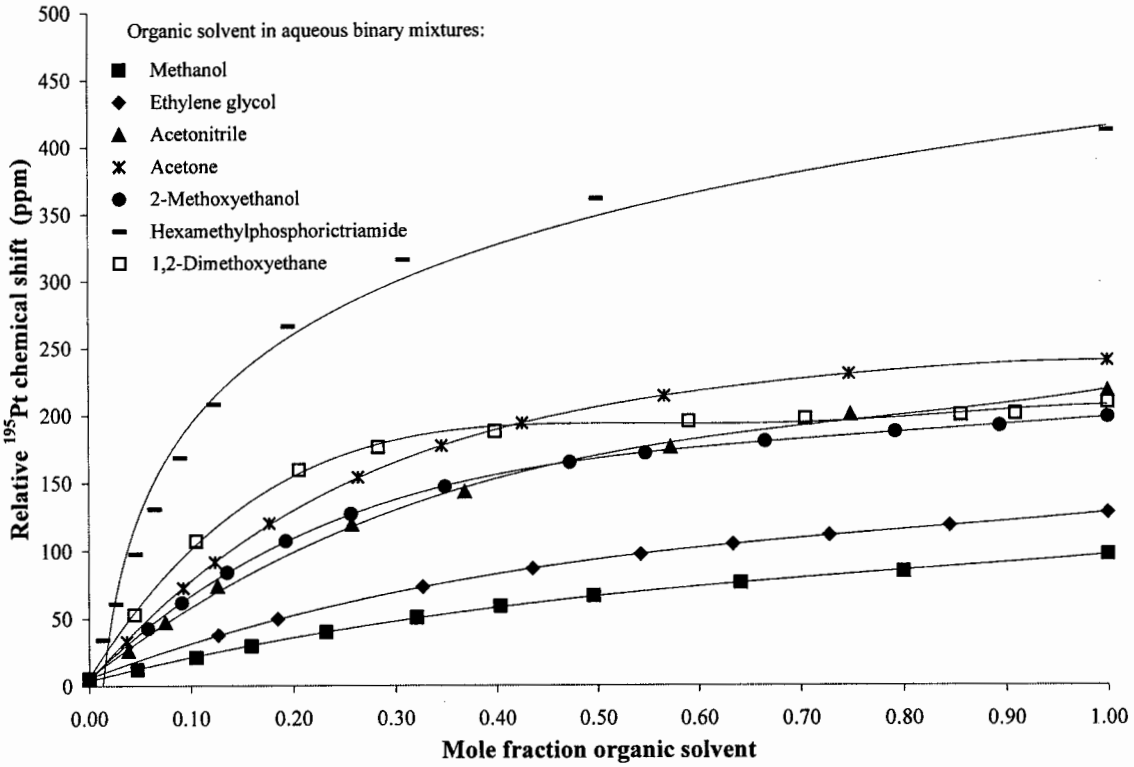

Fig. 4.4 The variation of $\delta_{Pt\text{-}195}$ as a function of bulk solvent composition for various aqueous binary solvent mixtures (D_2O + organic solvent) containing $PtCl_6^{2-}$; best-fit trendlines have been inserted.

Our investigations of the concentration dependence of the ^{195}Pt chemical shift for the PtX_6^{2-} (X = Cl, Br) anions in water, methanol and acetonitrile (see Section 5.3.1, Chapter 5), have shown that in water and methanol $\delta_{Pt\text{-}195}$ is concentration independent over the $[PtX_6^{2-}]$ range 0 – 0.12 M, while the $\delta_{Pt\text{-}195}$ variation in acetonitrile, over this concentration range, is 28 ppm for $PtCl_6^{2-}$ and 39 ppm for $PtBr_6^{2-}$. This indicates that variations in $[PtX_6^{2-}]$ will not account for the significant variations in shift observed in the different solvents (we have, in fact, ensured that $[PtX_6^{2-}] \sim 0.1$ M in all solutions). The observed $\delta_{Pt\text{-}195}$ changes are likely to be due to the manner in which the anions are solvated by the solvent molecules in the different solvents. In the present investigation we have attempted to correlate the observed ^{195}Pt chemical shifts for $PtCl_6^{2-}$ in the various pure solvents chosen (Table 4.1) with some solvent property which relates to the ability of the solvent to solvate ions, in order to elucidate the nature of the interaction between the hexachloroplatinate anion and the solvent molecules. Section 4.3.3.1 gives a brief summary of the solvent properties which are generally referred to in discussions of solvation, and in Section 4.3.3.2 the results of the present study are viewed with regard to these properties.

Stellenbosch University http://scholar.sun.ac.za

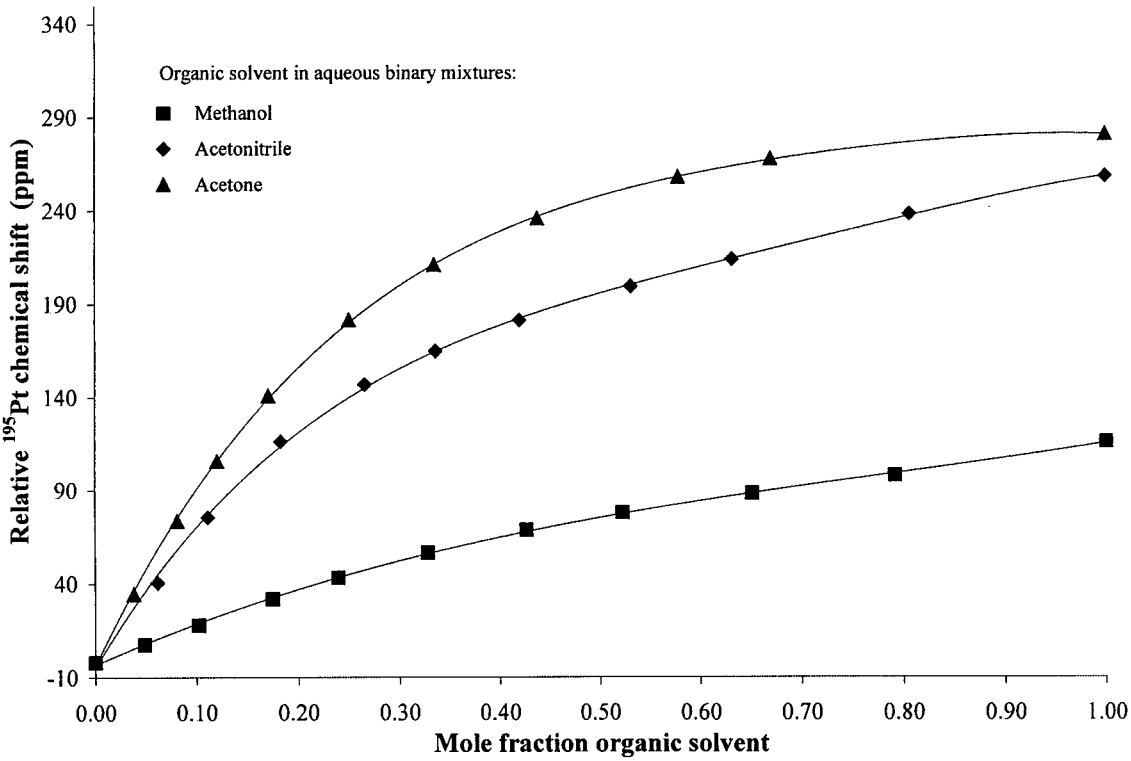

Fig. 4.5 The variation of $\delta_{Pt\text{-}195}$ as a function of bulk solvent composition for various aqueous binary solvent mixtures (D_2O + organic solvent) containing $PtBr_6^{2-}$; best-fit trendlines have been inserted.

4.3.3.1 The properties of solvents

Numerous reviews focusing on the properties of solvents are available in the literature,[1,5,6,45,46] most notably a recent and comprehensive publication by Yizhak Marcus.[46] In this section those properties which are generally used to describe the solvating power of a solvent, are briefly discussed.

Solvent polarity

The ability of a solvent to dissolve, and solvate, a solute is determined by a number of factors, which together make up the character of the solvent. This character is frequently referred to as the *polarity* of the solvent, and has been previously described as 'the sum of all the molecular properties responsible for all the interaction forces between solvent molecules and the solute, that lead to the overall solvation ability of the solvent'.[46] Due to the complexity of the solute-solvent interactions, it is not possible to determine solvent polarity by measuring a single, individual solvent property, but various parameters (or indices) have been devised to assess the polarity of a solvent. Some of these parameters are based on physical properties such as dipole moment and dielectric constant, while others are empirical parameters that are based on chemical properties of the solvents.

Stellenbosch University http://scholar.sun.ac.za

Molecules which possess a nonsymmetrical distribution of charge or electron density have a permanent dipole moment, μ, and are described as being dipolar. Solvents with dipolar molecules which are also able to donate an acidic hydrogen to form a hydrogen-bond, are termed *dipolar protic*, while those unable to form a hydrogen-bond are called *dipolar aprotic*. Solvents with highly symmetrical molecules have no permanent dipole moments, but are not necessarily *apolar* since they may be polarized by an induced dipole effect (or in an electric field); these solvents are termed *nonpolar/polarizable* (the term apolar should be used only for solvents which have molecules with a spherical charge distribution, *viz.* liquid xenon, neon). All the solvents of interest in the present investigation have permanent dipole moments, and may be classified as either dipolar protic (water, methanol, ethylene glycol, 2-methoxyethanol) or dipolar aprotic (1,2-dimethoxyethane, acetonitrile, acetone, hexamethylphosphorictriamide).

The dielectric constant (or relative permittivity), ε, is generally accepted as an indicator of the polarity of a solvent, and is measured by applying an electric field across the solvent between two plates of a capacitor. If the molecules of the solvent have a permanent dipole, they will orientate themselves according to the direction of the field (reducing the strength of the field). The electric field may also *induce* a dipole opposite to the applied field, even in solvents with no permanent dipole of their own. Since this behaviour is similar to the 'orientation' of a solvent around an electrolyte, ε is regarded as a good indicator of the ability of the solvent to *dissolve* an ionic compound. Solvents with $\varepsilon \leq 10$ are considered low dielectric constant solvents, and may be either polar or nonpolar; these solvents generally do not significantly dissolve electrolytes. Solvents with $\varepsilon \geq 30$ dissociate electrolytes almost completely, and are considered highly polar. Solvents with ε values between 10 and 30 allow some electrolyte dissociation, but considerable ion-pairing may also occur in them. Marcus cautions that the *solvation* properties of solvents are generally *not well* related to their dielectric properties.[46]

Empirical parameters which are based on the chemical properties of solvents, have also been used to estimate solvent polarities. For these empirical parameters a standard substance with some solvent sensitive spectroscopic characteristic (a phenomenon called solvatochromism), is used as a probe. The standard substance acts as a stand-in for the solute, and it is assumed that the solute under study will experience the same solvent polarity measured by the probe. Typically several standard substances with different functional groups are employed, to produce correlated values of such a solvent parameter, for which an average value can be determined. Marcus states that although many empirical polarity indexes have been developed over the years, the two that are employed most frequently are Dimroth and Reichardt's $E_T(30)$[47,48] and Kamlet and Taft's π^*[49,50] solvatochromic parameters. Both these indexes are based on the solvent-induced shifts of the lowest energy absorption bands (UV-visible region) of selected solvatochromic indicators.

Stellenbosch University http://scholar.sun.ac.za

The $E_T(30)$ solvent polarity scale developed by Dimroth and Reichardt is based on the solvent-induced shift of the longest wavelength charge transfer absorption band of the probe 2,6-diphenyl-4-(2,4,6-triphenyl-1-pyridino)-phenoxide in dilute solutions (values are expressed in kcal mol^{-1}).[47,48] This indicator (30^{th} in the series of probes investigated, hence the notation $E_T(30)$) is the most solvatochromic probe reported to date,[46,51] i.e. it exhibits a large variation in monitored probe wavelength with changing solvent polarity, and is thus a useful indicator of solvent polarity. Although not specifically designed to measure hydrogen-bonding interactions, $E_T(30)$ is also an indicator of the hydrogen-bond donating (or electron pair acceptance) ability of protic solvents.*

A different solvatochromic polarity parameter which is a measure of solvent polarity/polarizability, devoid of hydrogen bonding effects, is the Kamlet and Taft π^* parameter.[49,50] This parameter is derived by analysis of a series of nitro-substituted aromatic indicators, and is designed to eliminate specific interactions with solvent molecules.

Electron pair donicity.

Marcus points out that the ability of a solvent to solvate an electrolyte depends not only on its general polarity, which he describes as a non-specific property, but also on the solvents ability to interact in a specific way with the electrolyte. This interaction of a solvent with the solute may involve the donation of a non-bonding pair of electrons from an atom of the solvent molecule to the solute, or the acceptance of such an electron pair from the solute. Such specific interactions, Marcus continues, are often much stronger than the non-specific polar interactions.

Gutmann proposed the use of the donor number, *DN*, as a measure of the ability of a solvent to donate an electron pair of one of its donor atoms.[22,45] Gutmann's donor number is defined as the negative enthalpy for the reaction of equimolar quantities of the solvent with antimony pentachloride ($SbCl_5$), at room temperature in 1,2-dichloroethane. Values of *DN* are usually normalized using 1,2-dichloroethane (*DN* = 0 kcal mol^{-1}) and hexamethylphosphorictriamide (HMPA, *DN* = 38.8 kcal mol^{-1}) as reference solvents for the scale. This results in the parameter DN^N (which corresponds to *DN*/38.8), giving a unitless scale on which most solvents fall between 0 and 1. (Kamlet and Taft also developed a β scale as a measure of a solvent's ability to donate an electron pair;[50] this scale is closely related to the *DN* scale, and will therefore not be referred to.)

* Adams, Dyson and Tavener explain that $E_T(30)$ values are related to the ability of a solvent to stabilize charge separation in the solvatochromic probe, and that a correlation between $E_T(30)$ and ε might thus be expected.[51] Not all solvents show a good correlation, however. This is presumed to result from the fact that $E_T(30)$ is sensitive not only to the 'bulk, non-specific solvent polarity' but also incorporates contributions from specific interactions with solvent molecules, such as hydrogen bond donating ability. This point highlights the difficulty in developing a single parameter capable of assessing solvent polarity.

Stellenbosch University http://scholar.sun.ac.za

Electron pair acceptance / hydrogen-bond donation ability.

The acceptor number, *AN*, developed by Gutmann,[52] is a measure of the power of a solvent to form a hydrogen bond by accepting an electron pair from a donor atom in a solute. The evaluation of *AN* involves the measurement of the ^{31}P NMR chemical shift change when triethylphosphine oxide, $Et_3P{=}O$, is dissolved in the solvent of interest. Interestingly, aprotic and non-protogenic* solvents have non-zero acceptor numbers ($AN < 10$ for nonpolar solvents and between 10 and 20 for dipolar aprotic solvents), indicating that *AN* includes a non-specific polarity contribution. Protic solvents, however, generally have significantly higher *AN* values falling in the range 25 to 130. As has been pointed out, the $E_T(30)$ polarity parameter is also an indicator of the hydrogen-bond donating (or electron pair acceptance) ability of protic solvents, and a linear correlation exists between *AN* and $E_T(30)$ values.

Another measure of the hydrogen-bond donation ability of solvents which was developed to exclude contributions from 'non-specific solvent polarity' (and is therefore strictly speaking only valid for protic and protogenic solvents), is the Kamlet-Taft α parameter.[50]

Marcus summarizes this potentially confusing array of solvent parameters as follows: Solvents for electrolytes may be characterized by their *dielectric constants* (ε), and by their *donor* and *acceptor properties*.[53] The author holds that the dielectric constant is a measure of the power of a solvent to *dissociate* an electrolyte, while the donor and acceptor properties relate to the ability of the solvents to *solvate* the ion-pairs or ions produced on dissociation. Cations are described as Lewis acids, the solvation of which are determined mainly by the *donor properties* of the solvents. Anions, as Lewis bases, are considered not to be solvated much by aprotic solvents, even if dipolar, while protic solvents solvate anions well, with the solvent *acceptor properties* the determining factor in this respect.

Values for all the parameters introduced above for the solvents of interest, are given in Table 4.2.[46]

4.3.3.2 Relationship of $\delta_{Pt\text{-}195}$ (for $PtCl_6^{2-}$) in single solvents with solvent properties

The variation of $\delta_{Pt\text{-}195}$ with solvent dielectric constant for the solutions (single solvent) containing $PtCl_6^{2-}$ (Table 4.2) is shown in Fig. 4.6. It is clear that there is no correlation between the observed ^{195}Pt chemical shift and the dielectric constant of the solvent used. It may thus be concluded that ε is not *predominant* in determining the ^{195}Pt resonance position for the anion in solution; as Marcus points out, this parameter is non-specific and does not generally relate to the solvation ability of the solvent. It should be remembered that both of the platinum salts that were used ($H_2PtCl_6{\cdot}H_2O$ and H_2PtBr_6), introduce some protons (or

* Protogenic solvents are those for which only strongly basic solutes can induce hydrogen-bond formation. Examples of protogenic solvents include chloroform or nitromethane, as well as those solvents which have a methyl group adjacent to groups such as C=O or C≡N.

Table 4.2 Various solvent properties which are generally used to assess the abilities of solvents to dissociate electrolytes, and solvate the resulting ions or ion-pairs. ^{195}Pt chemical shifts for $PtCl_6^{2-}$ and $PtBr_6^{2-}$ in these solvents are also presented.

Solvent	$PtCl_6^{2-}$ $\delta_{Pt\text{-}195}$ (ppm)	$PtBr_6^{2-}$ $\delta_{Pt\text{-}195}$ (ppm)	μ (D)[a]	ε	$E_T(30)$ (kcal mol^{-1})	Kamlet-Taft π^*	DN^N [b]	AN	Kamlet-Taft α
D_2O	5	-2	1.85	78.36	63.1	1.09	0.85	54.8	1.17
Methanol	97	116	2.87	32.66	55.4	0.60	0.77	41.5	0.98
Ethylene glycol	127	-	2.31	37.7	56.3	0.92	0.52	43.4	0.90
2-Methoxyethanol	198	-	2.04	16.93	52.0	0.71		36.1	0.74
1,2-Dimethoxyethane	209	-	1.71	7.2	38.2	0.53	0.62	10.2	0.0
Acetonitrile	217	259	3.92	35.94	45.6	0.66	0.36	18.9	0.19
Acetone	240	281	2.69	20.56	42.2	0.62	0.44	12.5	0.08
Hexamethylphosphorictriamide	411	-	5.54	29.3	40.9	0.87	1	9.8	0.0

Values for solvent properties are taken from reviews by Marcus.[1,46]

[a] $D = 3.33564\times10^{-30}$ C·m

[b] Some uncertainty exists as to the donor numbers for water and methanol, the values depending on the method of determination.[46] DN^N values in this table are taken from reference [1].

Stellenbosch University http://scholar.sun.ac.za

Stellenbosch University http://scholar.sun.ac.za

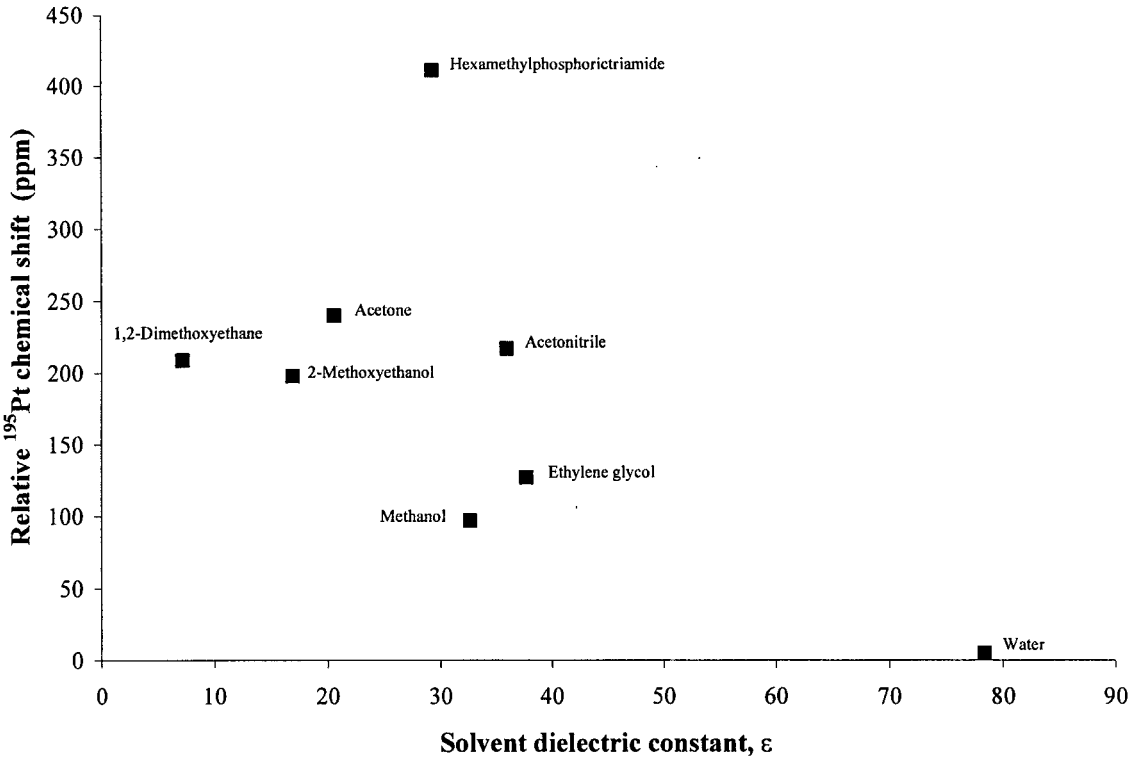

Fig. 4.6 ^{195}Pt chemical shift as a function of solvent dielectric constant (ε) for solutions of single solvents containing $PtCl_6^{2-}$.

hydronium ions, H_3O^+, in the case of $H_2PtCl_6{\cdot}H_2O$) into the solutions. The occurrence of ion-pair formation, particularly in solutions with low dielectric constants, might be considered accountable for the significant downfield shifts observed in the low dielectric solvents. We have studied ion-pair formation of Na^+ with both $PtCl_6^{2-}$ and $PtBr_6^{2-}$ in water, methanol and acetonitrile (see Chapter 5), and have found that the ^{195}Pt chemical shift is very sensitive to ion-ion association, but leads to an *upfield* shift of the $PtCl_6^{2-}$ resonance in these solvents. If it is accepted, based on these findings, that cation-PtX_6^{2-} (X = Cl, Br) association will generally lead to an *upfield* shift of $\delta_{Pt\text{-}195}$, the downfield shifts observed in the non-aqueous solvents cannot be attributed to significant ion-pair formation between $PtCl_6^{2-}$ and (H_3O^+) or (H^+·solvent).

Plots of $\delta_{Pt\text{-}195}$ *vs* μ and Kamlet-Taft π^* (not presented) also show no correlation between the ^{195}Pt chemical shift and either of these solvent polarity indexes. This indicates that neither the solvent dipole moment nor the solvent polarity/polarizability, as measured by the Kamlet-Taft π^* index, are predominant in determining the ^{195}Pt resonance positions.

The variation of $\delta_{Pt\text{-}195}$ with solvent $E_T(30)$ is shown in Fig. 4.7. In this figure a distinction between the protic (water, methanol, ethylene glycol, 2-methoxyethanol) and aprotic (1,2-dimethoxyethane, acetonitrile, acetone, hexamethylphosphorictriamide) solvents appears to exist. The ^{195}Pt chemical shift of $PtCl_6^{2-}$ in the protic solvents, which have relatively large $E_T(30)$ values, are generally more upfield than $\delta_{Pt\text{-}195}$ in the

Stellenbosch University http://scholar.sun.ac.za

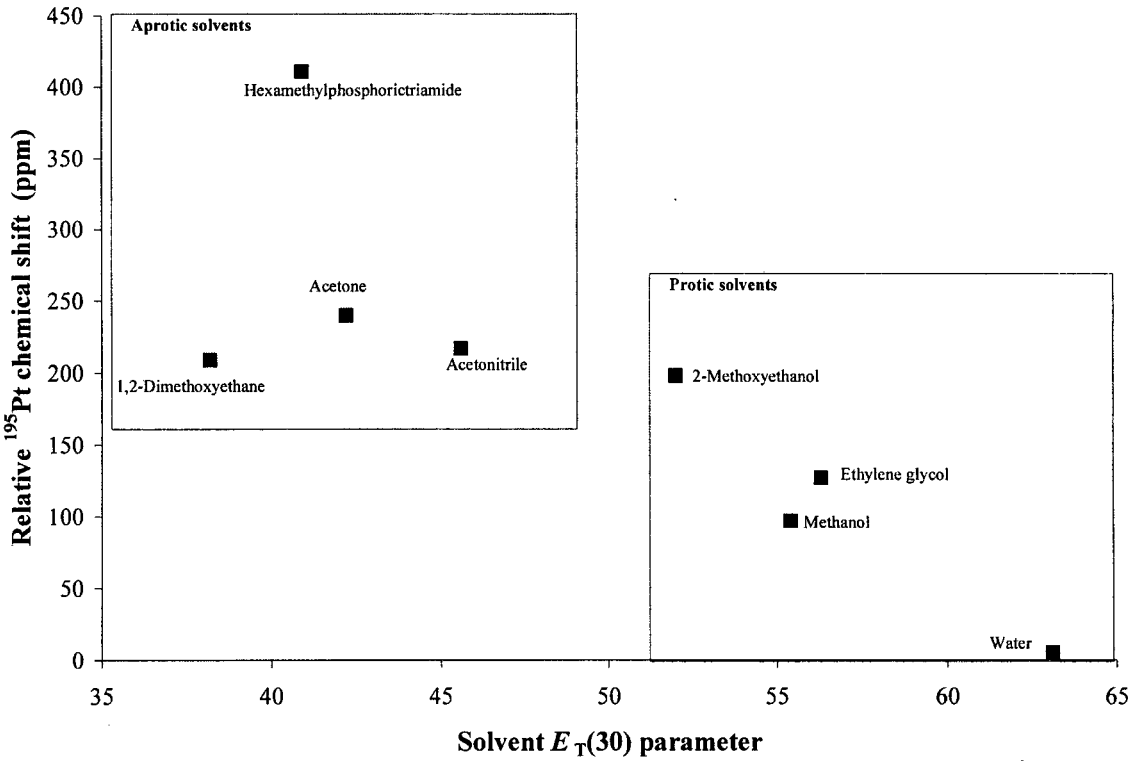

Fig. 4.7 ^{195}Pt chemical shift as a function of solvent $E_T(30)$ for solutions of single solvents containing $PtCl_6^{2-}$.

aprotic solvents. Furthermore, there is no simple relationship between the observed platinum chemical shifts and $E_T(30)$ for the aprotic solvents, but for the protic solvents there appears to be *generally* a downfield shift of $\delta_{Pt\text{-}195}$ with decreasing $E_T(30)$ for the solvents. The distribution of points for a plot of $\delta_{Pt\text{-}195}$ *vs* solvent acceptor number (*AN*) (not presented) is very similar to that shown in Fig. 4.7: there is no correlation between $\delta_{Pt\text{-}195}$ and *AN* for the aprotic solvents, but there appears to be generally a downfield shift of $\delta_{Pt\text{-}195}$ with decreasing *AN* for the protic solvents. This similarity is not surprising, considering the fact that a linear correlation exists between the $E_T(30)$ and *AN* indexes (see Section 4.3.3.1). The fact that some correlation appears to exist for the *protic* solvents in Fig. 4.7, and that *AN*, as well as $E_T(30)$, are indicators of the *hydrogen-bond donating ability* of protic solvents, suggests a relationship between solvent hydrogen-bond donicity and $\delta_{Pt\text{-}195}$. This is confirmed in a plot of $\delta_{Pt\text{-}195}$ *vs* solvent Kamlet-Taft α parameter, shown in Fig. 4.8 (α values are zero for 1,2-dimethoxyethane, and hexamethylphosphorictriamide, but non-zero for acetonitrile and acetone since the latter are classified as protogenic). The Kamlet-Taft α parameter is a measure of the hydrogen-bond donating ability of solvents, and Fig. 4.8 shows a *linear correlation* between $\delta_{Pt\text{-}195}$ and α for protic solvents: with decreasing α value for the protic solvents, there is a linear downfield shift of the ^{195}Pt resonance position for $PtCl_6^{2-}$, suggesting that as the hydrogen-bonding interaction between solvent and anion *diminishes*, the platinum nucleus of $PtCl_6^{2-}$ becomes *less shielded.* This considerable influence of the solvent hydrogen-bond donating ability on $\delta_{Pt\text{-}195}$ suggests that interaction of the protic solvents with the anion occurs *via* solvent H-bonding, which is

Stellenbosch University http://scholar.sun.ac.za

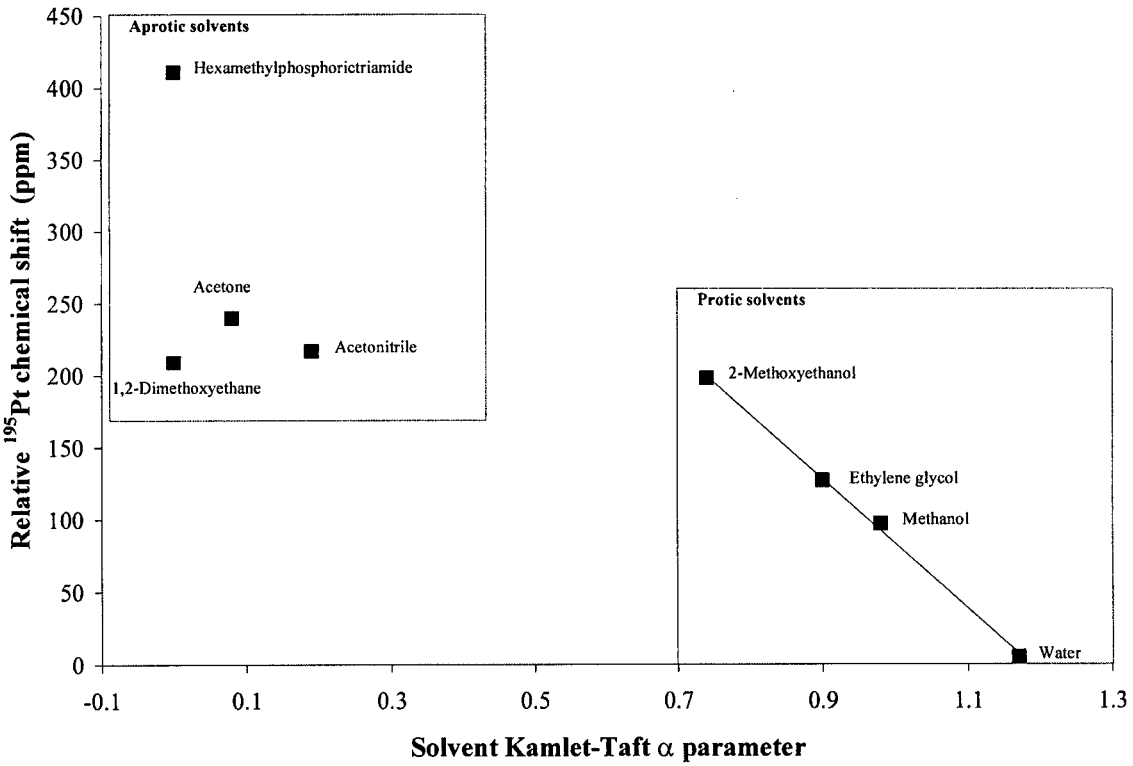

Fig. 4.8 ^{195}Pt chemical shift as a function of solvent Kamlet-Taft α parameter for solutions of single solvents containing $PtCl_6^{2-}$.

in accordance with the generally accepted view that anions are solvated by protic solvents by means of hydrogen-bonding interactions.[1]

Marcus suggests that solvent *donor* properties are important mainly in determining *cation* solvation, but a plot of $\delta_{Pt\text{-}195}$ *vs* solvent donor number (DN^N) is shown in Fig. 4.9, as a matter of interest. Although a possible correlation between $\delta_{Pt\text{-}195}$ and DN^N for the aprotic solvents acetonitrile, acetone, and hexamethylphosphorictriamide might be suggested, a reasonable explanation of anion solvation in terms of solvent electron pair donicity is not easily formulated.

The attempts to relate the observed ^{195}Pt chemical shift of $PtCl_6^{2-}$ in various solvents to some solvent property reveal that there is no correlation between $\delta_{Pt\text{-}195}$ in the *aprotic* solvents and the acceptor properties of these solvents, while there is a linear correlation of $\delta_{Pt\text{-}195}$ with the hydrogen-bond donation ability of the *protic* solvents. These results appear to reflect the generally accepted view that anions are not solvated much by aprotic solvents, even if dipolar, while protic solvents solvate anions well. Clearly, the ^{195}Pt chemical shift of the PtX_6^{2-} (X = Cl, Br) anions is extremely sensitive to the manner in which the solvent molecules interact with the anions, and theoretical studies are necessary to elucidate the effect of the ion-solvent interactions on the shielding of the platinum nucleus. DFT calculations of the ^{195}Pt chemical shift of $^{195}PtCl_xBr_{6-x}^{2-}$ complexes by Fowe *et al.*[38] have shown that the chemical shift of $PtBr_6^{2-}$ is extremely

Stellenbosch University http://scholar.sun.ac.za

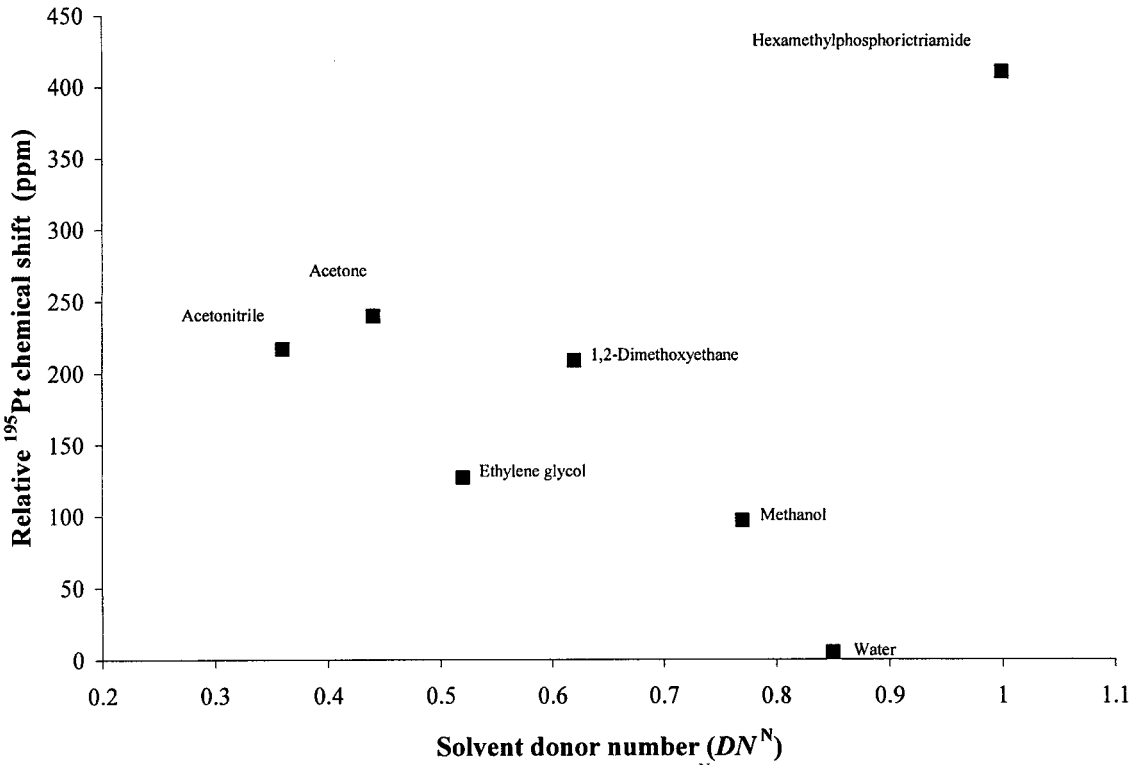

Fig. 4.9 ^{195}Pt chemical shift as a function of solvent donor number (DN^N) for solutions of single solvents containing $PtCl_6^{2-}$.

sensitive to a variation in Pt-Br bond lengths; an increase in chemical shift of 150 ppm pm^{-1} for a distance decrease, has been reported. It is conceivable that changes in the nature of the ion-solvent interactions may result in subtle changes of the Pt-X bond lengths in PtX_6^{2-} (X = Cl, Br), which may in turn lead to significant $\delta_{Pt\text{-}195}$ variations.

4.3.4 ^{195}Pt chemical shifts in pure solvents viewed in terms of nuclear shielding

It is generally accepted in NMR spectroscopy[14] that the Larmor resonance frequency, ν, for a particular nucleus may be expressed as:

$$\nu = \gamma H_O(1-\sigma_t)/2\pi \qquad (4.2)$$

where γ = the gyromagnetic ratio of the nucleus,

H_O = the applied magnetic field, and

σ_t = the total shielding (screening) constant.

Nuclear shielding and the total shielding constant, σ_t, are generally discussed in terms of the shielding theory developed by Ramsey.[54] The shielding of a nucleus, according to this theory, may be formulated as:

$$\sigma_t = \sigma_d + \sigma_p + \sigma_x \qquad (4.3)$$

Stellenbosch University http://scholar.sun.ac.za

where σ_d is the diamagnetic shielding parameter, and σ_p the paramagnetic shielding parameter. The parameter σ_x, represents the effect of ring currents and other anisotropic contributions, and does not need consideration in the present investigation. The diamagnetic shielding parameter, σ_d, corresponds to the uniform, symmetrical circulation of electrons about the nucleus in question, as if the atom were completely free. The rotation of electrons about a nucleus normally leads to a decrease in the effective magnetic field, and σ_d thus contributes to an upfield shift of the resonance position. The absolute value of this parameter is substantial, but its variation for a particular nucleus from one compound to another is small in comparison to the variation in the total screening that is observed. This is due to the fact that the magnitude of σ_d is dependent mainly on the core electrons, the wave functions of which are essentially not influenced by chemical bonding.[14] The paramagnetic shielding parameter, σ_p, however, has been shown to dominate the chemical shielding of heavy metal systems.[14,34-36]

Pesek and Mason,[35] and Pregosin,[36] have shown that σ_p for diamagnetic $5d^6$ octahedral Pt(IV) complexes may be expressed as:

$$\sigma_p = -\frac{4}{3}\beta^2 < r^{-3} > \left|C(t_{2g})\right|^2 \left\{24\left[\Delta E(^1T_{1g})\right]^{-1}\left|C(e_g)\right|^2\right\} \qquad (4.4)$$

where β = the Bohr magneton,

r^{-3} = the mean inverse cube distance of a metal *d* electron from the nucleus,

$C(t_{2g})$, $C(e_g)$ = the coefficients of the metal *d* orbitals in the molecular orbitals, and

$\Delta E(^1T_{1g})$ = the ligand field excitation ($^1T_{1g} \leftarrow {}^1A_{1g}$); the electronic ground state for the platinum(IV) halide complexes is $^1A_{1g}$.[55]

Thus, the chemical shielding of the platinum nucleus is dependent on at least three factors: i) the relative value of $<r^{-3}>$, ii) the *d* orbital coefficients in the molecular orbitals, and iii) the magnitude of the energy of the electronic transition $^1T_{1g} \leftarrow {}^1A_{1g}$ in the complex. According to equation (4.4), if changes in $<r^{-3}>$, and $C(t_{2g})$ and $C(e_g)$ are small for the halogenoplatinate ions with changing solvent, one might expect some correlation between $\delta_{Pt\text{-}195}$ and $\Delta E(^1T_{1g})$: for example, with increasing ligand field transition energy, a decrease in σ_p, and a increase in total shielding (an upfield shift of $\delta_{Pt\text{-}195}$), might be predicted. Freeman *et al.*[56] and Yamasaki *et al.*[57], were able to show a correlation between ^{59}Co chemical shifts and ligand field transition energies in a number of Co(III) complexes, based on a similar description of the paramagnetic shielding parameter. Although these investigations involved a large variety of Co(III) complexes, while only PtX_6^{2-} (X = Cl, Br) anions are considered in the present study, the remarkable sensitivity of $\delta_{Pt\text{-}195}$ of these anions in various solvents, prompted an attempt to correlate the observed ^{195}Pt chemical shifts in pure solvents with the appropriate electronic transition in the anions. Swihart and Mason presented detailed assignments of electronic spectra for a number of Pt(IV) complexes, amongst others $PtCl_6^{2-}$ and $PtBr_6^{2-}$, in a variety of non-aqueous solvents.[58] The authors assign a relatively weak band at ~360 nm in the absorbance spectrum of $PtCl_6^{2-}$ to the $^1T_{1g} \leftarrow {}^1A_{1g}$ transition, and report the position of this band in methanol,

Stellenbosch University http://scholar.sun.ac.za

acetonitrile and *N,N*-dimethylformamide at 27800 cm^{-1}, 27700 cm^{-1} and 27300 cm^{-1}, respectively. Similarly, a weak band at ~440 nm in the spectrum of $PtBr_6^{2-}$ is assigned to the $^1T_{1g} \leftarrow {}^1A_{1g}$ transition, with its position in methanol, acetonitrile and *N,N*-dimethylformamide reported at 22900 cm^{-1}, 22700 cm^{-1} and 22600 cm^{-1}, respectively. These results indicate that $\Delta E(^1T_{1g})$ *decreases* for the solvents in the order methanol > acetonitrile > *N,N*-dimethylformamide. If it is accepted that changes in $\langle r^{-3} \rangle$, and $C(t_{2g})$ and $C(e_g)$ are small, and that changes in σ_p are related predominantly to variations in $\Delta E(^1T_{1g})$, σ_p is expected to *increase* for the solvents in the order methanol < acetonitrile < *N,N*-dimethylformamide, resulting in increasing *downfield* shift of $\delta_{Pt\text{-}195}$ in the solvents in the order methanol, acetonitrile, *N,N*-dimethylformamide. This prediction is in accordance with the results presented for methanol and acetonitrile in Table 4.1, Section 4.3.1.

In order to investigate the apparent correlation between $\delta_{Pt\text{-}195}$ and $\Delta E(^1T_{1g})$ for $PtCl_6^{2-}$ in various solvents, solutions of the anion (as $H_2PtCl_6 \cdot H_2O$) in the solvents D_2O ($[PtCl_6^{2-}]$ = 0.00846 M), methanol ($[PtCl_6^{2-}]$ = 0.00874 M), acetonitrile ($[PtCl_6^{2-}]$ = 0.00715 M), acetone ($[PtCl_6^{2-}]$ = 0.00715 M), and hexamethylphosphorictriamide ($[PtCl_6^{2-}]$ = 0.00879 M) were prepared. Spectra for all these solutions were obtained in a 2 mm cuvette relative to a blank of the appropriate solvent. The spectra for the solutions of $PtCl_6^{2-}$ only in methanol and acetonitrile are presented in Fig. 4.10. The band for the $^1T_{1g} \leftarrow {}^1A_{1g}$ transition appears as a shoulder to a much more intense charge-transfer band which can be seen as starting to appear below 350 nm in the spectra in Fig. 4.10. Possibly due to the proximity of the $^1T_{1g} \leftarrow {}^1A_{1g}$ band to the intense charge-transfer band, we were unfortunately not able to unambiguously determine a position for the band of interest in any of the solutions. The spectra in Fig. 4.10 may indicate that the charge-transfer band in acetonitrile appears at longer wavelength than in methanol, suggesting a possible solvent dependence of the spectrum, but no conclusions regarding the $^1T_{1g} \leftarrow {}^1A_{1g}$ transition can be drawn. Attempts to determine the positions of the relevant *d-d* transition by calculating the first derivatives of the spectra, were also unsuccessful. The $^1T_{1g} \leftarrow {}^1A_{1g}$ transition for $PtBr_6^{2-}$ also appears as a weak shoulder to a much more intense charge-transfer band in the spectrum of $PtBr_6^{2-}$, and consequently spectral analysis for this anion was not attempted.

Thus, although the Swihart and Mason results in conjunction with findings of the present investigation, suggest a possible correlation of $\delta_{Pt\text{-}195}$ with $\Delta E(^1T_{1g})$ for $PtCl_6^{2-}$ and $PtBr_6^{2-}$ in various solvents, our spectral data was too insensitive to confirm such a relationship, and further theoretical study is called for in this regard.

Stellenbosch University http://scholar.sun.ac.za

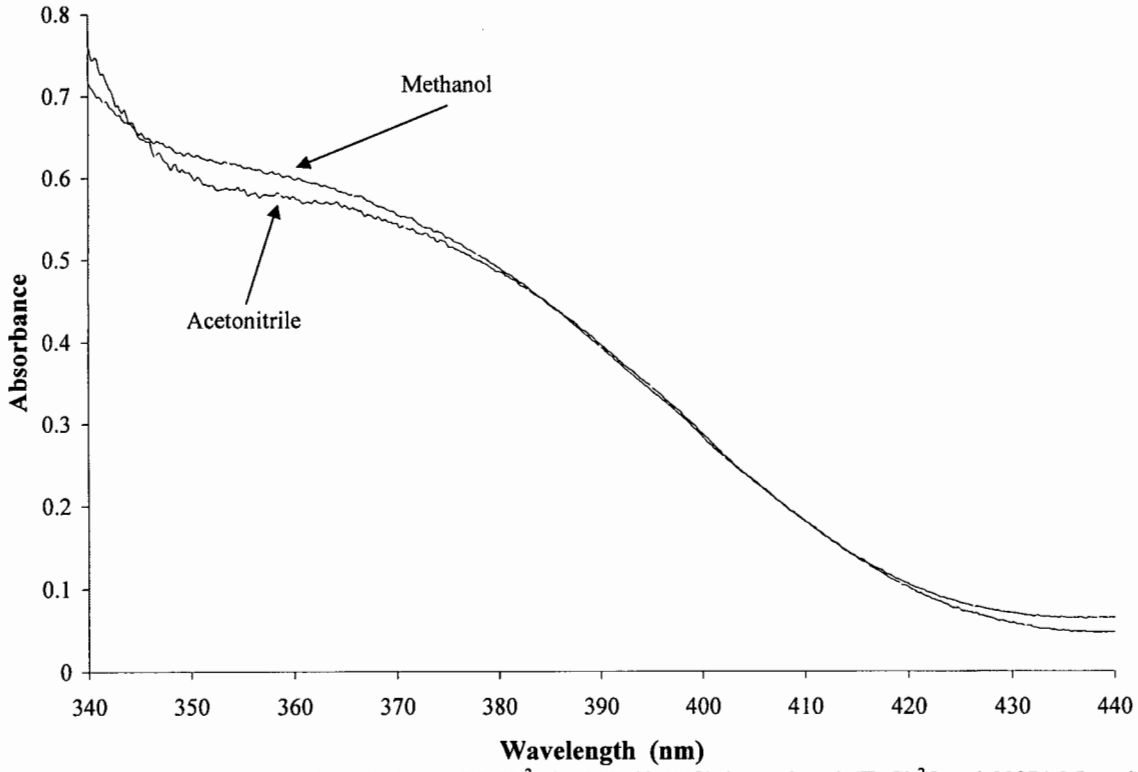

Fig. 4.10 UV-visible spectra for solutions of $PtCl_6^{2-}$ (as $H_2PtCl_6 \cdot H_2O$) in methanol ($[PtCl_6^{2-}]$ = 0.00874 M) and acetonitrile ($[PtCl_6^{2-}]$ = 0.00715 M). Spectra were recorded in a 2 mm quartz cuvette relative to the appropriate solvent as blank.

4.3.5 Interpretation of ^{195}Pt chemical shifts in aqueous binary solvent mixtures

A non-linear dependence of solute-nucleus NMR chemical shifts with changing bulk solvent composition in binary solvent mixtures, is generally regarded as evidence of *preferential solvation* of the ion under study by one of the solvents in the mixture.[1] In the binary mixture of solvents, the composition of the solvation shell of a solvated ion is expected to fluctuate about some average combination of solvent molecules in the first solvation shell. If the fluctuations are fast compared with the reciprocals of the solute-nucleus NMR chemical shift (in cycles per second), the observed chemical shift will be dependent on the average solvation shell composition. Changes in the composition of the solvation cage, due to changes in the bulk mixture, will be reflected in the observed chemical shift.[59] If the solvating abilities of the components of the solvent mixture are alike, the composition of the ion solvation shell will be the same as that of the bulk solvent mixture, and the observed chemical shifts are expected to describe a straight line between the shift values for the pure solvents with changing solvent composition. If, however, the solvents in the mixture have different solvating abilities, i.e. *if a solute interacts more strongly with one of the solvent components*, the solvation shell may *preferentially* contain one of the solvents, and observed chemical shifts, as a function of bulk composition, are expected to deviate from linearity.

Stellenbosch University http://scholar.sun.ac.za

The non-linear variations of $\delta_{Pt\text{-}195}$ with binary solvent composition shown in Figures 4.4 and 4.5, therefore suggest that $PtCl_6^{2-}$ and $PtBr_6^{2-}$ are preferentially solvated by one of the solvents in each binary solvent system studied. The fact that $\delta_{Pt\text{-}195}$, for both $PtCl_6^{2-}$ and $PtBr_6^{2-}$ in all the solvent systems studied, moves downfield more at lower mole fraction organic solvent with changing bulk mixture composition than at higher mole fraction organic solvent (0.5 – 1.0), i.e. the curves are all supraideal, suggests, according to the accepted view,[59,60] that *both anions are preferentially solvated by the non-aqueous solvents in the mixtures, i.e. the non-aqueous solvents interact more strongly with the anions than water.* This phenomenon is more clearly shown with reference to the so-called iso-solvation point.

The term iso-solvation point (or equisolvation point) was introduced by Frankel *et al.* to describe the propensity of a solvent to preferentially solvate an ion.[59,60] Frankel and co-workers investigated the preferential solvation of tris-acetylacetone complexes of Co(III) in CCl_3H-CCl_4 mixtures by ^{59}Co NMR, and defined the iso-solvation point as the bulk solvent composition at which the NMR chemical shift lies midway between the values for the pure solvents. The authors postulate that this is the bulk solvent composition at which both solvents participate equally in the solvation shell, i.e. the bulk composition at which the mole fraction of both solvents *in the solvation sphere* is 0.5; this qualitative measure for preferential solvation has been applied in several studies of the selective solvation of, for example, Na^+[23,24] and Tl^+.[44,61]

The iso-solvation points for each of the binary solvent systems in the present study have been determined according to the description by Frankel *et al.* from the available ^{195}Pt NMR data, and are summarized in Table 4.3; the data are ordered according to decreasing value of the iso-solvation point. For each system, the iso-solvation point lies at a mole fraction organic solvent less than 0.5. Thus, in each series the mole fraction organic solvent in the solvation sphere attains a value of 0.5 before the bulk solvent comprises a 1 : 1 mole composition, indicating that each of the non-aqueous solvents preferentially solvates the $PtCl_6^{2-}$ or $PtBr_6^{2-}$ anions.

Table 4.3 Iso-solvation points, and ^{195}Pt chemical shifts which determine these points, for various aqueous binary solvent systems containing $PtCl_6^{2-}$ and $PtBr_6^{2-}$.

Binary solvent system	$PtCl_6^{2-}$		$PtBr_6^{2-}$	
	$\delta_{Pt\text{-}195}$ (ppm) at the iso-solvation point	Iso-solvation point	$\delta_{Pt\text{-}195}$ (ppm) at the iso-solvation point	Iso-solvation point
D_2O/methanol	51	0.33	57	0.34
D_2O/ethylene glycol	67	0.28	-	-
D_2O/acetonitrile	111	0.24	129	0.22
D_2O/acetone	123	0.19	140	0.17
D_2O/2-methoxyethanol	102	0.18	-	-
D_2O/HMPA	209	0.12	-	-

Stellenbosch University http://scholar.sun.ac.za

Considering the generally accepted view that anions are solvated well by protic solvents, but not by aprotic solvents, even if dipolar,[1] it is a counter-intuitive and somewhat unexpected result that solvents such as acetonitrile, acetone, hexamethylphosphorictriamide and 1,2-dimethoxyethane should *preferentially* solvate $PtCl_6^{2-}$ or $PtBr_6^{2-}$ relative to water. Neither does it seem probable that methanol, ethylene glycol or 2-methoxyethanol, solvents which are protic but have lower hydrogen-bond donicities than water, will selectively solvate the halogenoplatinate anions above water. However, in a recent molecular dynamics simulation study of sodium chloride in water/methanol mixtures,[62,63] Hawlicka and co-workers found the anion (Cl^-) to be selectively solvated by methanol, and the cation (Na^+) to be preferentially hydrated in only water-deficient solutions. Interestingly, these authors conclude from their MD simulations that the preferential solvation of the ions is not due to ion-solvent interactions, but "is a consequence of the incompatibility of the structures of net water and net methanol." They suggest furthermore that in water-rich mixtures the "ions and methanol molecules cannot fit into the tetrahedral structure of water. They are forced to form 'common aggregates' – the preferentially solvated ions." A similar argument may account for the observations in the present investigation: the observed trend suggesting 'preferential solvation' of the anions by the non-aqueous solvents may thus not be related so much to the relative interactions of the solvent molecules with the solute, but may be due to the collective 'exclusion' of the non-aqueous solvent molecules and the anions from the hydrogen-bonded water structure; the much smaller and more mobile H^+ ions which are also in solution, will presumably not be 'excluded' from the H_2O structure since these ions are more easily accommodated. The $PtCl_6^{2-}$ and $PtBr_6^{2-}$ anions are larger (with radii of 313 pm and 342 pm, respectively[64]) than Cl^- (with a radius of 181 pm[64]), and will, due to their size, fit less well in the structure of water than the chloride ion. Moreover, Cl^-, $PtCl_6^{2-}$ and $PtBr_6^{2-}$ are *water structure breakers*; the average number of hydrogen bonds a water molecule near these anions experiences in solution, decreases relative to that in pure water. In pure water, the average number of hydrogen bonds per water molecule is ~ 1.55. Water molecules near a Cl^- ion participate on average in only 0.87 H-bonds, and in only 0.5 H-bonds on average, when near to a $PtCl_6^{2-}$ ion. It is thus conceivable that large anions such as $PtCl_6^{2-}$ and $PtBr_6^{2-}$, which do not fit, and cannot participate, in the hydrogen-bonding network of water molecules, are excluded from this network.

Although the detailed nature of the process which leads to the non-linear distributions in Figures 4.4 and 4.5, remains to be elucidated, it may be either by preferential solvation of the anion (as originally defined) or by collective 'exclusion' of the non-aqueous solvent and the anion, the data emphasizes a difference in composition of the anion solvation shell and the bulk mixture. Pursuant to our aim of utilizing ^{195}Pt NMR to probe the solvation spheres of the halogenoplatinate anions, we have analyzed the observed deviations by methods previously described in the literature for studying preferential solvation phenomena, and continue to use the concepts and terminology developed for this phenomenon.

Stellenbosch University http://scholar.sun.ac.za

4.3.6 Solvation sphere composition

In an investigation of the preferential solvation of the thallous ion in a formamide/pyrrolidine mixture by ^{205}Tl NMR, Dechter and Zink found that the cation was selectively solvated by pyrrolidine, and were able to determine the variation of the cation solvation sphere composition with changing bulk composition by interpreting the deviation from linearity of the observed $\delta_{Tl\text{-}205}$.[44] The method presented by these authors has been applied to the data obtained for $PtCl_6^{2-}$ and $PtBr_6^{2-}$, and is described below with reference to the D_2O/methanol binary solvent system containing $PtCl_6^{2-}$. Fig. 4.11 reproduces the relative ^{195}Pt chemical shift (ppm) *vs* mole fraction methanol data for $PtCl_6^{2-}$; the non-linear trend of the data is ascribed to the preferential solvation of the anion by methanol. If both solvents (D_2O and methanol) were to solvate the anion equally well, the chemical shift data would describe a straight line between the shift extremes (this line has been inserted in Fig. 4.11); the solvation sphere composition would then be the same as the mixture composition. Since the anion is preferentially solvated, the composition of the solvation sphere may be estimated by comparing the experimental curve with the straight line at various bulk solvent compositions. For example, for a bulk solvent composition of 0.33, the solvation sphere composition can be estimated on the *x*-axis by moving horizontally, at the observed chemical shift for that bulk composition (51 ppm), from the experimental curve to the straight line, yielding a value of 0.50; at a bulk solvent composition of 0.33

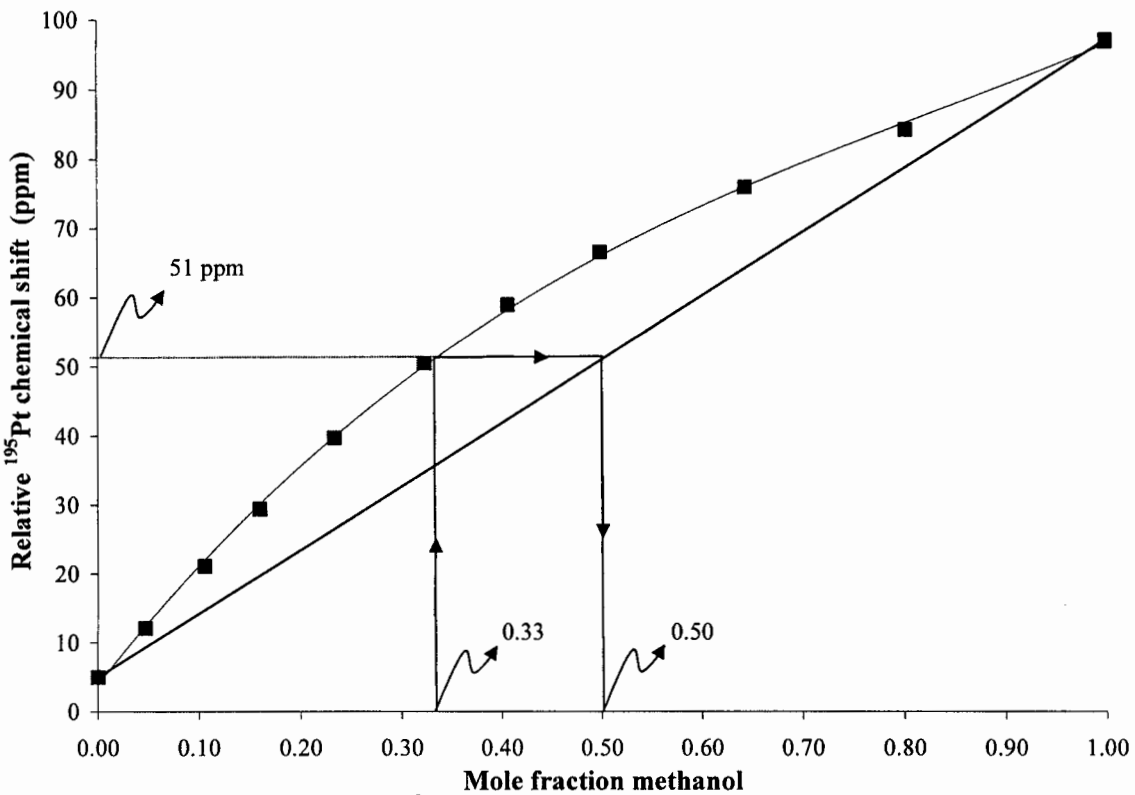

Fig. 4.11 The variation of $\delta_{Pt\text{-}195}$ (for $PtCl_6^{2-}$) as a function of solvent composition in the D_2O/methanol binary solvent system is shown (■; a best-fit polynomial trendline has been inserted). By relating the observed experimental data with the straight line drawn through the shift extremes, the solvation sphere composition at a given bulk composition may be estimated on the *x*-axis.

Stellenbosch University http://scholar.sun.ac.za

mole fraction methanol, the anion solvation sphere comprises a mole fraction methanol of 0.5. Repetition of these steps at various bulk solvent compositions, allows an estimated description of the variation of the solvation sphere composition with changing bulk composition. The estimated variation of the solvation sphere composition of $PtCl_6^{2-}$ with changing bulk solvent composition in the D_2O/methanol binary solvent system is shown graphically in Fig. 4.13.

For each of the binary solvent systems studied, a best-fit Excel trendline was fit onto the $\delta_{Pt\text{-}195}$ *vs* mole fraction organic solvent data. This is shown in Figures 4.1-Adm – 4.12-Adm (Addendum A); the Excel-generated R^2 value indicates the goodness-of-fit of the trendline in each case. Using the equation provided for the trendline, $\delta_{Pt\text{-}195}$ values were calculated for bulk mole fraction organic solvent values between 0.0 and 1.0, in steps of 0.1. These calculated $\delta_{Pt\text{-}195}$ values were inserted into an equation provided by Excel for a linear trendline fit through the shift extremes, in each case, to determine values for the solvation sphere composition at the chosen mixture composition; this data is presented in Tables 4.1B-Adm – 4.12B-Adm and Figures 4.1-Adm – 4.12-Adm, in Addendum A.

Naidoo and Koch *et al.* have recently established models of the solvation spheres of various of simple platinum group metal chloroanions ($PtCl_6^{2-}$, $RhCl_6^{2-}$, $PtCl_4^{2-}$, and $PdCl_4^{2-}$) by means of DFT calculations and molecular dynamics simulations.[12] The spatial probability densities for aqueous $PtCl_6^{2-}$, analyzed at a level 100 % greater than that found in bulk water, resulted in an hydration model for the anion (shown in Fig. 4.12) which reveals that there are on average 8 nearest neighbour solvent molecules around each anion. The water molecules are aligned with hydrogen densities closest to the anion, with the most highly occupied sites of the hydration shell centered above the 8 faces of the octahedral complex, equidistant from the three cofacial chloro ligands. Preliminary calculations for $PtCl_6^{2-}$ in methanol indicate a solvation shell structure similar to that determined for the anion in water, i.e. a first solvation shell comprising 8 methanol molecules.[65]

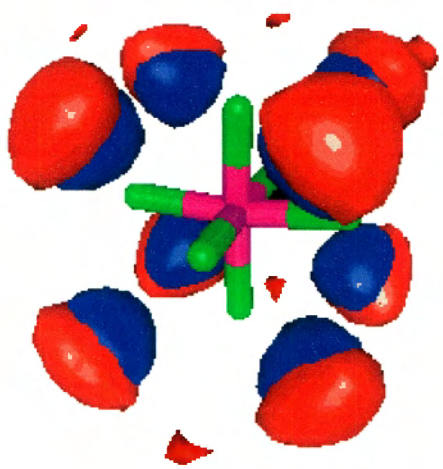

Fig. 4.12 Water isoprobability density surfaces (red = oxygen, blue = hydrogen) for $PtCl_6^{2-}$ at a level 100 % greater than that found in bulk water.[12]

Stellenbosch University http://scholar.sun.ac.za

If it is assumed that the solvation number of $PtCl_6^{2-}$ in binary mixtures of water and methanol is also on average 8, it is possible, with reference to the experimental estimates of the solvation sphere composition in the water/methanol system, to deduce the relative distribution of water and methanol molecules in the solvation sphere of the anion at different mixture compositions. Fig. 4.13 reproduces the solvation sphere composition: mole fraction methanol *vs* mole fraction methanol data. This data reveals that at a bulk mixture composition mole fraction methanol of 0.15, the $PtCl_6^{2-}$ solvation sphere comprises a mole fraction methanol of 0.25, i.e. at this mixture composition, there are on average 6 water and 2 methanol molecules surrounding each $PtCl_6^{2-}$ anion. By similar reasoning, the relative distributions of water : methanol molecules in the $PtCl_6^{2-}$ solvation sphere at mixture compositions of 0.33 and 0.61 mole fractions of methanol, will be 4 : 4 and 6 : 2 respectively, as illustrated in Fig. 4.13.

Notwithstanding the uncertainty that exists as to the nature of the process which leads to the observed non-linear variations of $\delta_{Pt\text{-}195}$ with changing bulk solvent composition, analysis of these variations allows the composition of the anion solvation sphere to be estimated; this emphasizes the potential of ^{195}Pt NMR for studying the hydration/solvation shells of the PtX_6^{2-} (X = Cl, Br) anions.

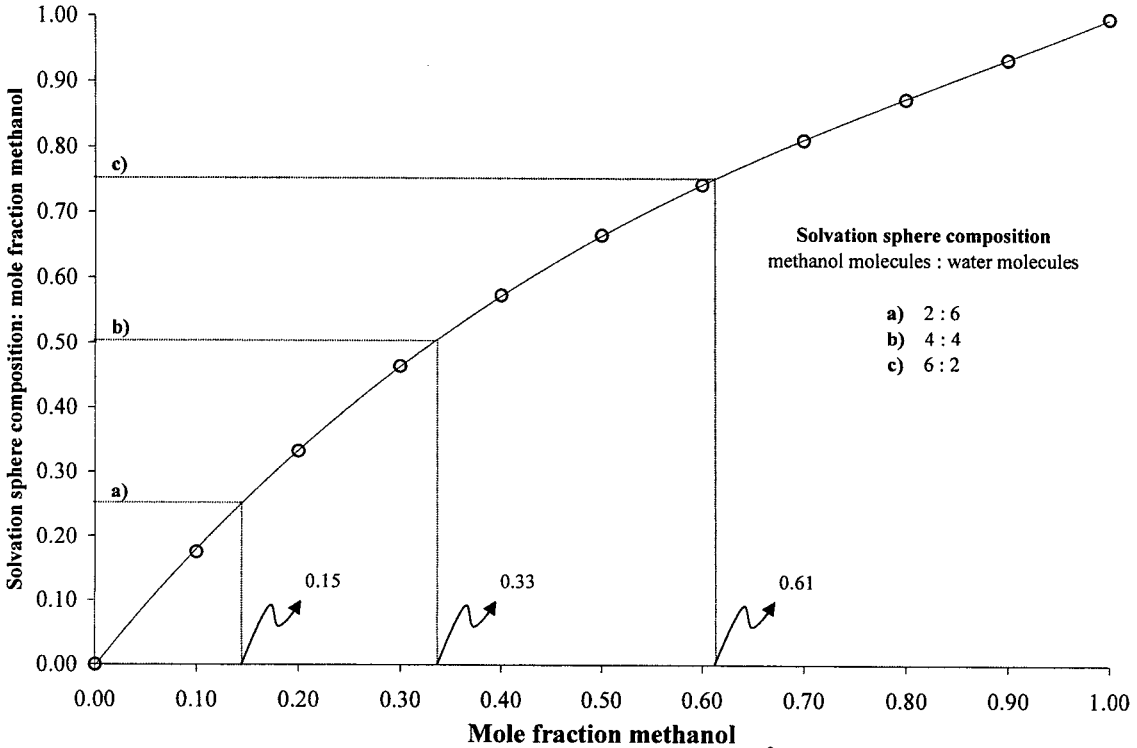

Fig. 4.13 The experimentally estimated solvation sphere composition for $PtCl_6^{2-}$ in the D_2O/methanol binary solvent system (O), in conjunction with the computationally derived solvation number of 8 for the anion in water and methanol, can be used to determine the relative distribution of water and methanol molecules in the anion solvation sphere at different mixture compositions.

Stellenbosch University http://scholar.sun.ac.za

4.3.7 Preferential solvation: a quantitative model

The concept of the preferential solvation of an ion in a binary solvent system may easily be described in a *qualitative* sense in terms of the isosolvation point, as has been done for the halogenoplatinate anions in Section 4.3.5. Attempts have also been made to describe the process of selective solvation in a more *quantitative* sense, by the determination of solvation equilibrium constants.[9,25] Recently, Ohtaki proposed the use of a parameter he defined as the *preferential solvation quotient*, K_{PSQ},[9] as a quantitative measure of the preferential solvation of an ion; this was done with reference to results published by Ozutsumi *et al.*[66] Ozutsumi and co-workers studied the solvation structure of the silver(I) ion in binary solvent mixtures of acetonitrile and *N,N*-dimethylformamide by means of X-ray diffraction, and found the cation to be preferentially solvated by acetonitrile in these solvent mixtures.[66] With reference to the work of Ozutsumi *et al.*, Ohtaki defines the preferential solvation quotient as follows:[9]

$$K_{PSQ} = \frac{[A]_{SS}/[B]_{SS}}{[A]_B/[B]_B} \qquad (4.5)$$

where $[A]_B$ and $[B]_B$ denote the concentrations of solvents A and B, in an A/B binary solvent system, in the bulk, and $[A]_{SS}$ and $[B]_{SS}$ the concentrations of A and B in the first solvation shell of the ion of interest. Ohtaki re-writes this expression in terms of mole fractions:

$$K_{PSQ} = \frac{{}^{SS}X_A/(1-{}^{SS}X_A)}{{}^{B}X_A/(1-{}^{B}X_A)} \qquad (4.6)$$

with ${}^{SS}X_A$ and ${}^{B}X_A$ the mole fractions of solvent A in the first solvation sphere and the bulk, respectively. Ohtaki points out that an ion is preferentially solvated with solvent A if K_{PSQ} is larger than 1. Using different values of K_{PSQ}, Ohtaki applies equation (4.6) to *calculate* various ${}^{SS}X_{acetonitrile}$ (mole fraction of acetonitrile in the solvation shell of Ag^+) *vs* ${}^{B}X_{acetonitrile}$ (mole fraction of acetonitrile in the bulk) series for the acetonitrile/*N,N*-dimethylformamide binary solvent system of the Ozutsumi *et al.* study. By graphically comparing the various calculated ${}^{SS}X_{acetonitrile}$ *vs* ${}^{B}X_{acetonitrile}$ series with the experimental ${}^{SS}X_{acetonitrile}$ *vs* ${}^{B}X_{acetonitrile}$ data, an estimated value for K_{PSQ} is derived; for Ag^+ in the acetonitrile/*N,N*-dimethylformamide binary solvent system, Ohtaki determines the value of K_{PSQ} to be about 2.[9]

For each of the binary solvent systems studied in the present investigation, with either $PtCl_6^{2-}$ or $PtBr_6^{2-}$ as anion, it has been possible to calculate the variation of the solvation sphere composition with varying bulk solvent composition (Section 4.3.6); the experimental ${}^{SS}X_{Organic\ solvent}$ (mole fraction of organic solvent in the solvation shell of the halogenoplatinate anion) *vs* ${}^{B}X_{Organic\ solvent}$ (mole fraction of organic solvent in the bulk) data have been presented in Tables 4.1B-Adm - 4.12B-Adm and in Figures 4.1-Adm - 4.12-Adm in Addendum A. For every system, various possible K_{PSQ} values were substituted into equation (4.6), re-written in the form:

$${}^{SS}X_{Organic\ solvent} = \left(\frac{K_{PSQ}\cdot{}^{B}X_{Organic\ solvent}}{1 - {}^{B}X_{Organic\ solvent}}\right)\Big/\left[1 + \left(\frac{K_{PSQ}\cdot{}^{B}X_{Organic\ solvent}}{1 - {}^{B}X_{Organic\ solvent}}\right)\right] \qquad (4.7)$$

Stellenbosch University http://scholar.sun.ac.za

together with the ${}^{B}X_{\text{Organic solvent}}$ range of values presented in Tables 4.1B-Adm - 4.12B-Adm, in order to *calculate* various ${}^{SS}X_{\text{Organic solvent}}$ *vs* ${}^{B}X_{\text{Organic solvent}}$ series. For example, for the D_2O/methanol binary solvent system containing $PtCl_6^{2-}$, K_{PSQ} values of 1, 2 and 3 were substituted into equation (4.7) together with ${}^{B}X_{met}$ values varying between 0.0 and 1.0 (in steps of 0.1) to obtain ${}^{SS}X_{met}$ *vs* ${}^{B}X_{met}$ series for each of the chosen K_{PSQ} values. The ${}^{SS}X_{met}$ *vs* ${}^{B}X_{met}$ series calculated for K_{PSQ} = 1.0 (■), K_{PSQ} = 2.0 (◆) and K_{PSQ} = 3.0 (▲) are shown in Fig. 4.14 together with the experimental ${}^{SS}X_{met}$ *vs* ${}^{B}X_{met}$ data (O). Note that the ${}^{SS}X_{met}$ points calculated for K_{PSQ} = 2.0 are practically identical to the experimental points at corresponding ${}^{B}X_{met}$ values, from which we may conclude that K_{PSQ} for the preferential solvation of $PtCl_6^{2-}$ by methanol in the D_2O/methanol binary solvent system, is 2.0. This process was repeated for each of the binary solvent systems, for both $PtCl_6^{2-}$ and $PtBr_6^{2-}$, in the present investigation. Estimated values, or value ranges, for K_{PSQ} were determined for each system by comparing the experimental and calculated ${}^{SS}X_{\text{Organic solvent}}$ *vs* ${}^{B}X_{\text{Organic solvent}}$ plots, and the results have been summarized in Table 4.4. Several systems allow a fairly precise graphical fit of the experimental and calculated ${}^{SS}X_{\text{Organic solvent}}$ *vs* ${}^{B}X_{\text{Organic solvent}}$ plots (as seen in Fig. 4.14 for the D_2O/methanol-$PtCl_6^{2-}$ series), while for most other binary mixtures only a range of K_{PSQ} values can be determined since the experimental points deviate between the calculated points for the given range of K_{PSQ} values. Table 4.4 shows that the order of the solvents according to decreasing iso-solvation point, correlates fairly well with the order according to increasing K_{PSQ} values/ranges.

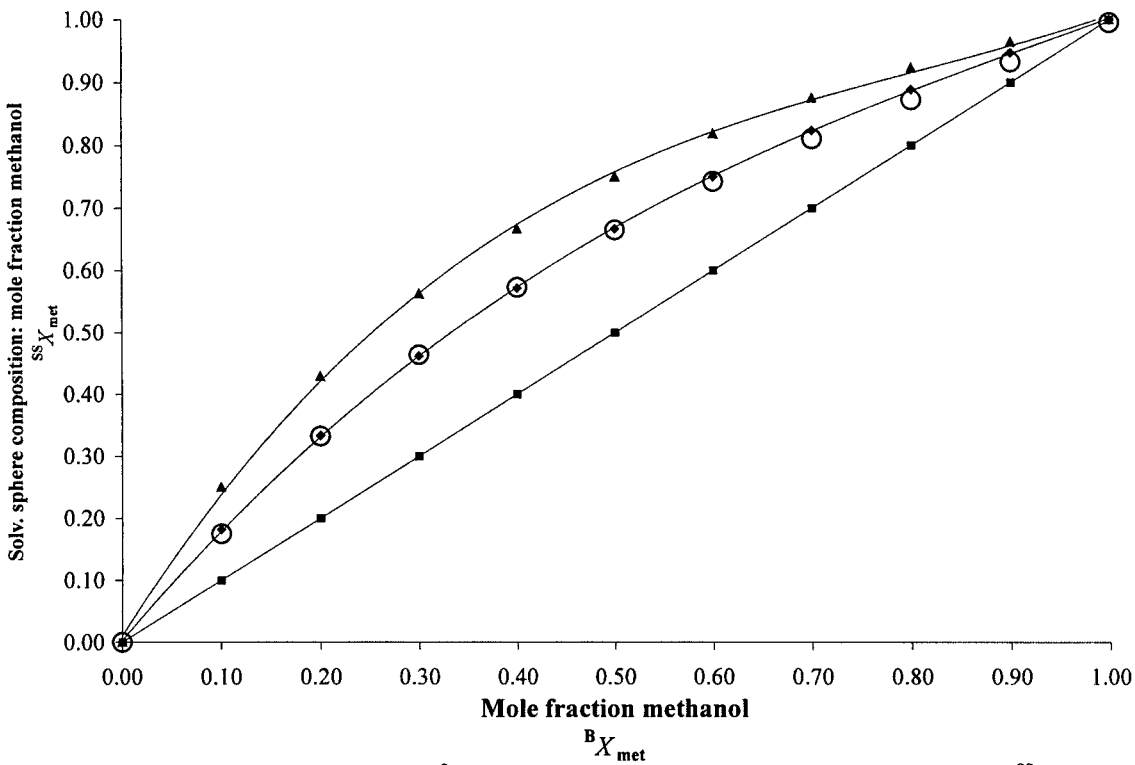

Fig. 4.14 Estimated variation of the $PtCl_6^{2-}$ solvation sphere composition (mole fraction methanol, ${}^{SS}X_{met}$) with changing bulk solvent composition (${}^{B}X_{met}$) determined experimentally, is shown (O). The ${}^{SS}X_{met}$ *vs* ${}^{B}X_{met}$ data *calculated* with equation (4.7) for K_{PSQ} = 1 (■), K_{PSQ} = 2 (◆) and K_{PSQ} = 3 (▲) are also depicted; best-fit trendlines have been inserted. K_{PSQ} for the preferential solvation of $PtCl_6^{2-}$ in the D_2O/methanol binary solvent system is *ca.* 2.0.

Stellenbosch University http://scholar.sun.ac.za

Table 4.4 Estimated values, or value ranges, for the preferential solvation quotient, K_{PSQ},[9] of the anions $PtCl_6^{2-}$ and $PtBr_6^{2-}$ in various aqueous binary solvent systems; iso-solvation points are also shown.

Binary solvent system	$PtCl_6^{2-}$ Iso-solvation point	K_{PSQ}	$PtBr_6^{2-}$ Iso-solvation point	K_{PSQ}
D_2O/methanol	0.33	2.0	0.34	2.0
D_2O/ethylene glycol	0.28	2.5	-	-
D_2O/acetonitrile	0.24	3 – 3.5	0.22	3 – 3.5
D_2O/acetone	0.19	4 – 6	0.17	4 - 8
D_2O/2-methoxyethanol	0.18	4 – 5	-	-
D_2O/HMPA	0.12	6 – 7	-	-

A more rigorous and thorough quantitative model for selective solvation than that described by Ohtaki, has been developed by Covington and co-workers in an investigation of the preferential solvation of various alkali metal halide salts in H_2O/H_2O_2 binary mixtures, by means of ^7Li, ^{23}Na, ^{87}Rb, ^{133}Cs, ^{19}F and ^{35}Cl NMR.[25,67-70] This model allows the calculation of equilibrium constants as the solvation shell of an ion X progressively changes from *n* molecules of solvent W to *n* molecules of solvent O in a series of binary solvent mixtures. The authors consider a mixture that contains 1 mole of ions X, *w* mole of solvent W and *o* mole of solvent O, and assume for simplicity in the derivation a solvation number *n* of 4 for X in all mixtures of W and O. With increasing mol fraction of solvent O, the solvation of ion X can be described by a series of successive equilibria in the form:

$$XW_4 + oO + (w-4)W \xleftrightarrow{K_1} XW_3O + (o-1)O + (w-3)W \xleftrightarrow{K_2} XW_2O_2 + (o-2)O + (w-2)W \xleftrightarrow{K_3}$$
$$XWO_3 + (o-3)O + (w-1)W \xleftrightarrow{K_4} XO_4 + (o-4)O + wW \qquad (4.8)$$

For each of the equilibria an equilibrium constant expression is formulated in terms of activities:

$$K_1 = \frac{a_{XW_3O} \cdot a_W}{a_{XW_4} \cdot a_O};\ K_2 = \frac{a_{XW_2O_2} \cdot a_W}{a_{XW_3O} \cdot a_O};\ K_3 = \frac{a_{XWO_3} \cdot a_W}{a_{XW_2O_2} \cdot a_O};\ K_4 = \frac{a_{XO_4} \cdot a_W}{a_{XWO_3} \cdot a_O} \qquad (4.9)$$

It is accepted for simplicity in the derivation that the activities of the solvated ionic species tend toward the species molality as the concentration of the solute in a particular binary solvent mixture tends toward zero, and that for solutions in which the moles of solute are low compared to the moles of solvent, the species molalities can be written as:

$$m_{XW_3O} = K_1 m_{XW_4}\left(\frac{a_O}{a_W}\right);\ m_{XW_2O_2} = K_1K_2 m_{XW_4}\left(\frac{a_O}{a_W}\right)^2;$$
$$m_{XWO_3} = K_1K_2K_3 m_{XW_4}\left(\frac{a_O}{a_W}\right)^3;\ m_{XO_4} = K_1K_2K_3K_4 m_{XW_4}\left(\frac{a_O}{a_W}\right)^4 \qquad (4.10)$$

The fundamental expression which relates the measured chemical shift, δ (the single, averaged resonance observed), to the intrinsic shifts of each species i, δ_i, is:

$$\delta = \sum_i X_i \delta_i \qquad (4.11)$$

Stellenbosch University http://scholar.sun.ac.za

with X_i the mole fraction of the species i, i.e.

$$X_i = \frac{m_i}{\sum_i m_i} \tag{4.12}$$

If the observed chemical shift *difference* for ion X in pure solvent W and pure solvent O is defined as δ_O, and it is assumed that the intrinsic shifts of the various species are proportional to the fraction of O molecules in the solvation sphere of the ion, then the following expressions may be formulated for δ_i:

$$\delta_{XW_4} = 0;\ \delta_{XW_3O} = \frac{\delta_O}{4};\ \delta_{XW_2O_2} = \frac{\delta_O}{2};\ \delta_{XWO_3} = \frac{3}{4}\delta_O;\ \delta_{XO_4} = \delta_O \tag{4.13}$$

Now substituting equations (4.10) and equations (4.13) into equation (4.11) and simplifying, leads to:

$$\frac{\delta}{\delta_O} = \frac{1}{4T}\left(K_1Y + 2K_1K_2Y^2 + 3K_1K_2K_3Y^3 + 4K_1K_2K_3K_4Y^4\right) \tag{4.14}$$

with

$$T = 1 + K_1Y + K_1K_2Y^2 + K_1K_2K_3Y^3 + K_1K_2K_3K_4Y^4$$

and

$$Y = \frac{a_O}{a_W}$$

Another simplifying assumption requires that the individual equilibrium constants, K_i, are related entirely by statistical requirements,* i.e. for $n = 4$:

$$K_1 = 4K';\ K_2 = \frac{3}{2}K';\ K_3 = \frac{2}{3}K';\ K_4 = \frac{1}{4}K' \tag{4.15}$$

where

$$K' = K^{\frac{1}{4}} = \left(K_1K_2K_3K_4\right)^{\frac{1}{4}} \tag{4.16}$$

and K is defined as the overall constant for the equilibrium:

$$XW_4 + 4O \overset{K}{\longleftrightarrow} XO_4 + 4W \tag{4.17}$$

Substituting equations (4.15) into equation (4.14) and factorizing gives:

$$\frac{\delta}{\delta_O} = \frac{K'Y}{1 + K'Y} = \frac{K^{\frac{1}{4}}Y}{1 + K^{\frac{1}{4}}Y} \tag{4.18}$$

* This assumption is based on the fact that the species XW_3O, for example, can lose solvent W from three different sites and the species XW_2O_2 can lose solvent O from two, hence $K_2 = 3/2K'$.

Covington points out that K' in equation (4.16) can be *reduced* to the K_{PSQ} defined by Ohtaki in equation (4.6).[9] This can be shown if equations (4.9) are substituted into equation (4.16), and the activity of the solvent in the inner solvation sphere is related to the activity of the solvated ion by a power equal to the number of solvent molecules in the solvation sphere.

Stellenbosch University http://scholar.sun.ac.za

This expression may be generalized for a solvation number *n*:

$$\frac{\delta}{\delta_o} = \frac{K^{\frac{1}{n}}Y}{1 + K^{\frac{1}{n}}Y} \tag{4.19}$$

and re-written in the form:

$$\frac{1}{\delta} = \frac{1}{\delta_o}\left(1 + \frac{1}{K^{\frac{1}{n}}Y}\right) \quad \text{or} \quad \frac{1}{\delta} = \frac{1}{\delta_o} + \left[\left(\frac{1}{\delta_o \cdot K^{\frac{1}{n}}}\right)\left(\frac{a_w}{a_o}\right)\right] \tag{4.20}$$

To allow the application of this expression, the activities of the solvents are substituted by their mole fractions:

$$Y = \frac{a_o}{a_w} \approx \frac{X_o}{X_w} \tag{4.21}$$

yielding:

$$\frac{1}{\delta} = \frac{1}{\delta_o} + \left[\left(\frac{1}{\delta_o \cdot K^{\frac{1}{n}}}\right)\left(\frac{X_w}{X_o}\right)\right] \tag{4.22}$$

with: δ = the observed chemical shift relative to the resonance of ion X in pure W,

δ_O = the total range of the chemical shifts, i.e. $\delta_{XO_n} - \delta_{XW_n}$

$K^{1/n}$ = the *derived preferential solvation equilibrium constant*, and

X_W, X_O = the mole fractions of the solvents W and O, respectively, in the mixture.

Thus, a plot of $1/\delta$ *vs* X_W/X_O is expected to yield a straight line, if the derived model with all its assumptions and simplifications is applicable, the gradient of which can be used to estimate a value for $K^{1/n}$.

For each of the binary solvent systems studied in the present investigation, with either $PtCl_6^{2-}$ or $PtBr_6^{2-}$ as anion, a value for $1/\delta_O$ can be calculated from the available experimental results, and $1/\delta$ *vs* X_W/X_O data can be determined from the information in Tables 4.1A-Adm - 4.12A-Adm. For example, for the D_2O/methanol binary solvent system containing $PtCl_6^{2-}$, Fig. 4.15 depicts a plot of $1/\delta$ *vs* ${}^BX_{water}/{}^BX_{methanol}$; δ_O = 92 ppm (see Table 4.1A-Adm), and the intercept for the linear trendline that has been inserted, is set at 0.01087. The Excel-generated R^2 value of 0.997 for this trendline emphasizes the linearity of the data points, and from the gradient of the straight line (0.006335), $K^{1/n}$ = 1.72 can be calculated. The data for each binary solvent system of the present study has been treated according to equation (4.22), and values for $K^{1/n}$ have been calculated. These values are presented in Table 4.5, together with the Excel-generated R^2 values for the linear trendlines.

Stellenbosch University http://scholar.sun.ac.za

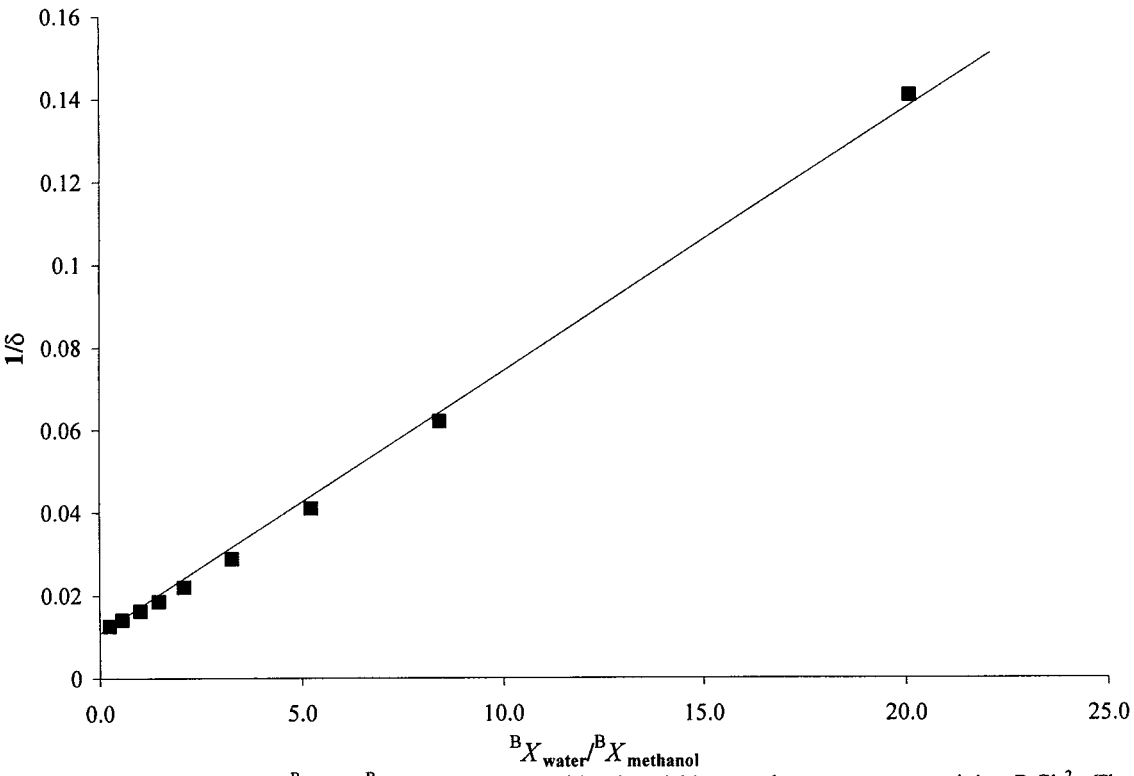

Fig. 4.15 A plot of $1/\delta$ *vs* $^{B}X_{water}/^{B}X_{methanol}$ for the D_2O/methanol binary solvent system containing $PtCl_6^{2-}$. The gradient of the linear trendline, with intercept fixed at $1/\delta_O$ ($R^2 = 0.997$), is used to determine the value of $K^{1/n}$ (1.72) for the system.

The R^2 values presented in Table 4.5 indicate that the plots of $1/\delta$ *vs* $X_{Water}/X_{Organic\ solvent}$ do yield very good straight lines in each case, although the D_2O/1,2-dimethoxyethane solvent system shows some degree of curvature. There is also, generally, fairly good agreement between values for K_{PSQ}, determined by application of the method of Ohtaki, and values for $K^{1/n}$, determined by Covington's method, for the different binary solvent systems

Table 4.5 Values of $K^{1/n}$, the Covington derived preferential solvation equilibrium constant,[25] calculated for $PtCl_6^{2-}$ and $PtBr_6^{2-}$ in various aqueous binary solvent mixtures, together with Excel-generated R^2 values for linear trendlines fit to the data from which the constants have been calculated. Iso-solvation points and K_{PSQ} values[9] are also presented.

Binary solvent system	$PtCl_6^{2-}$				$PtBr_6^{2-}$			
	Iso-solvation point	K_{PSQ}	$K^{1/n}$	R^2	Iso-solvation point	K_{PSQ}	$K^{1/n}$	R^2
D_2O/methanol	0.33	2.0	1.72	0.997	0.34	2.0	1.72	0.998
D_2O/ethylene glycol	0.28	2.5	2.50	1.000	-	-	-	-
D_2O/acetonitrile	0.24	3 – 3.5	2.86	0.995	0.22	3 – 3.5	3.07	0.992
D_2O/acetone	0.19	4 – 6	3.66	0.993	0.17	4 - 8	3.83	0.990
D_2O/2-methoxyethanol	0.18	4 – 5	4.03	0.994	-	-	-	-
D_2O/HMPA	0.12	6 – 7	5.63	0.997	-	-	-	-

Stellenbosch University http://scholar.sun.ac.za

In an investigation of the preferential solvation of the Na^+ ion in a variety of binary solvent mixtures, based on ^{23}Na NMR chemical shift data, Greenberg and Popov found, by applying the Covington model described above, that plots of the required data yielded straight lines for all the systems studied, except for an acetonitrile/pyridine combination.[24] Frankel *et al.*, who studied the selective solvation of Co^{3+} in binary mixtures of chloroform with acetone and *p*-dioxane by ^{59}Co NMR,[59] noted, in a treatment similar to that of Covington,* curvature in plots of the solvation isotherms. These authors ascribe the observed curvature to either weak solvent-solvent interactions, or to unequal solvation numbers of the cations in the solvents used. The Covington derivation is based on the assumption that the solvation numbers of the ion being studied are the same in the solvents of the mixture. The computational studies of Naidoo and Koch *et al.* have revealed that the solvation numbers of $PtCl_6^{2-}$ in water and methanol are the same.[12,65] Solvation numbers for $PtCl_6^{2-}$ and $PtBr_6^{2-}$ in the other non-aqueous solvents are not known, but it is likely that in solvents with bulkier molecules than H_2O, for example HMPA or 1,2-dimethoxyethane, the solvation numbers of the anions will be less than for water. However, despite the idealized assumptions which characterize the Covington model (requiring that a mixture be iso-dielectric, that it should exhibit ideal behaviour, and that solvation numbers must be equal), the results suggest that the approach is fairly successful, and appears to give a *quantitative* description of the selective solvation of the halogenoplatinate anion which shows some correlation with the more *qualitative* iso-solvation point for the various binary solvent mixtures (Table 4.5).

In an investigation of the preferential solvation of the thallous ion in binary solvent mixtures of *N,N*-dimethylformamide (DMF) with a variety of competing solvents by ^{205}Tl NMR, Dechter and Zink calculated preferential solvation equilibrium constants, $K^{1/n}$, for the binary systems by applying the Covington model.[61] These authors found a fair linear correlation of log $K^{1/n}$ and Gutmann's Donor Numbers (*DN*) for the solvents; solvents which had *DN* values higher than that of DMF preferentially solvated the thallous ion relative to DMF (log $K^{1/n} > 1$), while DMF preferentially solvated Tl^+ (log $K^{1/n} < 1$) in binary mixtures in which the competing solvent had a lower *DN* value than DMF.

Values of log $K^{1/n}$ for the preferential solvation of $PtCl_6^{2-}$ by the organic solvents in the aqueous binary solvent systems of the present investigation are presented in Table 4.6, together with values for various properties of the organic solvents. A plot of log $K^{1/n}$ *vs* $E_T(30)$ of the organic solvent in the aqueous binary solvent mixture is shown in Fig. 4.16. (The distribution of points for log $K^{1/n}$ *vs AN* (Acceptor Number) of the organic solvent in the binary mixture is very similar to that shown in Fig. 4.16, and is not presented). In Fig. 4.16, the data points for the aprotic and protic organic solvents appear to lie in distinct regions on the graph. In this figure there appears to be some correlation of log $K^{1/n}$ and the acceptor properties of the

* Frankel *et al.* derive the expression ${}^{SS}X_A/{}^{SS}X_B = K\,{}^{B}X_A/{}^{B}X_B$ for an A/B binary solvent system based on analogies of preferential solvation with preferential absorption phenomena,[59] and determine K from the gradient of ${}^{SS}X_A/{}^{SS}X_B$ *vs* ${}^{B}X_A/{}^{B}X_B$. The expression derived by Frankel *et al.* is the same as that for K_{PSQ} defined by Ohtaki,[9] i.e. ${}^{SS}X_A/(1 - {}^{SS}X_A) = K_{PSQ}\,[{}^{B}X_A/(1 - {}^{B}X_A]$ (equation 4.6).

Table 4.6 Values of $\log K^{1/n}$ calculated for the preferential solvation of $PtCl_6^{2-}$, by the organic solvent, in aqueous binary solvent systems (the organic solvent used in each binary system is indicated as the competing solvent), and various properties for the organic solvents.

Competing Solvent	$\log K^{1/n}$	μ (D)[a]	ε	$E_T(30)$ (kcal mol^{-1})	Kamlet-Taft π^*	DN^N	AN	Kamlet-Taft α
Methanol	0.24	2.87	32.66	55.4	0.6	0.77	41.5	0.98
Ethylene glycol	0.40	2.31	37.7	56.3	0.92	0.52	43.4	0.9
Acetonitrile	0.46	3.92	35.94	45.6	0.66	0.36	18.9	0.19
Acetone	0.56	2.69	20.56	42.2	0.62	0.44	12.5	0.08
2-Methoxyethanol	0.61	2.04	16.93	52	0.71		36.1	0.74
Hexamethylphosphorictriamide	0.75	5.54	29.3	40.9	0.87	1	9.8	0
1,2-Dimethoxyethane	0.83	1.71	7.2	38.2	0.53	0.62	10.2	0

Values for solvent properties are those published by Marcus.[46]
[a] $D = 3.33564 \times 10^{-30}$ C·m

Stellenbosch University http://scholar.sun.ac.za

Stellenbosch University http://scholar.sun.ac.za

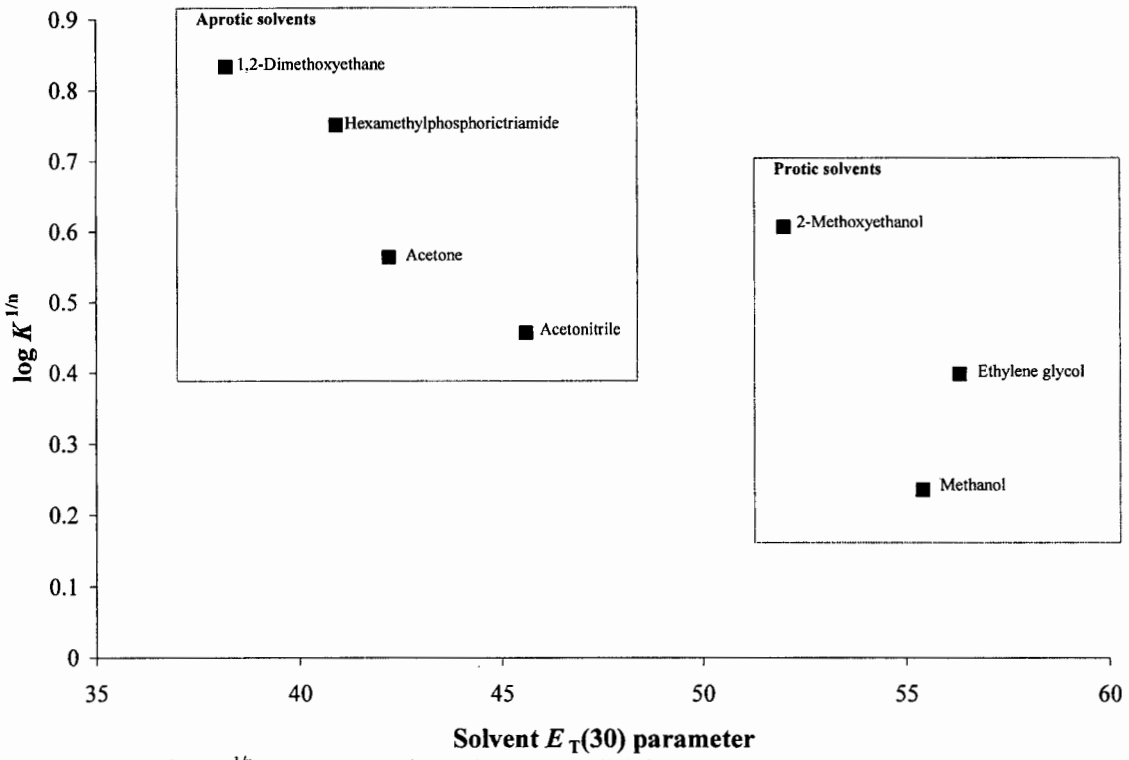

Fig. 4.16 Plot of log $K^{1/n}$ as a function of organic solvent $E_T(30)$ for aqueous binary solvent mixtures containing the organic solvent as indicated, and $PtCl_6^{2-}$.

aprotic solvents: there is generally an *increase* in log $K^{1/n}$ for the aprotic solvents with *decreasing* $E_T(30)$ parameter for these solvents. This seeming correlation however does not conform with the description that the solvent acceptance ability as indicated by the $E_T(30)$ parameter relates specifically to the hydrogen-bond donation ability of *protic* solvents. There is no apparent relationship between log $K^{1/n}$ and the $E_T(30)$ parameter for the protic solvents, however. A plot of log $K^{1/n}$ *vs* the Kamlet-Taft α parameter of the organic solvent in the aqueous binary solvent mixture (shown in Fig. 4.17) suggests that there may be a linear correlation between log $K^{1/n}$ and α for the protic solvents (the Kamlet-Taft α parameter is a measure of the hydrogen-bond donation ability of a solvent; protic and protogenic solvents have non-zero α values). With decreasing α for the protic solvents, there is linear increase in log $K^{1/n}$, i.e. the propensity of the protic solvents to solvate $PtCl_6^{2-}$ relative to water *increases* as the hydrogen-bonding ability of the solvent *decreases*. Plots of log $K^{1/n}$ *vs* solvent dipole moment (μ), dielectric constant (ε), the Kamlet-Taft π^* parameter, or normalized Donor Number (DN^N), reveal no correlation between log $K^{1/n}$ and these solvent parameters.

Stellenbosch University http://scholar.sun.ac.za

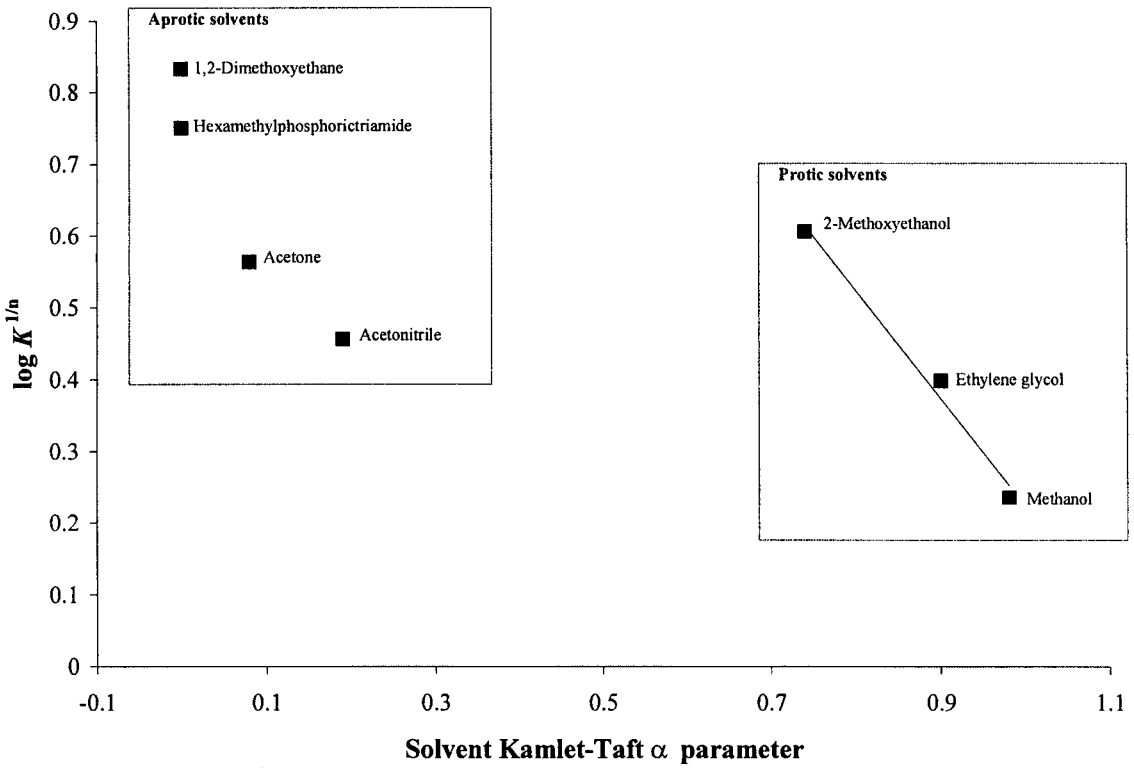

Fig. 4.17 Plot of log $K^{1/n}$ as a function of organic solvent Kamlet-Taft α parameter for aqueous binary solvent mixtures containing the organic solvent as indicated, and $PtCl_6^{2-}$.

The difficulty encountered in interpreting the values of log $K^{1/n}$ for the present study in terms of solvent properties, may be an indication that the observed preferential solvation is due more to the collective 'exclusion' of the organic solvent and anion from the water structure (see Section 4.3.5) than to the relative solvating abilities of water and the organic solvent in question, in which case log $K^{1/n}$ may possibly be a reflection of the 'ability' of water to exclude the organic solvent from its hydrogen-bonded structure.

4.4 Concluding Remarks

The ^{195}Pt NMR chemical shift of $PtCl_6^{2-}$ and $PtBr_6^{2-}$ shows a remarkable solvent dependence, varying by several hundred ppm in only a small selection of the most commonly used water-miscible solvents (methanol, acetonitrile, acetone, hexamethylphosphorictriamide, ethylene glycol, 2-methoxyethanol, and 1,2-dimethoxyethane), with protic solvents resulting in relatively more upfield resonance positions than the aprotic solvents. The ^{195}Pt resonance position is not determined predominantly by the non-specific polarity of the solvent, as measured by the dielectric constant or dipole moment, but appears to be related to the specific manner in which the solvent molecules interact with the PtX_6^{2-} (X = Cl, Br) anions. A linear correlation of $\delta_{Pt\text{-}195}$ for $PtCl_6^{2-}$ with the hydrogen-bond donating ability of protic solvents (a downfield shift of $\delta_{Pt\text{-}195}$ with decreasing H-bond donicity is observed) suggests that the anion is solvated *via* hydrogen-

Stellenbosch University http://scholar.sun.ac.za

bonding interactions with these solvent molecules. No relationship between $\delta_{Pt\text{-}195}$ for $PtCl_6^{2-}$ in aprotic solvents and the acceptor properties of the solvents is apparent, which reflects the generally accepted view that aprotic solvents do not solvate anions well.

For aqueous binary solvent mixtures with the water-miscible organic solvents, non-linear variations of the ^{195}Pt chemical shift of $PtCl_6^{2-}$ and $PtBr_6^{2-}$ with changing mixture composition are observed. These non-linear trends reflect the difference between the solvation sphere composition of the anions and the bulk solvent composition, and indicate that the organic solvents preferentially solvate the anions relative to water. This phenomenon may not be due to stronger interactions of the non-aqueous solvent molecules with the anions, considering the properties of the solvents in question, but possibly results from the collective 'exclusion' of the anions and organic solvent molecules from the hydrogen-bonded network of water. Nevertheless, the sensitivity of the ^{195}Pt chemical shift to the environment directly around the anions, yields shift variation data with which not only the compositions of the anion solvation spheres with changing bulk composition may be derived, but also allows the estimation of preferential solvation equilibrium constants for the anions in the binary solvent mixtures.

References

1 Y. Marcus, in *Ion Solvation*, Wiley-Interscience, Chichester, 1985.
2 J. F. Hinton and E. S. Amis, *Chemical Reviews*, 1967, **67**, 367.
3 A. I. Popov, *Pure and Applied Chemistry*, 1975, **41**, 275.
4 D. W. James, *Progress in Inorganic Chemistry*, 1985, **33**, 353.
5 J. J. Lagowski, in *The chemistry of non-aqueous solvents*, Academic Press Inc., New York, 1966.
6 J. F. Coetzee and C. D. Ritchie, in *Solute-solvent interactions*, Marcel Dekker, Inc., New York, 1969.
7 J. Burgess, in *Metal ions in solution*, Ellis Horwood Limited, Chichester, 1978.
8 J. Burgess, in *Ions in solution, Basic principles of chemical interactions*, Horwood Publishing Limited, Chichester, 1999.
9 H. Ohtaki, *Monatshefte fur Chemie*, 2001, **132**, 1237.
10 B. E. Conway, in *Ionic hydration in chemistry and biophysics*, Elsevier Scientific Publishing Company, Amsterdam, 1981.
11 A. Lienke, G. Klatt, D. J. Robinson, K. R. Koch and K. J. Naidoo, *Inorganic Chemistry*, 2001, **40**, 2352.
12 K. J. Naidoo, G. Klatt, K. R. Koch and D. J. Robinson, *Inorganic Chemistry*, 2002, **41**, 1845.
13 B. A. Moyer and P. V. Bonnesen, in *Supramolecular Chemistry of Anions*, Wiley-VCH, New York, 1997.
14 R. K. Harris and B. E. Mann, in *NMR and the Periodic Table*, Academic Press INC., London, 1978.
15 E. G. Bloor and R. G. Kidd, *Canadian Journal of Chemistry*, 1968, **46**, 3425.
16 R. H. Erlich, E. Roach and A. I. Popov, *Journal of the American Chemical Society*, 1970, **92**, 4989.
17 R. H. Erlich and A. I. Popov, *Journal of the American Chemical Society*, 1971, **93**, 5620.
18 M. Herlem and A. I. Popov, *Journal of the American Chemical Society*, 1972, **94**, 1431.
19 M. S. Greenberg, R. L. Bodner and A. I. Popov, *Journal of Physical Chemistry*, 1973, **77**, 2449.
20 M. S. Greenberg, D. S. Wied and A. I. Popov, *Spectrochimica Acta*, 1973, **29A**, 1927.
21 M. S. Greenberg and A. I. Popov, *Journal of Solution Chemistry*, 1976, **5**, 653.
22 V. Gutmann, in *Coordination chemistry in non-aqueous solutions*, Springer-Verlag, Vienna, 1968.
23 R. H. Erlich, M. S. Greenberg and A. I. Popov, *Spectrochimica Acta*, 1973, **29A**, 543.

Stellenbosch University http://scholar.sun.ac.za

24 M. S. Greenberg and A. I. Popov, *Spectrochimica Acta*, 1975, **31A**, 697.
25 A. K. Covington, T. H. Lilley, K. E. Newman and G. A. Porthouse, *Journal of the Chemical Society, Faraday Transactions I*, 1973, **69**, 963.
26 J. P. K. Tong, C. H. Langford and T. R. Stengle, *Canadian Journal of Chemistry*, 1974, **52**, 1721.
27 C. H. Langford and T. R. Stengle, *Journal of the American Chemical Society*, 1969, **91**, 4014.
28 T. R. Stengle, Y.-C. E. Pan and C. H. Langford, *Journal of the American Chemical Society*, 1972, **94**, 9037.
29 W. McFarlane, *Chemical Communications*, 1968, 393.
30 A. von Zelewsky, *Helvitica Chimica Acta*, 1968, **51**, 803.
31 S. M. Cohen and T. H. Brown, *Journal of Chemical Physics*, 1974, **61**, 2985.
32 P. L. Goggin, R. J. Goodfellow, S. R. Haddock, B. F. Taylor and I. R. H. MarshallI, *Journal of the Chemical Society, Dalton Transactions*, 1976, 459.
33 Y. Koie, S. Shinoda and Y. Saito, *Journal of the Chemical Society, Dalton Transactions*, 1981, 1082.
34 R. R. Dean and J. C. Green, *Journal of the Chemical Society (A), Inorganic Physical Theory*, 1968, 3047.
35 J. J. Pesek and W. R. Mason, *Journal of Magnetic Resonance*, 1977, **25**, 519.
36 P. S. Pregosin, *Coordination Chemistry Reviews*, 1982, **44**, 247.
37 T. M. Gilbert and T. J. Ziegler, *Journal of Physical Chemistry A*, 1999, **103**, 7535.
38 H. Chermette, P. Belser, E. P. Fowe and C. Daul, *Physical Chemistry Chemical Physics*, 2005, **7**, 1732.
39 A. I. Vogel, revised by B. S. Furniss, *Vogel's Textbook of Practical Organic Chemistry: including Qualitative Organic Analysis*, Longman Scientific and Technical, London, 1978.
40 I. M. Ismail, S. J. S. Kerrison and P. J. Sadler, *Journal of the Chemical Society, Chemical Communications*, 1980, 1175.
41 K. R. Koch, *Unpublished results*, 2005.
42 E. M. Kosower, *Journal of the American Chemical Society*, 1958, **80**, 3253.
43 G. E. Maciel, J. K. Hancock, L. F. Lafferty, P. A. Mueller and W. K. Musker, *Inorganic Chemistry*, 1966, **5**, 554.
44 J. J. Dechter and J. I. Zink, *Journal of the American Chemical Society*, 1975, **97**, 2937.
45 V. Gutmann and E. Vychera, *Inorg. Nucl. Chem. Lett.*, 1966, **2**, 257.
46 Y. Marcus, in *The Properties of Solvents*, John Wiley and Sons, Ltd, Chichester, 1999, and references cited therein.
47 K. Dimroth, C. Reichardt, T. Siepmann and F. Bohlmann, *Liebigs Annalen der Chemie*, 1966, **661**, 1.
48 C. Reichardt, *Chemical Reviews*, 1994, **94**, 2319.
49 M. J. Kamlet, J.-L. Abboud and R. W. Taft, *Journal of the American Chemical Society*, 1977, **99**, 6027.
50 M. J. Kamlet, J.-L. M. Abboud, M. H. Abraham and R. W. Taft, *Journal of Organic Chemistry*, 1983, **48**, 2877.
51 D. J. Adams, P. J. Dyson and S. J. Tavener, in *Chemistry in Alternative Reaction Media*, John Wiley and Sons Ltd, Chichester, 2004.
52 U. Mayer, V. Gutmann and W. Gerger, *Monatshefte fur Chemie*, 1975, **106**, 1235.
53 J. Hormadaly and Y. Marcus, *Journal of Physical Chemistry*, 1979, **83**, 2843.
54 N. F. Ramsey, *Physical Review*, 1950, **78**, 699.
55 A. B. P. Lever, in *Inorganic Electronic Spectroscopy*, Elsevier Science Publishers B. V., Amsterdam, 1984.
56 R. Freeman, G. R. Murray and R. E. Richards, *Proceedings of the Royal Society*, 1957, **A242**, 455.
57 A. Yamasaki, F. Yajima and S. Fujiwara, *Inorganica Chimica Acta*, 1968, **2**, 39.
58 Swihart, D. L. and W. R. Mason, *Inorganic Chemistry*, 1970, **9**, 1749.
59 L. S. Frankel, C. H. Langford and T. R. Stengle, *Journal of Physical Chemistry*, 1970, **74**, 1376.
60 L. S. Frankel, T. R. Stengle and C. H. Langford, *Chemical Communications*, 1965, 393.
61 J. J. Dechter and J. I. Zink, *Inorganic Chemistry*, 1976, **15**, 1690.
62 E. Hawlicka and D. Swiatla-Wojcik, *Journal of Molecular Liquids*, 1998, **78**, 7.
63 E. Hawlicka and D. Swiatla-Wojcik, *Journal of Physical Chemistry A*, 2002, **106**, 1336.
64 Y. Marcus, in *Ion Properties*, Marcel Dekker, Inc., New York, 1997.
65 K. J. Naidoo, A. S. Lopis, A. N. Westra, D. J. Robinson and K. R. Koch, *Journal of the American Chemical Society.*, 2003, **125**, 13330.
66 K. Ozutsumi, A. Kitakaze, M. Iinomi and H. Ohtaki, *Journal of Molecular Liquids*, 1997, **73/74**, 385.

Stellenbosch University http://scholar.sun.ac.za

67 A. K. Covington and K. E. Newman, *Journal of the Chemical Society; Faraday Transactions I*, 1973, **69**, 973.
68 A. K. Covington, I. R. Lantzke and J. M. Thain, *Journal of the Chemical Society; Faraday Transactions I*, 1974, **70**, 1869.
69 A. K. Covington and J. M. Thain, *Journal of the Chemical Society; Faraday Transactions I*, 1974, **70**, 1879.
70 A. D. Covington and A. K. Covington, *Journal of the Chemical Society; Faraday Transactions I*, 1975, **71**, 831.

Stellenbosch University http://scholar.sun.ac.za

Chapter 5

^{195}Pt NMR as a Sensitive Probe for the Estimation of $Na^{+}\cdots[PtX_6^{2-}]$ (X = Cl, Br) Ion-pairing in Non-aqueous Solution.*

The ^{195}Pt NMR chemical shifts of PtX_6^{2-} (X = Cl, Br) anions, as a function of $NaClO_4$ concentration, have been determined in water, methanol and acetonitrile solutions. Whereas variations of $\delta_{Pt\text{-}195}$ in water with increasing $[Na^+]$ are slight, significant variations of the chemical shift are observed in methanol and acetonitrile. We interpret these results as indicative of $\{Na^+[PtX_6^{2-}]\}^-$ (X = Cl, Br) *contact ion-pair formation* in water, methanol and acetonitrile, with ion-association occurring to a greater extent in the non-aqueous solvents. The ^{195}Pt chemical shift variations with $[Na^+]$ are used to estimate conditional ion-pair formation equilibrium quotients, Q (M^{-1}), in water, methanol and acetonitrile, and the Q-values are related to the polarities and the donor and acceptor properties of the solvents. Strong sodium complexing agents, such as 18-crown-6 and 15-crown-5, have been added to solutions in which $\{Na^+[PtX_6^{2-}]\}^-$ formation occurs to determine the effect of the crown ethers on the $Na^+\cdots PtX_6^{2-}$ association.

---

* Papers based in part on this chapter:
K. J. Naidoo, A. S. Lopis, A. N. Westra, D. J. Robinson, K. R. Koch, *JACS, Communications*, 2003, *125*, 13330-13331.
A. N. Westra, D. J. Robinson, A. S. Lopis, K. J. Naidoo, K. R. Koch, in *International Solvent Extraction Conference, ISEC 2005*, Conference Proceedings,Beijing, China, 2005, *in press*.

Paper in progress, based on this chapter:
A. N. Westra, A. S. Lopis, K. J. Naidoo, D. J. Robinson, K. R. Koch, *Inorganic Chemistry*, 2005, *to be submitted*.

Stellenbosch University http://scholar.sun.ac.za

5.1 Introduction

In very dilute solutions of electrolytes individual ions (cations and anions) are completely surrounded by solvent molecules over large distances, and the distance to the nearest ion, either cation or anion, is effectively infinite. At higher concentrations, the distances between ions decrease sufficiently for ion-ion interactions to become significant; oppositely charged ions may be held together at a short distance from each other by predominantly Coulombic forces for a reasonable period of time, resulting in so-called ion-pairs, before their thermal motion pulls them apart.[1] Bjerrum first introduced the concept of ion-pairing in 1926 to account for the behaviour of 'ionophores' (substances composed of ions which do not combine into covalently bonded molecules) in solvents of low dielectric constant.[2] Currently, three types of ion-paired species are generally accepted to exist in solution, depending on the solution concentration and the properties of the solvent.[1,3] These are:*

a. solvent-separated (or loose) ion-pairs - the primary solvation shells of the cation and anion remain intact, these primary shells being in contact (Fig. 5.1(a));
b. solvent-shared ion-pairs – the primary solvation shells of the ions interpenetrate, and they are held apart by a single layer of solvent molecules (Fig. 5.1(b));
c. contact (or intimate or tight) ion-pairs – no solvent molecules interpose between the two ions (Fig 5.1(c)).

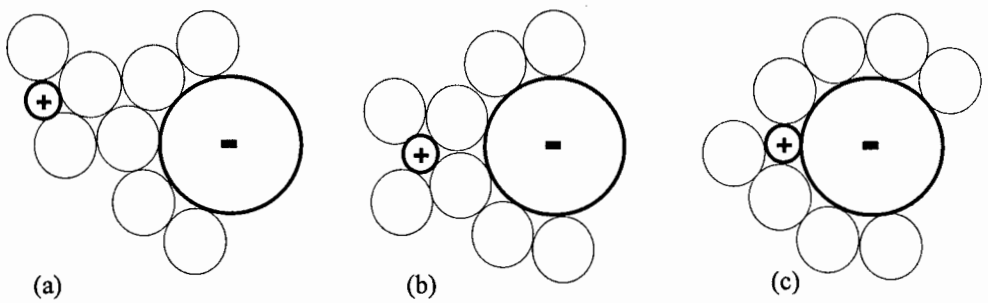

Fig. 5.1 Simplified schematic representation of a solvent-separated ion-pair (a), a solvent-shared ion-pair (b), and a contact ion-pair (c).[1]

Solvents are generally characterized by their dielectric constants (ε), as well as their donor and acceptor properties.[1,4,5] The dielectric constant determines the dissociating power of the solvent, and the donor and acceptor properties the ability of the solvent to solvate the ions (and ion-pairs, if these exist) that are produced on dissociation.[6,7] The *donor properties* are a measure of the ability of the solvent molecules to donate a non-bonding pair of electrons from a donor atom of the molecule to the solute, and determine the power of a solvent to solvate *cations* (Gutmann's donor number,[1,5,8] *DN*, or normalized donor number,

* The formation of so-called ion-triplets and higher aggregates have also been observed in solutions of very high concentrations with solvents of low dielectric constant, as well as 'penetrated' ion-pairs, discovered in studies of tetraalkylammonium tetrafluoroborates, [3] but these ion aggregates will not form part of the present discussion.

Stellenbosch University http://scholar.sun.ac.za

DN^N,[5] is used as a measure of the donicity of a solvent; see Section 4.3.3.1, Chapter 4). *Acceptor properties* relate to the ability of a solvent to accept an electron pair from a donor atom of the solute, and play a major role in the ability of solvents to solvate *anions* (the acceptor number,[1,9,10] *AN*, is used as a measure in this regard). In most instances in which the extent of ion-pairing is specifically described, authors refer mainly to the solvent dielectric constant and donor number.[1,11] It is generally accepted that a solvent with a low dielectric constant, ε, (which promotes the occurrence of ion-pairing in general) and a low donor number (which will result in only weak solvation of the cation), favours the formation of contact ion-pairs.[1,11,12] Conversely, ion-pairing is least prevalent in solvents, or solvent mixtures, of high dielectric constants and high donor numbers; molecules of solvents with high donor numbers are difficult to displace from the inner solvation spheres of cations, and therefore inhibit ion-pair formation. Mayer adds,[12] although this point is less often made in discussions of ion-pairing, that the so-called electrophilicity or anion solvating power of a solvent, of which the acceptor number (*AN*) is a measure, also plays a role in determining the occurrence of ion-pairing in solution; presumably molecules of solvents with high acceptor numbers are difficult to displace from the inner solvation spheres of anions, and may inhibit ion-pairing.

Popov and co-workers have extensively studied the concentration dependence of the ^{23}Na NMR chemical shift of a large variety of sodium salts in various solvents.[13-20] They have found, for example, that in general ^{23}Na chemical shifts for sodium perchlorate and sodium tetraphenylborate show no, or very little concentration dependence, while $\delta_{Na\text{-}23}$ for the iodide, bromide and thiocyanate sodium salts show considerable concentration dependence. A ^{19}F NMR chemical shift study of hexafluorophosphate salts in a number of non-aqueous solvents, also revealed a dependence of $\delta_{F\text{-}19}$ on salt concentration.[19] A linear dependence of the observed solute-nucleus chemical shift on salt concentration is ascribed to interactions during random collisions, while a non-linear dependence is interpreted as indicative of *ion-pair formation* in solution.[21] Popov *et al.* ascribed the concentration dependence of $\delta_{Na\text{-}23}$ of the sodium halide and thiocyanate solutions to the formation of contact ion-pairs,[11] and suggested that the dependence of $\delta_{F\text{-}19}$ on the hexafluorophosphate salt concentration also indicated anion-cation interactions.[19] Popov and co-workers have furthermore elucidated the important interplay between solvent dielectric constant and donor number in determining the extent of ion association in a study of sodium iodide solutions of dimethylsulphoxide and sulpholane by ^{23}Na NMR spectroscopy.[11] Dimethylsulphoxide and sulpholane have very similar dielectric constants (46.45 and 43.26, respectively[5]), but different normalized donor numbers (DN^N of 0.77 and 0.38, respectively[5]). Popov *et al.* found no evidence of ion-pairing in the solvent with the higher donor number (dimethylsulphoxide), but observed a marked concentration dependence of the ^{23}Na chemical shift, attributable to ion-pair formation, in the solvent with lower donicity (sulpholane).[11] Moreover, in an investigation of sodium thiocyanate in propylene carbonate by ^{23}Na NMR, Greenberg, Wied and Popov presented a model by means of which the $\{Na^+[SCN^-]\}$ *contact ion-pair formation equilibrium quotient* was estimated from the variation of $\delta_{Na\text{-}23}$ with salt concentration.[16]

Stellenbosch University http://scholar.sun.ac.za

Naidoo and Koch *et al.* have recently developed detailed geometric models of the *hydration* shells of $PtCl_6^{2-}$, $RhCl_6^{2-}$, $PtCl_4^{2-}$, and $PdCl_4^{2-}$ by means of DFT calculations and molecular dynamics simulations.[22,23] In similar simulations of the $PtCl_6^{2-}$ complex anion in *methanol*, including two Na^+ ions, these authors found that *solvent-shared* and *contact ion-paired* configurations are favoured, in contrast to the water solution simulations for which no ion-pairing was found.[24] In methanol, the contact ion-pair configuration is strongly preferred over the energetically less favourable solvent-shared ion-pair, with the Na^+ ion contacting in two possible positions, both perpendicular to the faces of the $PtCl_6^{2-}$ octahedron.

Our investigations of the $PtCl_6^{2-}$ and $PtBr_6^{2-}$ anions in mixed solvent systems by means of ^{195}Pt NMR (Chapter 4) have shown that the ^{195}Pt chemical shift is extremely sensitive to the immediate environment of these anions. With the aim of verifying the computational observations of Naidoo and Koch *et al.*, we have explored the possibility of utilizing ^{195}Pt NMR as a monitor of the occurrence of $Na^+\cdots PtX_6^{2-}$ (X = Cl, or Br) association in solution. We here present an investigation of $\{Na^+[PtX_6^{2-}]\}^-$ (X = Cl, Br) contact ion-pair formation in water, methanol and acetonitrile by means of ^{195}Pt, and ^{23}Na, NMR. The ^{195}Pt chemical shift is shown to be remarkably sensitive to the formation of $\{Na^+[PtX_6^{2-}]\}^-$ (X = Cl, Br) ion-pairs, and the significant chemical shift variations are used to determine conditional ion-pair formation equilibrium quotients for $\{Na^+[PtCl_6^{2-}]\}^-$ and $\{Na^+[PtBr_6^{2-}]\}^-$ in these solvents.

5.2 Experimental

5.2.1 Reagents

The platinum salts $H_2PtCl_6{\cdot}H_2O$ (Aldrich) and H_2PtBr_6 (Johnson Matthey PLC, Precious Metals Division), and the sodium salts $NaClO_4$ (Riedel de Haën) and NaCl (Merck) were of reagent grade quality; these were used without further purification and stored in a dessicator. $NaClO_4$ was dried at 100°C for 6 hours prior to use. The solvents methanol (Riedel de Haën, Chromasolv® for HPLC) and acetonitrile (Aldrich, HPLC grade) were used without further purification, and stored over freshly activated 4 Å molecular sieves (Aldrich). The macrocyclic polyethers 18-crown-6 and 15-crown-5 (Aldrich) were used as supplied, and stored at 4°C. Deionised water was obtained with a Milli-Q Millipore instrument.

5.2.2 Sample preparation

Solutions of $\mathbf{H_2PtCl_6{\cdot}H_2O}$ and $\mathbf{H_2PtBr_6}$, with varying anion concentrations, in **water**, **methanol**, and **acetonitrile**, were prepared as follows: Stock solutions in each solvent were prepared by weighing appropriate quantities of $H_2PtCl_6{\cdot}H_2O$, or H_2PtBr_6, into clean polytop containers, and pipetting 5 cm^3 of solvent onto the salt. Volumes of these stock solutions were pipetted into polytops, and the desired dilutions obtained by adding the required solvent to each polytop to achieve a final volume of 4 cm^3. Details of sample preparation are tabulated in Tables 5.1Adm - 5.6Adm in Addendum B.

Stellenbosch University http://scholar.sun.ac.za

For the solutions **$NaClO_4$ in H_2O, methanol** and **acetonitrile**, stock solutions of the sodium salt in each solvent were prepared by weighing quantities of $NaClO_4$ into clean polytop containers, and pipetting appropriate volumes of solvent onto the salt. For the aqueous samples, volumes of the stock solutions were pipetted into polytops, the solvent was evaporated off, and 0.7 cm^3 of deionised water was pipetted onto all the dry salt samples. For the methanol and acetonitrile samples, volumes of the stock solutions were pipetted into polytops and the desired Na^+ concentration range obtained by adding pure solvent to each polytop to achieve a final volume of 1 cm^3. For the solutions **NaCl in H_2O** and **methanol**, stock solutions of the sodium salt in each solvent were prepared by weighing quantities of NaCl into polytop containers, and pipetting appropriate volumes of solvent onto the salt. To complete each series, appropriate volumes of the stock solutions were pipetted into polytops and pure solvent was added to achieve a final volume of 1 cm^3. Details are given in Tables 5.7Adm - 5.11Adm in Addendum B.

Solutions of **$H_2PtCl_6 \cdot H_2O$ + $NaClO_4$ in water, methanol** and **acetonitrile**, and of **H_2PtBr_6 + $NaClO_4$ in water, methanol** and **acetonitrile**, were prepared: Stock solutions of $PtCl_6^{2-}$, $PtBr_6^{2-}$ and $NaClO_4$ in water, methanol and acetonitrile were prepared as before; solutions with $[PtCl_6^{2-}]$ in the range 0.05493 – 0.06332 M, and $[PtBr_6^{2-}]$ in the range 0.06044 – 0.06108 M were obtained. Into polytop containers was dispensed $NaClO_4$ as a solid, or as solution from the appropriate stock solution, such that the required range of Na^+ concentrations would be achieved in the final mixtures. Polytop containers with $NaClO_4$ *solutions* were placed in an oven to carefully evaporate off the solvent, until the salt was dry. 1 cm^3 or 0.7 cm^3 portions of the water, methanol, or acetonitrile stock solutions containing the desired halogenoplatinate anion, were pipetted onto the dry salt in each polytop. Details of solution preparation are shown in Tables 5.12Adm - 5.19Adm in Addendum B.

Solutions of **$NaClO_4$ + 18-crown-6 in methanol, $H_2PtCl_6 \cdot H_2O$ + $NaClO_4$ + 18-crown-6 in methanol, $H_2PtCl_6 \cdot H_2O$ + $NaClO_4$ + 18-crown-6 in acetonitrile**, and **$H_2PtCl_6 \cdot H_2O$ + $NaClO_4$ + 15-crown-5 in acetonitrile**, were prepared as described above, with the addition of appropriate quantities of the chosen crown ether. Details for each series are given in Tables 5.20Adm - 5.22Adm in Addendum B. For several solutions in these series', the mass of crown ether added was too large to leave the final volume unaffected. This was however considered a preliminary study in which only the *trends* of the observed chemical shifts were to be of interest, and thus the concentrations were calculated simply based on uncorrected sample volumes.

The concentrations of sodium perchlorate in the water, methanol and acetonitrile samples ranged from 0 – 7.275 M, 0 – 2.591 M and 0 – 2.211 M, respectively; for methanol and acetonitrile the highest concentrations are close to the saturation points.

Stellenbosch University http://scholar.sun.ac.za

5.2.3 Measurements

Appropriate volumes of the prepared solutions were transferred to 5 mm OD NMR tubes. ^{195}Pt and ^{23}Na NMR spectra were recorded of the solutions in the NMR tubes, together with a 2mm OD coaxial insert tube containing an appropriate reference solution. Separate reference solutions were used for ^{23}Na spectra (1.03 M NaCl in D_2O), for mixtures with $PtCl_6^{2-}$ (500 mg cm^{-3} $H_2PtCl_6 \cdot H_2O$ in 30 % v/v D_2O / 1 M HCl), and for mixtures with $PtBr_6^{2-}$ (250 mg cm^{-3} H_2PtBr_6 in 67 % v/v D_2O / 3 M HBr). ^{195}Pt (30°C) and ^{23}Na (25°C) NMR spectra were recorded with a Varian INOVA 600 MHz spectrometer operating at 128 MHz and 159 MHz, respectively. All chemical shifts are reported relative to the appropriate reference solution resonance; positive chemical shifts indicate resonance positions downfield, and negative δ values indicate positions upfield of the reference resonance peak. ^{195}Pt and ^{23}Na chemical shifts are estimated to be accurate to ± 2 ppm and ± 15 Hz, respectively. (The overall ^{23}Na chemical shift range, in ppm, was observed to be considerably smaller than that for $\delta_{Pt\text{-}195}$, and $\delta_{Na\text{-}23}$ values are for convenience sometimes presented in Hz.) The ^{195}Pt and ^{23}Na chemical shifts measured for the prepared samples are given in Tables 5.1Adm - 5.22Adm in Addendum B.

5.2.4 Bulk diamagnetic susceptibility corrections

The magnetic flux density B in a substance that is exposed to an external magnetic field is expressed as:[25]

$$B = \mu_0(H + M) \tag{5.1}$$

with H the field strength of the applied field, M the magnetization induced in the sample, and μ_0 the permeability, a constant equal to $4\pi \times 10^{-7}$ kg m s^{-2} A^{-2}. The magnetization, M, is dependent on the external field as follows:

$$M = \chi_v H \tag{5.2}$$

with χ_v a dimensionless constant, the volume magnetic susceptibility, which is characteristic of the solvent. The field strength which exists within an NMR tube in a spectrometer, is thus influenced by the magnetic susceptibility of the solvent. When an internal standard is used in an NMR sample, the reference substance and compound to be measured are exposed to the same magnetic environment, and no corrections need to be made to the recorded chemical shifts. If, however, an external standard is used, where the reference substance is contained in a coaxial insert tube and is dissolved in a solvent different to that used for the sample, the field strengths in the reference insert and the sample solution may be different due to the different volume susceptibilities of the solvents used. The recorded chemical shifts must then be corrected using a relationship developed by Live and Chan[26] for high-field spectrometers:

$$\delta_{corr} = \delta_{obs} - 4\pi/3\ (\chi_v^{Ref} - \chi_v^{Sample}) \tag{5.3}$$

with χ_v^{Ref} and χ_v^{Sample} the volume magnetic susceptibilities of the reference and sample solvent respectively, and δ_{corr} and δ_{obs} the corrected and observed chemical shifts (in ppm). The volume magnetic susceptibilities (χ_v) and correction terms, based on equation (5.3), for the solvents used in the present study, are presented in Table 5.1; the correction terms are applicable to the ^{23}Na and ^{195}Pt NMR data.

Stellenbosch University http://scholar.sun.ac.za

The ^{23}Na chemical shifts for methanol and acetonitrile samples have been corrected for differences in bulk diamagnetic susceptibility between the sample (solvent, methanol or acetonitrile) and the reference (solvent, water), using equation (5.3) and the χ_v-values given in Table 5.1; ^{23}Na chemical shifts in methanol have been corrected by -0.80 ppm (-126.6 Hz), and those in acetonitrile by -0.78 ppm (-124.0 Hz). Only the corrected values (in Hz) are presented in the tables in Addendum B. ^{195}Pt chemical shifts have not been corrected for the difference in magnetic susceptibility between sample and reference, since $\delta_{Pt\text{-}195}$ is estimated to be accurate to ± 2 ppm, and the corrections required (shown in Table 5.1) are smaller than this estimated error. Templeman and van Geet have estimated that the correction for the contribution of the *salt* to the susceptibility of an aqueous 9.65 M $NaClO_4$ solution is + 0.08 ppm (relative to an aqueous solution at infinite dilution);[27] total salt concentrations in the present study are considerably lower than 9.65 M, and it is safe to assume that susceptibility corrections due to the salt in solutions in this study are negligible.

Table 5.1 Volume magnetic susceptibilities (20°C)[28] and required chemical shift correction terms (equation (5.3)[26]) for the solvents used in this study; the correction terms are applicable to the ^{23}Na and ^{195}Pt NMR data.

	χ_v	$4\pi/3\ (\chi_v^{Ref} - \chi_v^{Sample})$
Water	0.7205	
Methanol	0.530	0.80
Acetonitrile	0.534	0.78

5.3 Results and Discussion

5.3.1 Dependence of $\delta_{Pt\text{-}195}$ on $[PtCl_6^{2-}]$ and $[PtBr_6^{2-}]$

Platinum-195 chemical shifts as a function of $[PtCl_6^{2-}]$ (as $H_2PtCl_6{\cdot}H_2O$) in water (■), methanol (◆) and acetonitrile (▲), and ^{195}Pt chemical shifts as a function of $[PtBr_6^{2-}]$ (as H_2PtBr_6) in water (□), methanol (◇) and acetonitrile (△), are shown in Fig. 5.2. The linear distributions of the chemical shifts for $PtCl_6^{2-}$ and $PtBr_6^{2-}$ in water and methanol, do not vary by more than 3 ppm through each series; the measured chemical shifts are estimated to be accurate to ± 2 ppm, and thus $\delta_{Pt\text{-}195}$ in water and methanol may reasonably be considered to be concentration independent for both anions over the concentration ranges studied. $\delta_{Pt\text{-}195}$ values for $PtCl_6^{2-}$ and $PtBr_6^{2-}$ in acetonitrile show some variation with salt concentration, with shift values for $PtCl_6^{2-}$ varying by ca. 28 ppm (upfield with increasing $[PtCl_6^{2-}]$), and $\delta_{Pt\text{-}195}$ values for $PtBr_6^{2-}$ varying by ca. 39 ppm (upfield with increasing $[PtBr_6^{2-}]$), over the concentration ranges studied. A non-linear dependence of observed chemical shift on salt concentration is generally ascribed to ion-pair formation,[21] and the variation of $\delta_{Pt\text{-}195}$ for $PtCl_6^{2-}$ and $PtBr_6^{2-}$ in acetonitrile may indicate cation-anion interactions. Acetonitrile has a lower normalized donor number and acceptor number than methanol ($DN^N_{acetonitrile} = 0.36$, $AN_{acetonitrile} = 18.9$, $DN^N_{methanol} = 0.77$, $AN_{methanol} = 41.5$[1,5]), indicating that cations and

Stellenbosch University http://scholar.sun.ac.za

anions are more weakly solvated in CH_3CN, thus, in general, favouring anion-cation interactions in this solvent at higher salt concentrations despite the fact that it has a slightly higher dielectric constant than methanol ($\varepsilon_{acetonitrile}$ = 35.94, $\varepsilon_{methanol}$ = 32.66).[5] The range of concentrations used in the present study is fairly low, however, which does not favour the occurrence of significant ion-pairing in these solutions.

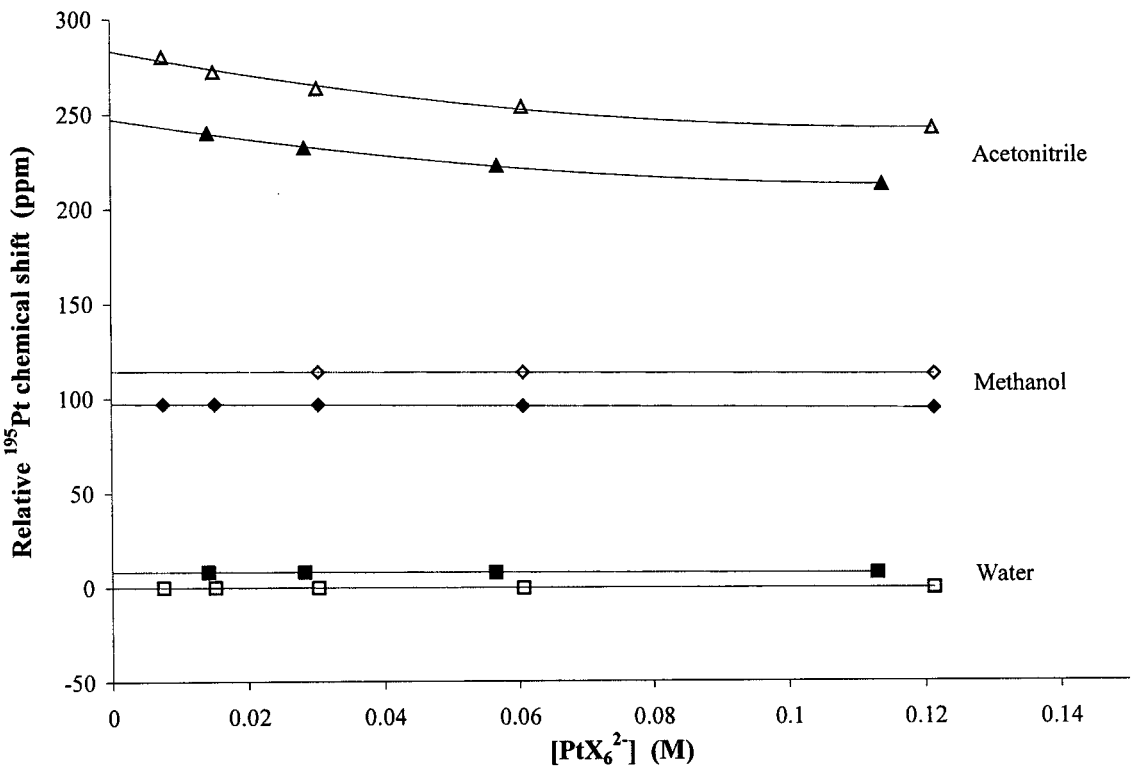

Fig. 5.2 Variation of the ^{195}Pt chemical shift as a function of halogenoplatinate anion concentration at 30°C. The chemical shifts have been extrapolated to infinite dilution; these values are given, together with curve legends, in parentheses below. ^{195}Pt Chemical shifts of $H_2PtCl_6 \cdot H_2O$ in water (■, 8 ppm), methanol (◆, 97 ppm) and acetonitrile (▲, 247 ppm) (X = Cl on x-axis), and of H_2PtBr_6 in water (□, 0 ppm), methanol (◇, 114 ppm) and acetonitrile (△, 283 ppm) (X = Br on x-axis). Separate reference solutions, as described in the experimental section, were used for $PtCl_6^{2-}$-containing and $PtBr_6^{2-}$-containing solutions.

5.3.2 Na^+ and ClO_4^- ion-pairing in water, methanol and acetonitrile

Although ion-pair formation of sodium and perchlorate in water, methanol and acetonitrile has been previously studied by Popov and co-workers, using ^{23}Na NMR,[14,18] similar studies were also performed in the present investigation in order to ensure that the chosen methodologies, with regard not only to the NMR spectroscopic experiments performed (Sections 5.3.4 and 5.3.5), but also the quantitative calculations based on the NMR data (Section 5.3.6), would lead to reliable results.

Stellenbosch University http://scholar.sun.ac.za

Solutions of $NaClO_4$ in water, methanol and acetonitrile were prepared as described in the Experimental Section, and ^{23}Na NMR spectra recorded. The sodium-23 chemical shifts (in ppm) as a function of $[Na^+]$ for **sodium perchlorate** in **water** (×), **methanol** (∗) and **acetonitrile** (+) observed in the present study, are shown in Fig. 5.3. Greenberg and Popov investigated sodium perchlorate solutions of several nonaqueous solvents and water by ^{23}Na, ^{35}Cl-NMR, infrared, and Raman spectroscopic techniques; these authors presented the variations of ^{23}Na chemical shifts (in ppm) with sodium perchlorate concentration.[18] The data for water, methanol and acetonitrile are reproduced in Fig. 5.3, together with the ^{23}Na shifts (in ppm) obtained in the present study. There is generally good agreement between the $\delta_{Na\text{-}23}$ *vs.* $[Na^+]$ data in water and methanol obtained in the present study and that reported by Greenberg and Popov. The chemical shifts in acetonitrile for the two studies differ by at most 0.7 ppm at corresponding sodium concentrations. ^{23}Na chemical shifts in both studies have been corrected for the difference in bulk diamagnetic susceptibility between sample and reference. Greenberg and Popov assert that the observed upfield shift in the ^{23}Na resonance position with increasing $[Na^+]$ is indicative of $\{Na^+[ClO_4^-]\}$ *contact ion-pair formation* in all three solvents.

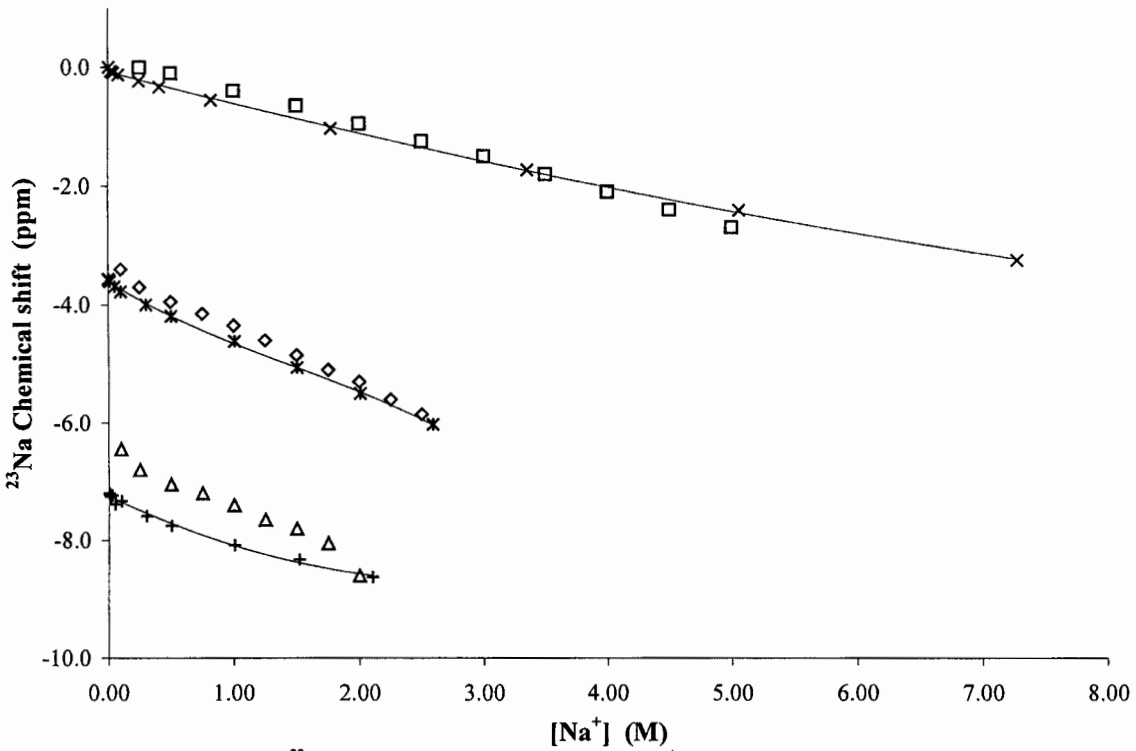

Fig. 5.3 The variation of the ^{23}Na chemical shift as a function of $[Na^+]$ obtained in the present study: (×) $NaClO_4$ in water, (∗) $NaClO_4$ in methanol, (+) $NaClO_4$ in acetonitrile; best-fit Excel trendlines have been included. Data previously reported by Greenberg and Popov[18] are also shown: (□) $NaClO_4$ in H_2O, (◇) $NaClO_4$ in CH_3OH, (△) $NaClO_4$ in CH_3CN. ^{23}Na chemical shifts in both studies (ppm) have been corrected for the difference in bulk diamagnetic susceptibility between sample and reference.

Stellenbosch University http://scholar.sun.ac.za

As the sodium perchlorate concentration in the prepared solutions increases, it is likely that ClO_4^- ions will disturb the solvation shells around the cations and will eventually replace solvent molecules in the first solvation spheres of these ions, leading to the formation of solvent-separated, solvent-shared and finally contact ion-pairs in solution.[1] The ^{23}Na chemical shift is known to be very sensitive to changes in the *inner* solvation sphere of the cation,[13-20,27,29-32] and the occurrence of close Na^+-ClO_4^- association will be reflected in the chemical shift of the sodium nucleus. The ^{23}Na chemical shift changes observed in Fig 5.3 are thus interpreted as indicative of $\{Na^+[ClO_4^-]\}$ contact ion-pair formation in methanol, acetonitrile *and* water, with increasing sodium perchlorate concentration. Popov emphasizes that ^{23}Na chemical shift measurements cannot be expected to differentiate between free solvated ions and solvent-separated/-shared ion pairs, but only between contact ion pairs and free solvated ions and/or solvent-separated/-shared ion pairs.[17] Although solvent-separated/-shared ion-pairs are presumed to form in solutions of the present study,[33] the observed shift changes with increasing salt concentration are interpreted as being related to predominantly contact ion-pair formation in solution. Under these conditions the observed ^{23}Na chemical shift can be formulated as the weighted average of the chemical shifts of the free and ClO_4^- contact ion-paired sodium ions:[16]

$$\delta_{Na\text{-}23\ obs} = X_{Na}\,\delta_{Na} + X_{ClO4\text{-}Na\ IP}\,\delta_{ClO4\text{-}Na\ IP} \qquad (5.4)$$

with X_{Na} and $X_{ClO4\text{-}Na\ IP}$ the mole fractions and δ_{Na} and $\delta_{ClO4\text{-}Na\ IP}$ the chemical shifts of the free and ClO_4^- ion-paired sodium ions, respectively. As the sodium perchlorate concentration increases, the contribution of $\{X_{ClO4\text{-}Na\ IP}\,\delta_{ClO4\text{-}Na\ IP}\}$ to $\delta_{Na\text{-}23\ obs}$ increases, and since the overall effect is an upfield shift in $\delta_{Na\text{-}23\ obs}$ it may be concluded that the $\delta_{ClO4\text{-}Na\ IP}$ value for each solvent lies *upfield* of the δ_{Na} value.

Both upfield and downfield ^{23}Na shifts with increasing salt concentrations have been observed for sodium salts,[17] the shift change depending on the anion, and it has been postulated that the change (upfield or downfield) is related to the paramagnetic shielding parameter, σ_p, of the screening constant, σ.[27,29] The paramagnetic shielding parameter represents the contribution to the screening due to the net orbital angular momentum of electrons in the valence orbitals of the nucleus under investigation, and always results in deshielding, contributing to a downfield shift. A solvated Na^+ ion will find its outer p orbitals overlapping with the outer s and p orbitals of neighbouring solvent molecules. The solvated Na^+ ion therefore acquires extra electron density in its valence orbitals, contributing to the net orbital angular momentum. The overlap, or occupancy, of the Na^+ 3*p* orbitals will be largest with solvent molecules with appreciable electron-donating ability, and will lead to lower field resonance positions. With contact ion-pair formation, the shift change (upfield or downfield) will depend on the relative electron-donating abilities of the solvent and the associated anion. Popov and co-workers suggest that replacement of a water, or methanol, or acetonitrile molecule in the Na^+ solvation shell by a ClO_4^- anion results in *decreased* electron density in the 3*p* orbitals of the cation, i.e. the anion acts as a poorer electron donor to Na^+ than do the solvent molecules it replaces when forming contact ion-pairs.[17,19] This leads to a smaller contribution to σ_p, and an upfield shift in the ^{23}Na resonance position, as seen in Fig. 5.3.

Stellenbosch University http://scholar.sun.ac.za

Although contact ion-pair formation involving perchlorate was first suggested by Geffeken in 1929,[34] it is generally believed that ClO_4^- is one of the least associating anions and that cation-ClO_4^- contact ion-pairing, particularly in water which has a high dielectric constant (78.36[5]), is negligible.[1] This is understandable in view of several reports on aqueous alkali metal perchlorate solutions studied by Raman spectroscopy[35-37] and ^{35}Cl-NMR spectroscopy[38] which concluded that contact association is *absent*. Yet as early as 1971, D'Aprano interpreted conductivity measurements of aqueous $NaClO_4$ as indicating that contact association between Na^+ and ClO_4^- does occur, albeit to a "marginal" extent.[39] Similar conclusions were reached by Templeman and van Geet based on ^{23}Na NMR relaxation times in aqueous $NaClO_4$,[27] and by Greenberg and Popov using NMR and vibrational spectroscopic techniques (see Fig. 5.3).[18] Moreover, careful analysis of the line shapes and line parameters in Raman spectra of aqueous solutions of Group 1 perchlorates, allowed Frost and co-workers to identify not only contact ion-pairs in solution, but also solvent-shared ion-pairs.[40] A similar Raman spectroscopic study of aqueous $NaClO_4$ and $NaClO_4$-NaOH mixtures allowed Miller and Macklin to confirm the existence of solvent-separated and contact ion-pairs in solution; these authors were also able to calculate association constants from their data.[33] Miller and Macklin further verified the occurrence of $\{Na^+[ClO_4^-]\}$ contact ion-pairing by studying the variation of the ^{35}Cl-NMR chemical shift and quadrupolar relaxation rate in aqueous $NaClO_4$ and $NaClO_4$-NaOH mixtures.[41] Several studies of $NaClO_4$ solutions of methanol [18,42] and acetonitrile [18,43-48] have also been performed; these investigations are based mainly on conductivity and NMR measurements. *All* the investigations confirm the generally accepted view that contact $\{Na^+[ClO_4^-]\}$ ion-pairing occurs in these solvents. Both methanol and acetonitrile have lower dielectric constants (ε) *and* normalized donor numbers (DN^N) than water, which favours the occurrence of ion-pairing in these solvents relative to water.

Results of our investigation confirm the existence of $\{Na^+[ClO_4^-]\}$ *contact ion-pairs* in not only methanol and acetonitrile, but also in water, with increasing sodium perchlorate concentration; although $\{Na^+[ClO_4^-]\}$ formation in water is very slight, resulting in sometimes only tentative conclusions as to its occurrence, ^{23}Na chemical shift experiments are clearly sensitive to this type of ion association in this medium.

5.3.3 Estimated conditional ion-pair formation equilibrium quotients: $\{Na^+[ClO_4^-]\}$ contact ion-pairing in water, methanol and acetonitrile

The ^{23}Na NMR data for the present study depicted in Fig. 5.3 shows *qualitatively* that Na^+ and ClO_4^- form contact ion-pairs in water, methanol and acetonitrile, in concentrated sodium perchlorate solutions. Analysis of this data has allowed an approximate *quantitative* estimation of the extent of contact ion-pair formation in these solutions. Ion-pair formation equilibrium quotients have been calculated: (a) by application of a least-squares curve fitting program, Sigmaplot,[49,50] with which the data were fit to an equation described by Greenberg *et al.*,[16] and (b) by utilization of the computer program SIRKO, which

Stellenbosch University http://scholar.sun.ac.za

was developed specifically for the calculation of equilibrium constants from not only NMR chemical shift data, but also from potentiometric and spectrophotometric data.[51]

(a) Calculation of conditional ion-pair formation equilibrium quotients by the method of Greenberg et al.:[16]

The model described by Greenberg *et al.* allows the calculation of association quotients for solutions of 1 : 1 electrolytes, based on NMR chemical shift data. In solutions of only sodium perchlorate, we may assume, due to the insensitivity of the ^{23}Na NMR technique to the presence of solvent-separated/-shared ion-pairs,[17] that the ^{23}Na chemical shift is dependent predominantly on two possible environments in which the ion finds itself: it may be surrounded solely by solvent molecules (including solvent-separated/-shared Na^+ ions), or it may be contact ion-paired with the counter anion.[16] If the exchange between the two environments is rapid compared with the NMR time scale, the observed chemical shift can be formulated as:

$$\delta_{\text{Na-23 obs}} = X_{\text{Na}}\,\delta_{\text{Na}} + X_{\text{ClO4-Na IP}}\,\delta_{\text{ClO4-Na IP}} \tag{5.4}$$

with X_{Na} and $X_{ClO4\text{-}Na\ IP}$ the mole fractions of Na^+ as solvated ion and as contact ion-pair, respectively, and δ_{Na} and $\delta_{ClO4\text{-}Na\ IP}$ the limiting chemical shifts for the cation in the two environments. Equation (5.4) may be re-written:

$$\delta_{\text{Na-23 obs}} = X_{\text{Na}}\,\delta_{\text{Na}} + (1 - X_{\text{Na}})\,\delta_{\text{ClO4-Na IP}} \tag{5.5}$$

Formulating the contact ion-pair formation equilibrium as:

$$Na^+ + [ClO_4^-] \xleftrightarrow{Q} \{Na^+[ClO_4^-]\} \tag{5.6}$$

the ion-pair formation equilibrium quotient may be expressed as:

$$Q = \frac{[\{Na^+[ClO_4^-]\}]}{[Na^+][ClO_4^-]} = \frac{C_{Na}^{\text{Total}} - [Na^+]}{[Na^+]^2} \tag{5.7}$$

with square-bracket terms denoting equilibrium concentrations, and C_{Na}^{Total} the total concentration of Na^+ ions present in the solution. The mole fraction term X_{Na} can be written as:

$$X_{\text{Na}} = \frac{[Na^+]}{C_{\text{Na}}^{\text{Total}}} \tag{5.8}$$

Substituting equation (5.8) into equation (5.5), and re-writing gives:

$$\delta_{\text{Na-23 obs}} = \frac{[Na^+]}{C_{\text{Na}}^{\text{Total}}}\left(\delta_{\text{Na}} - \delta_{\text{ClO4-Na IP}}\right) + \delta_{\text{ClO4-Na IP}} \tag{5.9}$$

Substituting a term for $[Na^+]$ derived from equation (5.7) into equation (5.9), and re-arranging yields:

$$\delta_{\text{Na-23 obs}} = \left[\frac{-1 + (1 + 4QC_{\text{Na}}^{\text{Total}})^{\frac{1}{2}}}{2QC_{\text{Na}}^{\text{Total}}}\right](\delta_{\text{Na}} - \delta_{\text{ClO4-Na IP}}) + \delta_{\text{ClO4-Na IP}} \tag{5.10}$$

This equation, together with the experimental data can be used to estimate the ion-pair formation equilibrium quotient, Q. Data describing the dependence of $\delta_{Na\text{-}23\ obs}$ on C_{Na}^{Total} are known (Table 5.7Adm -

Stellenbosch University http://scholar.sun.ac.za

5.9Adm, Addendum B), and the terms δ_{Na}, $\delta_{ClO4\text{-}Na\ IP}$ and Q are constants. The value of δ_{Na} can be assumed to be the ^{23}Na chemical shift at infinite dilution for each solvent,[16] and can be determined by extrapolation from the experimental data in Fig. 5.3; these values are presented in Table 5.2 (column (3)), and were *fixed* in the parameter refinement. Values of $\delta_{ClO4\text{-}Na\ IP}$ and Q were determined by application of the SigmaPlot nonlinear curve fitter.[49,50] This software allows one to specify the experimental data ($\delta_{Na\text{-}23\ obs}$ and C_{Na}^{Total} in this case) and the form of the equation to which the data must be fit (equation (5.10)), together with *initial estimates* of parameters that need to be refined ($\delta_{ClO4\text{-}Na\ IP}$ and Q). With this starting information, the initial estimates of the parameters are refined by application of equation (5.10), using an iterative process in which the curve fitter makes successively better 'guesses' about the parameter values until it reaches the best estimate, *i.e.* the parameter values that best fit the experimental data to equation (5.10). SigmaPlot employs the Marquardt-Levenberg algorithm to perform the fit.[50,52,53] This algorithm searches for the parameter values that minimize the squared sum of the difference between the experimental values and the values calculated from the nonlinear equation to be fit:

$$SS = \sum_{i=1}^{n} (y_i^{exp} - y_i^{calc})^2 \qquad (5.11)$$

with y_i^{exp} the observed values, y_i^{calc} the predicted values, and n the number of data points. Starting values for δ_{Na}, $\delta_{ClO4\text{-}Na\ IP}$ and Q used for the refinement are shown in Table 5.2, together with results obtained by application of the SigmaPlot curve fitter.

Table 5.2 Starting values input to SigmaPlot, and resultant refined parameters for Q and $\delta_{ClO4\text{-}Na\ IP}$.

	Experimental data	Infinite dilution $\delta_{Na\text{-}23}$ [a] (Hz)	Starting values Q (M^{-1})	Starting values $\delta_{ClO4\text{-}Na\ IP}$ (Hz)	Refinement parameters Q (M^{-1})	Q Std. Err. [b]	$\delta_{ClO4\text{-}Na\ IP}$ (Hz)	$\delta_{ClO4\text{-}Na\ IP}$ Std. Err. [b]
Water	Table 5.7Adm	-12	0.028	-750	0.024	0.004	-3856	484
Methanol	Table 5.8Adm	-571	0.2	-1309	0.047	0.016	-4425	1147
Acetonitrile	Table 5.9Adm	-1144	0.2	-1400	0.298	0.041	-1868	61

[a] Estimated by extrapolation of the data in Fig. 5.3.
[b] Std. Err. denotes standard errors calculated by SigmaPlot for the refined parameters.

The Q starting value used for $\{Na^+[ClO_4^-]\}$ contact ion-pair formation in water (0.028 M^{-1}) is a value reported by Miller and Macklin in 1985. These authors performed a detailed study of the variations in Raman spectra of aqueous $NaClO_4$ and $NaClO_4$-NaOH mixtures with changing $[Na^+]$, based upon resolution and assignment of components in the contours assigned to the $\nu_1(A_1)$ and $\nu_2(E)$ vibrations of the T_d perchlorate ion.[33] Careful analysis of the contours reveals separate bands that the authors attribute to contact and solvent-separated ion-pairs. The intensities of the bands were used to obtain an equilibrium quotient which includes both contact and solvent-separated ion-pairs, i.e. *free perchlorate → any ion-paired perchlorate (solvent-separated and/or contact)*, and one that includes only contact ion-pairs, i.e. *free*

Stellenbosch University http://scholar.sun.ac.za

and solvent-separated perchlorate → contact ion-paired perchlorate. A value of 0.14 M^{-1} was reported for the former, and 0.028 M^{-1} for the latter. The authors comment that the value of 0.14 M^{-1} obtained for the equilibrium *free perchlorate → any ion-paired perchlorate* shows good agreement with an association constant value K_A = 0.20 reported by D'Aprano for sodium perchlorate ion-pairing in aqueous medium, which was obtained by conductivity measurements.[39]■ Miller and Macklin emphasize that conductance measurements *do not differentiate between contact and solvent-separated ion-pairs*, and that all are included in the paired fraction,* i.e. the equilibrium *free perchlorate → any ion-paired perchlorate* is determined in conductivity measurements. It has been pointed out that the ^{23}Na NMR technique *cannot differentiate between free* Na^+ *and solvent-separated/-shared ion-paired* Na^+, and the association quotient value of 0.028 M^{-1} for the equilibrium *free and solvent-separated perchlorate → contact ion-paired perchlorate* reported by Miller *et al.* is thus more appropriate for the present study. The starting value for $\delta_{ClO4\text{-}Na\ IP}$ in water (-750 Hz) was *estimated* by extrapolation from the $\delta_{Na\text{-}23}$ *vs* $[Na^+]$ data (Table 5.7Adm), to which a best Excel trendline had been fit. The refined value for Q presented by SigmaPlot, 0.024 M^{-1} (Table 5.2), is in very good agreement with the value reported by Miller and Macklin, although $\delta_{ClO4\text{-}Na\ IP}$ is refined to be considerably more negative, -3856 Hz, than the starting value. The curve fitting process was however found to be consistent to a variety of starting values: with the Q starting value *varied* in the range 0.01 – 1.0 M^{-1} and starting $\delta_{ClO4\text{-}Na\ IP}$ set to -750 Hz, or with the $\delta_{ClO4\text{-}Na\ IP}$ starting value *varied* in the range -500 – -2000 Hz and starting Q set to 0.028 M^{-1}, SigmaPlot yielded practically the same final values as presented in Table 5.2. Constraining $\delta_{ClO4\text{-}Na\ IP}$ to a value > -1000 Hz in the refinement, led to a larger Q value of 0.178 M^{-1} (standard error 0.093, with $\delta_{ClO4\text{-}Na\ IP}$ being 'refined' to -1000 Hz), but also a considerably deteriorated overall fit (SigmaPlot provides a "Coefficient of Variation" term at the end of each run, which can be used as a measure of the goodness-of-fit of the refinement). We consider the value of Q = 0.024 M^{-1} for the formation of the $\{Na^+[ClO_4^-]\}$ contact ion-pair in the equilibrium *free and solvent-separated/-shared perchlorate → contact ion-paired perchlorate* in water, to be the correct value, in good agreement with the value reported by Miller *et al.*

■ Although D'Aprano reports a *unitless* association constant for $NaClO_4$ in water, K_A = 0.20 (as is generally the case for association constants calculated from conductance measurements), indicating a *thermodynamic* equilibrium constant, Miller and Macklin have reported the D'Aprano value as 0.20 M^{-1}, which indicates a *conditional* equilibrium constant, i.e. a constant calculated by exclusion of activity coefficients from the equilibrium constant expression. Equilibrium constants in the present investigation are *conditional* and are reported as M^{-1}.

* Although Miller and Macklin do not comment on the existence of solvent-shared ion-pairs in solution, these must also be presumed to be included in the paired fraction since this type of ion-pair is intermediate to the solvent-separated and contact types. Earlier literature[4] distinguishes only between contact ion-pairs and solvent-separated ion-pairs. The latter are described[4] as a type in which "ions are separated by one or several layers of solvent molecules", thus considering solvent-separated and solvent-shared ion-pairs collectively as one type of ion-pair. Presumably Miller and Macklin have used the collective description, in referring to solvent-separated ion-pairs.

Stellenbosch University http://scholar.sun.ac.za

Ion-pair formation is expected to be more pronounced in methanol and acetonitrile compared to water since these solvents have lower dielectric constants (32.66 and 35.94, respectively[5]) than water (ε = 78.36[5]), resulting in larger Q values than for water (0.028 M^{-1}). Conductance studies of sodium perchlorate in methanol and acetonitrile have enabled the calculation of association constants (*free perchlorate* → *any ion-paired perchlorate*) for these solvents (CH_3OH: 18.70[42]; CH_3CN: 10[44], 70.92[43]), but these values, as pointed out previously, are not appropriate to the equilibria under investigation in the present study (*free and solvent-separated/-shared perchlorate* → *contact ion-paired perchlorate*). Consequently, starting values of Q for $\{Na^+[ClO_4^-]\}$ contact ion-pair formation in methanol and acetonitrile were chosen to be 0.2 M^{-1}. The $\delta_{ClO4\text{-}Na\ IP}$ starting value for acetonitrile (-1400 Hz) was estimated by extrapolation from the $\delta_{Na\text{-}23}$ *vs* $[Na^+]$ data (Table 5.9Adm), to which a best Excel trendline had been fitted. Both the refined Q and $\delta_{ClO4\text{-}Na\ IP}$ values for the acetonitrile data (0.298 M^{-1} and -1868 Hz, respectively), as well as the calculated standard errors, appear reasonable. Contributing to the confidence in these results, furthermore, is the fact that, as with the refinement in the case of the aqueous data, the curve fitting process was found to be consistent to a variety of starting values: with the Q starting value *varied* in the range 0.01 – 1.0 M^{-1} and starting $\delta_{ClO4\text{-}Na\ IP}$ set to -1400 Hz, or with the $\delta_{ClO4\text{-}Na\ IP}$ starting value *varied* in the range 0 – -3600 Hz with starting Q set to 0.2 M^{-1}, SigmaPlot yielded practically the same final values. Unfortunately, a starting value for $\delta_{ClO4\text{-}Na\ IP}$ for the methanol medium could not be obtained from the available $\delta_{Na\text{-}23}$ *vs* $[Na^+]$ data (Table 5.8Adm); a best Excel trendline for this data predicts increasing upfield shifts for $\delta_{Na\text{-}23}$ with increasing $[Na^+]$, and cannot provide a limiting shift value. A value for $\delta_{ClO4\text{-}Na\ IP}$ for methanol was therefore simply chosen by adding the difference between the infinite dilution $\delta_{Na\text{-}23}$ values between methanol and water to the limiting $\delta_{ClO4\text{-}Na\ IP}$ starting value determined by extrapolation for water, *i.e.* ((-571 – (-12)) + (-750)) = -1309 Hz. SigmaPlot decreases the value of Q for $\{Na^+[ClO_4^-]\}$ formation in methanol (0.047 M^{-1}) relative to the starting value; although this value is higher than that for water (0.024 M^{-1}), indicating more pronounced ion-pair formation in methanol, the difference in the Q values for water and methanol is relatively small considering the significant difference in dielectric constants between these solvents, suggesting that the value of 0.047 M^{-1} for methanol may be under-estimated. The refined $\delta_{ClO4\text{-}Na\ IP}$ for the **$NaClO_4$ + methanol** data is significantly more negative (-4425 Hz) than the starting estimate, but this is to be expected considering the difficulty already experienced in extrapolating the $\delta_{Na\text{-}23}$ *vs* $[Na^+]$ data to a limiting shift value with Excel. The larger refinement standard errors presented by SigmaPlot for the methanol data, in comparison to the aqueous and acetonitrile data, illustrate that the overall fit for methanol is worse than that for H_2O and CH_3CN, but the refinement process for CH_3OH did appear consistent to a variety of starting values. Constraining the value for $\delta_{ClO4\text{-}Na\ IP}$ in methanol to > -1800 Hz in the refinement, leads to a Q value of 0.211 M^{-1} (standard error 0.083; $\delta_{ClO4\text{-}Na\ IP}$ is 'refined' -1800 Hz), but also results in considerable deterioration of the overall fit. A value of Q = 0.047 M^{-1} for $\{Na^+[ClO_4^-]\}$ contact ion-pair formation in methanol is considered the best-fit value, for the analysis by SigmaPlot.

Stellenbosch University http://scholar.sun.ac.za

In Fig. 5.4 the variation of $\delta_{Na\text{-}23}$, in Hz, with increasing sodium perchlorate concentration observed *experimentally*, is shown for **$NaClO_4$ + H_2O** (×), **$NaClO_4$ + methanol** (∗) and **$NaClO_4$ + acetonitrile** (+). The SigmaPlot *calculated* chemical shifts, based on δ_{Na} and the best-fit refined parameters $\delta_{ClO4\text{-}Na\ IP}$ and Q (Table 5.2) with equation (5.10), are shown as O for each series. Experimental and calculated values are practically identical, and the figure illustrates that the refined fit is optimized, i.e. these results are probably as good as a general curve-fitting program such as SigmaPlot can produce.

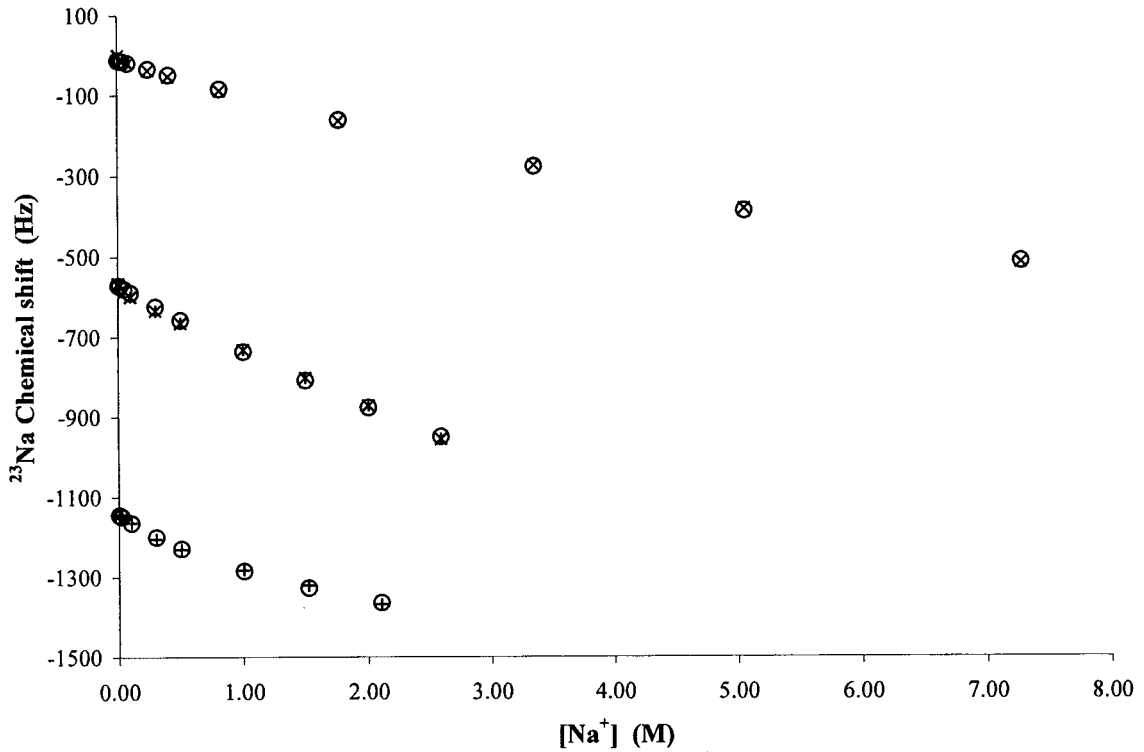

Fig. 5.4 Experimental values of ^{23}Na chemical shift with increasing $[Na^+]$ are shown as × for $NaClO_4$ in water, ∗ for $NaClO_4$ in methanol, and + for $NaClO_4$ in acetonitrile, together with *calculated* chemical shifts, indicated by O for each series, obtained by fitting the experimental data to equation (5.10) with SigmaPlot.

(b) Calculation of conditional ion-pair formation equilibrium quotients by application of SIRKO:[51]

The sodium chemical shift data was also analysed using the program SIRKO[51]. For its application, the equilibrium under study is formulated as:

$$Na^+ + [ClO_4^-] \overset{Q}{\longleftrightarrow} \{Na^+[ClO_4^-]\} \qquad (5.6)$$

and the equilibrium constant expression as:

$$Q = \frac{[\{Na^+[ClO_4^-]\}]}{[Na^+][ClO_4^-]} \qquad (5.7)$$

From an initial estimated value of Q and the analytical concentrations of the reagents (Na^+ and ClO_4^-), SIRKO calculates equilibrium concentrations of each species in solution from appropriate mass balance equations.[51] The program then iteratively refines the formation quotient by application of a so-called

Stellenbosch University http://scholar.sun.ac.za

universal response function that relates the calculated equilibrium concentrations to a given set of experimental data. The refinement is carried out by a least-squares method for which the best constants are those that minimize the weighted summation of the squared difference between calculated and measured experimental values:

$$SS = \sum_i \sum_j W_{ij} \left(F_{ij}^{\ exp} - F_{ij}^{\ calc} \right)^2 \tag{5.12}$$

where i is the number of experiments (one in each case of the present study), j is the number of experimental points, W_{ij} applies a weighting factor to each experimental point, and F_{ij} is the response function. The response function, which is unique to SIRKO (equation (5.13)), allows data from different physicochemical methods, such as spectrophotometry, potentiometry, calorimetry and NMR spectroscopy, to be used to perform the required calculations associated with the study of chemical equilibria. The response function is formulated as:

$$F = Y_0 + Y_e \sum_{k=1}^{s} E_k [C_k] - Y_l \log\left(\sum_{k=1}^{s} EH_k [C_k] \right) \tag{5.13}$$

where F is the measured value, s the number of components in solution, $[C_k]$ the equilibrium concentration of component k, Y_0 a constant for a given method (depending on the properties of the solvent), Y_l a constant used for potentiometric methods, Y_e a constant used for additive methods (such as spectrophotometry and NMR spectroscopy), E_k the physicochemical parameter of component k for additive methods, and EH_k a parameter of the k^{th} component for potentiometric methods.

It has been stated that in solutions of only sodium perchlorate, the ^{23}Na chemical shift may be expressed by equation (5.4):

$$\delta_{Na\text{-}23\ obs} = X_{Na}\, \delta_{Na} + X_{ClO4\text{-}Na\ IP}\, \delta_{ClO4\text{-}Na\ IP} \tag{5.4}$$

Since it also holds true that X_{Na} and $X_{ClO4\text{-}Na\ IP}$ may be written as:

$$X_{Na} = \frac{[Na^+]}{C_{Na}^{\ Total}} \tag{5.8}$$

and

$$X_{ClO4\text{-}Na\ IP} = \frac{[\{Na^+[ClO_4^-]\}]}{C_{Na}^{\ Total}} \tag{5.14}$$

equation (5.4) can be re-written as:

$$\delta_{Na\text{-}23\ obs}\, C_{Na}^{\ Total} = [Na^+]\, \delta_{Na} + [\{Na^+[ClO_4^-]\}]\, \delta_{ClO4\text{-}Na\ IP} \tag{5.15}$$

or, in a general form as:

$$F = \sum_{k=1}^{s} E_k [C_k] \tag{5.16}$$

Equation (5.16) is in fact the SIRKO universal response function (equation (5.13)) with Y_0 and Y_l set to zero, and Y_e set to 1. The SIRKO response function can thus be used to describe the dependence of the observed ^{23}Na chemical shift on the equilibrium concentrations of the 'free' (including solvent-separated/-shared ion-pairs) and contact ion-paired sodium ions in solution, and can be utilized to calculate values for Q. In this case F describes the product $\{\delta_{Na\text{-}23\ obs}\, C_{Na}^{\ Total}\}$, E_{Na} and $E_{ClO4\text{-}Na\ IP}$ are taken as the chemical shifts

Stellenbosch University http://scholar.sun.ac.za

of Na^+ (δ_{Na}) and $\{Na^+[ClO_4^-]\}$ ($\delta_{ClO4\text{-}Na\ IP}$), respectively, and [$C_{Na}$] and [$C_{ClO4\text{-}Na\ IP}$] are the equilibrium concentrations $[Na^+]$ and $[\{Na^+[ClO_4^-]\}]$, respectively. The results obtained by application of SIRKO, are shown in Table 5.3.

Table 5.3 Starting values input to SIRKO, and resultant refined parameters for Q and $\delta_{ClO4\text{-}Na\ IP}$.

	Experimental data	Infinite dilution $\delta_{Na\text{-}23}$ (Hz)	Starting values Q (M^{-1})	Starting values $\delta_{ClO4\text{-}Na\ IP}$ (Hz)	Refinement parameters Q (M^{-1})	Refinement parameters $\delta_{ClO4\text{-}Na\ IP}$ (Hz)	*R*-factor (%)
Water	Table 5.7Adm	-12	0.028	-750	0.022±0.002	-4108±250	0.97
Methanol	Table 5.8Adm	-571	0.2	-1309	0.167±0.003	-2027±17	2.12
Acetonitrile	Table 5.9Adm	-1144	0.2	-1400	0.327±0.003	-1830±4	0.34

Starting values for the parameters δ_{Na}, $\delta_{ClO4\text{-}Na\ IP}$ and Q, together with the analytical concentrations of Na^+ and ClO_4^- and the experimental ^{23}Na chemical shifts at those concentrations, were input to SIRKO for each data set. Starting values for δ_{Na} were taken as those determined for the SigmaPlot analyses (Table 5.3, column (3)), and were *fixed* in the refinement. The starting values for $\delta_{ClO4\text{-}Na\ IP}$ and Q were also taken as those previously determined for the SigmaPlot calculations; these parameters were refined. The SIRKO refined values for Q and $\delta_{ClO4\text{-}Na\ IP}$ for $\{Na^+[ClO_4^-]\}$ formation in water, 0.022 M^{-1} and -4108 Hz respectively, are practically identical to those obtained with SigmaPlot (see Table 5.2). The Q value presented by SIRKO for methanol (0.167 M^{-1}), is larger than that determined by SigmaPlot (0.047 M^{-1}); the refined $\delta_{ClO4\text{-}Na\ IP}$ is less negative (-2027 Hz) than that determined by SigmaPlot (-4425 Hz), and appears more reasonable on inspection of the $\delta_{Na\text{-}23}$ *vs* $[Na^+]$ data (Table 5.8Adm). The SIRKO Q value for acetonitrile (0.327 M^{-1}) is slightly larger than the SigmaPlot value (0.298 M^{-1}), while the $\delta_{ClO4\text{-}Na\ IP}$ values for the two methods do not differ significantly.

A so-called *R*-factor presented by SIRKO after each run may be used as a measure of the compatibility of the theoretical model with the experimental data. The *R*-factor is calculated with the equation:

$$R = \sqrt{\frac{SS}{\sum W_i (F_i^{exp})^2}} \qquad (5.17)$$

An *R*-factor of less than 5 % indicates an acceptable fit of the model to the data;[51,54] based on this factor, the overall fit for the methanol data is worse than for the other media, as is indicated by the SigmaPlot results. SIRKO provides the user the option of supplying errors on the experimental values; errors input were based on the estimated chemical shift errors, but any reasonable variation of these input error values had very little effect on the results presented by the program. *Calculated* chemical shifts, based on the

Stellenbosch University http://scholar.sun.ac.za

SIRKO refined parameters, are practically identical to the experimental values, and lead to a graphical representation of the goodness-of-fit closely resembling that already presented in Fig. 5.4.

The ^{23}Na chemical shift data for sodium perchlorate in water, methanol and acetonitrile presented by Greenberg and Popov in 1976 (referred to in Section 5.3.2),[18] were also analysed by the SigmaPlot and SIRKO methods, as has been described for the present data; the results for the Greenberg and Popov data and the present data are shown in Table 5.4. The Q values determined by SigmaPlot for $\{Na^+[ClO_4^-]\}$ formation in methanol and acetonitrile are 0.007 M^{-1} (standard error 0.011; $\delta_{Na\text{-}23}$ fixed at -3.4 ppm, $\delta_{ClO4\text{-}Na\ IP}$ started at -15 ppm) and 0.062 M^{-1} (standard error 0.066; $\delta_{Na\text{-}23}$ fixed at -6.3 ppm, $\delta_{ClO4\text{-}Na\ IP}$ started at -25 ppm), respectively; SigmaPlot could not satisfactorily fit the data for the aqueous medium. Refined Q values presented by SIRKO for water, methanol and acetonitrile are 0.060±0.002 (R-factor 6.99 %), 0.078±0.009 (R-factor 1.71 %) and 0.141±0.003 (R-factor 2.01), respectively. The respective Q values calculated with the Greenberg and Popov data illustrate that the extent of ion-pairing is greatest in acetonitrile and least in water, but the values differ notably from those determined from data in the present investigation. The errors calculated by the two programs for the Greenberg and Popov data are in general however larger than those for the present data, illustrating that the overall fit for the Greenberg and Popov data is poorer. Interestingly, the SIRKO Q values are larger than the SigmaPlot values; this response by the programs was also observed with the present data.

Table 5.4 Conditional ion-pair formation equilibrium quotients calculated by SigmaPlot and Sirko for the present data and the Greenberg and Popov data,[18] for $\{Na^+[ClO_4^-]\}$ contact ion-pair formation in water, methanol and acetonitrile.

	Present data				Greenberg and Popov data			
	SigmaPlot		SIRKO		SigmaPlot		SIRKO	
	Q (M^{-1})	Q Std. Err.	Q (M^{-1})	R-factor (%)	Q (M^{-1})	Q Std. Err.	Q (M^{-1})	R-factor (%)
Water	0.024	0.004	0.022±0.002	0.97	-	-	0.060±0.002	6.99
Methanol	0.047	0.016	0.167±0.003	2.12	0.007	0.011	0.078±0.009	1.71
Acetonitrile	0.298	0.041	0.327±0.003	0.34	0.062	0.066	0.141±0.003	2.01

The differences in the values of the refined parameters calculated by SigmaPlot and SIRKO are presumably due to the different approaches taken by the two programs in the refinement processes. Whereas SigmaPlot is a program that allows *generalized* and simple curve fitting, SIRKO was developed *specifically* for the calculation of equilibrium constants and could be regarded as the more sophisticated of the two approaches. The technique applied in the present study to analyze the data is subject to several constraints that deter the optimal use of a program such as SIRKO. The total number of experimental points in each of the data sets, for example, is rather small for accurate and rigorous curve fitting. Furthermore, data at high sodium perchlorate concentrations are not well represented, with only a few experimental points describing the

Stellenbosch University http://scholar.sun.ac.za

concentration ranges where contact ion-pairing may be considered to be significant; solubility constraints however preclude investigation at high salt concentrations, since solutions with a high predominance of contact ion-pairing will also rapidly experience salt precipitation. No provision has been made for the changing ionic strengths through each data set; typically, calculations of equilibrium constants with programs such as SIRKO are performed with experimental data obtained in constant ionic strength media,[55] but the chosen method for studying ion-pair formation necessitates the use of high analyte concentrations and disallows a constant medium system (the Q values are not thermodynamic constants, but are *conditional formation quotients*). Due to these constraints, which to a large degree are inherent to the technique, the calculated Q values are probably semi-quantitative at best, but they are extremely useful in indicating the *relative extent of ion-pairing* in the different solvents. The good agreement between the Q value obtained for $\{Na^+[ClO_4^-]\}$ formation in water in the present investigation (0.022 M^{-1}) and that previously reported by Miller and Macklin (0.028 M^{-1}[33]), however underscores the usefulness of the method applied in the present investigation to the study of ion-pair formation in solution.

Solvent properties relevant to the occurrence of ion-pairing in solution are shown for water, methanol and acetonitrile in Table 5.5, together with the SIRKO calculated conditional ion-pair formation equilibrium quotients, Q, for the formation of $\{Na^+[ClO_4^-]\}$ in these solvents. The DN^N and AN values for the solvents decrease in the order water > methanol > acetonitrile, indicating that Na^+ *and* ClO_4^- are progressively less well solvated from water, to methanol, to acetonitrile, which suggests that the extent of ion-pairing is likely to *increase* for the solvents in this order. The calculated Q values for $\{Na^+[ClO_4^-]\}$ contact ion-pair formation in these solvents do indicate that the extent of ion-pair formation increases for the solvents in the order water (Q = 0.022 M^{-1}) < methanol (Q = 0.167 M^{-1}) < acetonitrile (Q = 0.327 M^{-1}), corroborating the qualitative predictions based on solvent properties. Although methanol and acetonitrile have very similar dielectric constants, the extent of ion-pair formation is greater in acetonitrile, which has smaller values for DN^N and AN.

Table 5.5 Solvent properties relevant to the occurrence of ion-pairing for water, methanol and acetonitrile, and SIRKO calculated conditional ion-pair formation quotients, Q (M^{-1}), for $\{Na^+[ClO_4^-]\}$ formation in these solvents.

	ε	DN^N	AN	SIRKO Q (M^{-1})
Water	78.36	0.85	54.8	0.022
Methanol	32.66	0.77	41.5	0.167
Acetonitrile	35.94	0.36	18.9	0.327

Solvent properties were obtained from publications by Marcus.[1,5] Some uncertainty exists as to donor number values for water and methanol;[5] DN^N values in this table are taken from reference [1].

Stellenbosch University http://scholar.sun.ac.za

5.3.4 Ion-pair formation of Na^+ with $PtCl_6^{2-}$, and with $PtBr_6^{2-}$, in water, methanol and acetonitrile: a ^{23}Na NMR chemical shift study

Solutions of $H_2PtCl_6 \cdot H_2O$, or H_2PtBr_6, + $NaClO_4$ in water, methanol and acetonitrile were prepared as described in the Experimental Section, and ^{23}Na NMR spectra recorded. The variation of ^{23}Na chemical shift values with increasing log[Na^+] for the solutions **$H_2PtCl_6 \cdot H_2O$ + $NaClO_4$ in water** (■), **$H_2PtCl_6 \cdot H_2O$ + $NaClO_4$ in methanol** (◆), and **$H_2PtCl_6 \cdot H_2O$ + $NaClO_4$ in acetonitrile** (▲), as well as for the solutions **H_2PtBr_6 + $NaClO_4$ in water** (□), **H_2PtBr_6 + $NaClO_4$ in methanol** (◇), and **H_2PtBr_6 + $NaClO_4$ in acetonitrile** (△) are presented in Fig. 5.5. The sodium-23 chemical shifts as a function of log[Na^+] for **$NaClO_4$ in water** (×), **methanol** (✳) and **acetonitrile** (+) are also shown in Fig. 5.5.

Considering first only data for the solutions **$H_2PtCl_6 \cdot H_2O$ + $NaClO_4$ + CH_3OH** (◆) and **$NaClO_4$ + CH_3OH** (✳), Fig. 5.5 reveals a similar *general* trend for the solutions with and without the $PtCl_6^{2-}$ ion, i.e. an upfield shift in the ^{23}Na resonance position with increasing sodium perchlorate concentration. However, at lower overall sodium concentrations, the chemical shifts for solutions containing $PtCl_6^{2-}$ are more *downfield* than those for solutions without the anion.

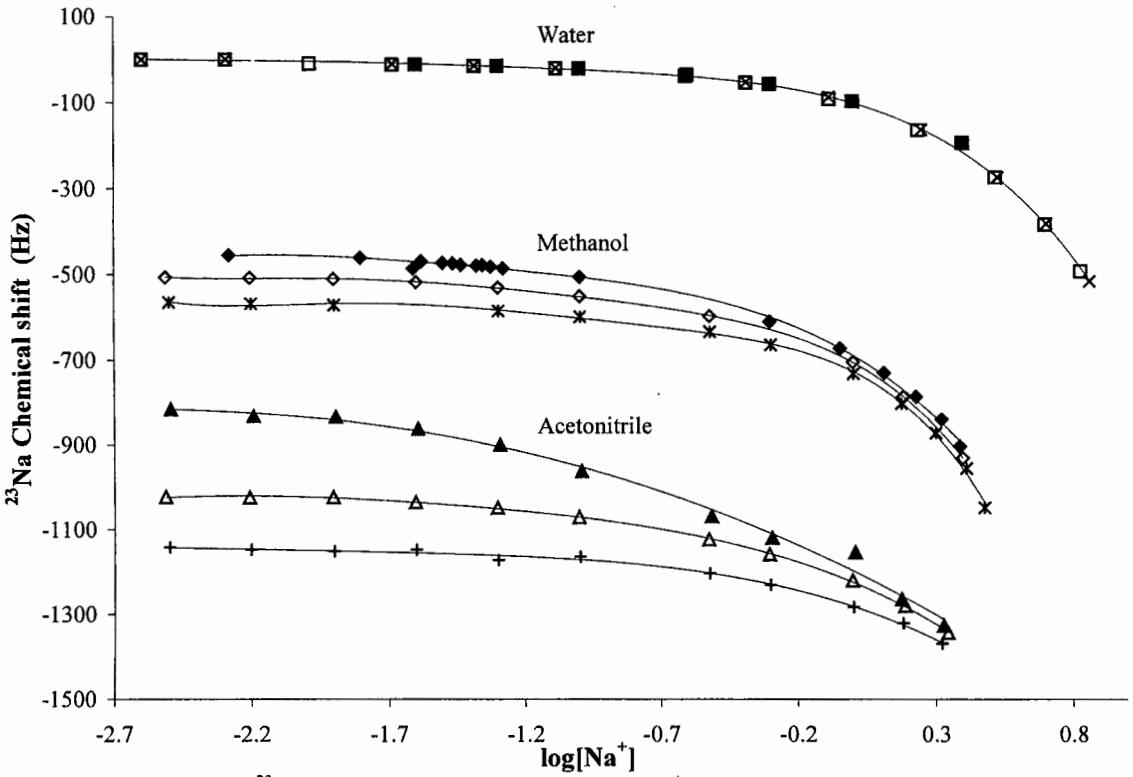

Fig. 5.5 Variation of the ^{23}Na chemical shift as a function of log[Na^+] for solutions of: (×) $NaClO_4$ in water, (■) $H_2PtCl_6 \cdot H_2O$ + $NaClO_4$ in water ([$PtCl_6^{2-}$] = 0.05493 M), (□) H_2PtBr_6 + $NaClO_4$ in water ([$PtBr_6^{2-}$] = 0.06108 M), (✳) $NaClO_4$ in methanol, (◆) $H_2PtCl_6 \cdot H_2O$ + $NaClO_4$ in methanol ([$PtCl_6^{2-}$] = 0.05885 M) , (◇) H_2PtBr_6 + $NaClO_4$ in methanol ([$PtBr_6^{2-}$] = 0.06089 M), (+) $NaClO_4$ in acetonitrile, (▲) $H_2PtCl_6 \cdot H_2O$ + $NaClO_4$ in acetonitrile ([$PtCl_6^{2-}$] = 0.06332 M), (△) H_2PtBr_6 + $NaClO_4$ in acetonitrile ([$PtBr_6^{2-}$] = 0.06044 M). ^{23}Na chemical shifts have been corrected for the difference in bulk diamagnetic susceptibility between sample and reference.

Stellenbosch University http://scholar.sun.ac.za

With reference to the discussion in Section 5.3.2, relating ^{23}Na chemical shift changes to the electron-donating ability of solvent molecules or a counter-anion in the inner solvation sphere of the cation, the downfield shift of the ^{23}Na resonance position at lower overall $[Na^+]$, where little or no $\{Na^+[ClO_4^-]\}$ ion-pairing is expected to occur, on addition of $H_2PtCl_6 \cdot H_2O$ to solutions of $NaClO_4$ in methanol, suggests that solvent molecules in the inner solvation sphere of some Na^+ ions are being replaced by a solution 'component' with *greater* electron donating ability than the methanol molecules. This 'component' is most likely to be the $PtCl_6^{2-}$ anion, thus indicating the occurrence of Na^+-$PtCl_6^{2-}$ association, i.e. *$\{Na^+[PtCl_6^{2-}]\}^-$ contact ion-pair formation*, in these solutions even at very low sodium concentrations (the $[PtCl_6^{2-}]$ remains constant through the series). The formation of solvated $\{(Na^+)_2[PtCl_6^{2-}]\}$ might reasonably be expected, but only at very high $[Na^+]$; solubility limitations of the sodium perchlorate and hexachloroplatinic acid however preclude investigations of more concentrated solutions. At low salt concentrations the observed ^{23}Na chemical shift will be a weighted average of the chemical shifts of the free and $PtCl_6^{2-}$ ion-paired sodium ions:

$$\delta_{Na\text{-}23\ obs} = X_{Na}\,\delta_{Na} + X_{PtCl6\text{-}Na\ IP}\,\delta_{PtCl6\text{-}Na\ IP} \qquad (5.18)$$

with X_{Na} and $X_{PtCl6\text{-}Na\ IP}$ the mole fractions and δ_{Na} and $\delta_{PtCl6\text{-}Na\ IP}$ the chemical shifts of the free and $PtCl_6^{2-}$ ion-paired Na^+, respectively. Hence it is not unreasonable to conclude that the downfield shift observed at low $[Na^+]$, is related to the formation of $\{Na^+[PtCl_6^{2-}]\}^-$, and that $\delta_{PtCl6\text{-}Na\ IP}$ is *downfield* of δ_{Na}.

Experimental results of the present study indicate that $\delta_{ClO4\text{-}Na\ IP}$ is *upfield* (Section 5.3.2) and $\delta_{PtCl6\text{-}Na\ IP}$ *downfield* of δ_{Na} in methanol. Greenberg, Bodner and Popov have stated that Na^+-anion association may lead to both upfield or downfield ^{23}Na shifts, the shift depending on the anion.[17] We have additionally investigated sodium *chloride* solutions of water and methanol with increasing salt concentration, using ^{23}Na NMR spectroscopy (details are presented in Tables 5.10Adm and 5.11Adm, Addendum B), and have found that, in contrast to the sodium *perchlorate* solutions in which there is an *upfield* shift of $\delta_{Na\text{-}23}$ with increasing salt concentration (see Fig. 5.5), the ^{23}Na resonance peak moves *downfield* with increasing sodium *chloride* concentration in water and methanol; this is illustrated graphically in Fig. 5.6. The observed chemical shift change is considered to be related to the formation of $\{Na^+[Cl^-]\}$ contact ion-pairs in solution.[18,21] The downfield ^{23}Na chemical shifts on replacement of H_2O or CH_3OH molecules in the inner solvation spheres of Na^+ ions by Cl^- ions, suggests *increased* electron density in the $3p$ orbitals of the cation, in contrast to the sodium perchlorate study in which the observed upfield shifts were related to a *decrease* in electron density in the $3p$ orbitals of Na^+ on contact ion-pair formation. These observations are in accordance with the relative donor numbers for Cl^- (DN = 1.01) and ClO_4^- (DN = 0).[9] The hexachloroplatinate anion, with its octahedral cage of six chloride ligands forming the first coordination sphere of the Pt(IV) ion, appears to have a similar influence on the ^{23}Na resonance position when ion-paired to the Na^+ cation as that of the chloride anion, resulting in the downfield shift of $\delta_{PtCl6\text{-}Na\ IP}$ relative to δ_{Na}.

Stellenbosch University http://scholar.sun.ac.za

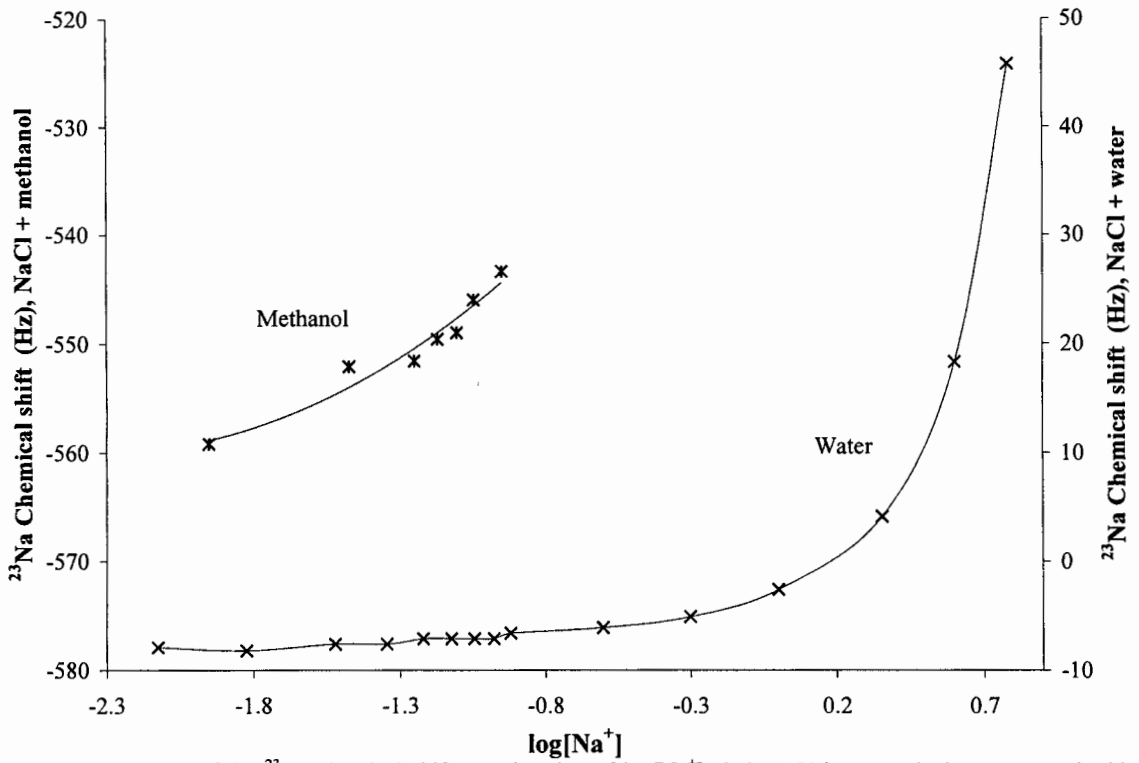

Fig. 5.6 Variation of the ^{23}Na chemical shift as a function of log[Na^+]: (×) NaCl in water (points connected with smoothed line), (∗) NaCl in methanol (a trendline has been inserted). ^{23}Na chemical shifts in methanol have been corrected for the difference in bulk diamagnetic susceptibility between sample and reference.

It has been pointed out that in Fig. 5.5 the data for the solutions **$H_2PtCl_6 \cdot H_2O$ + $NaClO_4$ + CH_3OH** (◆) and **$NaClO_4$ + CH_3OH** (∗) display a similar *general* trend. The upfield shift in $\delta_{Na\text{-}23}$ observed for the solutions **$H_2PtCl_6 \cdot H_2O$ + $NaClO_4$ + CH_3OH** (◆) with increasing [Na^+] is indicative, as is the case for the solutions of **$NaClO_4$ + CH_3OH** (∗) (Section 5.3.2), of {$Na^+[ClO_4^-]$} contact ion-pair formation as the sodium perchlorate concentration increases, which is consistent with the observation that $\delta_{Na\text{-}23}$ for the solutions with and without $PtCl_6^{2-}$ almost converge at very high [Na^+]. The observed chemical shift can be expressed as:

$$\delta_{Na\text{-}23\ obs} = X_{Na}\,\delta_{Na} + X_{PtCl6\text{-}Na\ IP}\,\delta_{PtCl6\text{-}Na\ IP} + X_{ClO4\text{-}Na\ IP}\,\delta_{ClO4\text{-}Na\ IP} \qquad (5.19)$$

$\delta_{ClO4\text{-}Na\ IP}$ lies upfield of δ_{Na}, and consequently the ^{23}Na peak moves further upfield with increasing salt concentration, as conditions become more favourable for {$Na^+[ClO_4^-]$} formation. The predominant contribution of {$X_{ClO4\text{-}Na\ IP}\,\delta_{ClO4\text{-}Na\ IP}$} to $\delta_{Na\text{-}23\ obs}$ at very high sodium salt concentrations, results in the convergence of curves for **$H_2PtCl_6 \cdot H_2O$ + $NaClO_4$ + CH_3OH** (◆) and **$NaClO_4$ + CH_3OH** (∗).

Fig. 5.5 shows that the general trend for the solutions **$H_2PtCl_6 \cdot H_2O$ + $NaClO_4$ + CH_3CN** (▲) is similar to that for **$H_2PtCl_6 \cdot H_2O$ + $NaClO_4$ + CH_3OH** (◆), from which we may conclude by analogy that Na^+-$PtCl_6^{2-}$ association, i.e. *{$Na^+[PtCl_6^{2-}]$}$^-$ contact ion-pair formation*, also occurs in the acetonitrile solutions, even at low overall Na^+ concentration, and that {$Na^+[ClO_4^-]$} contact ion-pairing becomes predominant at higher

Stellenbosch University http://scholar.sun.ac.za

sodium perchlorate concentrations. A similar assessment of the $\delta_{Na\text{-}23}$ trends for the solutions **H_2PtBr_6 + $NaClO_4$ + CH_3OH** (◇) and **H_2PtBr_6 + $NaClO_4$ + CH_3CN** (△), leads to the conclusion that in these solutions *$\{Na^+[PtBr_6^{2-}]\}^-$ contact ion-pairs* are formed. The observation that $\{Na^+[PtCl_6^{2-}]\}^-$ and $\{Na^+[PtBr_6^{2-}]\}^-$ ion-pairs form even at low sodium concentrations in methanol and acetonitrile, whereas $\{Na^+[ClO_4^-]\}$ ion-pairs form only at distinctly higher sodium perchlorate concentrations, suggests that Na^+-$PtCl_6^{2-}$ and Na^+-$PtBr_6^{2-}$ contact association occurs much more readily than Na^+-ClO_4^- association in these solvents.

Interestingly, $\delta_{Na\text{-}23}$ for the solutions **$NaClO_4$ in water** (×), **$H_2PtCl_6{\cdot}H_2O$ + $NaClO_4$ in water** (■), and **H_2PtBr_6 + $NaClO_4$ in water** (□) (Fig.5.5), describe identical curves, indicating that sodium exists only as free solvated Na^+ ions or as ClO_4^- ion-paired Na^+ ions in solution, with no clear indication of the occurrence of ion-pairing between $PtCl_6^{2-}$, or $PtBr_6^{2-}$, and Na^+ in the aqueous medium.

5.3.5 Ion-pair formation of Na^+ with $PtCl_6^{2-}$, and with $PtBr_6^{2-}$, in water, methanol and acetonitrile: a ^{195}Pt NMR chemical shift study

The occurrence of significant $\{Na^+[PtCl_6^{2-}]\}^-$ and $\{Na^+[PtBr_6^{2-}]\}^-$ contact ion-pair formation in methanol and acetonitrile, as suggested by the $\delta_{Na\text{-}23}$ *vs* log[Na^+] data in Fig. 5.5, is corroborated by ^{195}Pt NMR spectra recorded for the prepared samples. The variation of the ^{195}Pt chemical shift as a function of Na^+ concentration for the solutions **$H_2PtCl_6{\cdot}H_2O$ + $NaClO_4$ in water** (■), **methanol** (◆) and **acetonitrile** (▲), and for **H_2PtBr_6 + $NaClO_4$ in water** (□), **methanol** (◇) and **acetonitrile** (△), is depicted in Fig. 5.7. The trends of these curves reveal that for the aqueous solutions there is only a very slight upfield shift in $\delta_{Pt\text{-}195}$ with increasing [Na^+], while in methanol and acetonitrile there is a significant upfield shift of $\delta_{Pt\text{-}195}$ as the cation concentration increases. The ^{195}Pt nucleus has been shown to be very sensitive to changes in the *inner* solvation spheres around the $PtCl_6^{2-}$ and $PtBr_6^{2-}$ anions (Chapter 4, [56,57]) and thus if Na^+ ions disturb the solvent cages of the anions, due to ion-pairing, this will be reflected in the chemical shift of the platinum nucleus; at sufficiently high [Na^+], the cations may replace some solvent molecules in the solvation spheres of the anions, leading to solvent-separated, solvent-shared and finally contact ion pairs. We thus interpret the upfield shift trends in Fig. 5.7 as indicative of significant Na^+-$PtCl_6^{2-}$ and Na^+-$PtBr_6^{2-}$ association with increasing [Na^+] in the methanol and acetonitrile solutions, with very little association occurring in the aqueous solutions in the concentration ranges studied, thus supporting the conclusions derived from the $\delta_{Na\text{-}23}$ data (Fig. 5.5).

Thus far, solutions in which association of Na^+ and the halogenoplatinate anions occurs have had fixed PtX_6^{2-} (X = Cl, Br) concentrations, with sodium concentrations varying. A series of methanol solutions was also prepared in which the sodium perchlorate concentration was kept constant (at 0.01004 M) and the [$PtCl_6^{2-}$] was varied in the range 0.000527 – 0.1014 M (Table 5.18Adm, Addendum B). The $\delta_{Na\text{-}23}$ and

Stellenbosch University http://scholar.sun.ac.za

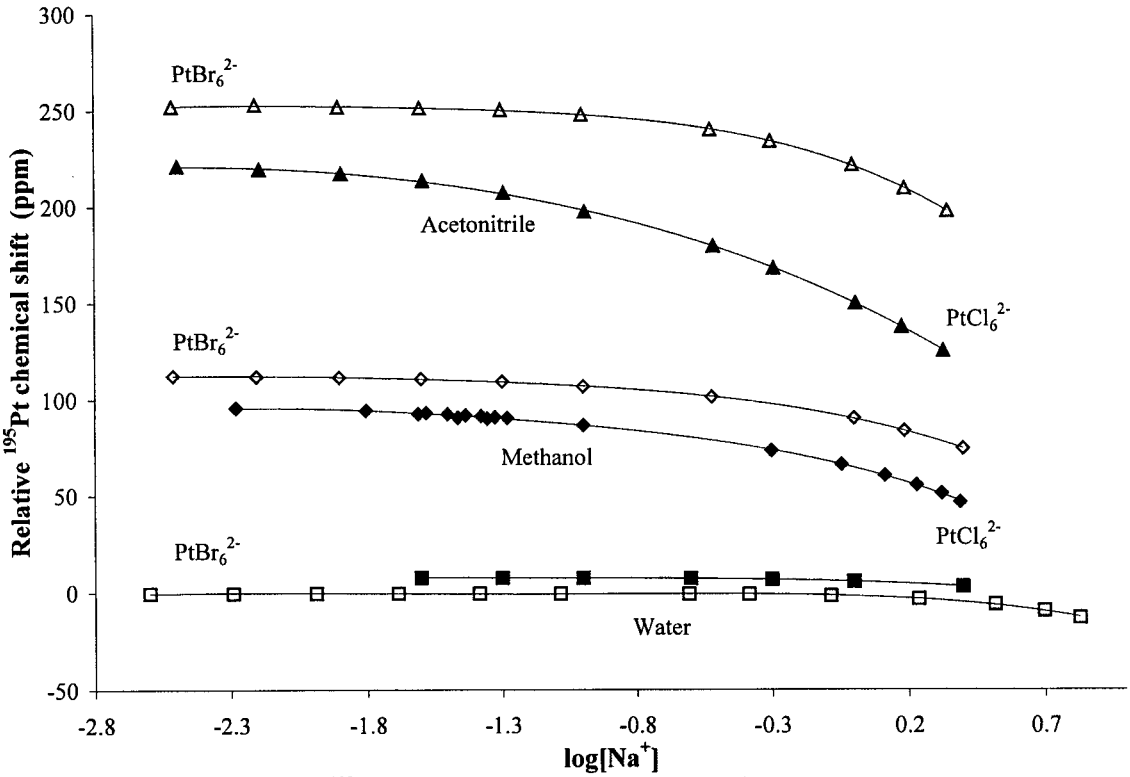

Fig. 5.7 Variation of the relative ^{195}Pt chemical shift as a function of log[Na^+]: (■) $H_2PtCl_6{\cdot}H_2O$ + $NaClO_4$ in water ([$PtCl_6^{2-}$] = 0.05493 M) , (□) H_2PtBr_6 + $NaClO_4$ in water ([$PtBr_6^{2-}$] = 0.06108 M), (◆) $H_2PtCl_6{\cdot}H_2O$ + $NaClO_4$ in methanol ([$PtCl_6^{2-}$] = 0.05885 M), (◇) H_2PtBr_6 + $NaClO_4$ in methanol ([$PtBr_6^{2-}$] = 0.06089 M), (▲) $H_2PtCl_6{\cdot}H_2O$ + $NaClO_4$ in acetonitrile ([$PtCl_6^{2-}$] = 0.06332 M), (△) H_2PtBr_6 + $NaClO_4$ in acetonitrile ([$PtBr_6^{2-}$] = 0.06044 M). Separate reference solutions, as described in the experimental section, were used for $PtCl_6^{2-}$-containing and $PtBr_6^{2-}$-containing solutions.

$\delta_{Pt\text{-}195}$ *vs* [$PtCl_6^{2-}$] data for these solutions is presented in Fig. 5.8; data for the solutions **$H_2PtCl_6{\cdot}H_2O$ in methanol** (◆) (Fig. 5.2) are also reproduced in Fig. 5.8. The $\delta_{Pt\text{-}195}$ *vs* [$PtCl_6^{2-}$] data for the solutions **$H_2PtCl_6{\cdot}H_2O$ + $NaClO_4$ in methanol** (constant [Na^+]) (●) reveal that the ^{195}Pt resonance position moves downfield with increasing [$PtCl_6^{2-}$], and *approaches* the linear distribution of the **$H_2PtCl_6{\cdot}H_2O$ in methanol** data (◆) at higher hexachloroplatinate concentrations. The fact that data for the solutions **$H_2PtCl_6{\cdot}H_2O$ in methanol** (◆) and **$H_2PtCl_6{\cdot}H_2O$ + $NaClO_4$ in methanol** (●) exhibit different chemical shift distributions, is indicative of the occurrence of ion-pairing in the sodium perchlorate containing solutions. The observed ^{195}Pt chemical shift in these solutions can be formulated as:

$$\delta_{Pt\text{-}195\,obs} = X_{PtX6}\delta_{PtX6} + X_{PtX6\text{-}Na\,IP}\delta_{PtX6\text{-}Na\,IP} \qquad (5.20)$$

Since the [Na^+] in the solutions **$H_2PtCl_6{\cdot}H_2O$ + $NaClO_4$ in methanol** (constant [Na^+]) is limited (0.01004 M), {$Na^+[PtCl_6^{2-}]$}$^-$ formation is inhibited by the 'shortage' of Na^+ ions at the highest $PtCl_6^{2-}$ concentrations in the series (these are points, for example, at which $PtCl_6^{2-}$ is as much as ten times in excess relative to Na^+, see Table 5.18Adm, Addendum B). Na^+-$PtCl_6^{2-}$ contact ion-pairing does occur, but the majority of the $PtCl_6^{2-}$ ions at high [$PtCl_6^{2-}$] are not ion-paired, and the term $\{X_{PtCl6}\ \delta_{PtCl6}\}$ in equation (5.20) predominantly contributes to $\delta_{Pt\text{-}195\,obs}$; chemical shifts for **$H_2PtCl_6{\cdot}H_2O$ in methanol** (◆) and **$H_2PtCl_6{\cdot}H_2O$ + $NaClO_4$ in**

Stellenbosch University http://scholar.sun.ac.za

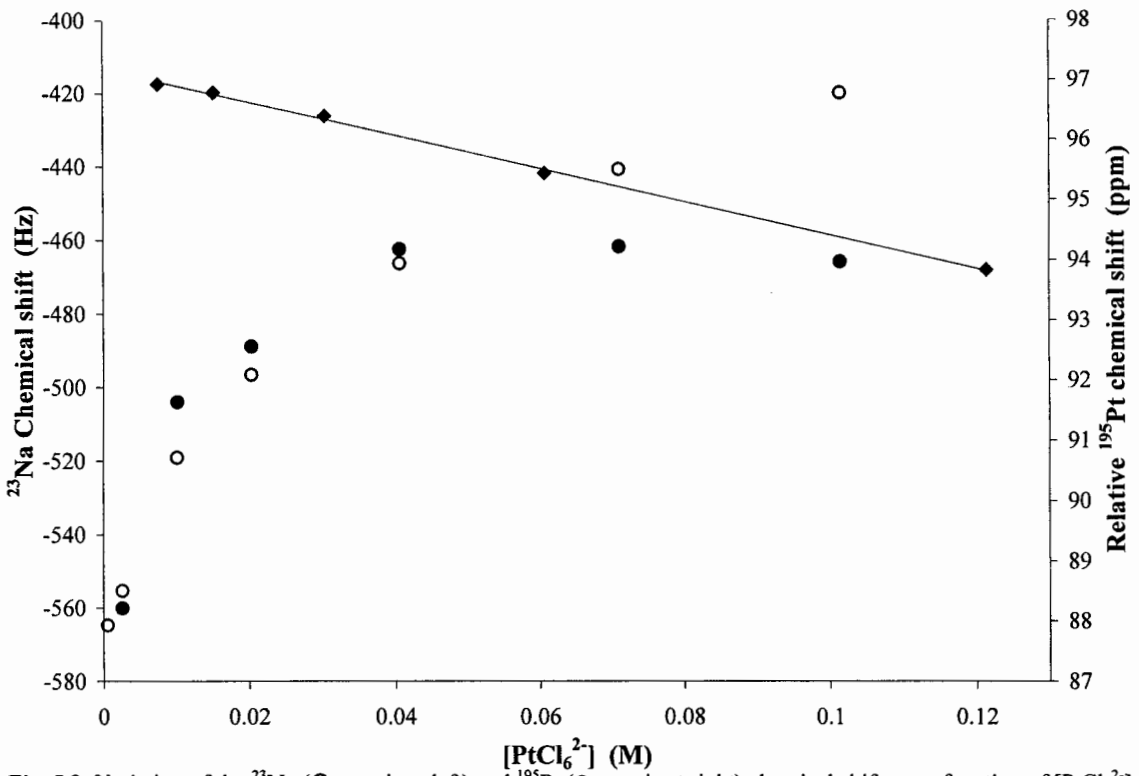

Fig. 5.8 Variation of the ^{23}Na (○, y-axis at left) and ^{195}Pt (●, y-axis at right) chemical shifts as a function of $[PtCl_6^{2-}]$ for the series **$H_2PtCl_6 \cdot H_2O$ + $NaClO_4$ in methanol** ($[Na^+]$ = 0.01004 M). Variation of the ^{195}Pt chemical shift as a function of $[PtCl_6^{2-}]$ for **$H_2PtCl_6 \cdot H_2O$ in methanol** (◆) has been reproduced from Fig. 5.2; a trendline has been inserted.

methanol (●) at the higher $PtCl_6^{2-}$ concentrations, will thus not differ considerably. As the $PtCl_6^{2-}$ concentration in the solutions **$H_2PtCl_6 \cdot H_2O$ + $NaClO_4$ in methanol** (constant $[Na^+]$) decreases, the fraction of $PtCl_6^{2-}$ ions which are not ion-paired decreases, and the contribution of the term $\{X_{PtCl6\text{-}Na\ IP}\ \delta_{PtCl6\text{-}Na\ IP}\}$ to $\delta_{Pt\text{-}195\ obs}$ becomes more significant. Data for the solutions **$H_2PtCl_6 \cdot H_2O$ + $NaClO_4$ in methanol** (◆, Fig. 5.7) have revealed that $\delta_{PtCl6\text{-}Na\ IP}$ is upfield of δ_{PtCl6}, and thus an increased contribution of $\{X_{PtCl6\text{-}Na\ IP}\ \delta_{PtCl6\text{-}Na\ IP}\}$ to $\delta_{Pt\text{-}195\ obs}$, will result in the observed upfield shift for the solutions **$H_2PtCl_6 \cdot H_2O$ + $NaClO_4$ in methanol** (constant $[Na^+]$) (●) with decreasing $[PtCl_6^{2-}]$.

The $\delta_{Na\text{-}23}$ *vs.* $[PtCl_6^{2-}]$ data for the series **$H_2PtCl_6 \cdot H_2O$ + $NaClO_4$ in methanol** (constant $[Na^+]$) (○, Fig. 5.8) shows a downfield shift in the ^{23}Na resonance position with increasing $[PtCl_6^{2-}]$. This trend is consistent with the observations in Section 5.3.4 that the addition of $H_2PtCl_6 \cdot H_2O$ to solutions of $NaClO_4$ in methanol, leads to a downfield shift in $\delta_{Na\text{-}23}$, and suggests that solvent molecules in the inner solvation sphere of some Na^+ ions are being replaced by the $PtCl_6^{2-}$ anion, resulting in the formation of $\{Na^+[PtCl_6^{2-}]\}^-$ contact ion-pairs.

Stellenbosch University http://scholar.sun.ac.za

5.3.6 Estimated conditional ion-pair formation equilibrium quotients: $\{Na^+[PtCl_6^{2-}]\}^-$ and $\{Na^+[PtBr_6^{2-}]\}^-$ contact ion-pairing in water, methanol and acetonitrile

The $\delta_{Na\text{-}23}$ and $\delta_{Pt\text{-}195}$ data shown in Figures 5.5 and 5.7 indicate that in the prepared solutions $\{Na^+[ClO_4^-]\}$, $\{Na^+[PtCl_6^{2-}]\}^-$ and $\{Na^+[PtBr_6^{2-}]\}^-$ ion-pairing occurs, to varying extents, depending on the solvent. For solutions of **$NaClO_4$ in water** (×), **methanol** (∗) and **acetonitrile** (+), the occurrence of $\{Na^+[ClO_4^-]\}$ ion-pairing must be considered. Since these solutions were prepared from a 1:1 electrolyte, and thus contain only Na^+ and ClO_4^- ions, it is possible to derive an equation (by the method of Greenberg *et al.*[16]), which relates the salt concentration and the observed ^{23}Na chemical shifts to the conditional ion-pair formation equilibrium quotient Q (equation (5.10)), which can be calculated by means of least-squares curve fitting. In solutions of **$H_2PtCl_6{\cdot}H_2O$ + $NaClO_4$ in water** (■), **methanol** (◆) and **acetonitrile** (▲), the trends in Figures 5.5 and 5.7 indicate that both $\{Na^+[ClO_4^-]\}$ and $\{Na^+[PtCl_6^{2-}]\}^-$ ion-pairs form, depending on the $[Na^+]$. A similar phenomenon takes place in solutions of **H_2PtBr_6 + $NaClO_4$ in water** (□), **methanol** (◇) and **acetonitrile** (△), with the formation of $\{Na^+[ClO_4^-]\}$ and $\{Na^+[PtBr_6^{2-}]\}^-$ ion-pairs. The ion-pair equilibria in the halogenoplatinate-containing solutions may be expressed as:

$$Na^+ + [ClO_4^-] \xleftrightarrow{Q_1} \{Na^+[ClO_4^-]\} \tag{5.6}$$

and

$$Na^+ + [PtX_6^{2-}] \xleftrightarrow{Q_{2X}} \{Na^+[PtX_6^{2-}]\}^- \tag{5.21}$$

with X = Cl, Br. The ion-pair formation equilibrium quotients are thus:

$$Q_1 = \frac{[\{Na^+[ClO_4^-]\}]}{[Na^+][ClO_4^-]} \tag{5.7}$$

and

$$Q_{2X} = \frac{[\{Na^+[PtX_6^{2-}]\}^-]}{[Na^+][PtX_6^{2-}]} \tag{5.22}$$

Formulating an expression in the form of equation (5.10), along similar lines to that described by Greenberg *et al* [16] (Section 5.3.3), for the calculation of Q_1 and Q_{2X} from ^{23}Na NMR data, or Q_{2X} from ^{195}Pt chemical shift data, cannot be simply done since the solutions now contain *two* analytes, and two equilibria (equations (5.6) and (5.21)) must be considered. The program SIRKO is however suitable for the analysis of such multi-component, multi-equilibrium systems. However, the ^{23}Na NMR data could not be used for the calculation of the formation quotients since the *variation* of the observed ^{23}Na chemical shift data *due to the formation of the $\{Na^+[PtX_6^{2-}]\}^-$ ion-pairs* is too small (Fig. 5.5). Higher relative errors were also expected for the ^{23}Na NMR data, due to the narrower overall shift range for this nucleus. SIRKO calculations were consequently carried out only with the ^{195}Pt chemical shift data.

For the solutions **$H_2PtCl_6{\cdot}H_2O$ + $NaClO_4$ in water** (■), **methanol** (◆) and **acetonitrile** (▲), as well as **H_2PtBr_6 + $NaClO_4$ in water** (□), **methanol** (◇) and **acetonitrile** (△), the ^{195}Pt chemical shift may be expressed as:

$$\delta_{Pt\text{-}195\,obs} = X_{PtX6}\delta_{PtX6} + X_{PtX6\text{-}Na\,IP}\delta_{PtX6\text{-}Na\,IP} \tag{5.20}$$

Stellenbosch University http://scholar.sun.ac.za

with X_{PtX6} and $X_{PtX6\text{-}Na\ IP}$ the mole fractions, and δ_{PtX6} and $\delta_{PtX6\text{-}Na\ IP}$ the limiting chemical shifts for the free and sodium contact ion-paired PtX_6^{2-} (X = Cl, Br), respectively. Expressions for X_{PtX6} and $X_{PtX6\text{-}Na\ IP}$ may be formulated as:

$$X_{PtX6} = \frac{[PtX_6^{2-}]}{[PtX_6^{2-}]^{Total}} \tag{5.23}$$

and:

$$X_{PtX6\text{-}Na\ IP} = \frac{[\{Na^+[PtX_6^{2-}]\}^-]}{[PtX_6^{2-}]^{Total}} \tag{5.24}$$

with $[PtX_6^{2-}]$ and $[\{Na^+[PtX_6^{2-}]\}^-]$ denoting equilibrium concentrations of the particular species, and $[PtX_6^{2-}]^{Total}$ the total halogenoplatinate concentration in solution. Equation (5.20) may be re-written in the form:

$$\delta_{Pt\text{-}195\,obs}\,[PtX_6^{2-}]^{Total} = [PtX_6^{2-}]\delta_{PtX6} + [\{Na^+[PtX_6^{2-}]\}^-]\delta_{PtX6\text{-}Na\ IP} \tag{5.25}$$

which can be formulated as a general expression:

$$F = \sum_{k=1}^{s} E_k[C_k] \tag{5.16}$$

with F the 'experimental values', *i.e.* $\{\delta_{Pt\text{-}195\,obs}\,[PtX_6^{2-}]^{Total}\}$, E_k representing the limiting chemical shifts for the anion in the two possible environments, *i.e.* δ_{PtX6} and $\delta_{PtX6\text{-}Na\ IP}$, and $[C_k]$ representing the equilibrium concentrations of the species involved. Thus, the SIRKO response function can be used to describe the dependence of the ^{195}Pt chemical shift on the equilibrium concentrations of the free and sodium ion-paired PtX_6^{2-} anions. If values of $\{\delta_{Pt\text{-}195\,obs}\,[PtX_6^{2-}]^{Total}\}$ as well as the analytical concentrations of the reagents for the relevant equilibria (equations (5.6) and (5.21)) are input to SIRKO, together with a value for Q_1 (see Section 5.3.3) and initial estimates of Q_{2X}, δ_{PtX6} and $\delta_{PtX6\text{-}Na\ IP}$, the program may be used to estimate values for the conditional ion-pair formation equilibrium quotient Q_{2X}. SIRKO uses the value for Q_1 and the initial estimate of Q_{2X}, and the analytical concentrations of the reagents, to calculate equilibrium concentrations of the species in the equilibria to be considered (equations (5.6) and (5.21)). It then iteratively refines Q_{2X}, and the parameters δ_{PtX6} and $\delta_{PtX6\text{-}Na\ IP}$, by application of the chosen response function (equation (5.25)), until it finds a 'model' which best fits the experimental data. The results are presented in Table 5.6.

In Table 5.6, the values for the parameters denoted **Fig. 5.2** δ_{PtCl6} and **Fig. 5.2** δ_{PtBr6} in column (2), are chemical shift values obtained from Fig. 5.2 for $PtCl_6^{2-}$ and $PtBr_6^{2-}$, at the halogenoplatinate concentrations reported in Tables 5.12Adm - 5.17Adm Addendum B, in the solvents water, methanol and acetonitrile in the absence of sodium perchlorate. The δ_{PtCl6} and δ_{PtBr6} values in column (6) are chemical shifts for the anions determined by extrapolation of the $\delta_{Pt\text{-}195}$ *vs* $[Na^+]$ data in Tables 5.12Adm - 5.17Adm to zero sodium perchlorate concentration. Corresponding values in columns (2) and (6) compare well, mostly within the estimated error of the chemical shift measurements (± 2 ppm), illustrating that the reproducibility of the measured data is satisfactory. The parameters denoted $\delta_{PtCl6\text{-}Na\ IP}$ and $\delta_{PtBr6\text{-}Na\ IP}$ (column (7)) are chemical shift values for the platinum nucleus in the ion-pairs $\{Na^+[PtCl_6^{2-}]\}^-$ and $\{Na^+[PtBr_6^{2-}]\}^-$,

Stellenbosch University http://scholar.sun.ac.za

Table 5.6 Starting values input to SIRKO, and resultant refined parameters for the formation of $\{Na^+[PtCl_6^{2-}]\}^-$ and $\{Na^+[PtBr_6^{2-}]\}^-$ in water, methanol and acetonitrile.

	Fig. 5.2 δ_{PtCl6} (ppm)	Experimental data Addendum B	Starting values Q_1 (M^{-1})	Q_{2Cl} (M^{-1})	δ_{PtCl6} (ppm)	$\delta_{PtCl6\text{-}Na\ IP}$ (ppm)	Calculated values Q_{2Cl} (M^{-1})	δ_{PtCl6} (ppm)	$\delta_{PtCl6\text{-}Na\ IP}$ (ppm)	*R*-fac (%)
Water	7.8	Table 5.12	0.022	0.022	7.7	0	0.13±0.01	7.8±0.1	12.7±0.1	0.39
Methanol	95.6	Table 5.13	0.167	0.167	92.6	50	0.71±0.14	93.5±1	13.4±6	1.44
Acetonitrile	219.9	Table 5.14	0.327	0.327	214.2	127	1.62±0.33	218.5±1	88.7±9	1.39

	Fig. 5.2 δ_{PtBr6} (ppm)	Experimental data Addendum B	Starting values Q_1 (M^{-1})	Q_{2Br} (M^{-1})	δ_{PtBr6} (ppm)	$\delta_{PtBr6\text{-}NaIP}$ (ppm)	Calculated values Q_{2Br} (M^{-1})	δ_{PtBr6} (ppm)	$\delta_{PtBr6\text{-}NaIP}$ (ppm)	*R*-fac (%)
Water	-0.3	Table 5.15	0.022	0.022	-0.5	"-50"	0.035±0.008	-0.3±0.2	-69±1	8.47
Methanol	113.0	Table 5.16	0.167	0.167	110.9	74	0.48±0.14	111.4±1	34.5±11	0.88
Acetonitrile	251.7	Table 5.17	0.327	0.327	251.7	192	0.16±0.03	252.1±1	-34.3±42	0.19

respectively, in each of the solvents. These values were *estimated* by extrapolation of best-fit trendlines on the relevant $\delta_{Pt\text{-}195}$ *vs* $[Na^+]$ data in Tables 5.12Adm - 5.17Adm. Unfortunately, a starting value for $\delta_{PtBr6\text{-}Na\ IP}$ in water could not be obtained from the $\delta_{Pt\text{-}195}$ *vs* $[Na^+]$ data for this medium; a best-fit Excel trendline for this data predicts increasing upfield shifts for $\delta_{PtBr6\text{-}Na\ IP}$ with increasing $[Na^+]$, and cannot provide a limiting shift value. The value given in Table 5.6 ("-50") was estimated by visual inspection from the available data. Starting values for Q_1 were chosen from the results obtained in Section 5.3.3 with SIRKO, and for *initial estimates* of Q_{2X} it was provisionally assumed that extent of $\{Na^+[PtX_6^{2-}]\}^-$ ion-pairing was comparable to that determined for $\{Na^+[ClO_4^-]\}$ in each of the media.

The *conditional ion-pair formation equilibrium quotients* calculated for the formation of $\{Na^+[PtCl_6^{2-}]\}^-$ in water, methanol and acetonitrile, Q_{2Cl} in column (8), show that ion-pairing occurs in all three solvents, and that the extent of ion-pair formation is greatest in acetonitrile, and least in water, as intuitively expected. The calculated values for δ_{PtCl6} (column (9)) compare well with the corresponding values in columns (2) and (6); the data is well represented at low $[Na^+]$, and this result is to be expected. The calculated values for $\delta_{PtCl6\text{-}Na\ IP}$ are also very reasonable by comparison to the estimated starting values. Fig. 5.9 illustrates the goodness-of-fit of the refined parameters obtained with SIRKO to the experimental data: the variation of $\delta_{Pt\text{-}195}$ with increasing sodium perchlorate concentration observed *experimentally* is shown for

$$Na^+ + [PtCl_6^{2-}] \xleftarrow{Q_{2Cl}} \{Na^+[PtCl_6^{2-}]\}^-$$

$$Na^+ + [PtBr_6^{2-}] \xleftarrow{Q_{2Br}} \{Na^+[PtBr_6^{2-}]\}^-$$

Stellenbosch University http://scholar.sun.ac.za

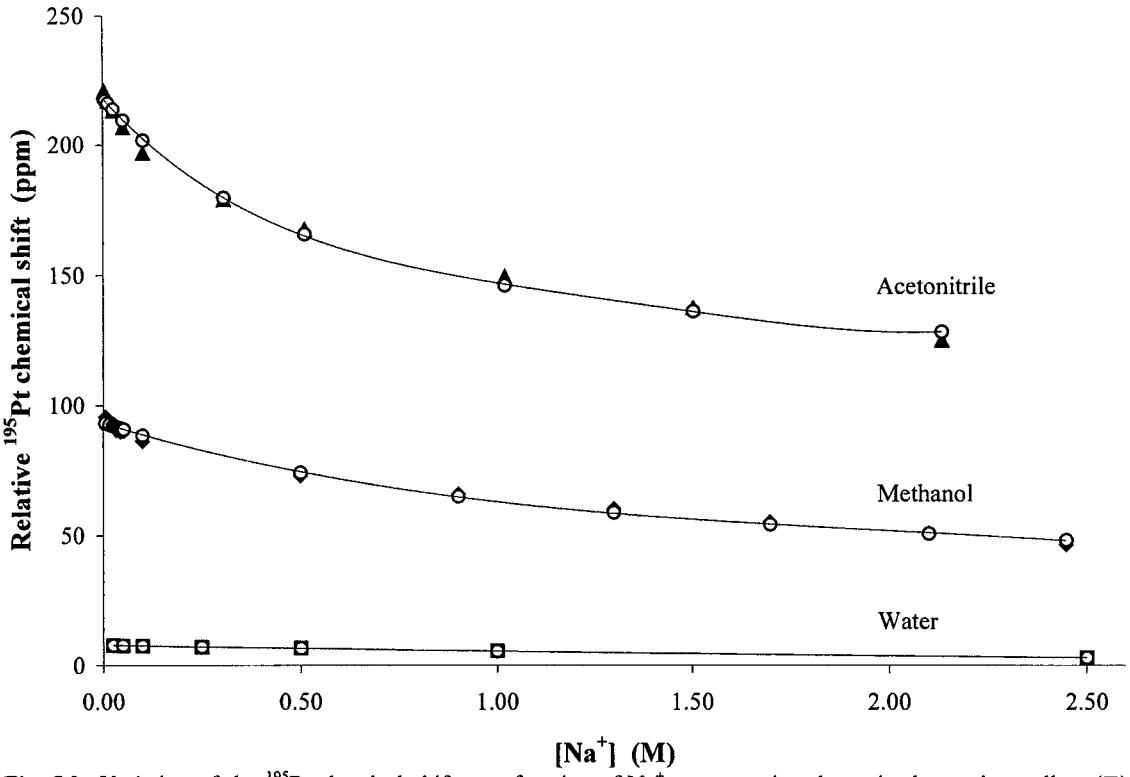

Fig. 5.9 Variation of the ^{195}Pt chemical shift as a function of Na^+ concentration determined experimentally: (■) $H_2PtCl_6 \cdot H_2O$ + $NaClO_4$ in water, (◆) $H_2PtCl_6 \cdot H_2O$ + $NaClO_4$ in methanol, (▲) $H_2PtCl_6 \cdot H_2O$ + $NaClO_4$ in acetonitrile. For each series the *calculated* chemical shifts, based on SIRKO analysis of the data, are shown by O, with best-fit trendlines inserted.

$H_2PtCl_6 \cdot H_2O$ + $NaClO_4$ in water (■), **$H_2PtCl_6 \cdot H_2O$ + $NaClO_4$ in methanol** (◆), and **$H_2PtCl_6 \cdot H_2O$ + $NaClO_4$ in acetonitrile** (▲), together with chemical shifts *calculated* by SIRKO based on its refined parameters; the latter points are shown as O for each series, with best-fit trendlines inserted. The experimental and calculated values are practically identical, and it can thus be accepted that, subject to the constraints of the method being employed, the best-fit parameters have been presented by SIRKO.

SIRKO refinement of the data for **H_2PtBr_6 + $NaClO_4$ in acetonitrile** leads to a value for $\delta_{PtBr6\text{-}Na\ IP}$ (-34.3 ppm, Table 5.6 column (10)) which is considerably smaller than the starting value (192 ppm) estimated by extrapolation of the available $\delta_{Pt\text{-}195}$ *vs* $[Na^+]$ data for acetonitrile; inspection of the experimental data indicates that this calculated value is unreasonable. The calculated Q_{2Br} value presented by SIRKO for the formation of $\{Na^+[PtBr_6^{2-}]\}^-$ in acetonitrile (0.16 M^{-1}, Table 5.6 column (8)) is also smaller than this parameter for the methanol medium (0.48 M^{-1}); based on the calculated Q_{2Cl} values obtained in the three solvents under investigation, one would expect Q_{2Br} for acetonitrile to be larger than Q_{2Br} for methanol. The parameter $\delta_{PtBr6\text{-}Na\ IP}$ was consequently *fixed* at a value of 192 ppm in the refinement for acetonitrile; although this leads to a deterioration in the goodness-of-fit, as indicated by the *R*-factor, the calculated value for Q_{2Br} (1.41 M^{-1}) appears much more reasonable (the *R*-factor still compares well with those for

Stellenbosch University http://scholar.sun.ac.za

refinements in the other media). The final *conditional ion-pair formation equilibrium quotients* calculated by SIRKO for the formation of $\{Na^+[PtBr_6^{2-}]\}^-$ in water (0.035 M^{-1}), methanol (0.48 M^{-1}) and acetonitrile (1.41 M^{-1}), Q_{2Br} in column (8), thus indicate that ion-pairing occurs in all three solvents, and that the extent of ion-pair formation is greatest in acetonitrile, and least in water, as was found for the formation of $\{Na^+[PtCl_6^{2-}]\}^-$ in these solvents. The calculated values for δ_{PtBr6} (column (9)) again compare well with the corresponding values in columns (2) and (6). The *R*-factor for the aqueous medium (8.47 %, column (11)), is larger than the limit of 5 % used to indicate the acceptability of the fit; this large value probably results from the fact that the data predicts increasing upfield shifts for $\delta_{Pt\text{-}195\ obs}$. The calculated chemical shifts, based on the refined SIRKO parameters, are practically identical to the experimental values, and a graphical representation of the goodness-of-fit shows the calculated and experimental points overlayed as in Fig. 5.9 (the fit with $\delta_{PtBr6\text{-}Na\ IP}$ fixed for acetonitrile, is worse than if this parameter is refined, as is indicated by the relevant *R*-factors).

Table 5.7 summarizes the solvent properties relevant to the occurrence of ion-pairing in solution for water, methanol and acetonitrile, together with the SIRKO calculated conditional ion-pair formation equilibrium quotients for the formation of $\{Na^+[ClO_4^-]\}$, $\{Na^+[PtCl_6^{2-}]\}^-$ and $\{Na^+[PtBr_6^{2-}]\}^-$ in these solvents. The decrease in DN^N and *AN* for the solvents in the order water > methanol > acetonitrile, indicates that cations and anions become progressively less well solvated, and suggests that the extent of ion-pairing will increase for the solvents in the order water < methanol < acetonitrile. The estimated *Q* values for $\{Na^+[ClO_4^-]\}$, $\{Na^+[PtCl_6^{2-}]\}^-$ and $\{Na^+[PtBr_6^{2-}]\}^-$ are in accordance with these qualitative predictions. The *Q* values indicate that the extent of ion-pair formation in water, methanol and acetonitrile is greater for both $\{Na^+[PtCl_6^{2-}]\}^-$ and $\{Na^+[PtBr_6^{2-}]\}^-$ than for $\{Na^+[ClO_4^-]\}$. Both $PtCl_6^{2-}$ and $PtBr_6^{2-}$ are larger anions (with radii of 313 pm and 342 pm, respectively) than ClO_4^- (with radius of 240 pm), and as a result are possibly less well solvated, leading to the larger ion-pair formation quotients for these anions. The $PtCl_6^{2-}$ anion is slightly smaller than $PtBr_6^{2-}$, and may thus have a higher charge density, which could favour ion-pair formation for this anion, as indicated by the larger *Q* values for $\{Na^+[PtCl_6^{2-}]\}^-$ in comparison to $\{Na^+[PtBr_6^{2-}]\}^-$.

Table 5.7 Solvent properties relevant to the occurrence of ion-pairing in water, methanol and acetonitrile, and SIRKO calculated conditional ion-pair formation quotients, *Q* (M^{-1}), for the formation of $\{Na^+[ClO_4^-]\}$, $\{Na^+[PtCl_6^{2-}]\}^-$ and $\{Na^+[PtBr_6^{2-}]\}^-$ in these solvents.

	ε	DN^N	*AN*	$\{Na^+[ClO_4^-]\}$ SIRKO *Q* (M^{-1})	$\{Na^+[PtCl_6^{2-}]\}^-$ SIRKO *Q* (M^{-1})	$\{Na^+[PtBr_6^{2-}]\}^-$ SIRKO *Q* (M^{-1})
Water	78.36	0.85	54.8	0.022	0.13	0.035
Methanol	32.66	0.77	41.5	0.167	0.71	0.48
Acetonitrile	35.94	0.36	18.9	0.327	1.62	1.41

Solvent properties were obtained from publications by Marcus.[1,5]

Stellenbosch University http://scholar.sun.ac.za

5.3.7 Estimated conditional thermodynamic quantities $\Delta H°$ and $\Delta S°$ for the contact ion-pair $\{Na^+[PtCl_6^{2-}]\}^-$ in acetonitrile: a determination based on the temperature dependence of the ion-pair formation equilibrium quotient

The investigation has shown that data describing the ^{195}Pt chemical shift dependence on $[Na^+]$ in solutions comprising $PtCl_6^{2-}$, or $PtBr_6^{2-}$, and sodium perchlorate, can be used to calculate sodium-halogenoplatinate ion association quotients, Q, albeit subject to the constraints of the experimental and calculation methods utilized. As a test of the estimated Q values, we have attempted to determine the thermodynamic quantities $\Delta H°$ and $\Delta S°$ for the observed ion-pairing, bearing in mind that the determination will be based on *conditional formation quotients* and not *thermodynamic equilibrium constants*. The well-known Gibbs free energy equation:

$$\Delta G° = \Delta H° - T\Delta S° = -RT \ln K \tag{5.26}$$

may be re-written in the form:

$$\log K = -\frac{\Delta H°}{2.303\,R}\cdot\frac{1}{T} + \frac{\Delta S°}{2.303\,R} \tag{5.27}$$

If the temperature dependence of $\log K$ for an equilibrium can be determined and a plot of $\log K$ *vs* $1/T$ is linear, values of $\Delta H°$ and $\Delta S°$ can be estimated from the gradient and intercept of the line:

$$\Delta H° = -2.303 \times R \times \text{gradient} \tag{5.28}$$

$$\Delta S° = 2.303 \times R \times \text{intercept} \tag{5.29}$$

A duplicate of the series **$H_2PtCl_6 \cdot H_2O$ + $NaClO_4$ in acetonitrile** was prepared (Table 5.19Adm, Addendum B); the solutions in the series were allowed to equilibrate at each of the temperatures 17.0±0.5°C, 40.6±0.5°C, 51.3±0.5°C and 62.1±0.5°C, and after equilibration ^{195}Pt NMR spectra were recorded at the given temperatures. The variation of $\delta_{Pt\text{-}195}$ with $[Na^+]$ for each temperature is shown in Fig. 5.10 (the data previously recorded at 30.0±0.5°C, Table 5.14Adm, has been included). Fig. 5.10 illustrates that the general trend for the dependence of $\delta_{Pt\text{-}195}$ on $[Na^+]$ already observed in Fig. 5.7, is evident even as the temperature of the system changes: significant upfield shift of $\delta_{Pt\text{-}195}$ with increasing cation concentration. It is clear however that as the temperature of the system increases, there is an *overall upfield shift* in the platinum resonance position; the shift change with changing temperature is significant, certainly greater than the accepted error on $\delta_{Pt\text{-}195}$ (±2 ppm). It is known that in general ^{195}Pt chemical shifts are temperature dependent,[58] but since an external reference was consistently used (see Experimental Section), it is reasonable to assume that the observed changes to the platinum resonance position are due to a temperature effect *on the ion-pairing phenomenon*, since the sample and reference solutions were recorded at the same temperature.

Stellenbosch University http://scholar.sun.ac.za

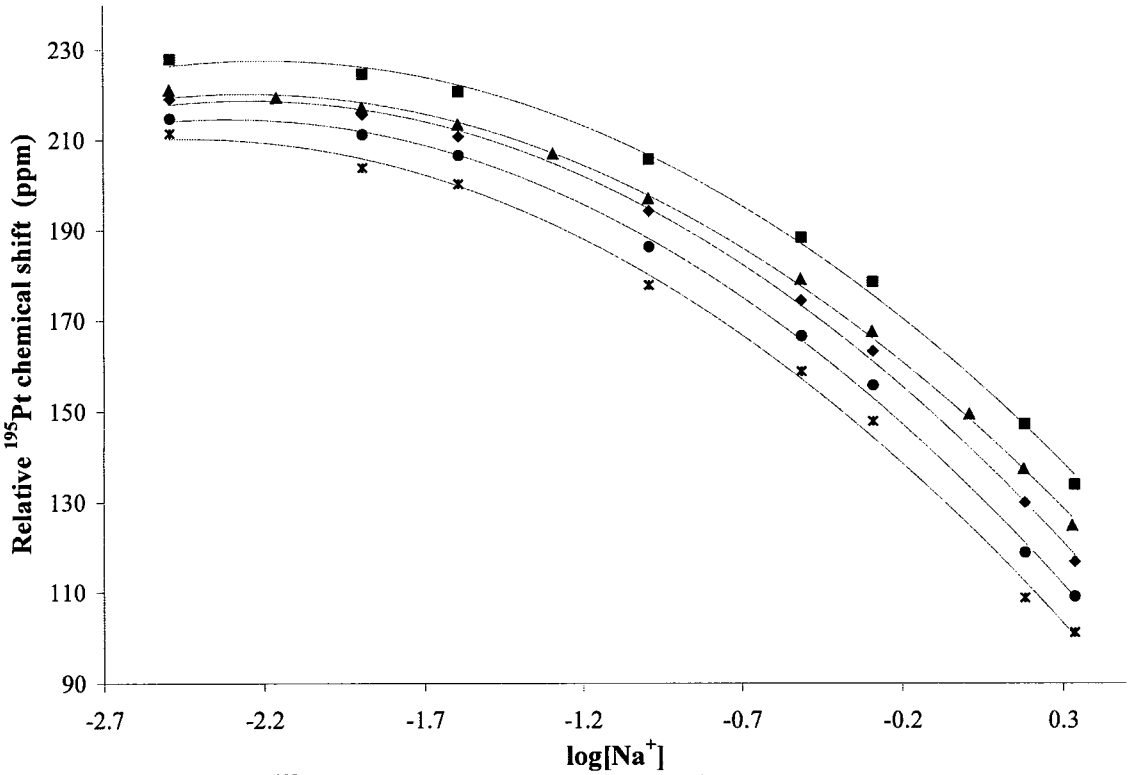

Fig. 5.10 Variation of the ^{195}Pt chemical shift as a function of log[Na^+] for the series $H_2PtCl_6 \cdot H_2O$ + $NaClO_4$ **in acetonitrile** at the temperatures: (■) 17.0±0.5°C, (▲) 30.0±0.5°C, (◆) 40.6±0.5°C, (●) 51.3±0.5°C, and (∗) 62.1±0.5°C. A best Excel trendline has been included for each data set.

The data was analysed using SIRKO, as in Section 5.3.6, with the available data to calculate values of Q_{2Cl} for the formation of $\{Na^+[PtCl_6^{2-}]\}^-$ in acetonitrile (equation (5.30), at the different temperatures.

$$Na^+ + [PtCl_6^{2-}] \xleftrightarrow{Q_{2Cl}} \{Na^+[PtCl_6^{2-}]\}^- \qquad (5.30)$$

These results are presented in Table 5.8. The starting values used were those that were obtained in Section 5.3.6 for Na^+-$PtCl_6^{2-}$ ion-pair formation in acetonitrile, i.e. Q_1 = 0.327 M^{-1}, Q_{2Cl} = 1.62 M^{-1}, δ_{PtCl6} = 219 ppm, and $\delta_{PtCl6\text{-}Na\ IP}$ = 89 ppm. All the refined parameters, Q_{2Cl}, δ_{PtCl6} and $\delta_{PtCl6\text{-}Na\ IP}$, as well as the concomitant *R*-factors appear reasonable. Fig. 5.11 graphically reproduces the temperature dependence of the SIRKO calculated conditional ion association constants (as logarithmic values). Error bars, based on the SIRKO derived errors, are included.

Fig. 5.11 illustrates that the variation of $\log Q_{2Cl}$ with temperature cannot be unambiguously established due to the relatively large errors on the constants. If it is assumed though, for the purpose of discussion, that the indicated values (■) do disclose the nature of the system, it would appear that as the temperature increases the value of Q_{2Cl} increases, suggesting that ion-pair formation becomes *more pronounced* at higher temperatures. This phenomenon is quite possibly related to the temperature dependence of the relative

Stellenbosch University http://scholar.sun.ac.za

Table 5.8 Temperature dependence of Q_{2Cl} for the formation of $\{Na^+[PtCl_6^{2-}]\}^-$ in **acetonitrile**, calculated with SIRKO.

Temperature (K)	Q_{2Cl} (M^{-1})	log Q_{2Cl}	δ_{PtCl6} (ppm)	$\delta_{PtCl6\text{-}Na\ IP}$ (ppm)	*R*-fac (%)
290.15	1.41±0.33	0.15±0.09	225.7±2	91.7±11	1.32
303.05	1.62±0.33	0.21±0.08	218.5±1	88.7±9	1.39
313.75	1.58±0.33	0.20±0.08	216.8±2	76.1±10	1.43
324.45	1.78±0.36	0.25±0.08	212.6±2	70.4±10	1.74
335.25	1.95±0.50	0.29±0.10	207.1±3	64.2±12	2.30

permitivity (ε) of the solvent. Marcus points out that such a temperature dependence is generally *negative*, due to increased thermal randomization and considerable decreased cooperativity between solvent dipoles as the temperature increases.[5] According to Marcus $d \ln\varepsilon / dT = -4.16\times10^{-3}\ K^{-1}$ for acetonitrile, i.e. a decrease of one unit in the relative permitivity for every Kelvin that the temperature increases.[5] This indicates that over the temperature range studied (17.0°C-62.1°C) there is a considerable decrease in the relative permitivity of the solvent (acetonitrile) with increasing temperature, which is consistent with the more pronounced ion-pair formation observed, despite the large relative errors obtained.

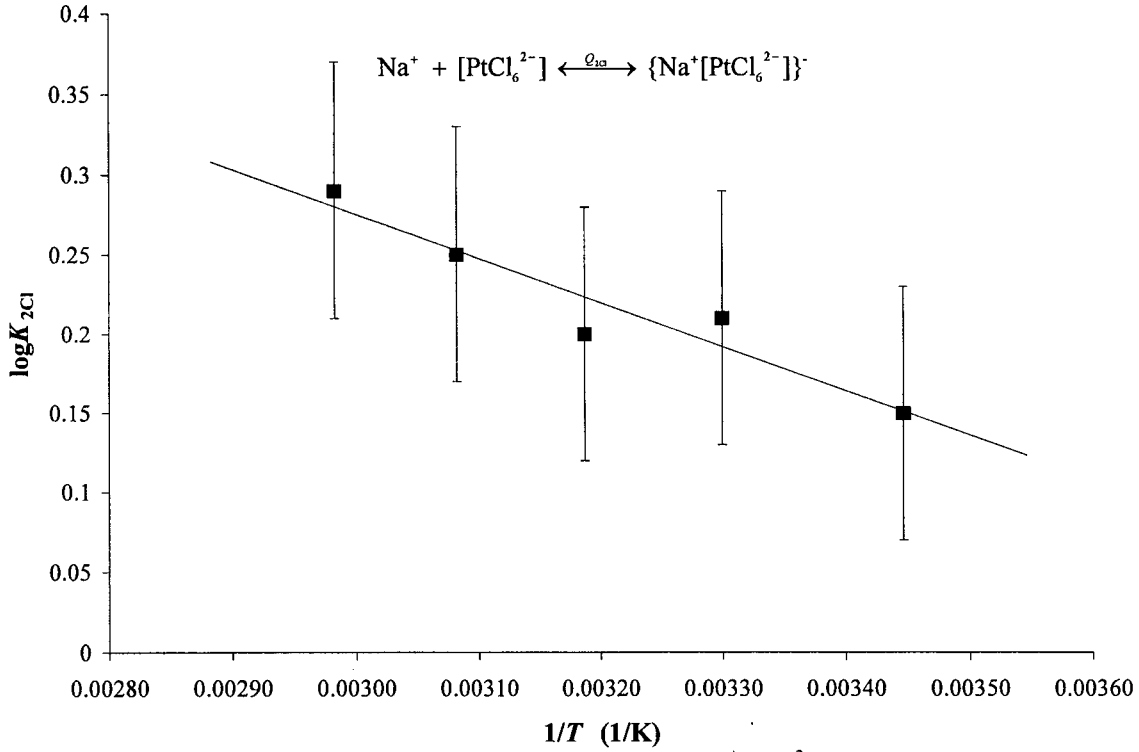

Fig. 5.11 Temperature dependence of $\log K_{2Cl}$ for the formation of $\{Na^+[PtCl_6^{2-}]\}^-$ in acetonitrile. Error bars are included as well as a best fit straight line.

Stellenbosch University http://scholar.sun.ac.za

Assuming that the straight line that has been fit to the data in Fig. 5.11 correctly characterizes the system, the gradient (-278.5) and intercept (1.111) can be used to estimate values of $\Delta H°$ (equation (5.28)) and $\Delta S°$ (equation (5.29)) for equilibrium (5.30): $\Delta H°$ = 5.3kJ mol^{-1} and $\Delta S°$ = 21.3 J K^{-1} mol^{-1}. These parameters indicate that the formation of $\{Na^+[PtCl_6^{2-}]\}^-$ in acetonitrile is an entropy-driven process. This is not an unreasonable result considering that the release of solvent molecules from the solvation shells of the ions that pair increases the number of particles in solution. Marcus reports that the standard molar entropy change on the formation of a contact ion-pair *is* positive.[1] Furthermore, a low $\Delta H°$ value is to be expected for the relatively "weak" ion-pairing interactions in the present study.

5.3.8 Effect of the addition of crown ethers (15-crown-5 and 18-crown-6) to solutions in which sodium ion-pairing occurs

The ability of crown ethers, such as 18-crown-6 and 15-crown-5, to strongly complex with alkali metal ions has been known for several decades, and the phenomenon is well-studied;[59-61] log*K* values for the formation of the $\{Na^+[18\text{-crown-6}]\}$ and $\{Na^+[15\text{-crown-5}]\}$ complexes in methanol have been determined to be 4.36 and 3.14, respectively, and for the formation of these complexes in acetonitrile, log*K* values of 4.8 and 4.9, respectively, have been determined.[62] Our results show that $\{Na^+[ClO_4^-]\}$, $\{Na^+[PtCl_6^{2-}]\}^-$ and $\{Na^+[PtBr_6^{2-}]\}^-$ contact ion-pairs form in methanol and acetonitrile solutions, with increasing sodium ion concentration. It was of interest to determine the effect that the addition of a strong sodium ion complexing agent, such as a 15-crown-5 or 18-crown-6, would have on the formation of these ion pairs; such competitive titrations are expected to corroborate the formation of $\{Na^+[PtX_6^{2-}]\}^-$ (X = Cl, Br) ion-pairs in solution.

Various samples were thus prepared as before, and appropriate quantities of either 18-crown-6 or 15-crown-5 were added to the solutions. Although the 18-crown-6 could be added to relatively high concentrations in methanol solutions containing the relevant components, it was not possible to repeat the experiments with 15-crown-5 due to rapid precipitate formation on addition of the crown ether. 18-crown-6 and 15-crown-5 could be added to acetonitrile solutions containing the components of interest, but only to limited concentrations of the crown ether, again as a result of precipitate formation at higher concentrations.

The solutions **$NaClO_4$ + 18-crown-6 in methanol**, **$H_2PtCl_6 \cdot H_2O$ + $NaClO_4$ + 18-crown-6 in methanol**, **$H_2PtCl_6 \cdot H_2O$ + $NaClO_4$ + 18-crown-6 in acetonitrile**, and **$H_2PtCl_6 \cdot H_2O$ + $NaClO_4$ + 15-crown-5 in acetonitrile**, were prepared such that the ratio crown ether : Na^+ was varied. Details of solution preparation, and the observed ^{23}Na and ^{195}Pt chemical shifts are given in Tables 5.20Adm - 5.22Adm in Addendum B; results are graphically presented in Figures 5.12 - 5.14.

Stellenbosch University http://scholar.sun.ac.za

Fig. 5.12 shows the $\delta_{Na\text{-}23}$ *vs* log[Na^+] data for the solutions **$NaClO_4$ in methanol** (∗) as well as the data for **$H_2PtCl_6{\cdot}H_2O$ + $NaClO_4$ in methanol** (◆), as shown in Fig. 5.5. On addition of 18-crown-6 to solutions of $NaClO_4$ in methanol, at a ratio Na^+ : crown ether of 1 : 1, the ^{23}Na resonance positions shift significantly more upfield (×, Fig. 5.12; **$NaClO_4$ + 18-crown-6 in methanol** – Na^+ : 18-c-6 at 1 : 1), and vary only slightly, by *ca.* 19 Hz, with increasing [Na^+] for these solutions, indicating that all Na^+ ions are most likely *complexed by the added crown ether*. This is to be expected considering the large value of the association constant for formation of the {Na^+[18-crown-6]} complex in methanol (log$K$ = 4.36 [62]).

If 18-crown-6 is added to solutions of $NaClO_4$ in methanol at a ratio Na^+ : crown ether of 2 : 1, the observed ^{23}Na chemical shifts (+, Fig. 5.12; **$NaClO_4$ + 18-crown-6 in methanol** – Na^+ : 18-c-6 at 2 : 1) lie approximately midway between data points for solutions **$NaClO_4$ in methanol** (∗) and **$NaClO_4$ + 18-crown-6 in methanol** – Na^+ : 18-c-6 at 1 : 1 (×). Only about half of all sodium ions are complexed by the added crown ether, largely precluding these ions from Na^+-ClO_4^- association, and resulting in the chemical shift distribution (+) approximately halfway between distributions for solutions in which no Na^+ ions are complexed (∗) and solutions in which all the cations are complexed by the crown ether (×). The remaining cations are either free or ClO_4^- ion-paired, thus resulting in a $\delta_{Na\text{-}23}$ *vs* log[Na^+] *trend* similar to that observed for the **$NaClO_4$ in methanol** series (∗), i.e. an upfield shift of $\delta_{Na\text{-}23}$ with increasing [Na^+].

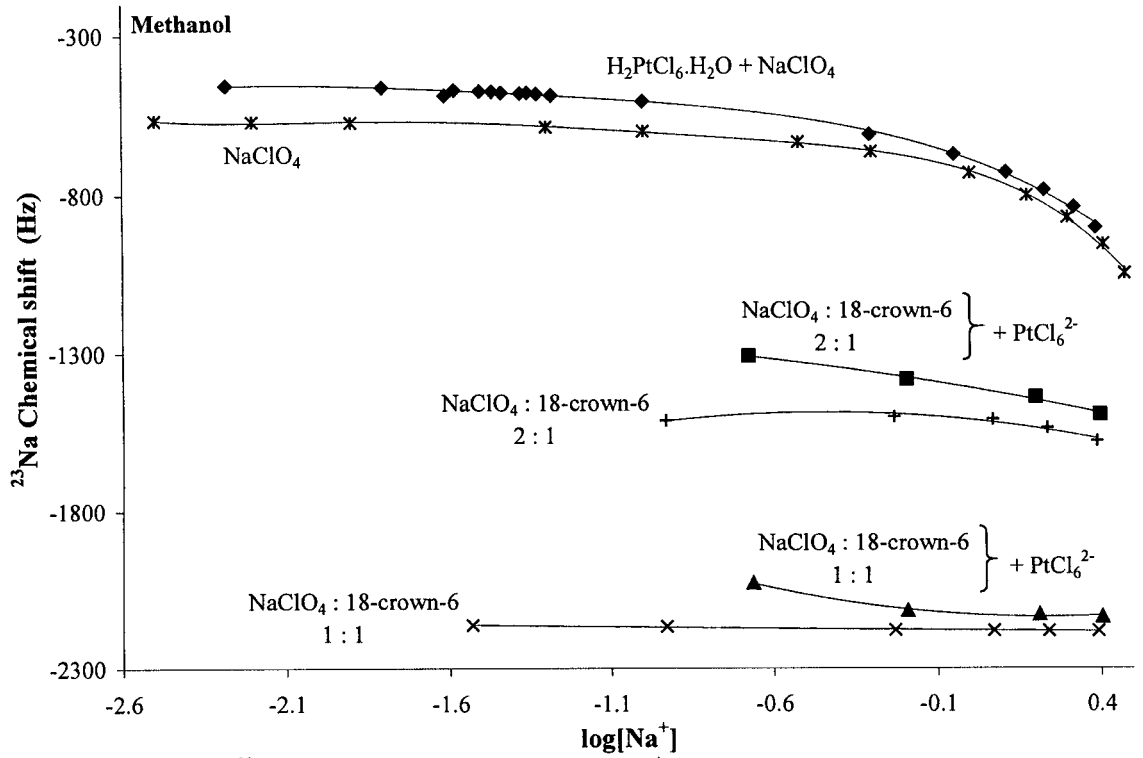

Fig. 5.12 Variation of ^{23}Na chemical shift as a function of log[Na^+]: (∗) $NaClO_4$ in methanol, (◆) $H_2PtCl_6{\cdot}H_2O$ + $NaClO_4$ in methanol, (×) $NaClO_4$ + 18-crown-6 in methanol (ratio Na^+ : crown ether at 1 : 1), (+) $NaClO_4$ + 18-crown-6 in methanol (ratio Na^+ : crown ether at 2 : 1), (▲) $H_2PtCl_6{\cdot}H_2O$ + $NaClO_4$ + 18-crown-6 in methanol (ratio Na^+ : crown ether at 1 : 1), (■) $H_2PtCl_6{\cdot}H_2O$ + $NaClO_4$ + 18-crown-6 in methanol (ratio Na^+ : crown ether at 2 : 1). Best fit Excel trendlines have been drawn for each series.

Stellenbosch University http://scholar.sun.ac.za

The data for solutions **$NaClO_4$ + 18-crown-6 in methanol** – Na^+ : 18-c-6 at 1 : 1, indicate that the addition of the crown ether excludes significant $\{Na^+[ClO_4^-]\}$ formation, and thus it might be expected that the addition of a crown ether to solutions in which the formation of, for example, $\{Na^+[PtCl_6^{2-}]\}^-$ had previously been observed, would also prevent Na^+-$PtCl_6^{2-}$ association. Fig. 5.12 reveals however that the data for **$H_2PtCl_6 \cdot H_2O$ + $NaClO_4$ + 18-crown-6 in methanol** – Na^+ : 18-c-6 at 1 : 1 (▲), or 1 : 2 (■) lie to *lower field* of that for corresponding solutions without the hexachloroplatinate anion (× and +, respectively). Considering that the downfield appearance of ^{23}Na resonances for solutions **$H_2PtCl_6 \cdot H_2O$ + $NaClO_4$ in methanol** (◆) relative to those for solutions **$NaClO_4$ in methanol** (∗) was interpreted as indicative of $\{Na^+[PtCl_6^{2-}]\}^-$ contact ion-pair formation (Section 5.3.4), the downfield appearance of data for solutions **$H_2PtCl_6 \cdot H_2O$ + $NaClO_4$ + 18-crown-6 in methanol** – Na^+ : 18-c-6 at 1 : 1 (▲), or 1 : 2 (■), suggests Na^+-$PtCl_6^{2-}$ association in methanol, *despite complexation of the cation by the crown ether*. This conclusion was corroborated with the ^{195}Pt NMR data for the **$H_2PtCl_6 \cdot H_2O$ + $NaClO_4$ + 18-crown-6 in methanol** samples, shown in Fig. 5.13.

In the previous analysis (Section 5.3.5) we found that the observed ^{195}Pt chemical shifts for $H_2PtCl_6 \cdot H_2O$ + $NaClO_4$ in methanol solutions may be expressed by equation (5.20):

$$\delta_{Pt\text{-}195\,obs} = X_{PtX6}\delta_{PtX6} + X_{PtX6\text{-}Na\,IP}\delta_{PtX6\text{-}Na\,IP} \qquad (5.20)$$

If the complexation of the Na^+ ions in solution by an added crown ether (with Na^+ : crown ether at 1 : 1)

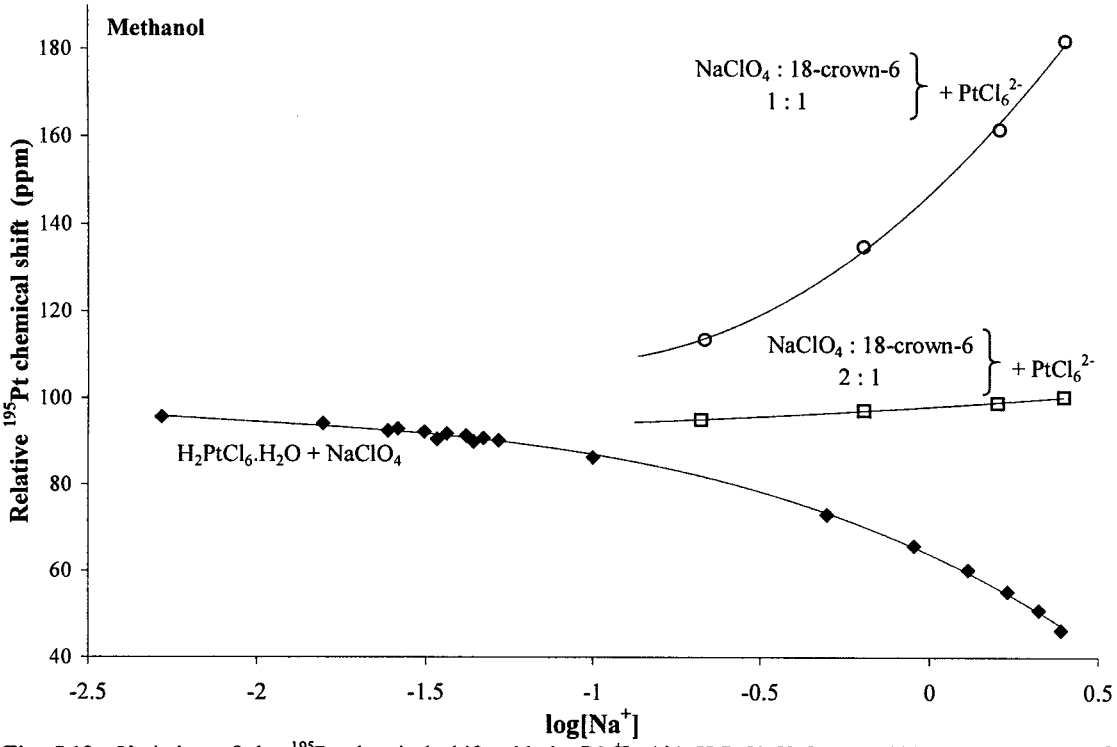

Fig. 5.13 Variation of the ^{195}Pt chemical shift with log[Na^+]: (◆) $H_2PtCl_6 \cdot H_2O$ + $NaClO_4$ in methanol, (○) $H_2PtCl_6 \cdot H_2O$ + $NaClO_4$ + 18-crown-6 in methanol (ratio Na^+ : crown ether at 1 : 1), (□) $H_2PtCl_6 \cdot H_2O$ + $NaClO_4$ + 18-crown-6 in methanol (ratio Na^+ : crown ether at 2 : 1). Best fit Excel trendlines have been drawn for each series.

Stellenbosch University http://scholar.sun.ac.za

were to effectively prohibit the association of the cation with $PtCl_6^{2-}$ in methanol, one would expect $\delta_{Pt\text{-}195}$ to present a linear *and unvarying* distribution at $\delta_{Pt\text{-}195} \approx 95$ ppm, i.e. the ^{195}Pt chemical shift at $[Na^+] = 0$ M in methanol, over the log$[Na^+]$ range -2.2 – 0.4; $\delta_{Pt\text{-}195}$ would be determined only by $\{X_{PtCl6}\delta_{PtCl6}\}$ in equation (5.20). The $\delta_{Pt\text{-}195}$ *vs* log$[Na^+]$ data for the solutions **$H_2PtCl_6{\cdot}H_2O$ + $NaClO_4$ + 18-crown-6 in methanol** – Na^+ : 18-c-6 at 1 : 1 (O, Fig. 5.13) however shows a marked *downfield* shift of the ^{195}Pt resonance position with increasing log$[Na^+]$. Moreover, if the ratio Na^+ : crown ether is 2 : 1, i.e. only half the Na^+ ions are complexed by the 18-crown-6, the observed $\delta_{Pt\text{-}195}$ *vs* log$[Na^+]$ data lies approximately *midway* (□, Fig. 5.13) between that for the solutions **$H_2PtCl_6{\cdot}H_2O$ + $NaClO_4$ in methanol** (◆, reproduced from Fig. 5.7) and for solutions **$H_2PtCl_6{\cdot}H_2O$ + $NaClO_4$ + 18-crown-6 in methanol** – Na^+ : 18-c-6 at 1 : 1 (O, Fig. 5.13). It appears from this data, as was the conclusion from the data in Fig. 5.12, that *Na^+-$PtCl_6^{2-}$ association persists in methanol even in samples where the cation is complexed to a crown ether.*

This phenomenon however appears to be solvent dependent. Fig. 5.14 reproduces the $\delta_{Pt\text{-}195}$ *vs* log$[Na^+]$ data for solutions **$H_2PtCl_6{\cdot}H_2O$ + $NaClO_4$ in acetonitrile**, as shown in Fig. 5.7 (▲), together with the data for solutions **$H_2PtCl_6{\cdot}H_2O$ + $NaClO_4$ + 18-crown-6 in acetonitrile** – Na^+ : 18-c-6 at 2 : 1 (□, Fig. 5.14), and **$H_2PtCl_6{\cdot}H_2O$ + $NaClO_4$ + 15-crown-5 in acetonitrile** – Na^+ : 15-c-5 at 2 : 1 (◇, Fig. 5.14). If the complexation of Na^+ ions in solution by an added crown ether *were to exclude $\{Na^+[PtCl_6^{2-}]\}^-$ formation in*

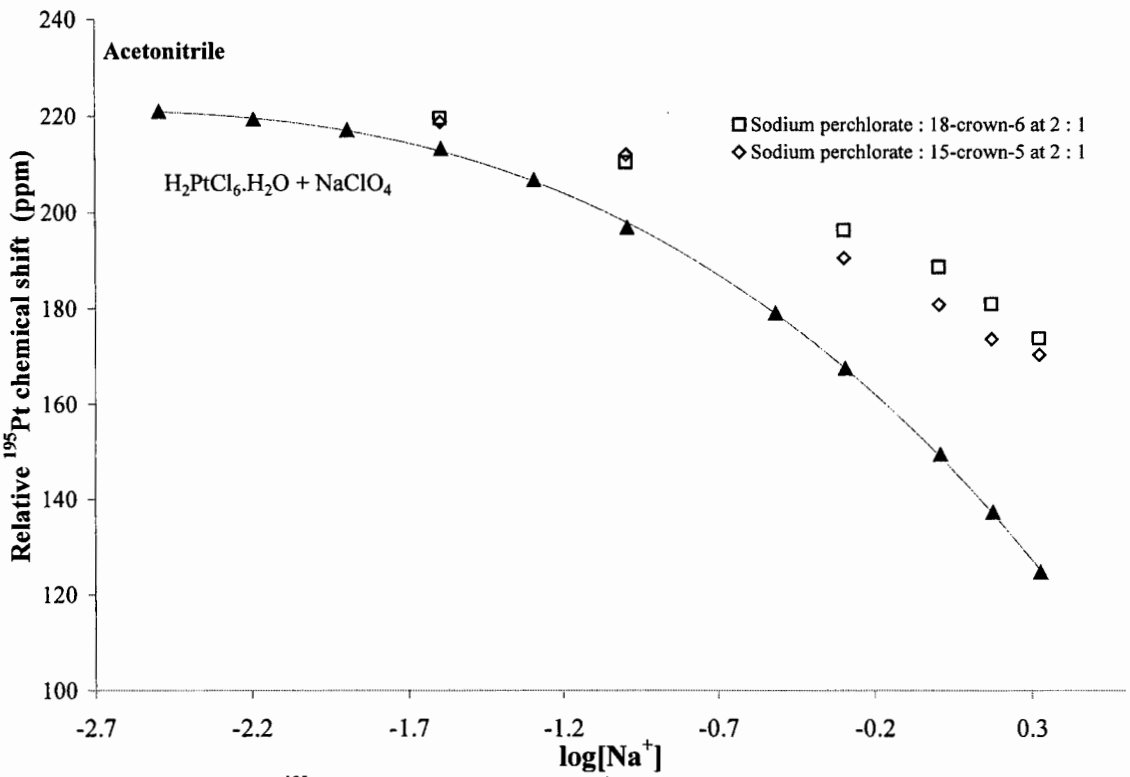

Fig. 5.14 Variation of the ^{195}Pt chemical shift with log$[Na^+]$: (▲) $H_2PtCl_6{\cdot}H_2O$ + $NaClO_4$ in acetonitrile, (□) $H_2PtCl_6{\cdot}H_2O$ + $NaClO_4$ + 18-crown-6 in acetonitrile (ratio Na^+ : crown ether at 2 : 1), (◇) $H_2PtCl_6{\cdot}H_2O$ + $NaClO_4$ + 15-crown-5 in acetonitrile (ratio Na^+ : crown ether at 2 : 1).

Stellenbosch University http://scholar.sun.ac.za

acetonitrile, one would expect, with a Na^+ : crown ether ratio of 1 : 1, $\delta_{Pt\text{-}195}$ to present a linear distribution at $\delta_{Pt\text{-}195} \approx 220$ ppm over the log[Na^+] range -2.2 – 0.4; at a Na^+ : crown ether ratio of 1 : 2, the $\delta_{Pt\text{-}195}$ *vs* log[Na^+] data should lie midway between this fairly linear distribution and the distribution for the solutions **$H_2PtCl_6 \cdot H_2O$ + $NaClO_4$ in acetonitrile**. The $\delta_{Pt\text{-}195}$ *vs* log[Na^+] data for **$H_2PtCl_6 \cdot H_2O$ + $NaClO_4$ + 18-crown-6 in acetonitrile** – Na^+ : 18-c-6 at 2 : 1 (□, Fig. 5.14) and **$H_2PtCl_6 \cdot H_2O$ + $NaClO_4$ + 15-crown-5 in acetonitrile** – Na^+ : 15-c-5 at 2 : 1 (◇, Fig. 5.14) do appear to lie halfway between $\delta_{Pt\text{-}195} \approx 220$ ppm and the distribution for **$H_2PtCl_6 \cdot H_2O$ + $NaClO_4$ in acetonitrile**; the prominent downfield shift observed in methanol under comparable experimental conditions, is not evident. This suggests that in acetonitrile the complexation of Na^+ by an added crown ether *does prohibit the association of such a sodium cation with* $PtCl_6^{2-}$.

5.4 Concluding Remarks

Significant variations of the ^{195}Pt NMR chemical shift for methanol and acetonitrile solutions of PtX_6^{2-} (X = Cl, Br) with increasing $NaClO_4$ concentrations are observed. The non-linear shift trends are indicative of $\{Na^+[PtX_6^{2-}]\}^-$ (X = Cl, Br) *contact ion-pair formation* in these solutions, and illustrate that ^{195}Pt NMR is a very sensitive monitor for $Na^+ \cdots PtX_6^{2-}$ ion association in non-aqueous solutions. By contrast, the variation of $\delta_{Pt\text{-}195}$ for aqueous solutions of the halogenoplatinate anions with increasing sodium perchlorate concentration is slight, revealing that $Na^+ \cdots PtX_6^{2-}$ ion association is not favoured in the higher dielectric aqueous medium. These observations are corroborated by ^{23}Na NMR chemical shift measurements of the solutions. *Conditional ion-pair formation equilibrium quotients*, Q (M^{-1}), for the $\{Na^+[PtCl_6^{2-}]\}^-$ and $\{Na^+[PtBr_6^{2-}]\}^-$ contact ion-pairs in water, methanol and acetonitrile can be estimated by analyzing the $NaClO_4$-concentration dependence of $\delta_{Pt\text{-}195}$ for the anions in each solvent, using the program SIRKO. For $\{Na^+[PtCl_6^{2-}]\}^-$ the quotients $Q_{water} = 0.13 \pm 0.01$ M^{-1}, $Q_{methanol} = 0.71 \pm 0.14$ M^{-1} and $Q_{acetonitrile} = 1.62 \pm 0.0.33$ M^{-1}, and for $\{Na^+[PtBr_6^{2-}]\}^-$ values of $Q_{water} = 0.035 \pm 0.008$ M^{-1}, $Q_{methanol} = 0.48 \pm 0.14$ M^{-1} and $Q_{acetonitrile} = 1.41 \pm 0.0.28$ M^{-1}, reveal that the extent of ion-pairing *increases* for both contact ion-pairs for solvents in the order water < methanol < acetonitrile. This is in accordance with a *decrease* in the cation and anion solvating powers of the solvents, as reflected by the normalized Donor Numbers (DN^N) and the Acceptor Numbers (AN) for water, methanol and acetonitrile. The magnitudes of estimated changes in enthalpy and entropy for the formation of $\{Na^+[PtCl_6^{2-}]\}^-$ in acetonitrile, based on the temperature dependence of Q, are reasonable, and underscore the usefulness of ^{195}Pt NMR for studying the occurrence of ion-pairing in non-aqueous solvents. The addition of 18-crown-6 to acetonitrile solutions containing $PtCl_6^{2-}$ and Na^+ prevents the formation of $\{Na^+[PtCl_6^{2-}]\}^-$, due to complexation of the cation by the crown ether. In methanol, however, $Na^+ \cdots PtCl_6^{2-}$ interactions appear to *persist* with the addition of 18-crown-6.

Stellenbosch University http://scholar.sun.ac.za

References

1 Y. Marcus, in *Ion Solvation*, Wiley-Interscience, Chichester, 1985.
2 N. Bjerrum, *Kgl. Danske Videnskab Selskab*, 1926, **7**, 3.
3 A. Macchioni, *Chemical Reviews*, 2005, **105**, 2039.
4 U. Mayer, *Coordination Chemistry Reviews*, 1976, **21**, 159.
5 Y. Marcus, in *The Properties of Solvents*, John Wiley and Sons, Ltd, Chichester, 1999.
6 J. Hormadaly and Y. Marcus, *Journal of Physical Chemistry*, 1979, **83**, 2843.
7 Y. Marcus, E. Pross and J. Hormadaly, *Journal of Physical Chemistry*, 1980, **84**, 2708.
8 V. Gutmann, in *Coordination chemistry in non-aqueous solutions.*, Springer-Verlag, Vienna (Austria), 1968.
9 Y. Marcus, in *Ion Properties*, Marcel Dekker, Inc., New York, 1997.
10 U. Mayer, V. Gutmann and W. Gerger, *Monatschefte fur Chemie*, 1975, **106**, 1265.
11 A. I. Popov, *Pure and Applied Chemistry*, 1975, **41**, 275.
12 U. Mayer, *Pure and Applied Chemistry*, 1975, **41**, 291.
13 R. H. Erlich, E. Roach and A. I. Popov, *Journal of the American Chemical Society*, 1970, **92**, 4989.
14 R. H. Erlich and A. I. Popov, *Journal of the American Chemical Society*, 1971, **93**, 5620.
15 M. Herlem and A. I. Popov, *Journal of the American Chemical Society*, 1972, **94**, 1431.
16 M. S. Greenberg, D. S. Wied and A. I. Popov, *Spectrochimica Acta*, 1973, **29A**, 1927.
17 M. S. Greenberg, R. L. Bodner and A. I. Popov, *Journal of Physical Chemistry*, 1973, **77**, 2449.
18 M. S. Greenberg and A. I. Popov, *Journal of Solution Chemistry*, 1976, **5**, 653.
19 W. J. deWitte and A. I. Popov, *Journal of Solution Chemistry*, 1976, **5**, 231.
20 L.-L. Soong, G. E. Leroi and A. I. Popov, *Journal of Solution Chemistry*, 1989, **18**, 561.
21 J. Burgess, in *Metal ions in solution.*, Ellis Horwood Limited, Chichester, 1978.
22 A. Lienke, G. Klatt, D. J. Robinson, K. R. Koch and K. J. Naidoo, *Inorganic Chemistry*, 2001, **40**, 2352.
23 K. J. Naidoo, G. Klatt, K. R. Koch and D. J. Robinson, *Inorganic Chemistry*, 2002, **41**, 1845.
24 K. J. Naidoo, A. S. Lopis, A. N. Westra, D. J. Robinson and K. R. Koch, *Journal of the American Chemical Society.*, 2003, **125**, 13330.
25 H. Gunter, in *NMR Spectroscopy*, John Wiley & Sons, 1980.
26 D. H. Live and S. I. Chan, *Analytical Chemistry*, 1970, **42**, 791.
27 G. J. Templeman and A. L. van Geet, *Journal of the American Chemical Society*, 1972, **94**, 5578.
28 *CRC Handbook of Chemistry and Physics*, CRC Press, Boca Raton, Fla., 85th, 2004-2005.
29 E. G. Bloor and R. G. Kidd, *Canadian Journal of Chemistry*, 1968, **46**, 3425.
30 A. L. van Geet, *Journal of the American Chemical Society*, 1972, **94**, 5583.
31 R. H. Erlich, M. S. Greenberg and A. I. Popov, *Spectrochimica Acta*, 1973, **29A**, 543.
32 M. S. Greenberg and A. I. Popov, *Spectrochimica Acta*, 1975, **31A**, 697.
33 A. G. Miller and J. W. Macklin, *Journal of Physical Chemistry*, 1985, **89**, 1193.
34 W. Geffeken, *Zeitschrift fur Physikalische Chemie, Abteilung B*, 1929, **5**, 118.
35 M. M. Jones, E. A. Jones, D. F. Harmon and R. T. Semmes, *Journal of the American Chemical Society*, 1961, **83**, 2038.
36 R. E. Hester and R. A. Plane, *Inorganic Chemistry*, 1964, **3**, 769.
37 M. I. S. Sastry and S. Singh, *Canadian Journal of Chemistry*, 1985, **63**, 1351.
38 H. A. Berman and T. R. Stengle, *Journal of Physical Chemistry*, 1975, **79**, 1001.
39 A. D'Aprano, *The Journal of Physical Chemistry*, 1971, **75**, 3290.
40 R. L. Frost, D. W. James, R. Appleby and R. E. Mayes, *Journal of Physical Chemistry*, 1982, **86**, 384.
41 A. G. Miller, J. A. Franz and J. W. Macklin, *Journal of Physical Chemistry*, 1985, **89**, 1190.
42 A. D'Aprano, *Journal of Physical Chemistry*, 1972, **76**, 2920.
43 S. Minc and L. Werblan, *Electrochimica Acta*, 1962, **7**, 257.
44 R. L. Kay, B. J. Hales and G. P. Cunningham, *Journal of Physical Chemistry*, 1967, **71**, 3925.
45 A. D'Aprano and R. Triolo, *Journal of Physical Chemistry*, 1967, **71**, 3474.
46 W. R. Fawcett, G. Liu, P. W. Faguy, C. A. Foss Jr and A. J. Motheo, *Journal of the Chemical Society, Faraday Transactions*, 1993, **89**, 811.
47 M. Chabanel, D. Legoff and K. Thouaj, *Journal of the Chemical Society, Faraday Transactions*, 1996, **92**, 4199.

Stellenbosch University http://scholar.sun.ac.za

48 J.-S. Seo, B.-S. Cheong and H.-G. Cho, *Spectrochimica Acta, Part A: Molecular and Biomolecular Spectroscopy*, 2002, **58A**, 1747.
49 J. Scientific, SigmaPlot for Windows, Version 1.01, San Rafael, CA, 1993.
50 M. B. Charland, in *SigmaPlot for Scientists*, Wm. C. Brown Communications, Inc., Dubuque, Iowa, 1995.
51 V. I. Vetrogon, N. G. Lukanenko, M.-J. Schwing-Weill and F. Arnaud-Neu, *Talanta*, 1994, **41**, 2105.
52 D. W. Marquardt, *Journal of the Society of Industrial and Applied Mathematics*, 1963, **11**, 431.
53 K. A. Levenberg, 1994, **2**, 164.
54 G. Ibrahim, G. M. Bouet, I. H. Hall and M. A. Khan, *Journal of Inorganic Biochemistry*, 2000, **81**, 29.
55 L. Johansson, *Coordination Chemistry Reviews*, 1974, **12**, 241.
56 J. J. Pesek and W. R. Mason, *Journal of Magnetic Resonance*, 1977, **25**, 519.
57 P. S. Pregosin, *Coordination Chemistry Reviews*, 1982, **44**, 247.
58 S. M. Cohen and T. H. Brown, *Journal of Chemical Physics*, 1974, **61**, 2985.
59 J. D. Lamb, R. M. Izatt, J. J. Christensen and D. J. Eatough, in *Coordination Chemistry of Macrocyclic Compounds*, Plenum Press, New York, 1979.
60 C. J. Pedersen, *Journal of the American Chemical Society*, 1967, **89**, 2495.
61 C. J. Pedersen, *Journal of the American Chemical Society*, 1967, **89**, 7017.
62 R. M. Izatt, J. S. Bradshaw, S. A. Nielsen, J. D. Lamb, J. J. Christensen and D. Sen, *Chemical Reviews*, 1985, **85**, 271-339; and references cited therein.

Stellenbosch University http://scholar.sun.ac.za

Chapter 6

Conclusions

Stellenbosch University http://scholar.sun.ac.za

The oxidative addition of elemental dihalogens to Pt(II) complexes of monopodal or bipodal *S,O*-donating aroylthioureas, has been shown to be a highly effective method for synthesizing the corresponding Pt(IV) compounds. ^{195}Pt NMR reveals that the oxidative addition is rapid and quantitative in solvents such as chloroform at room temperature. The number and relative distribution of the Pt(IV) oxidative addition products can be determined, and in the case of platinum metallamacrocycles, the technique reveals the formation, during the oxidative addition reaction, of mixed-valence Pt(II)/Pt(IV) complexes in solution. Although direct addition of I_2, Br_2 or Cl_2 does not always lead to the isolation of the desired Pt(IV) complex, the application of a simple glass electrolytic cell containing an appropriate Pt(II) precursor and halide salt, in which the halogen oxidants are produced *in situ* at the anode, has been shown to be a very successful alternative route of synthesis. This work reports on the use of electrolytic oxidative addition for the synthesis of only the 2 : 2 *trans*-Pt(IV)-bromo and -chloro metallamacrocycles of 3,3,3',3'-tetraethyl-1,1'-isophthaloylbis(thiourea), but preliminary investigations suggest that the method may also lead to the successful preparation and isolation of the, as yet elusive, 3 : 3 *trans*-Pt-X (X = I, Br, Cl) metallamacrocycles of 3,3,3',3'-tetra(*n*-butyl)-1,1'-terephthaloylbis(thiourea), as well as the *trans*-Pt(IV)-chloro analogues of the monopodal aroylthioureas.

Interestingly, direct treatment of a Pt(II) complex with I_2 does not necessarily lead to oxidative addition of the halogen. Whereas the Pt(II) complexes of the *N,N*-dialkyl-*N'*-benzoylthioureas undergo facile oxidative addition upon reaction with diiodine, similar treatment of *trans*-bis(*N*-benzoyl-*N'*-propylthiourea-κS)diiodoplatinum(II) leads to inclusion of the halogen in the lattice with the *trans*-Pt(II) complex upon crystallization. This suggests that the Pt(II) complexes of the *N,N*-dialkyl-*N'*-benzoylthioureas and the *N*-alkyl-*N'*-benzoylthioureas have distinctly different electrochemical properties. Moreover, the formation of the inclusion compound highlights the potential application of both the Pt(II) and Pt(IV) complexes of the aroylthioureas as building blocks for further assembly into higher order structures, and in novel host-guest phenomena; the Pt(II/IV)-iodo complexes in the present investigation have shown a particular propensity to undergo intermolecular I···I interactions in the solid state.

The investigations described in this thesis have relied heavily on the application of ^{195}Pt NMR chemical shifts as a tool to characterize not only the nature of platinum(II/IV) compounds themselves, but also the nature of the environment directly around halogenoplatinate(IV) complexes. The sensitivity of the platinum nucleus to changes in the solvation spheres of $PtCl_6^{2-}$ and $PtBr_6^{2-}$, results in remarkable variations of $\delta_{Pt\text{-}195}$ for the anions in different solvents, as well as in mixed solvent systems. The variations observed in binary solvent mixtures allow qualitative deductions regarding the 'preference' of the anions toward the component solvents in the mixture; the data reveals that the anions are preferentially solvated by organic solvents such as methanol, acetonitrile, acetone or hexamethylphosphorictriamide relative to water. Although the preferential solvation of ions in binary solvent mixtures is generally rationalized in terms of the relative solvating abilities of the component solvents in the mixture toward the ion under study, the

Stellenbosch University http://scholar.sun.ac.za

selective solvation of the anions by the organic solvents in the present investigation may result from the 'exclusion' of the ions and organic solvents from the hydrogen-bonded network of water. Nevertheless, the $\delta_{Pt\text{-}195}$ variations for the anions in the binary mixtures allow the estimation of the anion solvation sphere composition with changing bulk composition, as well as deductions regarding the relative distributions of solvent molecules in the solvation spheres.

The association of the anions ($PtCl_6^{2-}$ and $PtBr_6^{2-}$) with cations such as Na^+, in the formation of contact ion-pairs, is also distinctly reflected by the ^{195}Pt resonance position, allowing the utilization of the technique as a sensitive probe for the occurrence of PtX_6^{2-} (X = Cl, Br) ion-pair formation in solution. In addition to the *qualitative* deductions that can be made from the ^{195}Pt chemical shift variations of the PtX_6^{2-} anions in binary solvent mixtures and in media in which ion-pairing may occur, a further advantage of utilizing the technique is highlighted by *quantitative* results which can be obtained in terms of preferential solvation equilibrium constants, $K^{1/n}$, and conditional ion-pair formation equilibrium quotients, Q.

In this investigation the synthesis of Pt(IV) complexes of *N*-alkyl- and *N,N*-dialkyl-*N'*-benzoylthioureas has been achieved by the oxidative addition of various halogens to the Pt(II) precursors. Similarly, Pt(IV) complexes of the bipodal analogues, 3,3,3',3'-tetraalkyl-1,1'-phenylenedicarbonylbis(thioureas), have been successfully synthesized and characterized. These results form the basis of further investigations to elucidate the speciation of extracted species in solvent extraction processes with the *N,N*-alkyl-*N'*-aroyl(acyl)thioureas, as well as studies of the potential of Pt(IV) metallamacrocyclic complexes to act as building blocks for the synthesis of supramolecular assemblies. In addition, it has been shown that ^{195}Pt NMR spectroscopy is a powerful tool for probing the solvation shells of anions such as $PtCl_6^{2-}$ and $PtBr_6^{2-}$, and can, in conjunction with computational investigations, be effectively utilized to study the complicated ion-solvent and ion-ion interactions which prevail in industrial PGM separation processes.

Stellenbosch University http://scholar.sun.ac.za

Addendum A

Table 4.1A-Adm Stock solutions of D_2O and methanol containing $H_2PtCl_6 \cdot H_2O$ (Sol(A) and Sol(B)) were made and used to prepare the D_2O/methanol binary solvent system. Multiplication of the appropriate concentration term ("grams $H_2PtCl_6 \cdot H_2O$ per gram stock solution") with the mass of stock solution used, enables the determination of the mass contributions of $H_2PtCl_6 \cdot H_2O$ and solvents to each solution. The number of moles of solvent, and thus mole fraction non-aqueous solvent can be calculated. Bulk solvent composition and resultant ^{195}Pt chemical shifts (ppm) are indicated in the last two columns; see Fig. 4.1-Adm.

D_2O / METHANOL Binary Solvent System - $PtCl_6^{2-}$	
Solution A (Sol(A))	**Solution B (Sol(B))**
Solvent D_2O ($M_r = 20.03$ g mol^{-1})	Solvent Methanol ($M_r = 32.05$ g mol^{-1})
Mass of $H_2PtCl_6 \cdot H_2O$ = 0.2021 g	**Mass of $H_2PtCl_6 \cdot H_2O$ = 0.2045 g**
Mass of stock solution upon addition of 5.00 cm^3 of D_2O = 5.7326 g	**Mass of stock solution upon addition of 5.00 cm^3 of Methanol = 4.1477 g**
∴ 0.03526 g ($H_2PtCl_6 \cdot H_2O$) / g solution	**∴ 0.04930 g ($H_2PtCl_6 \cdot H_2O$) / g solution**

Sample	Mass Sol(A) (g)	Mass ($H_2PtCl_6 \cdot H_2O$) (g)	Mass D_2O (g)	Moles D_2O	Mass Sol(B) (g)	Mass ($H_2PtCl_6 \cdot H_2O$) (g)	Mass Methanol (g)	Moles Methanol	Total Moles Solvent	Total Mass ($H_2PtCl_6 \cdot H_2O$) (g)	Mole Fraction Methanol	^{195}Pt Chem Shift (ppm)
1	-	-	-	-	0	-	-	-	-	-	0	5
2	0.6123	0.02159	0.5907	0.02949	0.0494	0.002435	0.04696	0.001465	0.03095	0.02402	0.0473	12
3	0.5311	0.01872	0.5123	0.02558	0.1025	0.005053	0.0974	0.003040	0.02862	0.02378	0.1062	21
4	0.4713	0.01661	0.4546	0.02270	0.1464	0.00721	0.1391	0.004343	0.02704	0.02383	0.1606	29
5	0.3939	0.01388	0.3800	0.01897	0.1953	0.00962	0.1856	0.005793	0.02476	0.02351	0.2339	40
6	0.342	0.01205	0.3299	0.01647	0.2653	0.01307	0.2522	0.00787	0.02434	0.02513	0.3233	51
7	0.2595	0.00915	0.2503	0.01249	0.2884	0.01421	0.2741	0.00855	0.02105	0.02336	0.4063	59
8	0.2144	0.00756	0.2068	0.01032	0.3468	0.01709	0.3297	0.01028	0.02061	0.02465	0.4990	67
9	0.1354	0.00477	0.1306	0.00652	0.3972	0.01958	0.3776	0.01178	0.01830	0.02435	0.643	76
10	0.0654	0.00230	0.0630	0.00315	0.4304	0.02121	0.4091	0.01276	0.01591	0.02352	0.802	84
11	0	-	-	-	-	-	-	-	-	-	1	97

Table 4.1B-Adm Estimated $PtCl_6^{2-}$ solvation sphere composition (as mole fraction methanol) as a function of bulk solvent composition for the D_2O/methanol binary solvent system; see Fig. 4.1-Adm.

Bulk solvent composition Mole fraction methanol	**0**	**0.1**	**0.2**	**0.3**	**0.4**	**0.5**	**0.6**	**0.7**	**0.8**	**0.9**	**1.0**
Solvation sphere composition Mole fraction methanol	0.00	0.18	0.33	0.46	0.57	0.66	0.74	0.81	0.87	0.93	1.00

Stellenbosch University http://scholar.sun.ac.za

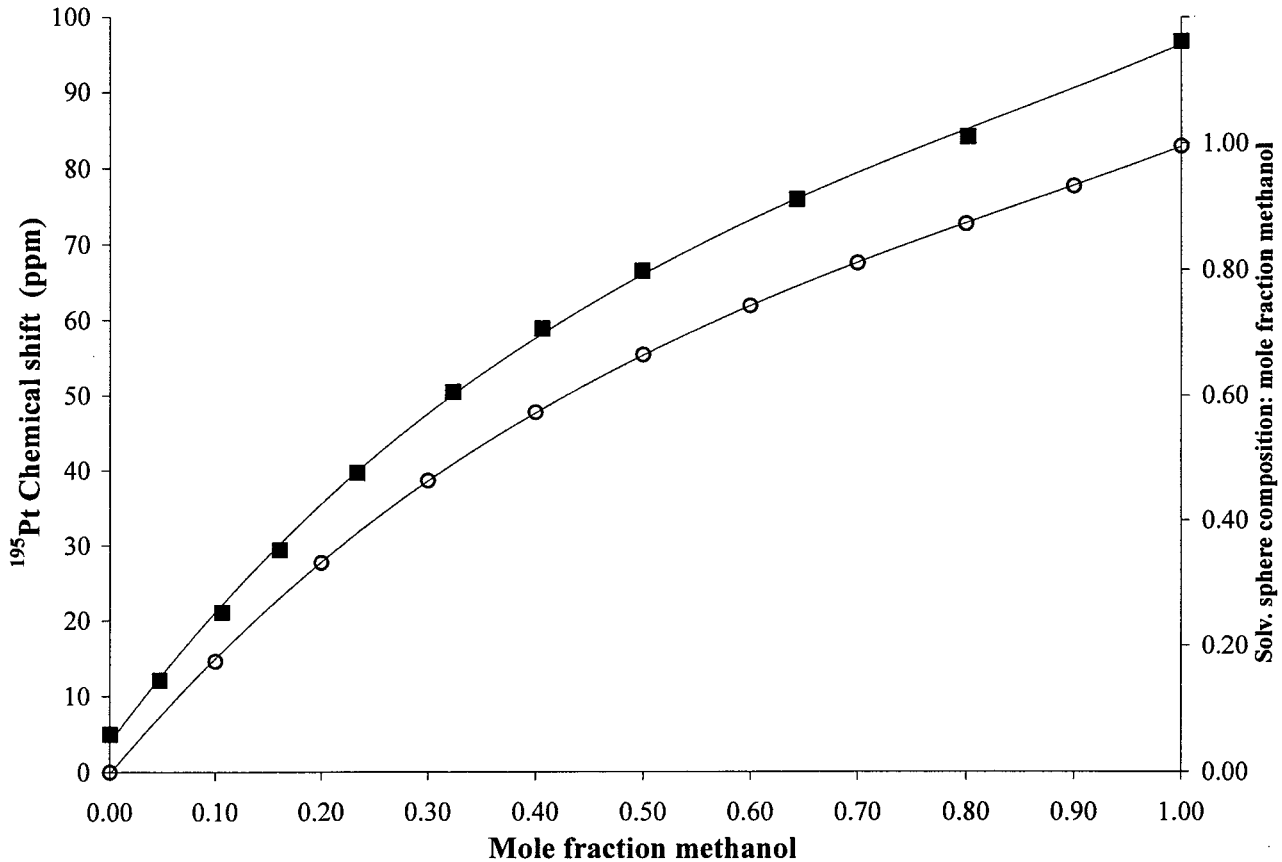

Fig. 4.1-Adm The ^{195}Pt (as $PtCl_6^{2-}$) chemical shift as a function of solvent composition in the D_2O/methanol binary solvent system (■). A best-fit polynomial trendline (3rd order) has been inserted; $y = 61.7x^3 - 156.1x^2 + 186.9x + 3.896$ ($R^2 = 0.999$). The estimated variation of the $PtCl_6^{2-}$ solvation sphere composition (mole fraction methanol) with changing bulk solvent composition is also depicted (O); a best-fit trendline has been inserted.

Stellenbosch University http://scholar.sun.ac.za

Table 4.2A-Adm Stock solutions of D_2O and ethylene glycol containing $H_2PtCl_6 \cdot H_2O$ were made and used to prepare the D_2O/ethylene glycol binary solvent system. Bulk solvent composition and resultant ^{195}Pt chemical shifts (ppm) are indicated in the last two columns; see Fig. 4.2-Adm

D_2O / ETHYLENE GLYCOL Binary Solvent System - $PtCl_6^{2-}$												
Solution A (Sol(A))					Solution B (Sol(B))							
Solvent D_2O (M_r = 20.03 g mol^{-1})					Solvent Ethylene Glycol (M_r = 62.08 g mol^{-1})							
Mass of $H_2PtCl_6 \cdot H_2O$ = 0.2072 g					**Mass of $H_2PtCl_6 \cdot H_2O$ = 0.2115 g**							
Mass of stock solution upon addition of 5.00 cm^3 of D_2O = 5.7298 g					**Mass of stock solution upon addition of 5.00 cm^3 of Ethylene Glycol = 5.6657 g**							
∴ 0.03616 g ($H_2PtCl_6 \cdot H_2O$) / g solution					**∴ 0.03733 g ($H_2PtCl_6 \cdot H_2O$) / g solution**							
Sample	**Mass Sol(A) (g)**	**Mass ($H_2PtCl_6 \cdot H_2O$) (g)**	**Mass D_2O (g)**	**Moles D_2O**	**Mass Sol(B) (g)**	**Mass ($H_2PtCl_6 \cdot H_2O$) (g)**	**Mass Ethylene Glycol (g)**	**Moles Ethylene Glycol**	**Total Moles Solvent**	**Total Mass ($H_2PtCl_6 \cdot H_2O$) (g)**	**Mole Fraction Ethylene Glycol**	**^{195}Pt Chem Shift (ppm)**
1	-	-	-	-	0	-	-	-	-	-	0	6
2	0.3848	0.01391	0.3709	0.01852	0.1732	0.00647	0.1667	0.002686	0.02120	0.02038	0.1267	38
3	0.3252	0.01176	0.3134	0.01565	0.2286	0.00853	0.2201	0.003545	0.01919	0.02029	0.1847	50
4	0.2206	0.00798	0.2126	0.01062	0.3324	0.01241	0.3200	0.00516	0.01577	0.02039	0.3269	73
5	0.1631	0.00590	0.1572	0.00785	0.3905	0.01458	0.3759	0.00606	0.01390	0.02048	0.4355	86
6	0.1199	0.004336	0.1156	0.00577	0.4413	0.01647	0.4248	0.00684	0.01261	0.02081	0.543	97
7	0.0885	0.003200	0.0853	0.004259	0.4747	0.01772	0.45698	0.00736	0.01162	0.02092	0.634	104
8	0.0597	0.002159	0.0575	0.002873	0.4957	0.01850	0.4772	0.00769	0.01056	0.02066	0.728	111
9	0.0317	0.001146	0.030554	0.001525	0.5362	0.02002	0.516	0.00831	0.00984	0.02116	0.845	118
10	0	-	-	-	-	-	-	-	-	-	1	127

Table 4.2B-Adm Estimated $PtCl_6^{2-}$ solvation sphere composition (as mole fraction ethylene glycol) as a function of bulk solvent composition for the D_2O/ethylene glycol binary solvent system; see Fig. 4.2-Adm.

Bulk solvent composition Mole fraction ethylene glycol	**0**	**0.1**	**0.2**	**0.3**	**0.4**	**0.5**	**0.6**	**0.7**	**0.8**	**0.9**	**1.0**
Solvation sphere composition Mole fraction ethylene glycol	0.00	0.21	0.38	0.52	0.63	0.72	0.79	0.85	0.90	095	1.00

Stellenbosch University http://scholar.sun.ac.za

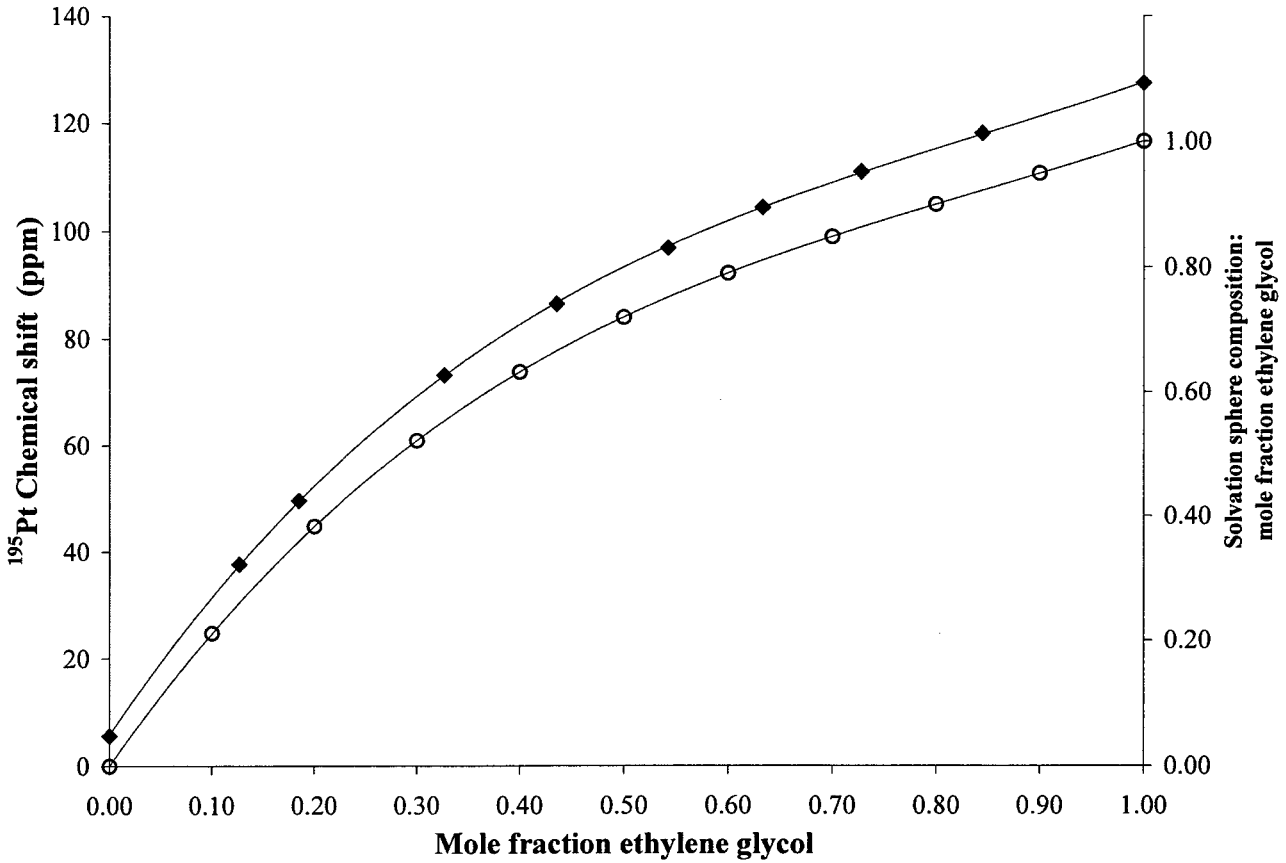

Fig. 4.2-Adm The ^{195}Pt (as $PtCl_6^{2-}$) chemical shift as a function of solvent composition in the D_2O/ethylene glycol binary solvent system (◆). A best-fit polynomial trendline (3rd order) has been inserted; $y = 107.0x^3 - 266.8x^2 + 281.7x + 5.78$ ($R^2 = 1.00$). The estimated variation of the $PtCl_6^{2-}$ solvation sphere composition (mole fraction ethylene glycol) with changing bulk solvent composition is also depicted (O); a best-fit trendline has been inserted.

Stellenbosch University http://scholar.sun.ac.za

Table 4.3A-Adm Stock solutions of D_2O and acetonitrile containing $H_2PtCl_6 \cdot H_2O$ were made and used to prepare the D_2O/acetonitrile binary solvent system. Bulk solvent composition and resultant ^{195}Pt chemical shifts (ppm) are indicated in the last two columns; see Fig. 4.3-Adm.

D_2O / ACETONITRILE Binary Solvent System - $PtCl_6^{2-}$	
Solution A (Sol(A))	**Solution B (Sol(B))**
Solvent D_2O ($M_r = 20.03$ g mol^{-1})	Solvent Acetonitrile ($M_r = 41.06$ g mol^{-1})
Mass of $H_2PtCl_6 \cdot H_2O$ = 0.2010 g	**Mass of $H_2PtCl_6 \cdot H_2O$ = 0.2036 g**
Mass of stock solution upon addition of 5.00 cm^3 of D_2O = 5.7300 g	**Mass of stock solution upon addition of 5.00 cm^3 of Acetonitrile = 4.1156 g**
∴ 0.03508 g ($H_2PtCl_6 \cdot H_2O$) / g solution	**∴ 0.04947 g ($H_2PtCl_6 \cdot H_2O$) / g solution**

Sample	Mass Sol(A) (g)	Mass ($H_2PtCl_6 \cdot H_2O$) (g)	Mass D_2O (g)	Moles D_2O	Mass Sol(B) (g)	Mass ($H_2PtCl_6 \cdot H_2O$) (g)	Mass Acetonitrile (g)	Moles Acetonitrile	Total Moles Solvent	Total Mass ($H_2PtCl_6 \cdot H_2O$) (g)	Mole Fraction Acetonitrile	^{195}Pt Chem Shift (ppm)
1	-	-	-	-	0	-	-	-	-	-	0	5
2	0.6033	0.02116	0.582	0.02906	0.0504	0.002493	0.04791	0.001167	0.03023	0.02366	0.0386	26
3	0.5315	0.01864	0.513	0.02560	0.0895	0.004428	0.0851	0.002072	0.02768	0.02307	0.0749	47
4	0.4442	0.01558	0.4286	0.02140	0.1335	0.00660	0.1269	0.003091	0.02449	0.02219	0.1262	74
5	0.3341	0.01172	0.3224	0.01609	0.2406	0.01190	0.2287	0.00557	0.02166	0.02362	0.2571	119
6	0.2476	0.00869	0.2389	0.01193	0.3004	0.01486	0.2855	0.00695	0.01888	0.02355	0.3683	143
7	0.1303	0.004571	0.1257	0.00628	0.3624	0.01793	0.3445	0.00839	0.01467	0.02250	0.572	176
8	0.072	0.002526	0.0695	0.003469	0.4462	0.02207	0.4241	0.01033	0.01380	0.02460	0.749	200
9	0	-	-	-	-	-	-	-	-	-	1	217

Table 4.3B-Adm Estimated $PtCl_6^{2-}$ solvation sphere composition (as mole fraction acetonitrile) as a function of bulk solvent composition for the D_2O/acetonitrile binary solvent system; see Fig. 4.3-Adm.

Bulk solvent composition Mole fraction acetonitrile	**0**	**0.1**	**0.2**	**0.3**	**0.4**	**0.5**	**0.6**	**0.7**	**0.8**	**0.9**	**1.0**
Solvation sphere composition Mole fraction acetonitrile	0.00	0.25	0.44	0.59	0.70	0.78	0.83	0.88	0.92	0.96	1.00

Stellenbosch University http://scholar.sun.ac.za

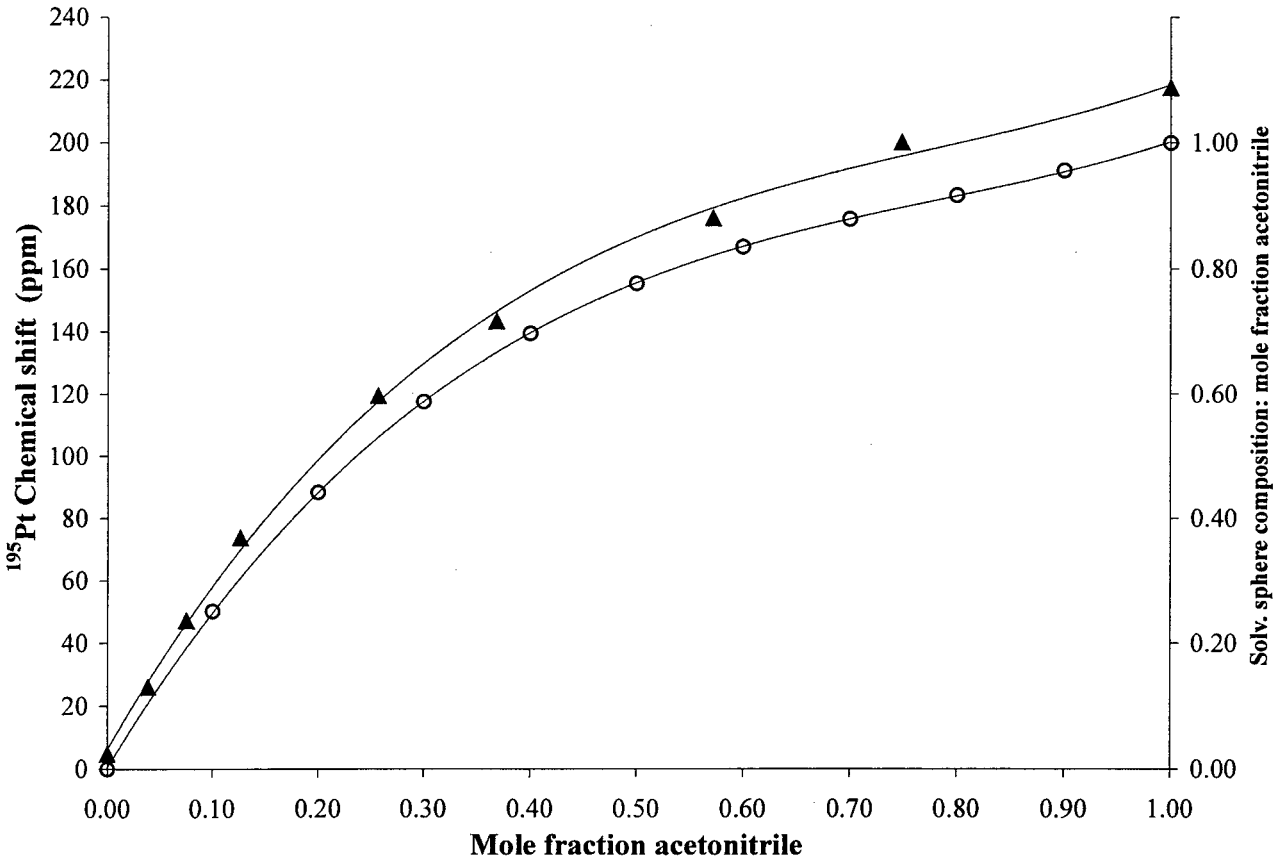

Fig. 4.3-Adm The ^{195}Pt (as $PtCl_6^{2-}$) chemical shift as a function of solvent composition in the D_2O/acetonitrile binary solvent system (▲). A best-fit polynomial trendline (3rd order) has been inserted; $y = 274.3x^3 - 642x^2 + 580x + 6.17$ ($R^2 = 0.999$). The estimated variation of the $PtCl_6^{2-}$ solvation sphere composition (mole fraction acetonitrile) with changing bulk solvent composition is also depicted (O); a best-fit trendline has been inserted.

Stellenbosch University http://scholar.sun.ac.za

Table 4.4A-Adm Stock solutions of D_2O and acetone containing $H_2PtCl_6 \cdot H_2O$ were made and used to prepare the D_2O/acetone binary solvent system. Bulk solvent composition and resultant ^{195}Pt chemical shifts (ppm) are indicated in the last two columns; see Fig. 4.5-Adm.

D_2O / ACETONE Binary Solvent System - $PtCl_6^{2-}$	
Solution A (Sol(A))	**Solution B (Sol(B))**
Solvent D_2O (M_r = 20.03 g mol^{-1})	Solvent Acetone (M_r = 58.09 g mol^{-1})
Mass of $H_2PtCl_6 \cdot H_2O$ = 0.2026 g	**Mass of $H_2PtCl_6 \cdot H_2O$ = 0.2129 g**
Mass of stock solution upon addition of 5.00 cm^3 of D_2O = 5.7394 g	**Mass of stock solution upon addition of 5.00 cm^3 of Acetone = 4.1640 g**
∴ 0.03530 g ($H_2PtCl_6 \cdot H_2O$) / g solution	**∴ 0.05113 g ($H_2PtCl_6 \cdot H_2O$) / g solution**

Sample	Mass Sol(A) (g)	Mass ($H_2PtCl_6 \cdot H_2O$) (g)	Mass D_2O (g)	Moles D_2O	Mass Sol(B) (g)	Mass ($H_2PtCl_6 \cdot H_2O$) (g)	Mass Acetone (g)	Moles Acetone	Total Moles Solvent	Total Mass ($H_2PtCl_6 \cdot H_2O$) (g)	Mole Fraction Acetone	^{195}Pt Chem Shift (ppm)
1	-	-	-	-	0	-	-	-	-	-	0	5
2	0.5693	0.02010	0.549	0.02742	0.0645	0.003298	0.0612	0.001054	0.02847	0.02339	0.0370	33
3	0.5076	0.01792	0.4897	0.02445	0.153	0.00782	0.1452	0.002499	0.02695	0.02574	0.0927	72
4	0.4695	0.01657	0.4529	0.02261	0.1955	0.01000	0.1855	0.003193	0.02581	0.02657	0.1237	92
5	0.4077	0.01439	0.3933	0.01964	0.2579	0.01319	0.2447	0.004213	0.02385	0.02758	0.1766	120
6	0.3164	0.01117	0.3052	0.01524	0.3335	0.01705	0.3164	0.00545	0.02069	0.02822	0.2633	154
7	0.2609	0.00921	0.2517	0.01257	0.4061	0.02076	0.3853	0.00663	0.01920	0.02997	0.3455	177
8	0.2125	0.00750	0.2050	0.01023	0.4637	0.02371	0.4400	0.00757	0.01781	0.03121	0.4253	194
9	0.1344	0.004744	0.1297	0.00647	0.5171	0.02644	0.4907	0.00845	0.01492	0.03118	0.566	214
10	0.07	0.002471	0.0675	0.003371	0.6098	0.03118	0.579	0.00996	0.01333	0.03365	0.747	230
11	0	-	-	-	-	-	-	-	-	-	1	240

Table 4.4B-Adm Estimated $PtCl_6^{2-}$ solvation sphere composition (as mole fraction acetone) as a function of bulk solvent composition for the D_2O/acetone binary solvent system; see Fig. 4.5-Adm.

Bulk solvent composition Mole fraction acetone	**0**	**0.1**	**0.2**	**0.3**	**0.4**	**0.5**	**0.6**	**0.7**	**0.8**	**0.9**	**1.0**
Solvation sphere composition Mole fraction acetone	0.00	0.31	0.53	0.68	0.78	0.85	0.90	0.94	0.97	0.99	1.00

Stellenbosch University http://scholar.sun.ac.za

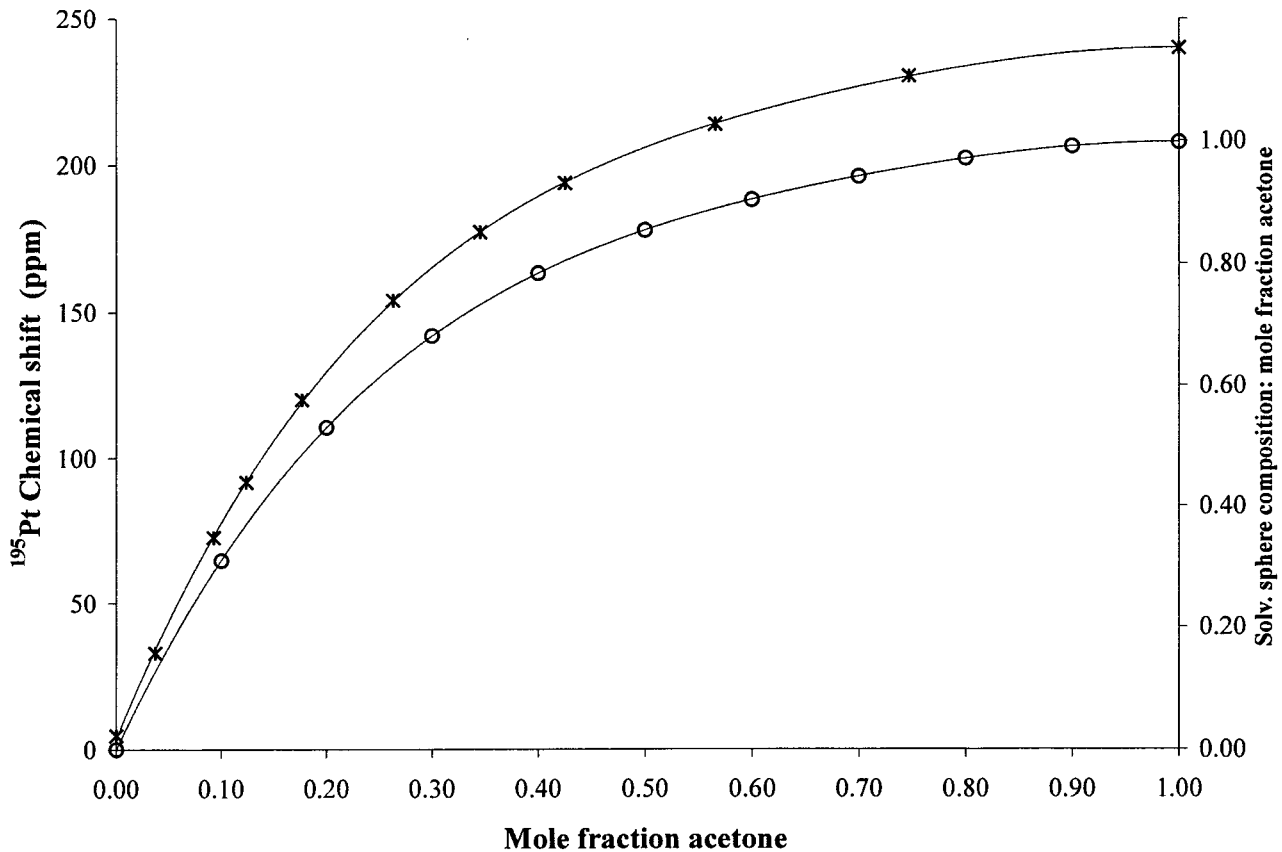

Fig. 4.4-Adm The ^{195}Pt (as $PtCl_6^{2-}$) chemical shift as a function of solvent composition in the D_2O/acetone binary solvent system (∗). A best-fit polynomial trendline (4th order) has been inserted; $y = -406.2x^4 + 1208x^3 - 1437x^2 + 871x + 3.663$ ($R^2 = 1.00$). The estimated variation of the $PtCl_6^{2-}$ solvation sphere composition (mole fraction acetone) with changing bulk solvent composition is also depicted (O); a best-fit trendline has been inserted.

Stellenbosch University http://scholar.sun.ac.za

Table 4.5A-Adm Stock solutions of D_2O and 2-methoxyethanol (2-MeOEt) containing $H_2PtCl_6 \cdot H_2O$ were made and used to prepare the D_2O/2-MeOEt binary solvent system. Bulk solvent composition and resultant ^{195}Pt chemical shifts (ppm) are indicated in the last two columns; see Fig. 4.6-Adm.

D_2O / 2-METHOXYETHANOL Binary Solvent System - $PtCl_6^{2-}$	
Solution A (Sol(A))	**Solution B (Sol(B))**
Solvent D_2O (M_r = 20.03 g mol^{-1})	Solvent 2-Methoxyethanol, 2-MeOEt (M_r = 76.1 g mol^{-1})
Mass of $H_2PtCl_6 \cdot H_2O$ = 0.2061 g	**Mass of $H_2PtCl_6 \cdot H_2O$ = 0.2116 g**
Mass of stock solution upon addition of 5.00 cm^3 of D_2O = 5.7364 g	**Mass of stock solution upon addition of 5.00 cm^3 of 2-Methoxyethanol = 4.9940 g**
∴ 0.03593 g ($H_2PtCl_6 \cdot H_2O$) / g solution	**∴ 0.04237 g ($H_2PtCl_6 \cdot H_2O$) / g solution**

Sample	Mass Sol(A) (g)	Mass ($H_2PtCl_6 \cdot H_2O$) (g)	Mass D_2O (g)	Moles D_2O	Mass Sol(B) (g)	Mass ($H_2PtCl_6 \cdot H_2O$) (g)	Mass 2-MeOEt (g)	Moles 2-MeOEt	Total Moles Solvent	Total Mass ($H_2PtCl_6 \cdot H_2O$) (g)	Mole Fraction 2-MeOEt	^{195}Pt Chem Shift (ppm)
1	-	-	-	-	0	-	-	-	-	-	0	6
2	0.4332	0.01556	0.4176	0.02085	0.1018	0.004313	0.0975	0.001281	0.02213	0.02020	0.0579	43
3	0.3818	0.01372	0.3681	0.01838	0.1464	0.00620	0.1402	0.001842	0.02022	0.02020	0.0911	62
4	0.3280	0.01179	0.3162	0.01579	0.1964	0.00832	0.1881	0.002472	0.01826	0.02034	0.1354	84
5	0.2700	0.00970	0.2603	0.01300	0.2459	0.01042	0.2355	0.003094	0.01609	0.02032	0.1923	107
6	0.2201	0.00791	0.2122	0.01059	0.2898	0.01228	0.2775	0.003647	0.01424	0.02035	0.2561	127
7	0.1643	0.005903	0.1584	0.00791	0.3363	0.01425	0.3221	0.004232	0.01214	0.02027	0.3486	147
8	0.1124	0.004039	0.1084	0.00541	0.3847	0.01630	0.3684	0.004841	0.01025	0.02042	0.4722	165
9	0.0888	0.003191	0.0856	0.004274	0.4101	0.01738	0.3927	0.00516	0.00943	0.02063	0.5470	172
10	0.0574	0.002062	0.0553	0.002763	0.4358	0.01846	0.4173	0.00548	0.00825	0.02057	0.665	180
11	0.0316	0.001135	0.03046	0.001521	0.4599	0.01949	0.44041	0.00579	0.00731	0.02064	0.792	187
12	0.0149	0.000535	0.01436	0.000717	0.4791	0.02030	0.4588	0.00603	0.00675	0.02085	0.894	192
11	0	-	-	-	-	-	-	-	-	-	1	198

Table 4.5B-Adm Estimated $PtCl_6^{2-}$ solvation sphere composition (as mole fraction 2-methoxyethanol) as a function of bulk solvent composition for the D_2O/2-methoxyethanol binary solvent system; see Fig. 4.6-Adm.

Bulk solvent composition Mole fraction 2-methoxyethanol	**0**	**0.1**	**0.2**	**0.3**	**0.4**	**0.5**	**0.6**	**0.7**	**0.8**	**0.9**	**1.0**
Solvation sphere composition Mole fraction 2-methoxyethanol	0.00	0.32	0.54	0.68	0.78	0.84	0.88	0.82	0.94	0.97	1.00

Stellenbosch University http://scholar.sun.ac.za

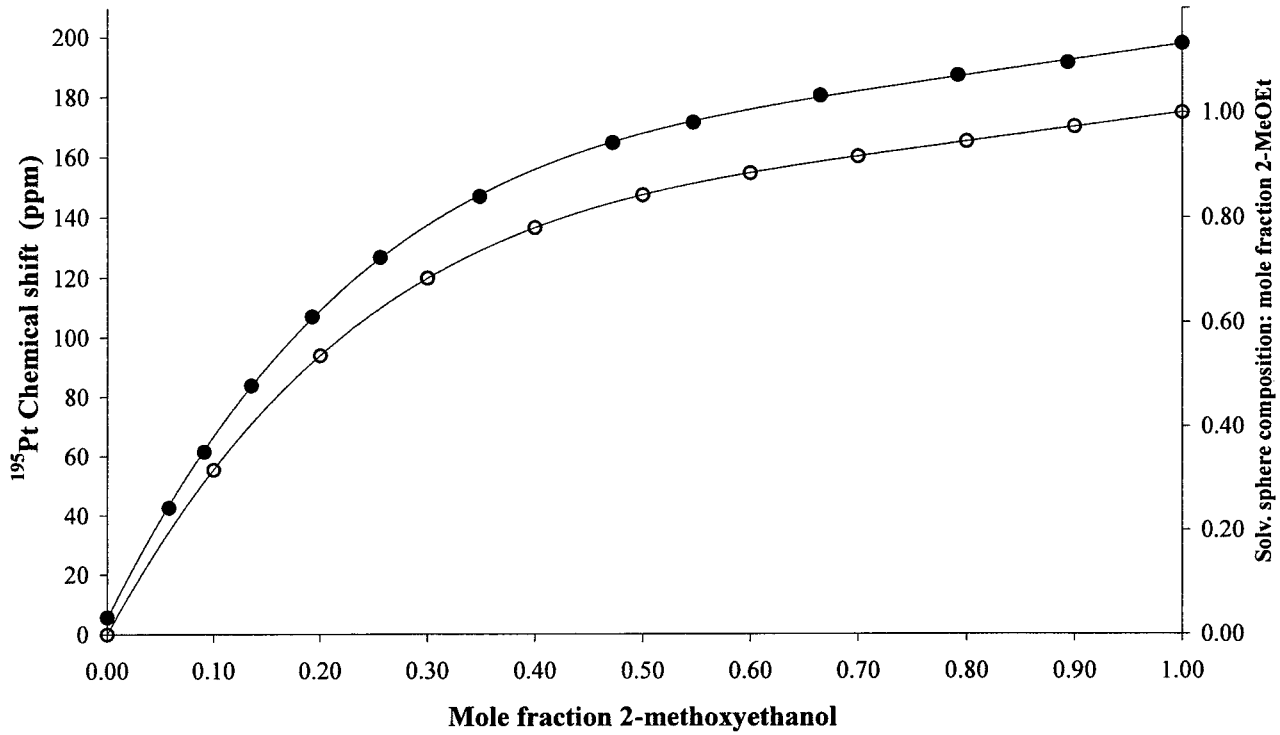

Fig. 4.5-Adm The ^{195}Pt (as $PtCl_6^{2-}$) chemical shift as a function of solvent composition in the D_2O/2-methoxyethanol binary solvent system (●). A best-fit polynomial trendline (4th order) has been inserted; $y = -298.0x^4 + 986x^3 - 1222x^2 + 727x + 5.20$ ($R^2 = 0.999$). The estimated variation of the $PtCl_6^{2-}$ solvation sphere composition (mole fraction 2-methoxyethanol) with changing bulk solvent composition is also depicted (O); a best-fit trendline has been inserted.

Stellenbosch University http://scholar.sun.ac.za

Table 4.6A-Adm Stock solutions of D_2O and hexamethylphosphorictriamide (HMPA) containing $H_2PtCl_6 \cdot H_2O$ were made and used to prepare the D_2O/HMPA binary solvent system. Bulk solvent composition and resultant ^{195}Pt chemical shifts (ppm) are indicated in the last two columns; see Fig. 4.7-Adm.

D_2O / HEXAMETHYLPHOSPHORICTRIAMIDE Binary Solvent System - $PtCl_6^{2-}$	
Solution A (Sol(A))	**Solution B (Sol(B))**
Solvent D_2O (M_r = 20.03 g mol^{-1})	Solvent Hexamethylphosphorictriamide, HMPA (M_r = 179.24 g mol^{-1})
Mass of $H_2PtCl_6 \cdot H_2O$ = 0.2045 g	**Mass of $H_2PtCl_6 \cdot H_2O$ = 0.2033 g**
Mass of stock solution upon addition of 5.00 cm^3 of D_2O = 5.7339 g	**Mass of stock solution upon addition of 5.00 cm^3 of HMPA = 5.3201 g**
∴ 0.03567 g ($H_2PtCl_6 \cdot H_2O$) / g solution	**∴ 0.03821 g ($H_2PtCl_6 \cdot H_2O$) / g solution**

Sample	Mass Sol(A) (g)	Mass ($H_2PtCl_6 \cdot H_2O$) (g)	Mass D_2O (g)	Moles D_2O	Mass Sol(B) (g)	Mass ($H_2PtCl_6 \cdot H_2O$) (g)	Mass HMPA (g)	Moles HMPA	Total Moles Solvent	Total Mass ($H_2PtCl_6 \cdot H_2O$) (g)	Mole Fraction HMPA	^{195}Pt Chem Shift (ppm)
1	-	-	-	-	0	-	-	-	-	-	0	6
2	0.5799	0.02069	0.559	0.02792	0.0713	0.002724	0.0686	0.0003826	0.02830	0.02341	0.0135	34
3	0.5179	0.01847	0.4994	0.02493	0.127	0.004853	0.1221	0.000682	0.02562	0.02333	0.0266	61
4	0.4585	0.01635	0.4421	0.02207	0.1977	0.00755	0.1901	0.001061	0.02314	0.02391	0.0459	98
5	0.3959	0.01412	0.38178	0.01906	0.2463	0.00941	0.2369	0.001322	0.02038	0.02353	0.0648	131
6	0.3372	0.01203	0.3252	0.01623	0.2992	0.01143	0.2878	0.001606	0.01784	0.02346	0.0900	169
7	0.2908	0.01037	0.2804	0.01400	0.3665	0.01400	0.3525	0.001967	0.01597	0.02438	0.1232	208
8	0.1962	0.00700	0.1892	0.00945	0.4281	0.01636	0.4117	0.002297	0.01174	0.02336	0.1956	266
9	0.1254	0.004473	0.1209	0.00604	0.5016	0.01917	0.4824	0.002692	0.00873	0.02364	0.3084	316
10	0.0616	0.002197	0.0594	0.002966	0.552	0.02109	0.531	0.002962	0.00593	0.02329	0.4997	361
11	0	-	-	-	-	-	-	-	-	-	1	411

Table 4.6B-Adm Estimated $PtCl_6^{2-}$ solvation sphere composition (as mole fraction HMPA) as a function of bulk solvent composition for the D_2O/HMPA binary solvent system; see Fig. 4.7-Adm.

Bulk solvent composition Mole fraction HMPA	**0**	**0.1**	**0.2**	**0.3**	**0.4**	**0.5**	**0.6**	**0.7**	**0.8**	**0.9**	**1.0**
Solvation sphere composition Mole fraction HMPA	0.00	0.46	0.63	0.72	0.79	0.84	0.89	0.92	0.96	0.98	1.00

Stellenbosch University http://scholar.sun.ac.za

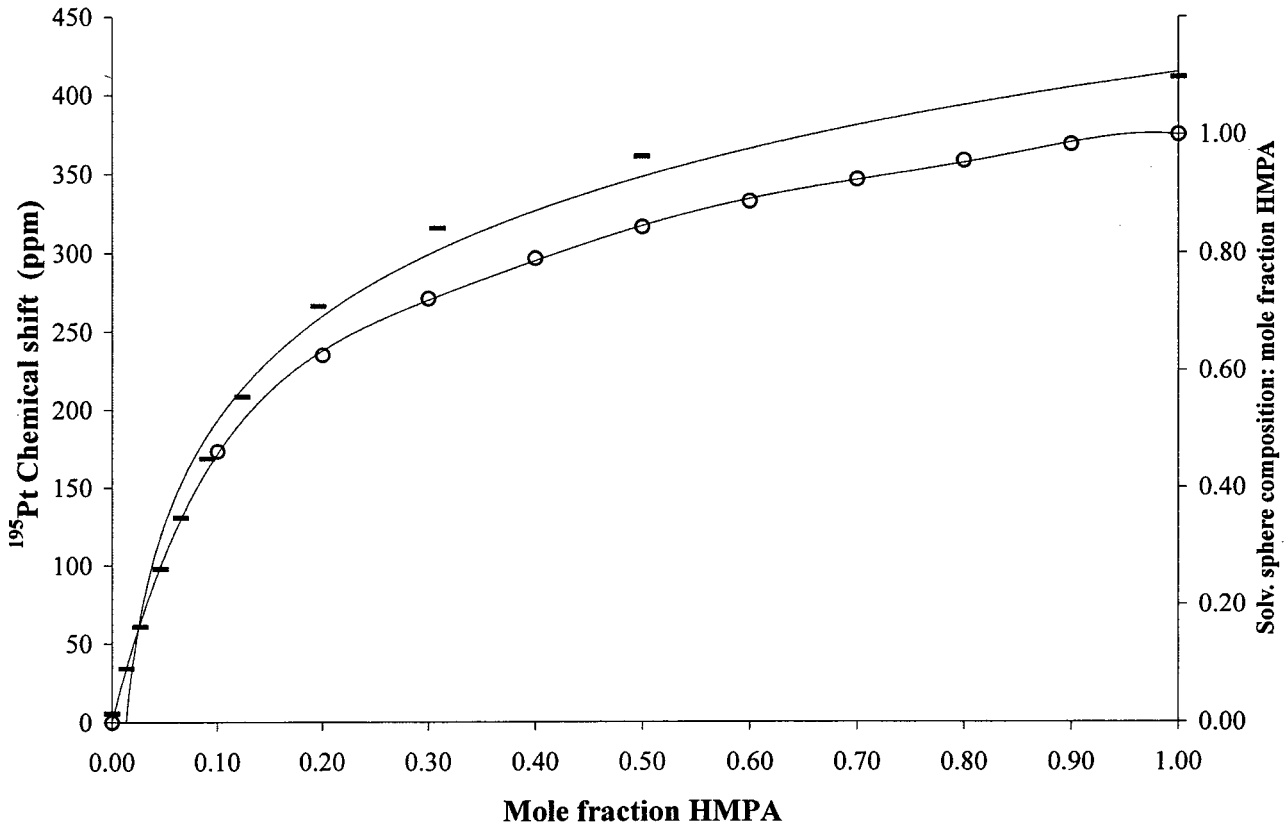

Fig. 4.6-Adm The ^{195}Pt (as $PtCl_6^{2-}$) chemical shift as a function of solvent composition in the D_2O/HMPA binary solvent system (-). A best-fit logarithmic trendline has been inserted; y = 96.2Ln(x) + 414.8 (R^2 = 0.982). The estimated variation of the $PtCl_6^{2-}$ solvation sphere composition (mole fraction HMPA) with changing bulk solvent composition is also depicted (O); a best-fit trendline has been inserted.

Stellenbosch University http://scholar.sun.ac.za

Table 4.7A-Adm Stock solutions of D_2O and 1,2-dimethoxyethane (1,2-DME) containing $H_2PtCl_6 \cdot H_2O$ were made and used to prepare the D_2O/1,2-DME binary solvent system. Bulk solvent composition and resultant ^{195}Pt chemical shifts (ppm) are indicated in the last two columns; see Fig. 4.8-Adm.

D_2O / 1,2-DIMETHOXYETHANE Binary Solvent System - $PtCl_6^{2-}$	
Solution A (Sol(A))	**Solution B (Sol(B))**
Solvent D_2O (M_r = 20.03 g mol^{-1})	Solvent 1,2-Dimethoxyethane, 1,2-DME (M_r = 90.12 g mol^{-1})
Mass of $H_2PtCl_6 \cdot H_2O$ = 0.2072 g	**Mass of $H_2PtCl_6 \cdot H_2O$ = 0.1631 g**
Mass of stock solution upon addition of 5.00 cm^3 of D_2O = 5.7298 g	**Mass of stock solution upon addition of 5.00 cm^3 of 1,2-Dimethoxyethane = 4.5108 g**
∴ 0.03616 g ($H_2PtCl_6 \cdot H_2O$) / g solution	**∴ 0.03616 g ($H_2PtCl_6 \cdot H_2O$) / g solution**

Sample	Mass Sol(A) (g)	Mass ($H_2PtCl_6 \cdot H_2O$) (g)	Mass D_2O (g)	Moles D_2O	Mass Sol(B) (g)	Mass ($H_2PtCl_6 \cdot H_2O$) (g)	Mass 1,2-DME (g)	Moles 1,2-DME	Total Moles Solvent	Total Mass ($H_2PtCl_6 \cdot H_2O$) (g)	Mole Fraction 1,2-DME	^{195}Pt Chem Shift (ppm)
1	-	-	-	-	0	-	-	-	-	-	0	6
2	0.4269	0.01544	0.4114	0.02054	0.0902	0.003262	0.0869	0.000965	0.02151	0.01870	0.04485	53
3	0.3254	0.01177	0.3136	0.01566	0.1726	0.00624	0.1664	0.001846	0.01750	0.01801	0.1055	107
4	0.2205	0.00797	0.2125	0.01061	0.2569	0.00929	0.2476	0.002748	0.01336	0.01726	0.2057	160
5	0.1644	0.00594	0.1585	0.00791	0.2922	0.01057	0.2816	0.003125	0.01104	0.01651	0.2832	176
6	0.1158	0.004187	0.1116	0.00557	0.3448	0.01247	0.3323	0.003688	0.00926	0.01666	0.3982	188
7	0.0597	0.002159	0.0575	0.002873	0.3870	0.01399	0.3730	0.004139	0.00701	0.01615	0.590	195
8	0.0376	0.001360	0.03624	0.001809	0.4037	0.01460	0.3891	0.004318	0.00613	0.01596	0.705	197
9	0.0158	0.000571	0.01523	0.000760	0.4226	0.01528	0.4073	0.004520	0.00528	0.01585	0.856	200
10	0.0095	0.0003435	0.00916	0.0004571	0.4287	0.01550	0.4132	0.004585	0.00504	0.01585	0.909	201
11	0	-	-	-	-	-	-	-	-	-	1	209

Table 4.7B-Adm Estimated $PtCl_6^{2-}$ solvation sphere composition (as mole fraction 1,2-dimethoxyethane) as a function of bulk solvent composition for the D_2O/1,2-dimethoxyethane binary solvent system; see Fig. 4.8-Adm.

Bulk solvent composition Mole fraction 1,2-dimethoxyethane	**0**	**0.1**	**0.2**	**0.3**	**0.4**	**0.5**	**0.6**	**0.7**	**0.8**	**0.9**	**1.0**
Solvation sphere composition Mole fraction 1,2-dimethoxyethane	0.00	0.47	0.73	0.87	0.91	0.92	0.92	0.93	0.95	0.97	1.00

Stellenbosch University http://scholar.sun.ac.za

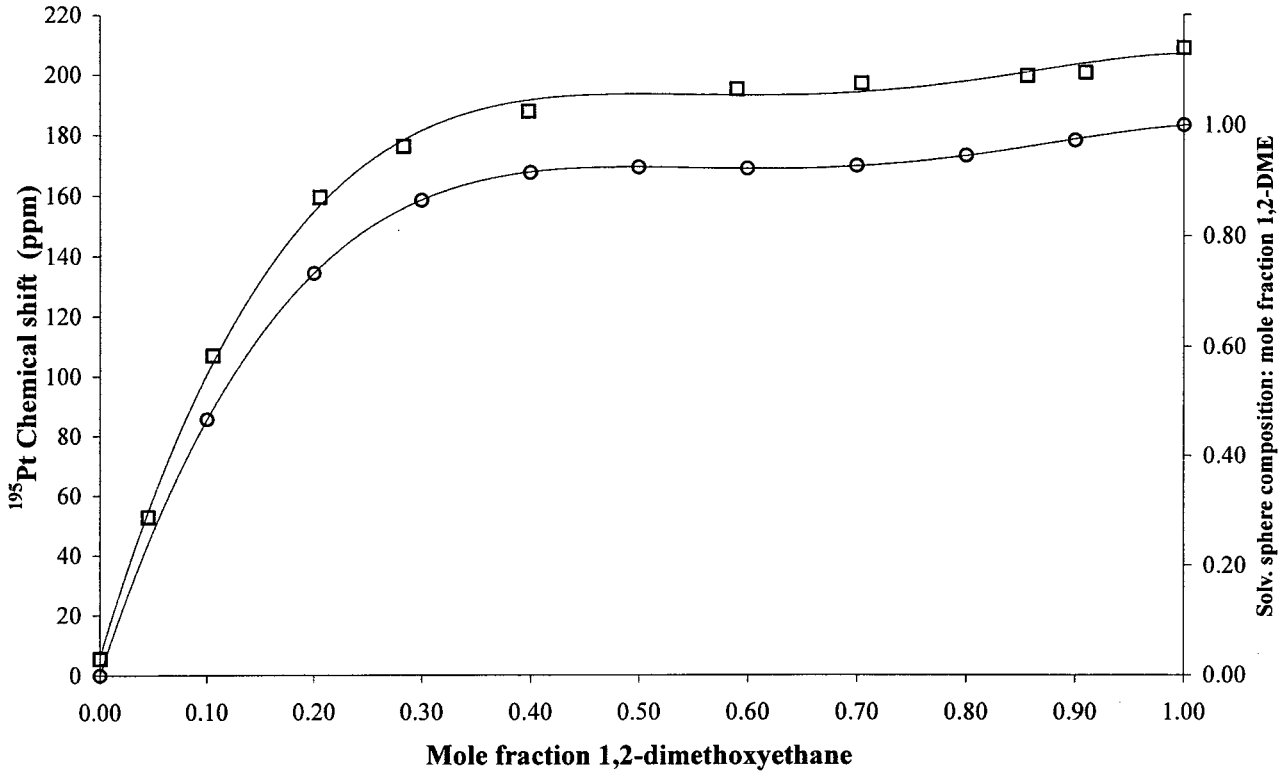

Fig. 4.7-Adm The ^{195}Pt (as $PtCl_6^{2-}$) chemical shift as a function of solvent composition in the D_2O/1,2-dimethoxyethane binary solvent system (□). A best-fit polynjomial trendline (4th order) has been inserted; $y = -984x^4 + 2775x^3 - 2788x^2 + 1198x + 6.02$ ($R^2 = 0.999$). The estimated variation of the $PtCl_6^{2-}$ solvation sphere composition (mole fraction 1,2-dimethoxyethane) with changing bulk solvent composition is also depicted (O); a best-fit trendline has been inserted.

Stellenbosch University http://scholar.sun.ac.za

Table 4.8A-Adm Stock solutions of D_2O and *N,N*-dimethylformamide (DMF) containing $H_2PtCl_6 \cdot H_2O$ were made and used to prepare the D_2O/DMF binary solvent system. Bulk solvent composition and resultant ^{195}Pt chemical shifts (ppm) are indicated in the last two columns; see Fig. 4.4-Adm. (This solvent was stored over solid KOH, which may cause decomposition of the solvent; the data must be considered with some uncertainty, and is not included in the Results and Discussion).

D_2O / *N,N*-DIMETHYLFORMAMIDE Binary Solvent System - $PtCl_6^{2-}$	
Solution A (Sol(A))	**Solution B (Sol(B))**
Solvent D_2O (M_r = 20.03 g mol^{-1})	Solvent *N,N*-Dimethylformamide, DMF (M_r = 73.11 g mol^{-1})
Mass of $H_2PtCl_6 \cdot H_2O$ = 0.2126 g	**Mass of $H_2PtCl_6 \cdot H_2O$ = 0.2137 g**
Mass of stock solution upon addition of 5.00 cm^3 of D_2O = 5.7421 g	**Mass of stock solution upon addition of 5.00 cm^3 of DMF = 4.9509 g**
∴ 0.03703 g ($H_2PtCl_6 \cdot H_2O$) / g solution	**∴ 0.04316 g ($H_2PtCl_6 \cdot H_2O$) / g solution**

Sample	Mass Sol(A) (g)	Mass ($H_2PtCl_6 \cdot H_2O$) (g)	Mass D_2O (g)	Moles D_2O	Mass Sol(B) (g)	Mass ($H_2PtCl_6 \cdot H_2O$) (g)	Mass DMF (g)	Moles DMF	Total Moles Solvent	Total Mass ($H_2PtCl_6 \cdot H_2O$) (g)	Mole Fraction DMF	^{195}Pt Chem Shift (ppm)
1	-	-	-	-	0	-	-	-	-	-	0	5
2	0.6222	0.02304	0.599	0.02991	0.0666	0.002875	0.0637	0.000872	0.03078	0.02591	0.02831	37
3	0.5449	0.02018	0.525	0.02620	0.1186	0.00512	0.1135	0.001552	0.02775	0.02530	0.0559	64
4	0.4728	0.01751	0.4553	0.02273	0.1837	0.00793	0.1758	0.002404	0.02513	0.02544	0.0957	98
5	0.4064	0.01505	0.3914	0.01954	0.2412	0.01041	0.2308	0.003157	0.02270	0.02546	0.1391	131
6	0.3595	0.01331	0.3462	0.01728	0.3057	0.01319	0.2925	0.004001	0.021284	0.02651	0.1880	163
7	0.2152	0.00797	0.2072	0.01035	0.4318	0.01864	0.4132	0.005651	0.01600	0.02661	0.3533	235
8	0.1517	0.00562	0.1461	0.00729	0.4755	0.02052	0.4550	0.00622	0.01352	0.02614	0.4604	261
9	0.0729	0.002700	0.0702	0.003504	0.5371	0.02318	0.514	0.00703	0.01053	0.02588	0.667	285
10	0	-	-	-	-	-	-	-	-	-	1	341

Table 4.8B-Adm Estimated $PtCl_6^{2-}$ solvation sphere composition (as mole fraction *N,N*-dimethylformamide) as a function of bulk solvent composition for the D_2O/*N,N*-dimethylformamide binary solvent system; see Fig. 4.4-Adm.

Bulk solvent composition Mole fraction *N,N*-dimethylformamide	**0**	**0.1**	**0.2**	**0.3**	**0.4**	**0.5**	**0.6**	**0.7**	**0.8**	**0.9**	**1.0**
Solvation sphere composition Mole fraction *N,N*-dimethylformamide	0.00	0.29	0.49	0.63	0.72	0.78	0.81	0.84	0.87	0.92	1.00

Stellenbosch University http://scholar.sun.ac.za

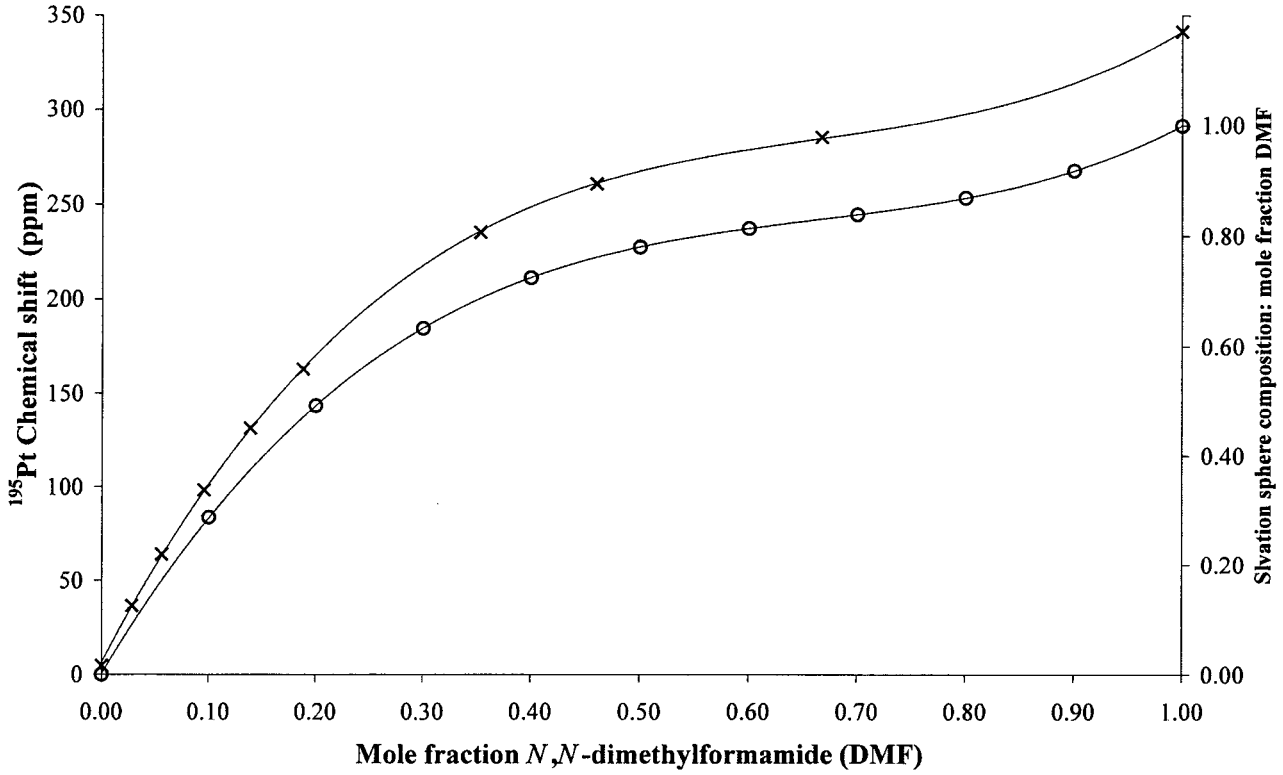

Fig. 4.8-Adm The ^{195}Pt (as $PtCl_6^{2-}$) chemical shift as a function of solvent composition in the D_2O/DMF binary solvent system (×). A best-fit polynomial trendline (3rd order) has been inserted: $y = 769x^3 - 1528x^2 + 1094x + 6.27$ ($R^2 = 1.00$). The estimated variation of the $PtCl_6^{2-}$ solvation sphere composition (mole fraction DMF) with changing bulk solvent composition is also depicted (O); a best-fit trendline has been inserted.

Stellenbosch University http://scholar.sun.ac.za

Table 4.9A-Adm Stock solutions of D_2O and methanol containing H_2PtBr_6 were made and used to prepare the D_2O/methanol binary solvent system. Bulk solvent composition and resultant ^{195}Pt chemical shifts (ppm) are indicated in the last two columns; see Fig. 4.9-Adm.

D_2O / METHANOL Binary Solvent System - $PtBr_6^{2-}$												
Solution A (Sol(A))					**Solution B (Sol(B))**							
Solvent D_2O (M_r = 20.03 g mol^{-1})					Solvent Methanol (M_r = 32.05 g mol^{-1})							
Mass of H_2PtBr_6 = 0.4057 g					**Mass of H_2PtBr_6 = 0.4047 g**							
Mass of stock solution upon addition of 5.00 cm^3 of D_2O = 5.9333 g					**Mass of stock solution upon addition of 5.00 cm^3 of 1,2-Dimethoxyethane = 4.3412 g**							
∴ 0.06838 g (H_2PtBr_6) / g solution					**∴ 0.09322 g (H_2PtBr_6) / g solution**							
Sample	**Mass Sol(A) (g)**	**Mass (H_2PtBr_6) (g)**	**Mass D_2O (g)**	**Moles D_2O**	**Mass Sol(B) (g)**	**Mass (H_2PtBr_6) (g)**	**Mass Methanol (g)**	**Moles Methanol**	**Total Moles Solvent**	**Total Mass (H_2PtBr_6) (g)**	**Mole Fraction Methanol**	**^{195}Pt Chem Shift (ppm)**
1	-	-	-	-	0	-	-	-	-	-	0	-2
2	0.6795	0.04646	0.633	0.03160	0.0573	0.00534	0.0520	0.001621	0.03323	0.0518	0.0488	8
3	0.5817	0.03978	0.542	0.02706	0.1088	0.01014	0.0987	0.003078	0.03013	0.04992	0.1022	18
4	0.5105	0.03491	0.4756	0.02374	0.1777	0.01657	0.1611	0.005028	0.02877	0.0515	0.1747	32
5	0.4336	0.02965	0.4040	0.02017	0.2242	0.02090	0.2033	0.00634	0.02651	0.0505	0.2393	43
6	0.3637	0.02487	0.3388	0.01692	0.2918	0.02720	0.2646	0.00826	0.02517	0.0521	0.3280	56
7	0.2812	0.01923	0.2620	0.01308	0.3439	0.03206	0.3118	0.00973	0.02281	0.0513	0.4266	69
8	0.2149	0.01469	0.2002	0.01000	0.3863	0.03601	0.3503	0.01093	0.02092	0.0507	0.522	78
9	0.1455	0.00995	0.1356	0.00677	0.4462	0.04159	0.4046	0.01262	0.01939	0.0515	0.651	88
10	0.0792	0.00542	0.0738	0.003684	0.4937	0.04602	0.4477	0.01397	0.01765	0.0514	0.791	98
11	0	-	-	-	-	-	-	-	-	-	1	116

Table 4.9B-Adm Estimated $PtBr_6^{2-}$ solvation sphere composition (as mole fraction methanol) as a function of bulk solvent composition for the D_2O/methanol binary solvent system; see Fig. 4.9-Adm.

Bulk solvent composition Mole fraction methanol	**0**	**0.1**	**0.2**	**0.3**	**0.4**	**0.5**	**0.6**	**0.7**	**0.8**	**0.9**	**1.0**
Solvation sphere composition Mole fraction methanol	0.00	0.17	0.33	0.46	0.56	0.65	0.73	0.80	0.86	0.93	1.00

Stellenbosch University http://scholar.sun.ac.za

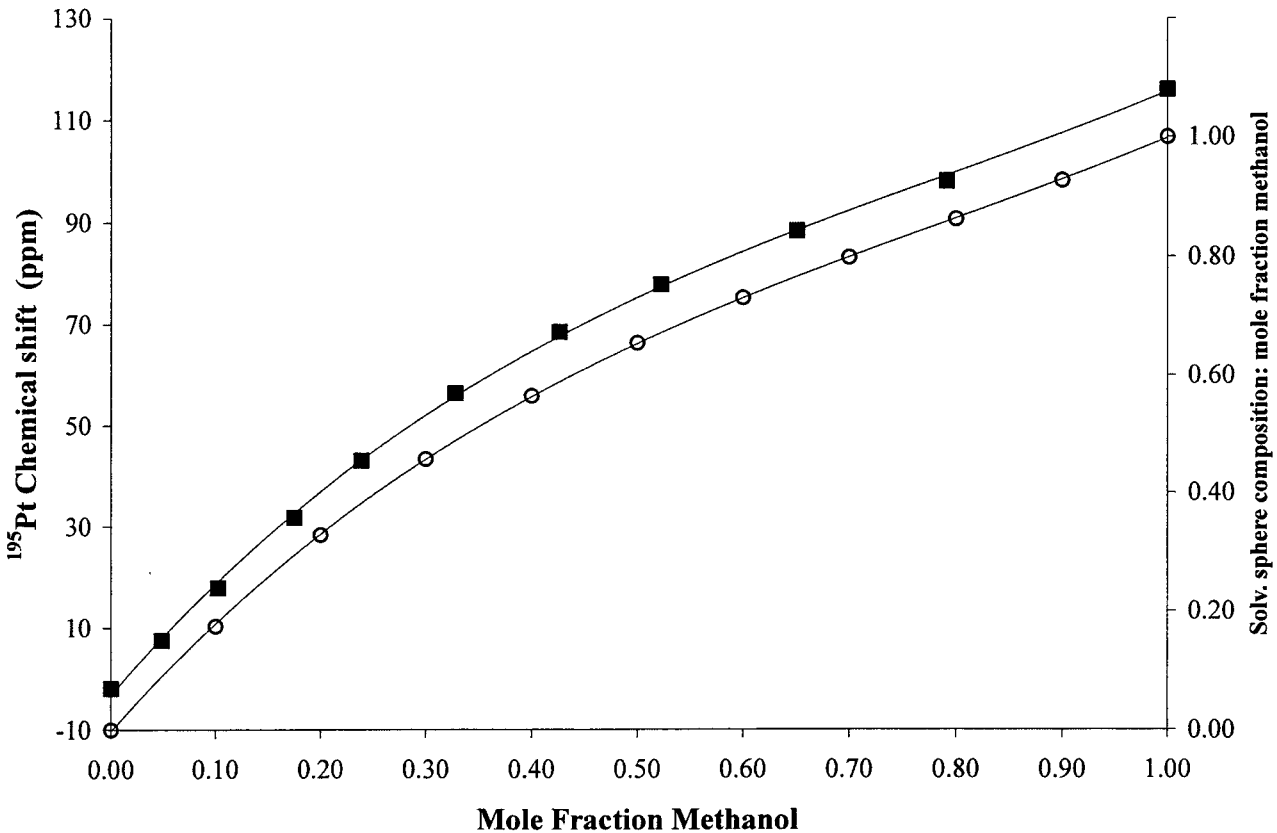

Fig. 4.9-Adm The ^{195}Pt (as $PtBr_6^{2-}$) chemical shift as a function of solvent composition in the D_2O/methanol binary solvent system (■). A best-fit polynomial trendline (3rd order) has been inserted; $y = 87.3x^3 - 207.0x^2 + 238.5x - 3.222$ ($R^2 = 1.00$). The estimated variation of the $PtBr_6^{2-}$ solvation sphere composition (mole fraction methanol) with changing bulk solvent composition is also depicted (O); a best-fit trendline has been inserted.

Stellenbosch University http://scholar.sun.ac.za

Table 4.10A-Adm Stock solutions of D_2O and acetonitrile containing H_2PtBr_6 were made and used to prepare the D_2O/acetonitrile binary solvent system. Bulk solvent composition and resultant ^{195}Pt chemical shifts (ppm) are indicated in the last two columns; see Fig. 4.10-Adm.

D_2O / ACETONITRILE Binary Solvent System - $PtBr_6^{2-}$												
Solution A (Sol(A)) - Solvent D_2O (M_r = 20.03 g mol^{-1})					**Solution B (Sol(B))** - Solvent Acetonitrile (M_r = 41.06 g mol^{-1})							
Mass of H_2PtBr_6 = 0.2101 g					**Mass of H_2PtBr_6 = 0.2145 g**							
Mass of stock solution upon addition of 5.00 cm^3 of D_2O = 5.7201 g					**Mass of stock solution upon addition of 5.00 cm^3 of Acetonitrile = 4.1249 g**							
∴ 0.03673 g (H_2PtBr_6) / g solution					**∴ 0.05200 g (H_2PtBr_6) / g solution**							
Sample	**Mass Sol(A) (g)**	**Mass (H_2PtBr_6) (g)**	**Mass D_2O (g)**	**Moles D_2O**	**Mass Sol(B) (g)**	**Mass (H_2PtBr_6) (g)**	**Mass Acetonitrile (g)**	**Moles Acetonitrile**	**Total Moles Solvent**	**Total Mass (H_2PtBr_6) (g)**	**Mole Fraction Acetonitrile**	**^{195}Pt Chem Shift (ppm)**
1	-	-	-	-	0	-	-	-	-	-	0	-2
2	0.5768	0.02119	0.556	0.02774	0.0790	0.004108	0.0749	0.001824	0.02956	0.02529	0.0617	41
3	0.5448	0.02001	0.525	0.02620	0.1421	0.00739	0.1347	0.003281	0.02948	0.02740	0.1113	75
4	0.4583	0.01683	0.4415	0.02204	0.2136	0.01111	0.2025	0.004932	0.02697	0.02794	0.1828	116
5	0.3811	0.01400	0.3671	0.01833	0.2871	0.01493	0.2722	0.00663	0.02496	0.02893	0.2656	147
6	0.3171	0.01165	0.3055	0.01525	0.3344	0.01739	0.3170	0.00772	0.02297	0.02904	0.3361	165
7	0.2583	0.00949	0.2488	0.01242	0.3894	0.02025	0.3692	0.00899	0.02141	0.02974	0.4199	181
8	0.1956	0.00718	0.1884	0.00941	0.4614	0.02399	0.4374	0.01065	0.02006	0.03118	0.531	199
9	0.1457	0.00535	0.1403	0.00701	0.5199	0.02703	0.4929	0.01200	0.01901	0.03239	0.631	214
10	0.0693	0.002545	0.0668	0.003333	0.6022	0.03131	0.571	0.01390	0.01724	0.03386	0.807	238
11	0	-	-	-	-	-	-	-	-	-	1	259

Table 4.10B-Adm Estimated $PtBr_6^{2-}$ solvation sphere composition (as mole fraction acetonitrile) as a function of bulk solvent composition for the D_2O/acetonitrile binary solvent system; see Fig. 4.10-Adm.

Bulk solvent composition Mole fraction acetonitrile	**0**	**0.1**	**0.2**	**0.3**	**0.4**	**0.5**	**0.6**	**0.7**	**0.8**	**0.9**	**1.0**
Solvation sphere composition Mole fraction acetonitrile	0.00	0.28	0.47	0.60	0.69	0.76	0.81	0.86	0.91	0.96	1.00

Stellenbosch University http://scholar.sun.ac.za

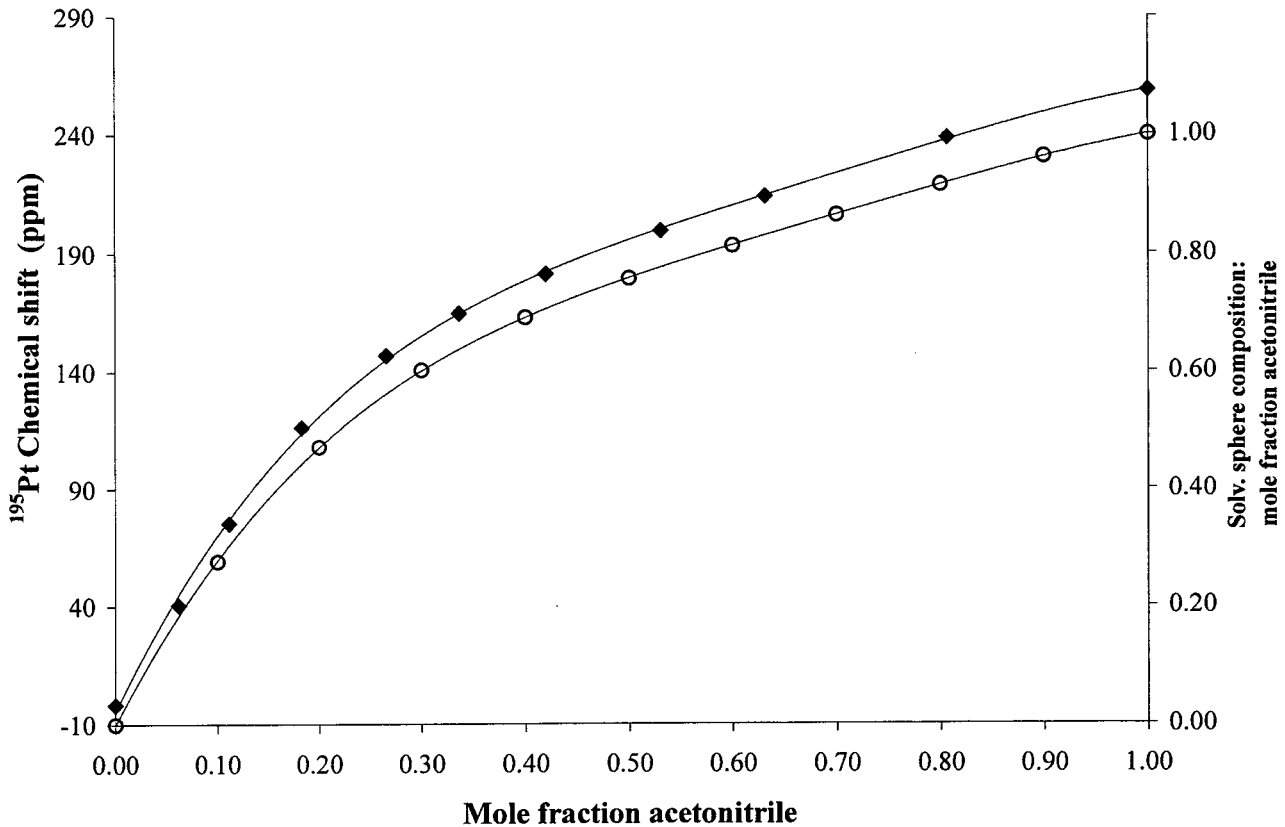

Fig. 4.10-Adm The ^{195}Pt (as $PtBr_6^{2-}$) chemical shift as a function of solvent composition in the D_2O/acetonitrile binary solvent system (◆). A best-fit polynomial trendline (4th order) has been inserted; $y = -534x^4 + 1511x^3 - 1606x^2 + 892x - 4.497$ ($R^2 = 0.999$). The estimated variation of the $PtBr_6^{2-}$ solvation sphere composition (mole fraction acetonitrile) with changing bulk solvent composition is also depicted (O); a best-fit trendline has been inserted.

Stellenbosch University http://scholar.sun.ac.za

Table 4.11A-Adm Stock solutions of D_2O and acetone containing H_2PtBr_6 were made and used to prepare the D_2O/acetone binary solvent system. Bulk solvent composition and resultant ^{195}Pt chemical shifts (ppm) are indicated in the last two columns; see Fig. 4.11-Adm.

D_2O / ACETONE Binary Solvent System - $PtBr_6^{2-}$	
Solution A (Sol(A))	**Solution B (Sol(B))**
Solvent D_2O (M_r = 20.03 g mol^{-1})	Solvent Acetone (M_r = 58.09 g mol^{-1})
Mass of H_2PtBr_6 = 0.4007 g	**Mass of H_2PtBr_6 = 0.4051 g**
Mass of stock solution upon addition of 5.00 cm^3 of D_2O = 5.9187 g	**Mass of stock solution upon addition of 5.00 cm^3 of Acetone = 4.3425 g**
∴ 0.06770 g (H_2PtBr_6) / g solution	**∴ 0.0933 g (H_2PtBr_6) / g solution**

Sample	Mass Sol(A) (g)	Mass (H_2PtBr_6) (g)	Mass D_2O (g)	Moles D_2O	Mass Sol(B) (g)	Mass (H_2PtBr_6) (g)	Mass Acetone (g)	Moles Acetone	Total Moles Solvent	Total Mass (H_2PtBr_6) (g)	Mole Fraction Acetone	^{195}Pt Chem Shift (ppm)
1	-	-	-	-	0	-	-	-	-	-	0	-2
2	0.4599	0.03114	0.4288	0.02141	0.0542	0.00506	0.04914	0.000846	0.02225	0.03619	0.0380	34
3	0.4125	0.02793	0.3846	0.01920	0.1086	0.01013	0.0985	0.001695	0.02090	0.03806	0.0811	73
4	0.3807	0.02577	0.3549	0.01772	0.1554	0.01450	0.1409	0.002426	0.02015	0.04027	0.1204	106
5	0.3424	0.02318	0.3192	0.01594	0.2103	0.01962	0.1907	0.003283	0.01922	0.04280	0.1708	141
6	0.2668	0.01806	0.2487	0.01242	0.2655	0.02477	0.2407	0.004144	0.01656	0.04283	0.2502	181
7	0.2113	0.01431	0.1970	0.00984	0.3172	0.02959	0.2876	0.004951	0.01479	0.04390	0.3348	211
8	0.1565	0.01060	0.1459	0.00728	0.3635	0.03391	0.3296	0.00567	0.01296	0.04451	0.4379	236
9	0.1069	0.00724	0.0997	0.004976	0.4373	0.04080	0.3965	0.00683	0.01180	0.04803	0.578	258
10	0.0796	0.00539	0.0742	0.003705	0.4816	0.04493	0.4367	0.00752	0.01122	0.0503	0.670	268
11	0	-	-	-	-	-	-	-	-	-	1	281

Table 4.11B-Adm Estimated $PtBr_6^{2-}$ solvation sphere composition (as mole fraction acetone) as a function of bulk solvent composition for the D_2O/acetone binary solvent system; see Fig. 4.11-Adm.

Bulk solvent composition Mole fraction acetone	**0**	**0.1**	**0.2**	**0.3**	**0.4**	**0.5**	**0.6**	**0.7**	**0.8**	**0.9**	**1.0**
Solvation sphere composition Mole fraction acetone	0.00	0.33	0.56	0.71	0.82	0.88	0.93	0.96	0.98	1.00	1.00

Stellenbosch University http://scholar.sun.ac.za

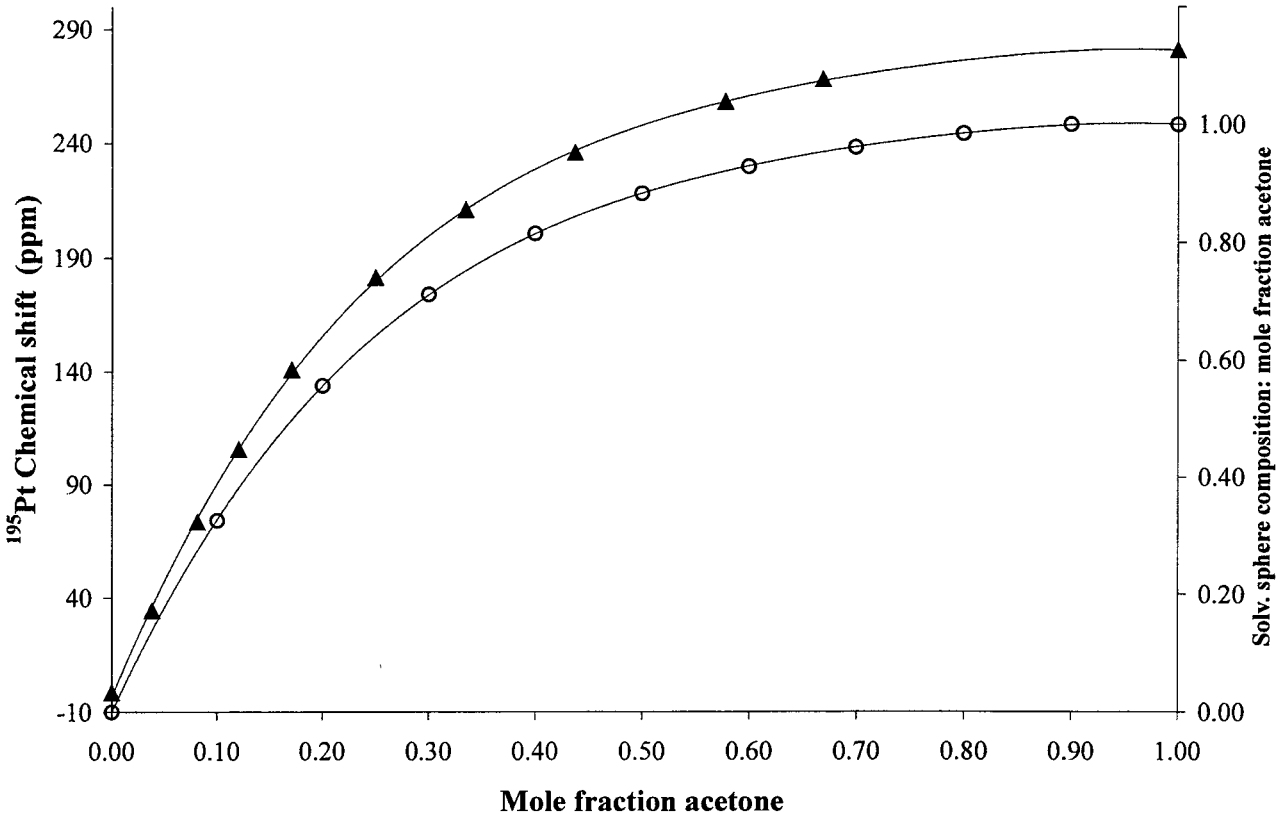

Fig. 4.11-Adm The ^{195}Pt (as $PtBr_6^{2-}$) chemical shift as a function of solvent composition in the D_2O/acetone binary solvent system (▲). A best-fit polynomial trendline (4th order) has been inserted; $y = -523.4x^4 + 1569x^3 - 1873x^2 + 1112x - 3.536$ ($R^2 = 1.00$). The estimated variation of the $PtBr_6^{2-}$ solvation sphere composition (mole fraction acetone) with changing bulk solvent composition is also depicted (O); a best-fit trendline has been inserted.

Stellenbosch University http://scholar.sun.ac.za

Table 4.12A-Adm Stock solutions of D_2O and *N,N*-dimethylformamide (DMF) containing H_2PtBr_6 were made and used to prepare the D_2O/DMF binary solvent system. Bulk solvent composition and resultant ^{195}Pt chemical shifts (ppm) are indicated in the last two columns; see Fig. 4.12-Adm. (This solvent was stored over solid KOH, which may cause decomposition of the solvent; the data must be considered with some uncertainty, and is not included in the Results and Discussion).

D_2O / *N,N*-DIMETHYLFORMAMIDE Binary Solvent System - $PtBr_6^{2-}$	
Solution A (Sol(A))	**Solution B (Sol(B))**
Solvent D_2O (M_r = 20.03 g mol^{-1})	Solvent *N,N*-Dimethylformamide, DMF (M_r = 73.11 g mol^{-1})
Mass of H_2PtBr_6 = 0.4464 g	**Mass of H_2PtBr_6 = 0.4453 g**
Mass of stock solution upon addition of 5.00 cm^3 of D_2O = 5.9761 g	**Mass of stock solution upon addition of 5.00 cm^3 of DMF = 5.1768 g**
∴ 0.07470 g (H_2PtBr_6) / g solution	**∴ 0.0860 g (H_2PtBr_6) / g solution**

Sample	Mass Sol(A) (g)	Mass (H_2PtBr_6) (g)	Mass D_2O (g)	Moles D_2O	Mass Sol(B) (g)	Mass (H_2PtBr_6) (g)	Mass DMF (g)	Moles DMF	Total Moles Solvent	Total Mass (H_2PtBr_6) (g)	Mole Fraction DMF	^{195}Pt Chem Shift (ppm)
1	-	-	-	-	0	-	-	-	-	-	0	-2
2	0.6228	0.04652	0.5763	0.02877	0.0635	0.00546	0.0580	0.000794	0.02956	0.0520	0.02685	36
3	0.5599	0.04182	0.5181	0.02587	0.1144	0.00984	0.1046	0.001430	0.02730	0.0517	0.0524	68
4	0.4923	0.03677	0.4555	0.02274	0.1828	0.01572	0.1671	0.002285	0.02503	0.0525	0.0913	110
5	0.4131	0.03086	0.3822	0.01908	0.231	0.01987	0.2111	0.002888	0.02197	0.0507	0.1314	146
6	0.3572	0.02668	0.3305	0.01650	0.3014	0.02593	0.2755	0.003768	0.02027	0.0526	0.1859	188
7	0.2798	0.02090	0.2589	0.01293	0.3472	0.02987	0.3173	0.004341	0.01727	0.0508	0.2514	228
8	0.2795	0.02088	0.2586	0.01291	0.4052	0.03486	0.3703	0.00507	0.01798	0.0557	0.2818	242
9	0.1507	0.01126	0.1394	0.00696	0.4586	0.03945	0.4192	0.00573	0.01269	0.0507	0.4516	296
10	0.0960	0.00717	0.0888	0.004435	0.5083	0.04372	0.4646	0.00635	0.01080	0.0509	0.589	317
11	0	-	-	-	-	-	-	-	-	-	1	364

Table 4.12B-Adm Estimated $PtBr_6^{2-}$ solvation sphere composition (as mole fraction *N,N*-dimethylformamide) as a function of bulk solvent composition for the D_2O/*N,N*-dimethylformamide binary solvent system; see Fig. 4.12-Adm.

Bulk solvent composition Mole fraction *N,N*-dimethylformamide	**0**	**0.1**	**0.2**	**0.3**	**0.4**	**0.5**	**0.6**	**0.7**	**0.8**	**0.9**	**1.0**
Solvation sphere composition Mole fraction *N,N*-dimethylformamide	0.00	0.33	0.55	0.69	0.78	0.84	0.88	0.91	0.94	0.97	1.00

Stellenbosch University http://scholar.sun.ac.za

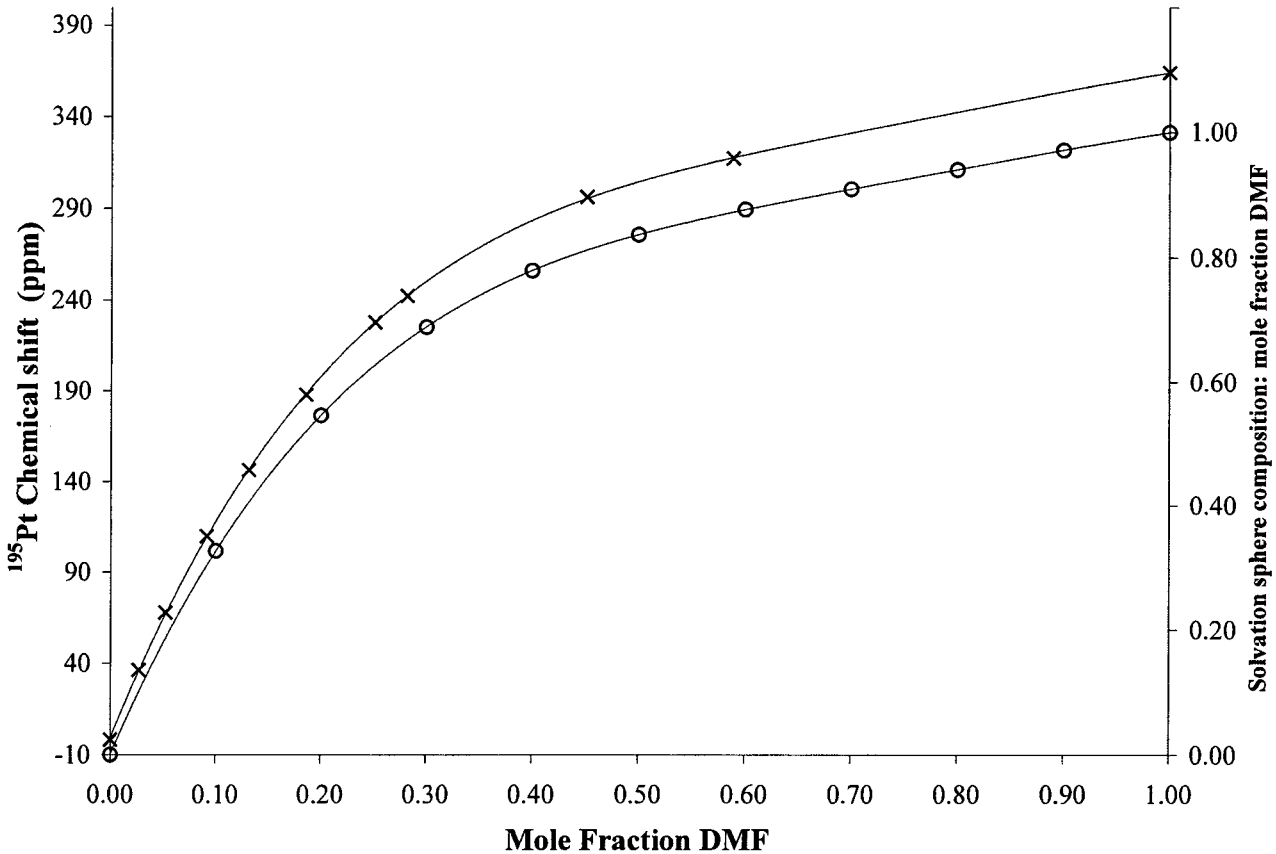

Fig. 4.12-Adm The ^{195}Pt (as $PtBr_6^{2-}$) chemical shift as a function of solvent composition in the D_2O/*N*,*N*-dimethylformamide binary solvent system (×). A best-fit polynomial trendline (4th order) has been inserted; $y = -681x^4 + 2142x^3 - 2512x^2 + 1416x - 0.747$ ($R^2 = 1.00$). The estimated variation of the $PtBr_6^{2-}$ solvation sphere composition (mole fraction *N*,*N*-dimethylformamide) with changing bulk solvent composition is also depicted (O); a best-fit trendline has been inserted.

Stellenbosch University http://scholar.sun.ac.za

Stellenbosch University http://scholar.sun.ac.za

Addendum B

Table 5.1Adm Solution preparation, resultant $PtCl_6^{2-}$ concentrations, and ^{195}Pt chemical shifts for the dilution series: **$H_2PtCl_6 \cdot H_2O$ in H_2O.**

Sample	Mass $H_2PtCl_6 \cdot H_2O$ (g)	Vol. Sample 1 (cm^3)	Vol. deion. H_2O (cm^3)	$[PtCl_6^{2-}]$ (M)	$\delta^{195}Pt$ (Hz)
1	0.2417		5.000	0.1130	7.3
2		2.000	2.000	0.05650	7.7
3		1.000	3.000	0.02825	8.1
4		0.500	3.500	0.01413	8.2

0.2417 g $H_2PtCl_6 \cdot H_2O$ was weighed into a polytop and 5 cm^3 of deionised water pipetted onto it. For Samples 2-4 volumes of Sample 1 (column (3)) were pipetted into polytops, after which appropriate volumes of deionised water (column (4), pipet) were added to achieve a final volume of 4.000 cm^3 for each sample. (M_r ($H_2PtCl_6 \cdot H_2O$) = 427.82 g mol^{-1}).
The ^{195}Pt chemical shifts were determined for each solution relative to the ^{195}Pt external reference solutions (^{195}Pt reference solution: 500 mg.ml^{-1} $H_2PtCl_6 \cdot H_2O$ in 30 % v/v D_2O / 1 M HCl).

Table 5.2Adm Solution preparation, resultant $PtCl_6^{2-}$ concentrations, and ^{195}Pt chemical shifts for the dilution series: **$H_2PtCl_6 \cdot H_2O$ in Methanol.**

Sample	Mass $H_2PtCl_6 \cdot H_2O$ (g)	Vol. Sample 1 (cm^3)	Vol. methanol (cm^3)	$[PtCl_6^{2-}]$ (M)	$\delta^{195}Pt$ (Hz)
1	0.2597		5.000	0.1214	93.8
2		2.000	2.000	0.06070	95.4
3		1.000	3.000	0.03035	96.4
4		0.500	3.500	0.01518	96.8
5		0.250	3.750	0.00759	96.9

0.2597 g $H_2PtCl_6 \cdot H_2O$ was weighed into a polytop and 5 cm^3 of methanol pipetted onto it. For Samples 2-5 volumes of Sample 1 (column (3)) were pipetted into polytops, after which appropriate volumes of methanol (column (4), pipet) were added to achieve a final volume of 4.000 cm^3 for each sample. (M_r ($H_2PtCl_6 \cdot H_2O$) = 427.82 g mol^{-1}).
The ^{195}Pt chemical shifts were determined for each solution relative to the ^{195}Pt external reference solutions (^{195}Pt reference solution: 500 mg.ml^{-1} $H_2PtCl_6 \cdot H_2O$ in 30 % v/v D_2O / 1 M HCl).

Stellenbosch University http://scholar.sun.ac.za

Table 5.3Adm Solution preparation, resultant $PtCl_6^{2-}$ concentrations, and ^{195}Pt chemical shifts for the dilution series: **$H_2PtCl_6 \cdot H_2O$ in Acetonitrile**.

Sample	Mass $H_2PtCl_6 \cdot H_2O$ (g)	Vol. Sample 1 (cm^3)	Vol. acetonitrile (cm^3)	$[PtCl_6^{2-}]$ (M)	$\delta^{195}Pt$ (Hz)
1	0.2439		5.000	0.1140	211.7
2		2.000	2.000	0.05700	222.1
3		1.000	3.000	0.02850	231.8
4		0.500	3.500	0.01425	239.8

0.2439 g $H_2PtCl_6 \cdot H_2O$ was weighed into a polytop and 5 cm^3 of acetonitrile pipetted onto it. For Samples 2-4 volumes of Sample 1 (column (3)) were pipetted into polytops, after which appropriate volumes of acetonitrile (column (4), pipet) were added to achieve a final volume of 4.000 cm^3 for each sample. (M_r ($H_2PtCl_6 \cdot H_2O$) = 427.82 g mol^{-1}).
The ^{195}Pt chemical shifts were determined for each solution relative to the ^{195}Pt external reference solutions (^{195}Pt reference solution: 500 mg.ml^{-1} $H_2PtCl_6 \cdot H_2O$ in 30 % v/v D_2O / 1 M HCl).

Table 5.4Adm Solution preparation, resultant $PtBr_6^{2-}$ concentrations, and ^{195}Pt chemical shifts for the dilution series: **H_2PtBr_6 in H_2O**.

Sample	Mass H_2PtBr_6 (g)	Vol. Sample 1 (cm^3)	Vol. deion. H_2O (cm^3)	$[PtBr_6^{2-}]$ (M)	$\delta^{195}Pt$ (Hz)
1	0.4104		5.000	0.1213	-0.6
2		2.000	2.000	0.06065	-0.4
3		1.000	3.000	0.03033	-0.2
4		0.500	3.500	0.01516	0
5		0.250	3.750	0.00758	0

0.4104 g H_2PtBr_6 was weighed into a polytop and 5 cm^3 of deionised water pipetted onto it. For Samples 2-5 volumes of Sample 1 (column (3)) were pipetted into polytops, after which appropriate volumes of deionised water (column (4), pipet) were added to achieve a final volume of 4.000 cm^3 for each sample. (M_r (H_2PtBr_6) = 676.50 g mol^{-1}).
The ^{195}Pt chemical shifts were determined for each solution relative to the ^{195}Pt external reference solution (^{195}Pt reference solution: 250 mg.ml^{-1} H_2PtBr_6 in 67 % v/v D_2O / 3 M HBr).

Stellenbosch University http://scholar.sun.ac.za

Table 5.5Adm Solution preparation, resultant $PtBr_6^{2-}$ concentrations, and ^{195}Pt chemical shifts for the dilution series: **H_2PtBr_6 in Methanol.**

Sample	Mass H_2PtBr_6 (g)	Vol. Sample 1 (cm^3)	Vol. methanol (cm^3)	$[PtBr_6^{2-}]$ (M)	$\delta^{195}Pt$ (Hz)
1	0.4105		5.000	0.1214	111.8
2		2.000	2.000	0.06070	113.1
3		1.000	3.000	0.03035	113.5

0.4105 g H_2PtBr_6 was weighed into a polytop and 5 cm^3 of methanol pipetted onto it. For Samples 2-3 volumes of Sample 1 (column (3)) were pipetted into polytops, after which appropriate volumes of methanol (column (4), pipet) were added to achieve a final volume of 4.000 cm^3 for each sample. (M_r (H_2PtBr_6) = 676.50 g mol^{-1}).
The ^{195}Pt chemical shifts were determined for each solution relative to the ^{195}Pt external reference solution (^{195}Pt reference solution: 250 mg.ml^{-1} H_2PtBr_6 in 67 % v/v D_2O / 3 M HBr).

Table 5.6Adm Solution preparation, resultant $PtBr_6^{2-}$ concentrations, and ^{195}Pt chemical shifts for the dilution series: **H_2PtBr_6 in Acetonitrile.**

Sample	Mass H_2PtBr_6 (g)	Vol. Sample 1 (cm^3)	Vol. acetonitrile (cm^3)	$[PtBr_6^{2-}]$ (M)	$\delta^{195}Pt$ (Hz)
1	0.4108		5.000	0.1214	241.2
2		2.000	2.000	0.06070	253.1
3		1.000	3.000	0.03035	263.1
4		0.500	3.500	0.01518	271.9
5		0.250	3.750	0.00759	279.9

0.4108 g H_2PtBr_6 was weighed into a polytop and 5 cm^3 of acetonitrile pipetted onto it. For Samples 2-5 volumes of Sample 1 (column (3)) were pipetted into polytops, after which appropriate volumes of acetonitrile (column (4), pipet) were added to achieve a final volume of 4.000 cm^3 for each sample. (M_r (H_2PtBr_6) = 676.50 g mol^{-1}).
The ^{195}Pt chemical shifts were determined for each solution relative to the ^{195}Pt external reference solution (^{195}Pt reference solution: 250 mg.ml^{-1} H_2PtBr_6 in 67 % v/v D_2O / 3 M HBr).

Stellenbosch University http://scholar.sun.ac.za

Table 5.7Adm Solution preparation, resultant Na^+ concentrations, and ^{23}Na chemical shifts for the series: **$NaClO_4$ in H_2O**.

Sample	Mass $NaClO_4$ (g)		Vol. deion. H_2O (cm^3)	$[Na^+]$ (M)	$\log[Na^+]$	$\delta^{23}Na$ (Hz)
1	0.6235		0.700	7.275	0.862	-516.8
2	0.4338		0.700	5.061	0.704	-382.8
3	0.2875		0.700	3.354	0.526	-274.8
4	0.1522		0.700	1.776	0.249	-164.1
5	0.3025		3.000	0.824	-0.0841	-88.2
		Vol. Sample 5 (cm^3)				
6		0.350		0.4118	-0.385	-53.02
7		0.210		0.2471	-0.607	-37.6
8		0.070		0.0824	-1.084	-20.7
9		0.150	2.850	0.04118	-1.385	-14.7
		Vol. Sample 9 (cm^3)				
10		0.350		0.02059	-1.686	-11.0
11		0.087		0.005118	-2.291	0.0

For samples 1-5, $NaClO_4$ was weighed (column (2)) into polytops and a volume of deionised water (column (4)) pipetted onto the salt. For samples 6-9, volumes of Sample 5 (column (3)) were measured into clean polytops; Sample 9 was completed by adding a further 2.850 cm^3 of deionised water (column (4), pipet). For samples 10-11, volumes of Sample 9 (column (3)) were measured into polytops. The solvent was evaporated off Samples 6, 7, 8, 10 and 11 in an oven, whereafter 0.700 cm^3 of deionised water was pipetted onto the cooled salt for each sample to affect the desired $[Na^+]$. (M_r ($NaClO_4$) = 122.44 g mol^{-1}).
The ^{23}Na chemical shifts were determined for each solution relative to the ^{23}Na external reference solution (1.034 M NaCl in D_2O).

Stellenbosch University http://scholar.sun.ac.za

Table 5.8Adm Solution preparation, resultant Na^+ concentrations, and ^{23}Na chemical shifts (corrected for the difference in bulk diamagnetic susceptibility between sample and reference) for the series: **$NaClO_4$ in Methanol**.

Sample	Mass $NaClO_4$ (g)		Vol. Methanol (cm^3)	$[Na^+]$ (M)	$log[Na^+]$	$\delta^{23}Na$ (Hz)
1	0.3173		1.000	2.591	0.413	-956.3
2	0.2457		1.000	2.007	0.303	-872.4
3	0.1840		1.000	1.503	0.177	-802.7
4	0.6163		5.000	1.007	0.00303	-732.6
		Vol. Sample 5 (cm^3)				
5		0.500	0.500	0.5035	-0.298	-665.3
6		0.300	0.700	0.3021	-0.520	-634.6
7		0.100	0.900	0.1007	-0.997	-599.5
8		0.250	4.750	0.05035	-1.298	-585.8
		Vol. Sample 9 (cm^3)				
9		0.250	0.750	0.01259	-1.900	-572.0
10		0.125	0.875	0.00629	-2.201	-568.8
11		0.063	0.937	0.003172	-2.499	-565.3

For samples 1-4, $NaClO_4$ was weighed (column (2)) into polytops and a volume of methanol (column (4)) pipetted onto the salt. For samples 5-8, dilutions of Sample 4 (column (3)) were made by pipetting volumes of this sample (column (3)) into clean polytops and adding an appropriate volume of methanol (column (4), pipet) to achieve a final volume of 1 cm^3 (Samples 5-7) or 5 cm^3 (Sample 8). For samples 9-11, dilutions of Sample 8 were made by pipetting volumes of this sample (column (3)) into polytops and adding an appropriate volume of methanol (column (4)) to achieve a final volume of 1 cm^3. (M_r ($NaClO_4$) = 122.44 g mol^{-1}).

The ^{23}Na chemical shifts were determined for each solution relative to the ^{23}Na external reference solution (1.034 M NaCl in D_2O).

Stellenbosch University http://scholar.sun.ac.za

Table 5.9Adm Solution preparation, resultant Na^+ concentrations, and ^{23}Na chemical shifts (corrected for the difference in bulk diamagnetic susceptibility between sample and reference) for the series: **$NaClO_4$ in Acetonitrile**.

Sample	Mass $NaClO_4$ (g)		Vol. Acetonitrile (cm^3)	$[Na^+]$ (M)	$log[Na^+]$	$\delta^{23}Na$ (Hz)
1	0.2577		1.000	2.105	0.323	-1368.9
2	0.1864		1.000	1.522	0.182	-1321.2
3	0.6158		5.000	1.006	0.00260	-1282.4
		Vol. Sample 3 (cm^3)				
4		0.500	0.500	0.503	-0.298	-1230.6
5		0.300	0.700	0.3018	-0.520	-1204.0
6		0.100	0.900	0.1006	-0.997	-1163.8
7		0.250	4.750	0.0503	-1.298	-1172.0
		Vol. Sample 7 (cm^3)				
8		0.500	0.500	0.02515	-1.599	-1147.5
9		0.250	0.750	0.01258	-1.900	-1151.6
10		0.125	0.875	0.00629	-2.201	-1147.5
11		0.063	0.937	0.003169	-2.499	-1142.0

For samples 1-3, $NaClO_4$ was weighed (column (2)) into polytops and a volume of acetonitrile (column (4)) pipetted onto the salt. For samples 4-7, dilutions of Sample 3 were made by pipetting volumes of this sample (column (3)) into clean polytops and adding the appropriate volume of acetonitrile (column (4), pipet) to achieve a final volume of 1 cm^3 (Samples 4-6) or 5 cm^3 (Sample 7). For samples 8-11, dilutions of Sample 7 were made by pipetting volumes of this sample (column (3)) into polytops and adding the appropriate volume of acetonitrile (column (4), pipet) to achieve a final volume of 1 cm^3. (M_r ($NaClO_4$) = 122.44 g mol^{-1}).
The ^{23}Na chemical shifts were determined for each solution relative to the ^{23}Na external reference solution (1.034 M NaCl in D_2O).

Stellenbosch University http://scholar.sun.ac.za

Table 5.10Adm Solution preparation, resultant Na^+ concentrations, and ^{23}Na chemical shifts for the series: **NaCl in H_2O**.

Sample	Mass NaCl (g)		Vol. deion. H_2O (cm^3)	$[Na^+]$ (M)	log$[Na^+]$	$\delta^{23}Na$ (Hz)
1	0.3543		1.000	6.063	0.783	45.8
2	0.2330		1.000	3.987	0.601	18.3
3	0.1319		1.000	2.257	0.354	4.1
4	0.5844		10.000	1.000	0	-2.6
		Vol. Sample 4 (cm^3)				
5		0.500	0.500	0.5000	-0.301	-5.1
6		0.250	0.750	0.2500	-0.602	-6.1
7		0.120	0.880	0.1200	-0.921	-6.6
8		0.105	0.895	0.1050	-0.979	-7.1
9		0.090	0.910	0.0900	-1.046	-7.1
10		0.075	0.925	0.0750	-1.125	-7.1
11		0.600	9.400	0.0600	-1.222	-7.1
		Vol. Sample 11 (cm^3)				
12		0.750	0.250	0.04500	-1.347	-7.6
13		0.500	0.500	0.03000	-1.523	-7.6
14		0.250	0.750	0.01500	-1.824	-8.2
15		0.125	0.875	0.00750	-2.125	-7.9

For samples 1-4, NaCl was weighed (column (2)) into polytops and a volume of deionised water (column (4)) pipetted onto the salt. For samples 5-11, dilutions of Sample 4 were made by pipetting volumes of this sample (column (3)) into clean polytops and adding an appropriate volume of deionised water (column (4), pipet) to achieve a final volume of 1 cm^3 (Samples 5-10) or 10 cm^3 (Sample 11). For samples 12-15, dilutions of Sample 11 were made by pipetting volumes of this sample (column (3)) into polytops and adding an appropriate volume of deionised water (column (4), pipet) to achieve a final volume of 1 cm^3. (M_r (NaCl) = 58.44 g mol^{-1}).
The ^{23}Na chemical shifts were determined for each solution relative to the ^{23}Na external reference solution (1.034 M NaCl in D_2O).

Stellenbosch University http://scholar.sun.ac.za

Table 5.11Adm Solution preparation, resultant Na^+ concentrations, and ^{23}Na chemical shifts (corrected for the difference in bulk diamagnetic susceptibility between sample and reference) for the series: **NaCl in Methanol.**

Sample	Vol. 0.1121 M NaCl (cm^3)	Vol. methanol (cm^3)	$[Na^+]$ (M)	$\log[Na^+]$	$\delta^{23}Na$ (Hz)
1	1.000	0	0.1121	-0.950	-543.4
2	0.800	0.200	0.0897	-1.047	-546.0
3	0.700	0.300	0.0785	-1.105	-549.0
4	0.600	0.400	0.0673	-1.172	-549.6
5	0.500	0.500	0.0561	-1.251	-551.6
6	0.300	0.700	0.0336	-1.474	-552.1
7	0.100	0.900	0.0112	-1.951	-559.2

0.0655 g NaCl was weighed into a polytop, and 10 cm^3 of methanol pipetted onto it; $[Na^+]$ = 0.1121 M. Volumes of this 0.1121 M NaCl solution (column (2)) were pipetted into separate polytops, after which appropriate volumes of pure methanol (column (3)) were added to achieve a final volume of 1.000 cm^3. (M_r (NaCl) = 58.44 g mol^{-1}).
The ^{23}Na chemical shifts were determined for each solution relative to the ^{23}Na external reference solution (1.034 M NaCl in D_2O).

Stellenbosch University http://scholar.sun.ac.za

Table 5.12Adm Solution preparation, resultant Na^+ concentrations, and ^{195}Pt and ^{23}Na chemical shifts for the series: **$H_2PtCl_6 \cdot H_2O$ + $NaClO_4$ in H_2O.**

Sample	Vol. 2.501 M $NaClO_4$ (cm^3)	$[Na^+]$ (M)	log$[Na^+]$	$\delta^{195}Pt$ (ppm)	$\delta^{23}Na$ (Hz)
1	1.000	2.501	0.398	2.9	-194.9
2	0.400	1.000	0	5.5	-97.9
3	0.200	0.5002	-0.301	6.6	-57.4
	Vol. 0.2501 M $NaClO_4$ (cm^3)				
4	1.000	0.2501	-0.602	7.1	-36.3
5	0.400	0.1000	-1	7.4	-21.1
6	0.200	0.05002	-1.301	7.6	-15.2
7	0.100	0.02501	-1.602	7.7	-11.7

1.5310 g $NaClO_4$ was weighed into a polytop and 5 cm^3 of deionised H_2O pipetted onto it; $[Na^+]$ = 2.501 M. 0.500 cm^3 of this solution was diluted accurately to 5 cm^3 with deionised H_2O; $[Na^+]$ = 0.2501 M. Volumes of 2.501 M $NaClO_4$ solution and of 0.2501 M $NaClO_4$ solution (column (2)) were pipetted into separate polytops, which were placed in an oven overnight at 60-70°C to allow the solvent to evaporate off. 0.2350 g $H_2PtCl_6 \cdot H_2O$ was weighed into a polytop and 10 cm^3 of deionised water pipetted onto it; **$[PtCl_6^{2-}]$ = 0.05493 M**. Exactly 1cm^3 of the 0.05493 M $H_2PtCl_6 \cdot H_2O$ solution was then pipetted into each of the polytops containing $NaClO_4$ from which the water had been evaporated, to affect the desired $[Na^+]$. (M_r ($H_2PtCl_6 \cdot H_2O$) = 427.82 g mol^{-1}; M_r ($NaClO_4$) = 122.44 g mol^{-1}). The ^{195}Pt and ^{23}Na chemical shifts were determined for each solution relative to the ^{195}Pt and ^{23}Na external reference solutions respectively (^{195}Pt reference solution: 500 mg.ml^{-1} $H_2PtCl_6 \cdot H_2O$ in 30 % v/v D_2O / 1 M HCl; ^{23}Na reference solution: 1.034 M NaCl in D_2O).

Stellenbosch University http://scholar.sun.ac.za

Table 5.13Adm Solution preparation, resultant Na^+ concentrations, and ^{195}Pt and ^{23}Na chemical shifts for the series: **$H_2PtCl_6 \cdot H_2O$ + $NaClO_4$ in Methanol.**

Sample	Vol. 0.05235 M $NaClO_4$ (cm^3)	$[Na^+]$ (M)	log$[Na^+]$	$\delta^{195}Pt$ (ppm)	$\delta^{23}Na$ (Hz)
1	0.100	0.005235	-2.281	95.6	-455.4
2	0.300	0.01571	-1.804	94.1	-461.7
3	0.500	0.02618	-1.582	92.9	-470.4
4	0.600	0.03141	-1.503	92.2	-473.5
5	0.700	0.03665	-1.436	91.7	-478.6
6	0.800	0.04188	-1.378	91.3	-480.6
7	0.900	0.04712	-1.327	90.7	-482.6
8	1.000	0.05235	-1.281	90.2	-486.5
	Vol. 2.448 M $NaClO_4$ (cm^3)				
9	0.014	0.03427	-1.465	90.5	-475.1
10	0.018	0.04406	-1.356	89.9	-479.0
11	0.041	0.1004	-0.998	86.3	-506.6
12	0.204	0.4994	-0.302	73.0	-611.0
13	0.368	0.901	-0.045	65.8	-673.6
14	0.531	1.300	0.114	60.2	-730.7
15	0.694	1.699	0.230	55.2	-786.2
16	0.858	2.100	0.322	50.9	-839.7
17	1.000	2.448	0.389	46.3	-904.3

0.0641 g $NaClO_4$ was weighed into a polytop and 10 cm^3 of methanol pipetted onto it; $[Na^+]$ = 0.05235 M. 2.9973 g $NaClO_4$ dissolved in 10 cm^3 of methanol gave a solution with $[Na^+]$ = 2.448 M. Volumes of these sodium perchlorate solutions (column (2)) were pipetted into separate polytops, which were placed in a vacuum dessicator to evacuate off the solvent. 0.2505 g $H_2PtCl_6 \cdot H_2O$ was weighed into a polytop and 10 cm^3 of methanol pipetted onto it; **$[PtCl_6^{2-}]$ = 0.05855 M**. 0.2530 g $H_2PtCl_6 \cdot H_2O$ dissolved in 10 cm^3 of methanol gave a solution with **$[PtCl_6^{2-}]$ = 0.05914 M**. Exactly 1cm^3 of the 0.05855 M $H_2PtCl_6 \cdot H_2O$ solution was then pipetted into the polytops to complete Samples 1-8, and 1cm^3 of the 0.05914 M $H_2PtCl_6 \cdot H_2O$ solution pipetted into polytops to complete Samples 9-17. (M_r ($H_2PtCl_6 \cdot H_2O$) = 427.82 g mol^{-1}; M_r ($NaClO_4$) = 122.44 g mol^{-1}).
The ^{195}Pt and ^{23}Na chemical shifts were determined for each solution relative to the ^{195}Pt and ^{23}Na external reference solutions respectively (^{195}Pt reference solution: 500 mg.ml^{-1} $H_2PtCl_6 \cdot H_2O$ in 30 % v/v D_2O / 1 M HCl; ^{23}Na reference solution: 1.034 M NaCl in D_2O). ^{23}Na chemical shifts have been corrected for the difference in bulk diamagnetic susceptibility between sample and reference.

Stellenbosch University http://scholar.sun.ac.za

Table 5.14Adm Solution preparation, resultant Na^+ concentrations, and ^{195}Pt and ^{23}Na chemical shifts for the series: **$H_2PtCl_6 \cdot H_2O$ + $NaClO_4$ in Acetonitrile.**

Sample	Mass $NaClO_4$ (g)		$[Na^+]$ (M)	log$[Na^+]$	$\delta^{195}Pt$ (ppm)	$\delta^{23}Na$ (Hz)
1	0.1830		2.135	0.329	124.7	-1326.1
2	0.1290		1.505	0.178	137.2	-1264.2
		Vol. 1.021 M $NaClO_4$ (cm^3)				
3		0.700	1.021	0.00903	149.4	-1153.8
4		0.350	0.5105	-0.292	167.4	-1119.8
5		0.210	0.3063	-0.514	179.0	-1068.7
6		0.070	0.1021	-0.991	196.9	-962.4
		Vol. 0.05105 M $NaClO_4$ (cm^3)				
7		0.700	0.05105	-1.292	206.8	-900.5
8		0.350	0.02553	-1.593	213.2	-862.3
9		0.175	0.01277	-1.894	217.1	-833.0
10		0.088	0.00642	-2.193	219.3	-831.7
11		0.044	0.003209	-2.494	220.9	-815.3

0.2709 g $H_2PtCl_6 \cdot H_2O$ was weighed into a polytop and 10 cm^3 of acetonitrile pipetted onto it; **$[PtCl_6^{2-}] = 0.06332$ M**. 0.3750 g $NaClO_4$ was weighed into a polytop, and 3 cm^3 of acetonitrile pipetted onto it; $[Na^+] = 1.021$ M. 0.150 cm^3 of this solution was diluted to 3 cm^3; $[Na^+] = 0.05105$ M. For Samples 1 & 2, $NaClO_4$ was weighed (column (2)) into polytops. For Samples 3-6 volumes of the 1.021 M $NaClO_4$ solution, and for Samples 7-11 volumes of the 0.05105 M $NaClO_4$ solution, were pipetted (column (3)) into polytops. Samples 3-11 were placed in an oven at 60-70°C to allow the solvent to evaporate off. Exactly 0.700 cm^3 of the 0.06332 M $H_2PtCl_6 \cdot H_2O$ solution was pipetted into each of the polytops containing $NaClO_4$, to affect the desired $[Na^+]$. (M_r ($H_2PtCl_6 \cdot H_2O$) = 427.82 g mol^{-1}; M_r ($NaClO_4$) = 122.44 g mol^{-1}).
The ^{195}Pt and ^{23}Na chemical shifts were determined for each solution relative to the ^{195}Pt and ^{23}Na external reference solutions respectively (^{195}Pt reference solution: 500 mg.ml^{-1} $H_2PtCl_6 \cdot H_2O$ in 30 % v/v D_2O / 1 M HCl; ^{23}Na reference solution: 1.034 M NaCl in D_2O). ^{23}Na chemical shifts have been corrected for the difference in bulk diamagnetic susceptibility between sample and reference.

Stellenbosch University http://scholar.sun.ac.za

Table 5.15Adm Solution preparation, resultant Na^+ concentrations, and ^{195}Pt and ^{23}Na chemical shifts for the series: **H_2PtBr_6 + $NaClO_4$ in H_2O.**

Sample	Mass $NaClO_4$ (g)		$[Na^+]$ (M)	log$[Na^+]$	$\delta^{195}Pt$ (ppm)	$\delta^{23}Na$ (Hz)
1	0.5782		6.746	0.829	-13.2	-494.2
2	0.4275		4.988	0.698	-9.6	-385.3
3	0.2820		3.290	0.517	-6.3	-275.0
4	0.1478		1.724	0.237	-3.4	-165.0
		Vol. 0.8222 M $NaClO_4$ (cm^3)				
5		0.700	0.822	-0.0850	-1.9	-92.6
6		0.350	0.4111	-0.386	-1.2	-54.6
7		0.210	0.2467	-0.608	-0.9	-38.5
8		0.070	0.0822	-1.085	-0.6	-21.1
		Vol. 0.04111 M $NaClO_4$ (cm^3)				
9		0.700	0.04111	-1.386	-0.5	-15.2
10		0.350	0.02056	-1.687	-0.5	-12.1
11		0.175	0.01028	-1.988	-0.5	-10.1
12		0.087	0.005109	-2.292	-0.5	0
13		0.043	0.002525	-2.598	-0.5	0

0.4132 g H_2PtBr_6 was weighed into a polytop and 10 cm^3 of deionised water pipetted onto it; **$[PtBr_6^{2-}]$ = 0.06108 M**. 0.3020 g $NaClO_4$ was weighed into a polytop, and 3 cm^3 of deionised water pipetted onto it; $[Na^+]$ = 0.8222 M. 0.150 cm^3 of this solution was diluted to 3 cm^3; $[Na^+]$ = 0.04111 M. For Samples 1-4, $NaClO_4$ was weighed (column (2)) into polytops. For Samples 5-8 volumes of the 0.8222 M $NaClO_4$ solution, and for Samples 9-13 volumes of the 0.04111 M $NaClO_4$ solution, were pipetted (column (3)) into polytops. Samples 5-13 were placed in an oven at 60-70°C to allow the solvent to evaporate off. Exactly 0.700 cm^3 of the 0.06108M H_2PtBr_6 solution was pipetted into each of the polytops containing $NaClO_4$, to affect the desired $[Na^+]$. (M_r (H_2PtBr_6) = 676.50 g mol^{-1}; M_r ($NaClO_4$) = 122.44 g mol^{-1}).

The ^{195}Pt and ^{23}Na chemical shifts were determined for each solution relative to the ^{195}Pt and ^{23}Na external reference solutions respectively (^{195}Pt reference solution: 250 mg.ml^{-1} H_2PtBr_6 in 67 % v/v D_2O / 3 M HBr; ^{23}Na reference solution: 1.034 M NaCl in D_2O).

Stellenbosch University http://scholar.sun.ac.za

Table 5.16Adm Solution preparation, resultant Na^+ concentrations, and ^{195}Pt and ^{23}Na chemical shifts for the series: **H_2PtBr_6 + $NaClO_4$ in Methanol.**

Sample	Mass $NaClO_4$ (g)		$[Na^+]$ (M)	log$[Na^+]$	$\delta^{195}Pt$ (ppm)	$\delta^{23}Na$ (Hz)
1	0.2150		2.509	0.400	74.0	-931.8
2	0.1313		1.532	0.185	83.4	-786.0
		Vol. 1.003 M $NaClO_4$ (cm^3)				
3		0.700	1.003	0.00130	89.9	-705.7
4		0.210	0.3009	-0.522	100.9	-597.9
5		0.070	0.1003	-0.999	106.6	-552.1
		Vol. 0.05015 M $NaClO_4$ (cm^3)				
6		0.700	0.05015	-1.300	109.0	-531.9
7		0.350	0.02508	-1.601	110.6	-518.6
8		0.175	0.01254	-1.902	111.5	-511.2
9		0.087	0.00623	-2.206	111.9	-508.3
10		0.043	0.00308	-2.511	112.3	-506.8

0.4119 g H_2PtBr_6 was weighed into a polytop and 10 cm^3 of methanol pipetted onto it; **$[PtBr_6^{2-}] = 0.06089$ M.** 0.3685 g $NaClO_4$ was weighed into a polytop, and 3 cm^3 of acetonitrile pipetted onto it; $[Na^+] = 1.003$ M. 0.150 cm^3 of this solution was diluted to 3 cm^3; $[Na^+] = 0.05015$ M. For Samples 1 & 2, $NaClO_4$ was weighed (column (2)) into polytops. For Samples 3-5 volumes of the 1.003 M $NaClO_4$ solution, and for Samples 6-10 volumes of the 0.05015 M $NaClO_4$ solution, were pipetted (column (3)) into polytops. Samples 3-10 were placed in an oven at 60-70°C to allow the solvent to evaporate off. Exactly 0.700 cm^3 of the 0.06089M H_2PtBr_6 solution was pipetted into each of the polytops containing $NaClO_4$, to affect the desired $[Na^+]$. (M_r (H_2PtBr_6) = 676.50 g mol^{-1}; M_r ($NaClO_4$) = 122.44 g mol^{-1}).

The ^{195}Pt and ^{23}Na chemical shifts were determined for each solution relative to the ^{195}Pt and ^{23}Na external reference solutions respectively (^{195}Pt reference solution: 250 mg.ml^{-1} H_2PtBr_6 in 67 % v/v D_2O / 3 M HBr; ^{23}Na reference solution: 1.034 M NaCl in D_2O). ^{23}Na chemical shifts have been corrected for the difference in bulk diamagnetic susceptibility between sample and reference.

Stellenbosch University http://scholar.sun.ac.za

Table 5.17Adm Solution preparation, resultant Na^+ concentrations, and ^{195}Pt and ^{23}Na chemical shifts for the series: **H_2PtBr_6 + $NaClO_4$ in Acetonitrile.**

Sample	Mass $NaClO_4$ (g)		$[Na^+]$ (M)	log$[Na^+]$	$\delta^{195}Pt$ (ppm)	$\delta^{23}Na$ (Hz)
1	0.1895		2.211	0.345	197.0	-1343.3
2	0.1325		1.546	0.189	208.7	-1280.3
		Vol. 0.998 M $NaClO_4$ (cm^3)				
3		0.700	0.998	-0.00087	220.9	-1220.2
4		0.350	0.499	-0.302	233.2	-1158.7
5		0.210	0.2994	-0.524	239.5	-1123.7
6		0.070	0.0998	-1.001	247.4	-1071.0
		Vol. 0.04990 M $NaClO_4$ (cm^3)				
7		0.700	0.0499	-1.302	249.8	-1048.8
8		0.350	0.02495	-1.603	251.0	-1036.0
9		0.175	0.01248	-1.904	251.5	-1023.7
10		0.087	0.00620	-2.208	252.8	-1024.2
11		0.043	0.00307	-2.513	252.1	-1022.7

0.4089 g H_2PtBr_6 was weighed into a polytop and 10 cm^3 of acetonitrile pipetted onto it; **$[PtBr_6^{2-}]$ = 0.06044 M**. 0.3666 g $NaClO_4$ was weighed into a polytop, and 3 cm^3 of acetonitrile pipetted onto it; $[Na^+]$ = 0.998 M. 0.150 cm^3 of this solution was diluted to 3 cm^3; $[Na^+]$ = 0.04990 M. For Samples 1 & 2, $NaClO_4$ was weighed (column (2)) into polytops. For Samples 3-6 volumes of the 0.998 M $NaClO_4$ solution, and for Samples 7-11 volumes of the 0.04990 M $NaClO_4$ solution, were pipetted (column (3)) into polytops. Samples 3-11 were placed in an oven at 60-70°C to allow the solvent to evaporate off. Exactly 0.700 cm^3 of the 0.06044 M H_2PtBr_6 solution was pipetted into each of the polytops containing $NaClO_4$, to affect the desired $[Na^+]$. (M_r (H_2PtBr_6) = 676.50 g mol^{-1}; M_r ($NaClO_4$) = 122.44 g mol^{-1}).
The ^{195}Pt and ^{23}Na chemical shifts were determined for each solution relative to the ^{195}Pt and ^{23}Na external reference solutions respectively (^{195}Pt reference solution: 250 mg.ml^{-1} H_2PtBr_6 in 67 % v/v D_2O / 3 M HBr; ^{23}Na reference solution: 1.034 M NaCl in D_2O). ^{23}Na chemical shifts have been corrected for the difference in bulk diamagnetic susceptibility between sample and reference.

Stellenbosch University http://scholar.sun.ac.za

Table 5.18Adm Solution preparation, resultant $PtCl_6^{2-}$ concentrations, and ^{195}Pt and ^{23}Na chemical shifts for the series: **$H_2PtCl_6 \cdot H_2O$ + $NaClO_4$ in Methanol** (constant $[Na^+]$).

Sample	Vol. 0.1014 M $H_2PtCl_6 \cdot H_2O$ (cm^3)	$[PtCl_6^{2-}]$ (M)	$\delta^{195}Pt$ (ppm)	$\delta^{23}Na$ (Hz)
1	0.500	0.1014	94.0	-420.1
2	0.350	0.0710	94.2	-440.8
3	0.200	0.04056	94.2	-466.3
	Vol. 0.02028 M $H_2PtCl_6 \cdot H_2O$ (cm^3)			
4	0.500	0.02028	92.6	-496.5
5	0.250	0.01014	91.7	-519.1
6	0.063	0.002555	88.2	-555.2
7	0.013	0.000527		-564.7

0.1735g $H_2PtCl_6 \cdot H_2O$ was weighed into a polytop and 4 cm^3 of methanol pipetted onto it; **$[PtCl_6^{2-}]$ = 0.1014 M**. 0.400 cm^3 of this solution was diluted to 2.000 cm^3 with methanol; **$[PtCl_6^{2-}]$ = 0.02028 M**. 0.6145 g $NaClO_4$ was weighed into a polytop and 5 cm^3 of methanol pipetted onto it; $[Na^+]$ = 1.004 M. 0.050 cm^3 of this solution was diluted to 5 cm^3 with methanol; $[Na^+]$ = 0.01004 M. For Samples 1-3 volumes of the 0.1014M $H_2PtCl_6 \cdot H_2O$ solution, and for Samples 4-7 volumes of the 0.02028 M $H_2PtCl_6 \cdot H_2O$ solution (column (2)), were pipetted into clean polytop containers. The samples were placed in a vacuum dessicator to evaporate off all the solvent. To each dry $H_2PtCl_6 \cdot H_2O$ sample was added 0.500cm^3 of 0.01004M $NaClO_4$ solution. (M_r ($H_2PtCl_6 \cdot H_2O$) = 427.82 g mol^{-1}; M_r ($NaClO_4$) = 122.44 g mol^{-1}).

The ^{195}Pt and ^{23}Na chemical shifts were determined for each solution relative to the ^{195}Pt and ^{23}Na external reference solutions respectively (^{195}Pt reference solution: 500 mg.ml^{-1} $H_2PtCl_6 \cdot H_2O$ in 30 % v/v D_2O / 1 M HCl; ^{23}Na reference solution: 1.034 M NaCl in D_2O). ^{23}Na chemical shifts have been corrected for the difference in bulk diamagnetic susceptibility between sample and reference.

Stellenbosch University http://scholar.sun.ac.za

Table 5.19Adm Solution preparation, resultant Na^+ concentrations, and temperature dependence of the ^{195}Pt chemical shifts for the series: **$H_2PtCl_6 \cdot H_2O$ + $NaClO_4$ in Acetonitrile**

Sample	Mass $NaClO_4$ (g)		$[Na^+]$ (M)	$\log[Na^+]$	17.0°C $\delta^{195}Pt$ (ppm)	40.6°C $\delta^{195}Pt$ (ppm)	51.3°C $\delta^{195}Pt$ (ppm)	62.1°C $\delta^{195}Pt$ (ppm)
1	0.1864		2.175	0.338	133.8	116.7	109.0	101.1
2	0.1303		1.520	0.182	147.1	129.8	118.7	108.7
		Vol. 1.026 M $NaClO_4$ (cm^3)						
3		0.350	0.5130	-0.290	178.4	163.2	155.7	147.8
4		0.210	0.3078	-0.512	188.3	174.3	166.5	158.7
5		0.070	0.1026	-0.989	205.6	194.1	186.2	177.8
		Vol. 0.05130 M $NaClO_4$ (cm^3)						
6		0.350	0.02565	-1.591	220.6	210.6	206.5	200.2
7		0.175	0.01283	-1.892	224.6	215.6	211.1	203.8
8		0.044	0.003225	-2.491	227.9	219.0	214.8	211.4

0.2694 g $H_2PtCl_6 \cdot H_2O$ was weighed into a polytop and 10 cm^3 of acetonitrile pipetted onto it; **$[PtCl_6^{2-}] = 0.06297$ M**. 0.3769 g $NaClO_4$ was weighed into a polytop, and 3 cm^3 of acetonitrile pipetted onto it; $[Na^+] = 1.026$ M. 0.150 cm^3 of this solution was diluted to 3 cm^3; $[Na^+] = 0.05130$ M. For Samples 1 & 2, $NaClO_4$ was weighed (column (2)) into polytops. For Samples 3-5 volumes of the 1.026 M $NaClO_4$ solution, and for Samples 6-8 volumes of the 0.05130 M $NaClO_4$ solution, were pipetted (column (3)) into polytops. Samples 3-8 were placed in an oven at 60-70°C to allow the solvent to evaporate off. Exactly 0.700 cm^3 of the 0.06297 M $H_2PtCl_6 \cdot H_2O$ solution was pipetted into each of the polytops containing $NaClO_4$, to affect the desired $[Na^+]$. (M_r ($H_2PtCl_6 \cdot H_2O$) = 427.82 g mol^{-1}; M_r ($NaClO_4$) = 122.44 g mol^{-1}).

The ^{195}Pt and chemical shifts were determined for each solution relative to the ^{195}Pt external reference solution (^{195}Pt reference solution: 500 mg.ml^{-1} $H_2PtCl_6 \cdot H_2O$ in 30 % v/v D_2O / 1 M HCl).

Stellenbosch University http://scholar.sun.ac.za

Table 5.20Adm Solution preparation, resultant Na^+ concentrations, and ^{23}Na chemical shifts (corrected for the difference in bulk diamagnetic susceptibility between sample and reference) for the series: **$NaClO_4$ + 18-crown-6 in Methanol.**

Sample	Vol. 2.459 M $NaClO_4$ (cm^3)	Mass 18-crown-6 (g)	mols 18-crown-6 / mols Na^+	$[Na^+]$ (M)	$\log[Na^+]$	$\delta^{23}Na$ (Hz)
1	0.700	0.4569	1.00	2.459	0.391	-2182
2	0.493	0.3253	1.02	1.732	0.239	-2182
3	0.335	0.2170	1.00	1.176	0.0704	-2181
	Vol. 0.5882 M $NaClO_4$ (cm^3)					
4	0.700	0.1098	1.01	0.5882	-0.230	-2179
5	0.140	0.0231	1.06	0.1176	-0.930	-2167
6	0.035	0.0060	1.10	0.02941	-1.532	-2163
	Vol. 2.459 M $NaClO_4$ (cm^3)					
a	0.700	0.2299	0.51	2.459	0.391	-1579
b	0.493	0.1596	0.50	1.732	0.239	-1537
c	0.335	0.1077	0.50	1.176	0.0704	-1510
	Vol. 0.5882 M $NaClO_4$ (cm^3)					
d	0.700	0.0550	0.51	0.5882	-0.230	-1502
e	0.140	0.0109	0.50	0.1176	-0.930	-1513

3.0110 g $NaClO_4$ was weighed into a polytop and 10 cm^3 of methanol pipetted onto it; $[Na^+]$ = 2.459 M. 1.196 cm^3 of this solution was diluted accurately to 5 cm^3 with methanol; $[Na^+]$ = 0.5882 M. Volumes of 2.459 M $NaClO_4$ solution and of 0.5882 M $NaClO_4$ solution (column (2)) were pipetted into separate polytops, which were placed in an oven overnight at 60-70°C to allow the solvent to evaporate off. 0.700 cm^3 of methanol was pipetted onto the dry salt in each polytop, after which an appropriate mass of 18-crown-6 was added (column 3). (M_r ($NaClO_4$) = 122.44 g mol^{-1}; M_r (18-crown-6) = 264.32 g mol^{-1}).
The ^{23}Na chemical shifts were determined for each solution relative to the ^{23}Na external reference solution (1.034 M NaCl in D_2O).

Stellenbosch University http://scholar.sun.ac.za

Table 5.21Adm Solution preparation, resultant Na^+ concentrations, and ^{195}Pt and ^{23}Na chemical shifts for the series: **$H_2PtCl_6 \cdot H_2O$ + $NaClO_4$ + 18-crown-6 in Methanol**.

Sample	Mass 18-crown-6 (g)	Mass $NaClO_4$ (g)	mols 18-crown-6 / mols Na^+	$[Na^+]$ (M)	$\log[Na^+]$	$\delta^{195}Pt$ (ppm)	$\delta^{23}Na$ (Hz)
1	0.0265	0.0259	0.47	0.2115	-0.675	95.0	-1309
2	0.0843	0.0787	0.50	0.6427	-0.192	97.1	-1383
3	0.2081	0.1952	0.49	1.594	0.202	98.9	-1440
4	0.3323	0.3077	0.50	2.513	0.400	100.3	-1495
5	0.0528	0.0266	0.92	0.2172	-0.663	113.5	-2030
6	0.1661	0.0787	0.98	0.6427	-0.192	134.9	-2118
7	0.4186	0.1987	0.98	1.623	0.210	161.6	-2130
8	0.6642	0.3101	0.99	2.532	0.403	181.8	-2137

Appropriate masses of 18-crown-6 (column (2)) were weighed into clean polytops, after which the masses of $NaClO_4$ indicated in column (3) were added. 0.2505 g $H_2PtCl_6 \cdot H_2O$ was weighed into a polytop and 10 cm^3 of methanol pipetted onto it; **$[PtCl_6^{2-}] = 0.05856$ M**. 1.000 cm^3 of the 0.05856 M $H_2PtCl_6 \cdot H_2O$ solution was pipetted into each polytop. (M_r ($H_2PtCl_6 \cdot H_2O$) = 427.82 g mol^{-1}; M_r ($NaClO_4$) = 122.44 g mol^{-1}; M_r (18-crown-6) = 264.32 g mol^{-1}).
The ^{195}Pt and ^{23}Na chemical shifts were determined for each solution relative to the ^{195}Pt and ^{23}Na external reference solutions respectively (^{195}Pt reference solution: 500 $mg.ml^{-1}$ $H_2PtCl_6 \cdot H_2O$ in 30 % v/v D_2O / 1 M HCl; ^{23}Na reference solution: 1.034 M NaCl in D_2O). ^{23}Na chemical shifts have been corrected for the difference in bulk diamagnetic susceptibility between sample and reference.

Stellenbosch University http://scholar.sun.ac.za

Table 5.22Adm Solution preparation, resultant Na^+ concentrations, and ^{195}Pt chemical shifts for the series: **$H_2PtCl_6 \cdot H_2O$ + $NaClO_4$ + 18-crown-6 in Acetonitrile** and **$H_2PtCl_6 \cdot H_2O$ + $NaClO_4$ + 15-crown-5 in Acetonitrile**.

Sample	Vol. 2.114 M $NaClO_4$ (cm^3)	Mass 18-crown-6 (g)	mols 18-crown-6 / mols Na^+	$[Na^+]$ (M)	log$[Na^+]$	$\delta^{195}Pt$ (Hz)
1	0.700	0.1951	0.50	2.114	0.325	173.7
2	0.493	0.1371	0.50	1.489	0.173	180.9
3	0.335	0.0953	0.51	1.012	0.00518	188.7
	Vol. 0.5057 M $NaClO_4$ (cm^3)					
4	0.700	0.0458	0.49	0.5057	-0.296	196.4
5	0.140	0.0087	0.46	0.1011	-0.995	210.4
6	0.035	0.0025	0.53	0.02529	-1.597	219.6
	Vol. 2.120 M $NaClO_4$ (cm^3)	Mass 15-crown-5 (g)	mols 15-crown-5 / mols Na^+			
a	0.700	0.1746	0.53	2.120	0.326	170.3
b	0.493	0.1156	0.50	1.493	0.174	173.5
c	0.335	0.0778	0.50	1.015	0.00647	180.8
	Vol. 0.5071 M $NaClO_4$ (cm^3)					
d	0.700	0.0383	0.49	0.5071	-0.295	190.6
e	0.140	0.0097	0.62	0.1014	-0.994	212.0
f	0.035	0.0027	0.69	0.02536	-1.596	218.8

2.5886 g $NaClO_4$ was weighed into a polytop and 10 cm^3 of acetonitrile pipetted onto it; $[Na^+]$ = 2.114 M. 1.196 cm^3 of this solution was diluted accurately to 5 cm^3 with acetonitrile; $[Na^+]$ = 0.5057 M. 2.5956 g $NaClO_4$ was weighed into a polytop and 10 cm^3 of acetonitrile pipetted onto it; $[Na^+]$ = 2.120 M. 1.196 cm^3 of this solution was diluted accurately to 5 cm^3 with acetonitrile; $[Na^+]$ = 0.5071 M. Volumes of the 2.114 M, 0.5057 M, 2.120 M and 0.5071 M $NaClO_4$ solutions (column (2)) were pipetted into separate polytops, which were placed in an oven overnight at 60-70°C to allow the solvent to evaporate off. 0.2648 g $H_2PtCl_6 \cdot H_2O$ was weighed into a polytop and 10 cm^3 of acetonitrile pipetted onto it; **$[PtCl_6^{2-}]$ = 0.06190 M**. 0.2630 g $H_2PtCl_6 \cdot H_2O$ was weighed into a polytop and 10 cm^3 of acetonitrile pipetted onto it; **$[PtCl_6^{2-}]$ = 0.06147 M**. 0.700 cm^3 of the 0.06190 M $H_2PtCl_6 \cdot H_2O$ solution was pipetted into the polytops to complete Samples 1-6, and 0.700 cm^3 of the 0.06147 M $H_2PtCl_6 \cdot H_2O$ solution was pipetted into the polytops to complete Samples a-f. Appropriate masses of 18-crown-6 (column 3) were weighed into Samples 1-6, and 15-crown-5 weighed into Samples a-f. (M_r ($H_2PtCl_6 \cdot H_2O$) = 427.82 g mol^{-1}; M_r ($NaClO_4$) = 122.44 g mol^{-1}; M_r (18-crown-6) = 264.32 g mol^{-1}; M_r (15-crown-5) = 220.27 g mol^{-1}). The ^{195}Pt chemical shifts were determined for each solution relative to the ^{195}Pt external reference solution (^{195}Pt reference solution: 500 mg.ml^{-1} $H_2PtCl_6 \cdot H_2O$ in 30 % v/v D_2O / 1 M HCl).

Stellenbosch University http://scholar.sun.ac.za

Stellenbosch University http://scholar.sun.ac.za

Addendum C

Stellenbosch University http://scholar.sun.ac.za

ON THE LIQUID-LIQUID EXTRACTION OF Pt(IV/II) FROM HYDROCHLORIC ACID BY *N*-ACYL(AROYL)-*N'*,*N'*-DIALKYLTHIOUREAS: A MULTINUCLEAR (^{1}H, ^{13}C AND ^{195}Pt) NMR SPECIATION STUDY OF THE EXTRACTED COMPLEXES

Klaus R Koch * , Jörn Miller and Arjan N Westra

Department of Chemistry, University of Stellenbosch, Matieland

An investigation into the nature of the complex species which are formed by the extraction of Pt(IV/II) from hydrochloric acid using *N*-benzoyl-*N'*,*N'*-diethylthiourea and *N*-benzoyl-*N'*,*N'*-di(n-butyl)thiourea in chloroform and toluene, has been carried out. The study reveals that for Pt^{IV} extraction a remarkably complicated distribution of complex species is obtained, arising from *inter alia* possible redox reactions between Pt^{IV} and the ligands. In the case of Pt^{II} extraction with *N*-acyl(aroyl)-*N'*,*N'*-dialkylthioureas, which is relatively simpler, several protonated species containing coordinated chloride ions ([Pt(L-*S*,*O*)(HL-*S*)Cl], *cis*-[Pt(HL-*S*)$_2$Cl$_2$] and *trans*-[Pt(HL-*S*)$_2$Cl$_2$]) as well as the well-known *cis*-[Pt(L-*S*,*O*)$_2$] complex (depending on the extraction conditions), are found in the organic phase.

INTRODUCTION

Although the discovery of platinum in the sixteenth century did not lead to an immediate realisation of any usefulness for it, it has become one of the most sought-after metals today. With applications for this transition metal as diverse as the manufacture of autocatalysts, to the development of new anti-cancer drugs based on *cis*-platin and its derivatives, to the making of jewellery and ornaments, it is not surprising that research into improved separation of this precious metal, and the other platinum group metals (PGMs), is ongoing. While previous processes for the separation of the platinum group metals (Pt, Pd, Ru, Rh, Os and Ir) were based on the selective precipitation of the metals from a solution mixture, solvent extraction has proven to be more advantageous in many respects, *viz.* efficiency, yield and operating time [1], and investigations into the selective solvent extraction of the platinum group metals are therefore of continued interest.

The ligands *N*-acyl(aroyl)-*N'*-alkylthiourea (H_2L) and *N*-acyl(aroyl)-*N'*,*N'*-dialkylthiourea (HL) have been shown to form very stable neutral complexes with many metal ions, particularly so with the platinum group metals [2,3]. In fact, these ligands have been found to *selectively* coordinate the PGMs making them ideal candidates for use in the liquid-liquid extraction [4,5], as well as preconcentration and separation [6,7], of the PGMs.

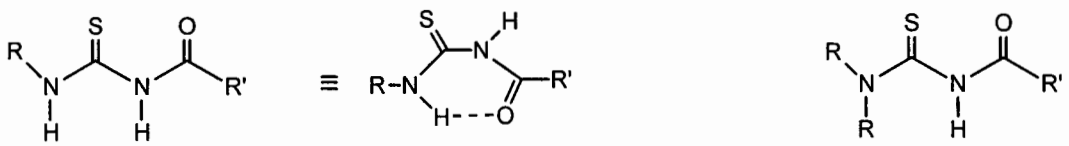

H_2L **HL**

R' = phenyl or alkyl group

International Solvent Extraction Conference, ISEC 2002,
Ed. K. C. Sole, P. M. Cole, J. S. Preston and D. J. Robinson
South African Institute of Mining and Metallurgy, 2002, pp. 327-334

Stellenbosch University http://scholar.sun.ac.za

In a study by König *et al* [4] the efficacy of several *N*-benzoyl-*N'*,*N'*-**dialkyl**thioureas as extraction reagents was illustrated (**dialkyl** = dimethyl, diethyl, di-n-propyl, di-n-butyl, di-n-hexyl). The authors found that by controlling the pH of the aqueous phase, the PGMs (Pt^{II}, Pd^{II}, Ru^{III}, Rh^{III}, Os^{III}, Ir^{III}) can be separated from several important metals such as iron, cobalt, nickel, copper and zinc. Furthermore, by controlling the pH and the temperature it is, to some degree, also possible to separate the platinum group metals from each other. Ligands with longer alkyl moieties produce larger distribution coefficients, better phase separation and thus improved extraction. The differences in the extractive abilities of the ligands was ascribed to varying solubilities of the ligands and complexes in the solvents used, as well as to the large variation in complex stabilities; the longer alkyl groups lead, due to larger +I-effects, to increased electron density at the coordinative centers of the ligands (the O- and S-atoms) and thus to more stable complexes. A subsequent investigation by Vest *et al* [5] showed that the dialkyl-substituted benzoylthioureas, HL, are far more efficient in the liquid-liquid extraction of the PGMs than the monoalkyl-substituted analogues, H_2L.

In both the afore-mentioned investigations, however, no description of the coordination chemistry of Pt^{II} (or the other PGMs) with the *N*-acyl(aroyl)-*N'*-alkylthioureas, H_2L, and *N*-acyl(aroyl)-*N'*,*N'*-dialkylthioureas, HL, was given, but in recent years several papers have appeared in this regard. Investigations have shown that the potentially bidentate H_2L ligands co-ordinate to the Pt^{II} through the S-atom only, similar to simple unsubstituted thioureas, and not via the O-atom also [8, 9, 10]. Crystallographic evidence reveals the monoalkyl-substituted ligands to be locked into a planar six-membered O-C-N-C-N-H ring by means of an intramolecular N-H···O hydrogen bond thus disallowing coordination via the carbonyl oxygen (Fig. 1 (a)). The HL ligands, however, coordinate to the Pt^{II} via both the S- and the O-atom forming essentially square-planar bis-complexes with loss of the thioamidic proton (Fig. 1 (b)). Coordination to Pt^{II} by the monoalkyl- and dialkyl-substituted ligands differs in another respect in that the *N*-acyl(aroyl)-*N'*-alkylthioureas react with $PtCl_4^{2-}$ in neutral aqueous solution to yield mixtures of *cis*- and *trans*-[$Pt(H_2L\text{-}S)_2Cl_2$] complexes whilst complexation with *N*-acyl(aroyl)-*N'*,*N'*-dialkylthioureas in most cases yields only *cis*-[$Pt(L\text{-}S,O)_2$] complexes. *N*-naphthoyl-*N'*,*N'*-dibutylthiourea is the only dialkyl-substituted ligand of this type to have been reported to yield *trans*- as well as *cis*- isomers [11].

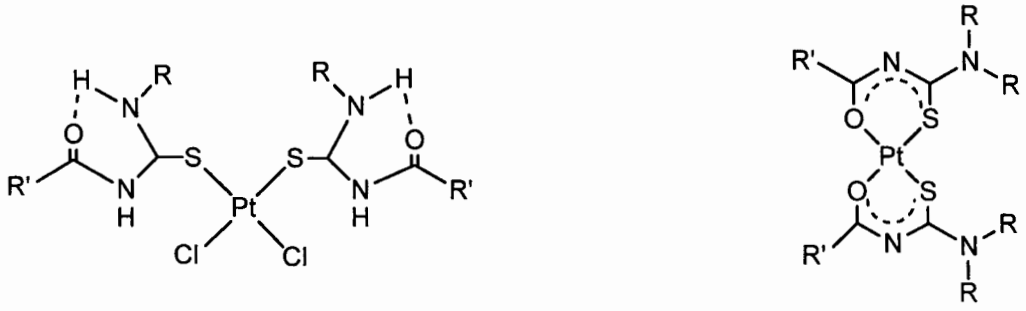

(a) *cis*-[$Pt(H_2L\text{-}S)_2Cl_2$] (b) *cis*-[$Pt(L\text{-}S,O)_2$]

Figure 1. Complexation of Pt^{II} with N-acyl(aroyl)-N'-alkylthioureas leads to mixtures of cis-, (a), and trans- isomers whilst complexation with N-acyl(aroyl)-N',N'-dialkylthioureas leads predominantly to cis-, (b), isomers.

Whereas the investigations [8-11] into the fundamental coordination chemistry of the H_2L and HL type ligands of the PGMs have been performed in essentially neutral solutions, the solvent extraction studies by Vest *at al* [5] revealed that optimum extraction of the PGMs by the ligands of interest occurred in 2 molar hydrochloric acid media, conditions under which Pt^{II} species other than those already identified [8-11] might also exist. An investigation of the acid-base chemistry of various *cis*-[$Pt(\mathbf{L}\text{-}S,O)_2$] complexes [12] elucidated this point (**HL** = *N*-benzoyl-*N'*,*N'*-di(n-butyl)thiourea, *N*-(4Br-phenyl)-*N'*,*N'*-di(n-butyl)thiourea, *N*-(4NO_2-phenyl)-

Stellenbosch University http://scholar.sun.ac.za

N',*N'*-di(n-butyl)thiourea). It was shown that treatment of a solution of the uncharged complex *cis*-[Pt(L-*S*,*O*)$_2$] in chloroform with hydrochloric acid solution results in the formation of three protonated complexes: a partially ring-opened [Pt(L-*S*,*O*)(HL-*S*)Cl] complex which, in the presence of excess *conc.* HCl, disappeared, presumably becoming further protonated in the acid medium to yield a *cis*-[Pt(HL-*S*)$_2$Cl$_2$] complex which in turn isomerizes slowly to the *trans*-[Pt(HL-*S*)$_2$Cl$_2$] complex.

The results of investigations by Koch and co-workers give an indication of the types of Pt^{II} species that possibly exist in the extraction processes described by Vest *et al.* Since much of the platinum in the extractive industrial process streams occurs in the oxidation state +4 however (as the species $PtCl_6^{2-}$), investigations into the extraction of Pt^{IV} and the resultant Pt^{IV} species are therefore also of importance. The Pt^{IV} chloro-complex ($PtCl_6^{2-}$) is however kinetically less labile than the Pt^{II} chloro-complex ($PtCl_4^{2-}$) and this results in slower formation of the extractable Pt^{IV} species; the system is thus more difficult to investigate. Moreover, the possibility of a redox reaction between Pt^{IV} and the thiourea ligands cannot be excluded. Vest *et al* improved the rate of extraction of Pt^{IV} by addition of tin(II) chloride [13], a reagent which, apart from labilizing Pt—Cl bonds, also reduces the Pt^{IV} to Pt^{II} [14].

This paper reports on our preliminary attempts at Pt^{IV} speciation in the extraction of this ion with ***N*-benzoyl-*N'*,*N'*-diethylthiourea**, **HL^1**, and ***N*-benzoyl-*N'*,*N'*-di(n-butyl)thiourea**, **HL^2**, as well as Pt^{II} speciation in the coordination of this ion with ***N*-propanoyl-*N'*-morpholinothiourea**, **HL^3**.

EXPERIMENTAL

Preparation of ligands and *cis*-[Pt(L^3-*S*,*O*)$_2$] complex

All ligands, HL^1 – HL^3, were prepared as previously described [9] and were characterised by means of ^{1}H and ^{13}C NMR spectroscopy. The neutral complex *cis*-[Pt(L^3-*S*,*O*)$_2$] was also prepared and characterized as previously reported [9].

Solvent extraction procedure

Phase intermixture in the extractions was achieved either by the use of a shaking apparatus or by means of magnetic stirring. In the first case 1.0 mL of an acidified (2 M HCl) aqueous $H_2PtCl_6{\cdot}H_2O$ solution (initial concentration of platinum was 23.1 g/L) and 1.0 mL of a $CDCl_3$ solution of HL^1 (metal/ligand ratio 1:4) were thoroughly mixed at room temperature in a tightly stoppered test-tube on a shaking apparatus for 24 hours. The organic layer was filtered through Extrelut® (to remove traces of water) directly into an NMR tube and spectra acquired. In the second instance extractions were performed by magnetically stirring the two phases in a water-jacketted reaction vessel; the latter allowed temperature control. 10.0 mL of an acidified (2 M HCl) aqueous $H_2PtCl_6{\cdot}H_2O$ solution (initial concentration of platinum was 22.1 g/L) was vigorously stirred with 10.0 mL of a toluene solution of HL^2 (metal/ligand ratio 1:8) at 80°C. After 3 hours of stirring a sample of the organic phase was filtered through Extrelut® directly into an NMR tube and spectra acquired.

Protonation experiments

An aliquot of 0.15 mL 6 M aqueous HCl was added directly to an NMR tube containing 0.6 mL of *cis*-[Pt(L^3-*S*,*O*)$_2$] complex in $CDCl_3$. After vigorously shaking the tube to ensure thorough intermixing of the two phases, the acidified organic layer was allowed to separate and NMR spectra were recorded ca. 7 minutes after acid addition. After spectral acquisition the mineral acid was removed, the organic layer washed with water and then treated with 5 M ammonia solution, and NMR spectra were re-acquired.

Stellenbosch University http://scholar.sun.ac.za

NMR spectroscopy

^{1}H and ^{195}Pt NMR spectra were recorded in 5 mm tubes in chloroform-d (^{1}H and ^{195}Pt) or toluene-d_8 (^{195}Pt) solution, using a Varian INOVA 600 MHz spectrometer operating at 600 and 128 MHz respectively (^{1}H at 25°C and ^{195}Pt at 30°C). ^{1}H chemical shifts are quoted relative to the residual $CDCl_3$ solvent resonance at 7.26 ppm. The ^{195}Pt NMR spectra were recorded using spectral widths typically 130 kHz with 15 μs pulses (~90°) and 1.0 s pulse delay. All ^{195}Pt chemical shifts are quoted relative to external H_2PtCl_6 (500mg ml^{-1} in 30% v/v D_2O/1 M HCl) and are estimated to be accurate to ±4 ppm.

RESULTS AND DISCUSSION

Pt^{IV} speciation

In the first attempt at characterising the Pt^{IV} species that occur in the extraction of $[PtCl_6^{2-}]$ with an *N*-acyl(aroyl)-*N'*,*N'*-dialkylthiourea, an acidified aqueous solution of Pt^{IV} was vigorously mixed with a $CDCl_3$ solution containing *N*-benzoyl-*N'*,*N'*-diethylthiourea, HL^1, on a shaking apparatus for 24 hours as described in the experimental section. The organic layer coloured dark yellow indicating the formation of platinum complexes and NMR spectra of this solution were acquired. ^{195}Pt spectra in the region between 220 and –3700 ppm, relative to the external standard, were recorded; uncertainty as to the species that had formed necessitated this large spectral region but the limits were based on the premise that both Pt^{IV} and Pt^{II} species would be found in this range. The only indication of platinum in the organic layer however was a very broad (334 Hz) and undefinable peak at –3646 ppm which, despite a long acquisition time (9 hours), was of extremely low intensity. The appearance of this peak, as well as a very complex ^{1}H spectrum different from that of the ligand, is proof that extraction of the metal had taken place but the very low intensity of the ^{195}Pt peak suggested that several species were extracted and that the extent of metal separation had been very poor.

To improve the extent of metal separation a second extraction was performed at higher temperature with a toluene solution containing *N*-benzoyl-*N'*,*N'*-di(n-butyl)thiourea, HL^2, as described in the experimental section. König *et al* [4] had concluded that ligands with longer alkyl moieties lead to improved platinum extraction, as does a higher operating temperature; the latter change necessitated the use of an organic solvent with a higher boiling point. After 3 hours of phase contact at 80°C the toluene solution had an extremely dark brown/red appearance indicating significant metal extraction; this was confirmed by the ^{1}H spectrum which revealed a plethora of peaks the complexity of which prevented interpretation. To ensure that all possible species would be registered, the platinum spectral region from 3500 to –6000 ppm (relative to the external standard) was scanned, but ^{195}Pt peaks were only observed between –3100 and –3700 ppm. In this range several peaks appeared (at least 7) with varying line-widths (64 – 208 Hz) but again with surprisingly low intensity despite an acquisition time of 13½ hours. After several days a white/yellow precipitate had formed in the toluene solution. The precipitate was separated, rinsed and re-dissolved in $CDCl_3$ and NMR spectra acquired. The ^{1}H NMR spectrum is consistent with a species that contains the *N*-benzoyl-*N'*,*N'*-di(n-butyl)thiourea ligand. Moreover, the presence of a ^{1}H peak at 11.16 ppm, characteristic of an N-H resonance, confirms that the thioamidic N-atom of the ligand is protonated. The corresponding ^{195}Pt spectrum of this solution consists of a single, relatively sharp (180 Hz), resonance at -3205 ppm. In the investigation of the acid-base chemistry of various *cis*-$[Pt^{II}(L\text{-}S,O)_2]$ complexes by Koch *et al* [12], the complex *cis*-bis(*N*-benzoyl-*N'*,*N'*-di(n-butyl)thiourea)platinum(II) was prepared and the ^{1}H and ^{195}Pt NMR spectra of this complex and its protonated forms acquired. The authors concluded that one of the doubly protonated forms of *cis*-bis(*N*-benzoyl-*N'*,*N'*-di(n-butyl)thiourea)platinum(II) was a complex denoted as *cis*-$[Pt^{II}(HL^2\text{-}S)_2Cl_2]$ in which the carbonyl O-donor of the ligand had been displaced from the metal centre by a coordinating chloride ion upon protonation of the thioamidic nitrogen. The resultant N-H resonance was found to appear at 11.14 ppm and the

Stellenbosch University http://scholar.sun.ac.za

platinum resonance for this protonated complex was reported at -3218 ppm. Comparison of these ^{1}H and ^{195}Pt chemical shifts (11.14 ppm and -3218 ppm respectively) with those obtained for the re-dissolved precipitate in the present investigation (11.16 ppm and -3205 ppm respectively) suggests that *cis*-$[Pt^{II}(HL^{2}\text{-}S)_2Cl_2]$ is one of the species formed in the extraction of Pt^{IV} with *N*-benzoyl-*N'*,*N'*-di(n-butyl)thiourea and thus that some Pt^{IV} is reduced to Pt^{II} in the process of extraction. The reduction of Pt^{IV} by the ligands was not unexpected since several investigations into anti-cancer drugs have revealed that many sulfur-containing biomolecules act as reducing agents, reducing antitumour-active platinum(IV) drugs to their platinum(II) analogues [15].

Although the serendipitous crystallization of one of extracted platinum species has allowed its characterisation, the complexity of the extracted mixture, as revealed by the ^{1}H and ^{195}Pt NMR spectra, indicates that the speciation in the liquid-liquid extraction of Pt^{IV} with the ligands of interest must be approached in a piecemeal fashion. This would entail the preparation of possible complex species under experimental conditions relevant to the extraction process, characterisation of these species by means of multinuclear (^{1}H, ^{13}C and ^{195}Pt) NMR spectroscopy and subsequent correlation of these species-characterisation results with the results obtained from extraction experiments. Since the preparation and characterisation of Pt^{II} species will elucidate not only speciation in the solvent extraction of Pt^{II} but also that of Pt^{IV}, attention was first focused on Pt^{II} speciation; a description of the complexes of Pt^{II} with *N*-propanoyl-*N'*-morpholinothiourea, HL^{3}, follows.

Pt^{II} speciation

Reaction of *N*-propanoyl-*N'*-morpholinothiourea with $PtCl_4^{2-}$ (see the Experimental section) yields a product the ^{195}Pt NMR spectrum of which shows only a single resonance at $\delta(^{195}Pt)$ = -2743 ppm (Fig. 2(a)).

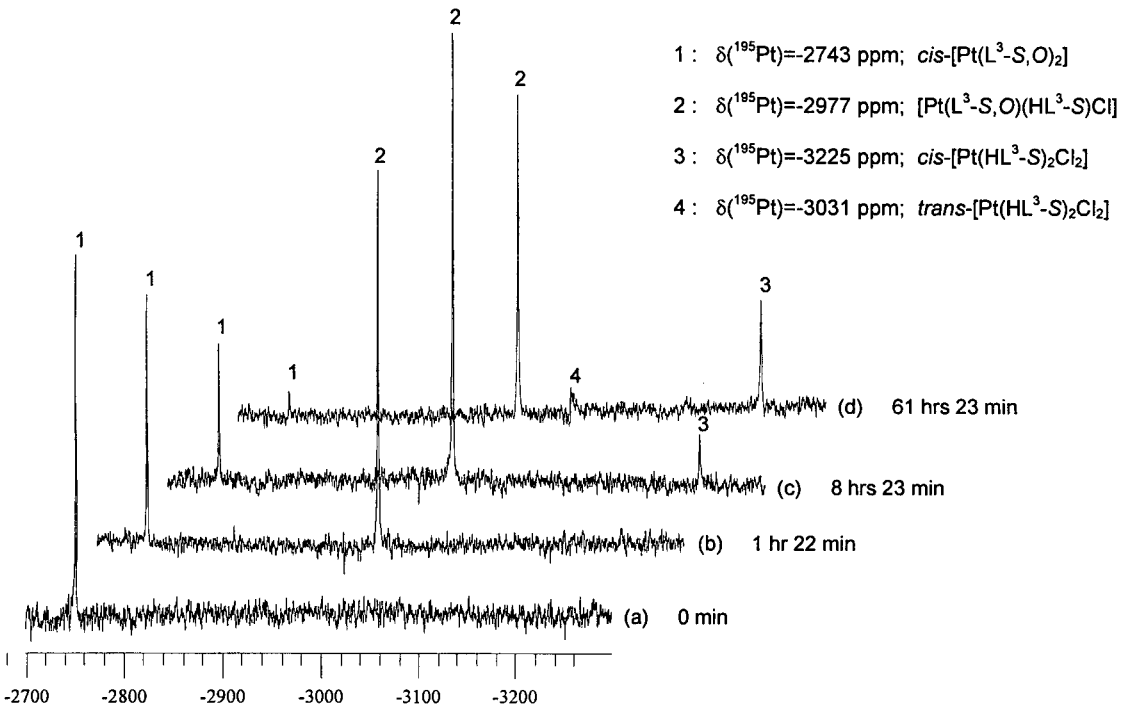

Figure 2. (a) ^{195}Pt NMR spectrum of cis-$[Pt(L^{3}\text{-}S,O)_2]$ in $CDCl_3$ before acid addition. (b)-(d) Spectra of solution (a) to which 6 M HCl has been added, acquired at the time intervals as indicated.

Stellenbosch University http://scholar.sun.ac.za

Although *trans* configurations of Pt^{II} complexes with *N*-acyl(aroyl)-*N'*,*N'*-dialkylthioureas are known [11], formation of exclusively the *cis* isomer predominates [12] and since the ^{195}Pt chemical shift obtained for the product (-2743 ppm) is consistent with ^{195}Pt shift trends reported by Koch *et al* for several *cis*-[Pt(L-*S*,*O*)$_2$] complexes [10, 12, 16], it is concluded that the product obtained is *cis*-bis(*N*-propanoyl-*N'*-morpholinothiourea)platinum(II) (*cis*-[Pt(L^3-*S*,*O*)$_2$]; Fig. 4). The corresponding ^1H NMR spectrum is consistent with only a single unprotonated complex species, as confirmed by the absence of the characteristic amido N-H resonance in the 10-12 ppm range (detailed ^1H assignments are trivial and will not be given here).

Addition of 0.15 mL 6 M HCl directly to the NMR tube containing *cis*-[Pt(L^3-*S*,*O*)$_2$] in $CDCl_3$ as described in the experimental section, yields a ^1H spectrum (acquired ca. 7 min after addition of the HCl) showing the presence of at least two additional species in solution, characterised by N-H resonances at 10.70 and 10.57 ppm (Fig. 3(i)). The appearance of the two N-H resonances reveals that the additional species occur as a result of the protonation of the coordinated ligands by some HCl partitioned into the $CDCl_3$ phase. After 1 hour 23 min a third protonated species becomes evident, as indicated by an N-H resonance at 10.29 ppm (Fig. 3(ii)); the corresponding ^{195}Pt spectrum at this time (Fig. 2(b)) consists of only two resonances at δ = -2743 and -2977 ppm. With time the concentrations of two of the protonated species increase, as indicated by the increasing intensities of the peaks at 10.57 and 10.29 ppm (Fig. 3(iii)-3(viii)) and eventually exist at concentrations which enable them to be detected in the ^{195}Pt spectra, $\delta(^{195}Pt)$ = -3225 and -3031 ppm (Fig. 2(c) and 2(d)). The protonated species giving rise to the ^1H peak at 10.70 ppm and the ^{195}Pt peak at -2977 ppm slowly increases and then decreases in concentration whilst the original unprotonated complex, $\delta(^{195}Pt)$ = -2743 ppm, decreases markedly with time.

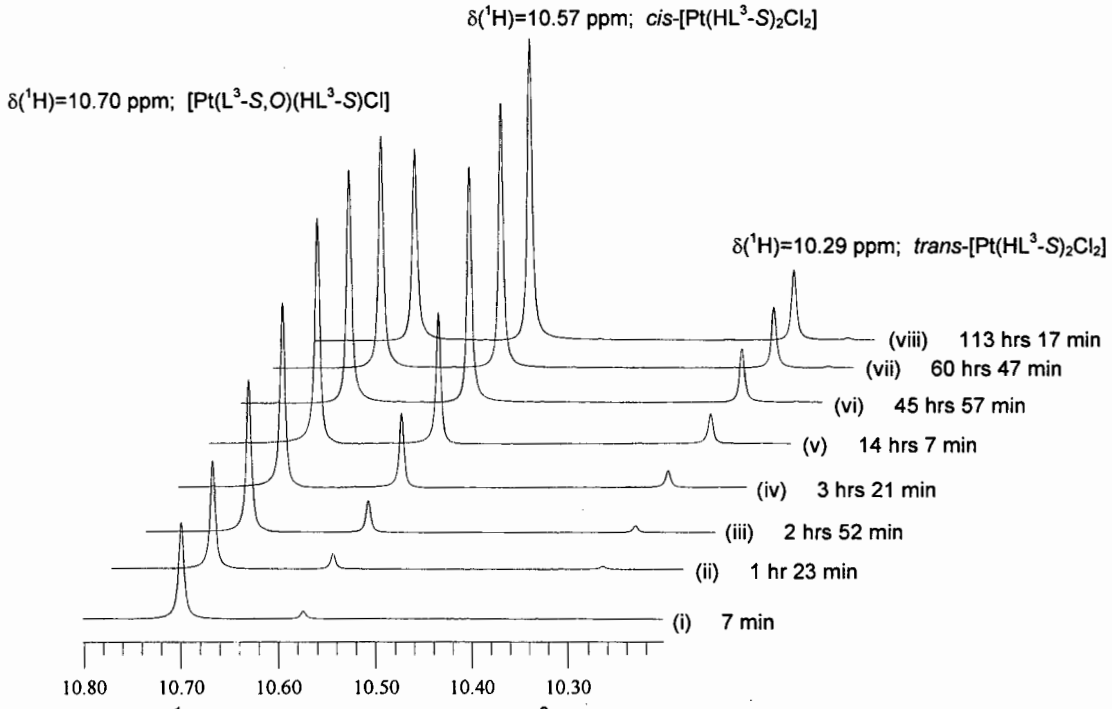

Figure 3. Partial ^1H NMR spectra of cis-[Pt(L^3-S,O)$_2$] in $CDCl_3$ acquired as a function of time after addition of 6 M HCl.

Treatment of the $CDCl_3$ phase with a small volume of 5 M ammonia as described in the experimental section, results in ^1H and ^{195}Pt spectra which are identical to those of the initial *cis*-[Pt(L^3-*S*,*O*)$_2$] complex with no evidence of any other complex species in solution. Whereas the protonation steps had taken several hours to occur, the solution treated with base had reverted to the original *cis*-[Pt(L^3-*S*,*O*)$_2$] complex within minutes (ca. 10 min)

Stellenbosch University http://scholar.sun.ac.za

indicating that the deprotonation reactions take place much more rapidly across the phase boundary.

In a previous investigation by Koch *et al* [8] the ^{195}Pt spectrum of a mixture of *cis*- and *trans*-bis(*N*-benzoyl-*N'*-propylthiourea)dichloroplatinum(II) in $CDCl_3$ showed two resonances at -3219 and -3040 ppm. The resonance at -3219 ppm has been assigned to the *cis*- bis(*N*-benzoyl-*N'*-propylthiourea)dichloroplatinum(II)complex (which has also been characterised by means of x-ray crystallography) and the one at -3040 ppm to the *trans*- isomer. Based on these assignments the ^{195}Pt peak at -3225 ppm in the present investigation is assigned to the doubly protonated species *cis*-[Pt(HL^3-*S*)$_2$Cl$_2$] (Fig. 4); a species formed when, upon protonation of the thioamidic N-atoms of *cis*-[Pt(L^3-*S*,*O*)$_2$], the carbonyl O-donor atoms are displaced from the metal centre by coordinating chloride ions leaving the ligands monodentately coordinated through the S-atoms only. The smaller ^{195}Pt peak which develops over time at -3031 ppm is assigned to the *trans*-[Pt(HL^3-*S*)$_2$Cl$_2$] isomer (Fig. 4), resulting from the isomerization of the *cis* complex. These assignments are consistent with the generally observed trend that the *cis* isomers for complexes of the type [PtA$_2$X$_2$] usually appear 200-500 ppm upfield of the *trans* isomers, depending on the nature of the donor atom of ligand A (X = Cl$^-$) [17]. The ^{195}Pt peak at -2977 ppm is assigned to a singly protonated species [Pt(L^3-*S*,*O*)(HL^3-*S*)Cl] (Fig. 4), a species in which only one of the ligands has been protonated to become monodentately (*S*-) coordinated to the platinum centre whilst the second ligand remains bidentately (*S*,*O*-) bound. ^{195}Pt chemical shifts are extremely sensitive to changes in the coordination sphere of the metal [17] and an upfield shift change of 234 ppm {-2743 ppm – (-2977 ppm)} as compared to an upfield shift change of 482 ppm {-2743 ppm – (-3225 ppm)}, known to result from a change in coordination sphere from two O-atoms to two chloride ions, would indicate a species in which only one O-atom has been replaced by only a single chloride ion.

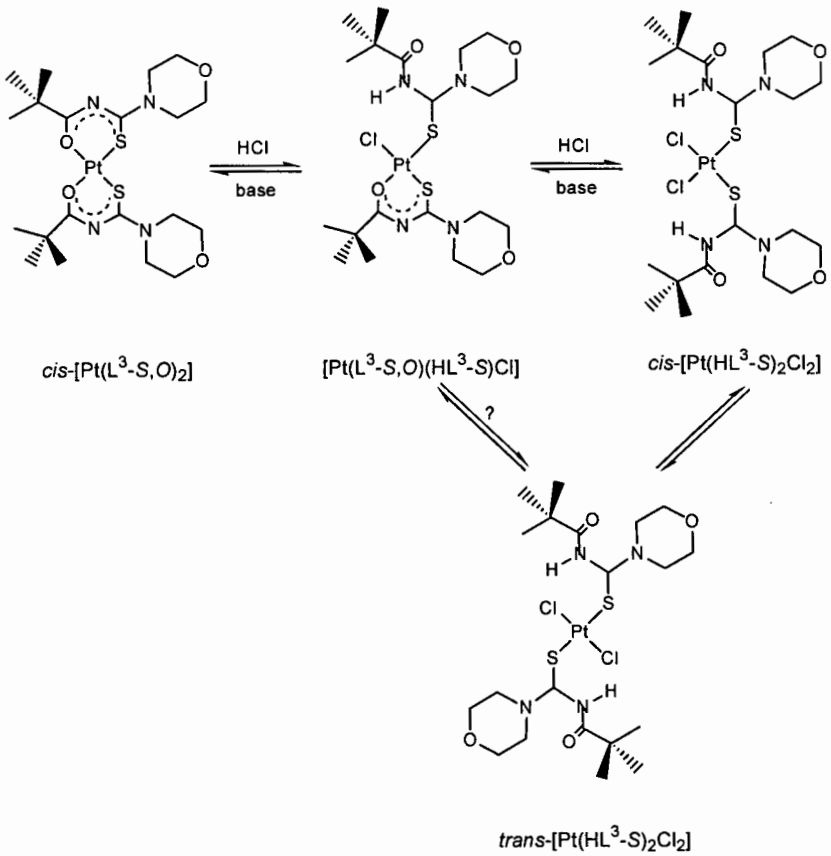

Figure 4. Schematic representation of the formation of various Pt^{II} species on addition of HCl to a $CDCl_3$ solution of cis-[Pt(L^3-S,O)$_2$].

Stellenbosch University http://scholar.sun.ac.za

CONCLUSION

The results of our investigation confirm that Pt^{IV} complex species are indeed extracted by *N*-acyl(aroyl)-*N'*,*N'*-dialkylthioureas yielding remarkably complex ^{1}H and ^{195}Pt NMR spectra of the extracts which are difficult to interpret directly. The possibility of redox reactions between Pt^{IV} and the ligands cannot be excluded at present, warranting further study (currently in progress). Nevertheless ^{1}H and ^{195}Pt NMR studies of the simpler Pt^{II} system shows that under acidic extractive conditions a variety of protonated complexes such as $[Pt(L^3\text{-}S,O)(HL^3\text{-}S)Cl]$, *cis*-$[Pt(HL^3\text{-}S)_2Cl_2]$ and *trans*-$[Pt(HL^3\text{-}S)_2Cl_2]$, may exist in equilibrium in the organic phase. Treatment of the acidified solution with dilute alkali results in reversion to the *cis*-$[Pt(L^3\text{-}S,O)_2]$ complex.

ACKNOWLEDGEMENTS

We thank the University of Stellenbosch, the National Research Foundation (NRF) and Anglo Platinum for financial assistance.

REFERENCES

1 F. Hartley (1991), Chemistry of the Platinum Group Metals: Recent Developments, Elsevier, Amsterdam, pp.9-31.
2 L. Beyer, E. Hoyer, J. Liebscher and H. Hartmann (1981), *Z. Chem.*, **21**, 81-91.
3 P. Muhl, K. Gloe, F. Dietze, E. Hoyer and L. Beyer (1986), *Z. Chem.*, **26**, 81-94.
4 K.-H. König, M. Schuster, B. Steinbrech, G. Schneeweis and R. Schlodder (1985), *Fres. Z. Anal. Chem.*, **321**, 457-460.
5 P. Vest, M. Schuster and K.-H. König (1989), *Fres. Z. Anal. Chem.*, **335**, 759-763.
6 M. Schuster (1992), *Fres. Z. Anal. Chem.*, **342**, 791-794.
7 K. R. Koch (2001), *Coord. Chem. Rev.*,**216-217**, 473-488.
8 S. Bourne and K. R. Koch (1993), *J. Chem. Soc., Dalton Trans.*, 2071-2072.
9 K. R. Koch, C. Sacht and S. Bourne (1995), *Inorg. Chim. Acta.*, **232**, 109-115.
10 K. R. Koch, C. Sacht, T. Grimmbacher and S Bourne (1995), *S. Afr. J. Chem.*, **48**, 71-77.
11 K. R.Koch, J. du Toit, M. Caira and C. Sacht (1994), *J. Chem. Soc., Dalton Trans.*, 785-786.
12 K. R. Koch, T. Grimmbacher and C. Sacht (1998), *Polyhedron*, **17**, 267-274.
13 P. Vest, M. Schuster and K.-H. König (1991), *Fres. J. Anal. Chem.*, **339**, 142-144.
14 K. R. Koch and J. Yates (1983), *Anal. Chim. Acta*, **147**, 235-245.
15 T. Shi, J. Berglund and L. Elding (1997), *J. Chem. Soc., Dalton Trans.*, 2073-2077.
16 A. Irving, K. R. Koch and M. Matoetoe (1993), *Inorg. Chim. Acta*, **206**, 193-199.
17 P. Pregosin (1982), *Coord. Chem. Rev.*, **44**, 247-291.